ILENR/AE-87/02

A PRACTICAL SYSTEM FOR THE USE OF ALCOHOL IN DIESEL ENGINES

Illinois Department of Energy and Natural Resources
OFFICE OF SOLID WASTE & RENEWABLE RESOURCES

ILENR/AE-87/02
Printed: November 1987
Contracts AE-13, 3-ALT

A PRACTICAL SYSTEM FOR THE USE OF ALCOHOL IN DIESEL ENGINES
Final Report

Prepared by:

University of Illinois at Urbana-Champaign
Department of Mechanical and Industrial Engineering
Urbana, Il. 61801

Principal Investigators

Dr. L.D. Savage
Dr. R.A. White

Prepared For:

Illinois Department of Energy and Natural Resources
Office of Solid Waste and Renewable Resources
325 West Adams Street, Room 300
Springfield, Illinois 62704-1892

Additional copies are available by calling the ENR Clearinghouse
at 800/252-8955 (within Illinois)
or 217/785-2800 (outside Illinois)

Statements and comments expressed herein do not
necessarily reflect the view of the Department.

Additional information is available from
Manager, Alternative Energy Development Program
at 217/524-5454

This document printed with U.S. DOE funds.

FOREWORD

The Illinois ethanol fuel industry has grown to be an important part of our state's economy over the past 10 years. It provides an additional market for Illinois' abundant corn production, provides many industrial jobs and substitutes a home-grown renewable energy resource for imported oil. More than 30 percent of all gasoline sold in Illinois contains 10 percent ethanol.

Gasoline engines readily accept ethanol blends and, with minor modifications, can run on pure ethanol. However, diesel engines, which power much of our transportation equipment and agricultural machinery, are not so obliging. The objective of this research effort was to develop a simple method of using ethanol in diesel engines in place of diesel fuel. The project was supported by grants from ENR's Alternative Energy Bond Fund Program and Alternative Transportation Fuels Program.

The resulting system shows great promise for retrofitting or as optional equipment on diesel engines. The information from this project should prove to be usable in many applications, such as on farm tractors, city buses and over-the-road trucks. ENR is pleased to have supported this research project and will continue to support development and field testing of the ethanol fuel systems.

Don Etchison, Director
Illinois Department of Energy
and Natural Resources

EXECUTIVE SUMMARY

The widespread use of diesel engines in the farm community coupled with the capability to produce fuel grade ethyl alcohol from farm grains has generated extensive research into the use of ethanol as an alternate diesel fuel. Since ethanol's basic combustion characteristics and consequent low cetane number make it a poor diesel fuel when directly injected into diesel engines, most studies have emphasized either mixtures of alcohol and diesel fuel or dual fueling systems such as fumigation of the alcohol with the inducted air charge.

This study utilized fumigation of ethanol with the aim of developing a simple and practical microchip controlled alcohol injection system suitable for all engine operating conditions. In contrast to most previous fumigation systems, the method selected used multiple injectors with one at each inlet valve location. This provided for uniform cylinder-to-cylinder air-alcohol mixtures in order to avoid reduction in energy replacement potential due to one cylinder setting the limiting condition and allowed the use of different alcohol injection cycles. the latter is important since it provides a method for controlling the composition of the air-alcohol charge in terms of the percent vapor or droplets and consequently the tendency to detonate (knock) or burn with the pilot diesel fuel.

The results of the investigation have shown that alcohol fumigation of diesel engines is practical in terms of energy replacement and in terms of proof level of alcohol needed. This is based on five major conclusions which can be summarizes as:

1. The alcohol injection cycle is critical to avoid damaging knock. A two-step injection process is needed which controls the form of knock and allows energy replacement levels of up to 90 percent at low loads and 35 percent at high loads.

2. Improved performance can be obtained by modification to the diesel pilot fuel injection timing.

3. 100 proof ethanol provides performance equivalent to or slightly better than either straight diesel fuel or 190 to 200 proof ethanol.

4. Three distinct knock types can be identified in the fumigated diesel engine. Only one of these causes damaging pressure levels as energy replacement levels are increased and apparently can be avoided by the proper choice of alcohol injection cycle.

5. Multipoint port injection provides improved fumigation control, increased energy replacement capability, and permits injection cycle change for modification of the air-alcohol charge and its burning characteristics.

TABLE OF CONTENTS

INTRODUCTION

The search for alternatives to petroleum based fuels is not new nor is it confined to particular countries or cultures. Typically it has been based on need due to war or appliances which resulted in uncontrollable restrictions on fuel delivers. More recently, however, it has been recognized that long-term energy requirements will need to be based on additional sources for chemically stored heat energy to drive the various types of heat engines of modern society. Transportation in particular has special needs due to the twin requirements of relatively high energy density and energy per unit volume. With transportation consuming approximately 25 percent of all energy used in the United States and almost 60 percent of that produced from oil, this sector is strongly dependent on guarantees for reliable future sources of liquid fuel.

The farm community with its rural base and dependence on large equipment for the efficient production of food must have fuel available at reasonable cost at specific times, nature does not wait for the convenience of man. Consequently, the farms states have been leaders in the understanding of the need for alternate fuels. Fortunately, grain derived alcohols, ethanol in particular, meets almost all of the requirements. Its production is well developed, although this has been primarily driven by the beverage aspects of this liquid. It is renewable, it can be relatively easily produced by the individual farmer or on a large scale, and it has good to excellent energy density and volume.

Indeed, ethanol has been used as fuel but primarily as a spark ignition engine fuel due to its high octane rating (in excess of 100). For farm type equipment and the over the highway industry, the diesel engine is the engine of preference due to efficiency and longevity. Unfortunately the one characteristic of ethanol which makes is so suitable as a spark ignition fuel, is its octane rating, makes it a poor diesel fuel. If its low cetane rating can be overcome, ethanol is at least an attractive supplement as a diesel fuel.

Consequently there exists an extensive body of literature based on research studies covering the various means of using alcohol in diesel engines. These range from direct injection as is done with straight diesel fuel to simple induction of small mounts with the air stream or fumigation as it is called. In general, each of the various methods has advantages and disadvantages which must be taken into account. One important factor is the degree of modification to existing engines required to use alcohol as a fuel since new engines designed for alcohol use will not significantly impact energy use in the next generation due to the tens of millions of existing engines in the farm/industrial fleet.

Recognizing that all of the practical alcohol systems are based on using the alcohol as a supplement and not as a complete replacement for diesel fuel and that of these fumigation readily allows dual fueling with few if any modifications. Unfortunately the amount of energy replacement with fumigation has been reported as being limited (Baranescu) due to heavy knock and excessive rates of change of cylinder pressure. The range of energy replacement has also been the subject of considerable variation with no satisfactory explanation for the large difference reported by different investigators.

The attractive practical features of alcohol fumigation, in particular the ability to easily retrofit existing engines and continued normal operation on diesel fuel in case of shutdown, led to the selection of this approach for this investigation. The following sections examine and discuss the results of the study and show that ethanol fumigation of diesel engines is a practical and efficient method for the use of alcohol as an alternate and supplement fuel in these engines.

APPLICATION OF FUMIGATION

hile various methods for the use of fumigation have been tried, the most approach has been to introduce the alcohol in the intake before the ld and in the case of turbocharged engines downstream of the turbo- r. This approach has the disadvantage of producing cylinder-to-cylinder ions in the air-to-fuel ratio of the inducted charge. Indeed, the m is more severe than that occurring with the carbureted spark ignition since diesel intake manifolds are not designed for the flow of an air- ixture but simple air.

hus it was decided to utilize the rapidly developing technology of oint port injection used in the automotive industry. This choice im- ely leads to several important advantages in addition to the guarantee iform cylinder-to-cylinder air fuel ratios which prevents the limiting ion being established by any single cylinder and its charge. In ad- , the multipoint system at the intake port also allows changes in the f cycle and timing of the alcohol addition relative to the engine cycle . This latter factor is important in that it permits some control over tratification of the in-cylinder charge of air and alcohol and con- tly its combustion/detonation characteristics.

he initial alcohol injection cycle selected is one in which one-half of lcohol is injected on each engine revolution. Thus one-half of the l lies on the intake valve where it absorbs heat and partially ates for one engine revolution while the other half is injected during me the intake valve is open. this will be referred to as the DIT or injection timing cycle. This cycle was originally selected since it y simplifies design the electronics and associated logic for timing the relative to top dead center.

he engine used in the investigation was an International Harvester (now ar International) DT-436 four-stroke turbocharged six-cylinder diesel. gine was nominally rates at 175 hp at 2,500rpm. The engine was com- y instrumented including modifications for cylinder pressure measurement e multipoint port injectors. Data included cylinder pressure at every of crackshaft rotation and air flow, fuel flow, exhaust temperatures, harger inlet and outlet conditions, coolant and lubrication temper- , and exhaust emissions. The additional cycles were added to the system lity later in the program. These allow the examination of different nce times for the alcohol in the manifold and consequent vapor liquid These cycles are:

SIO, or single injection of all alcohol during the intake value open engine revolution and

SOC, or single injection of all alcohol during the intake value closed engine revolution.

DISCUSSION OF RESULTS

This investigation has resulted to date in the publications of three master of science theses and a Society of Automotive Energy technical paper. Copies of all four are included as APPENDIX I through APPENDIX IV. An additional master of science degree thesis will be completed during the Fall of 1986. The major conclusions and results of these studies are discussed below.

The initial study which was undertaken by Roberts (APPENDIX I) aimed at defining the engines operations field using the multipoint port injection system and DIT cycle. This was essential to determine if the port injection concept had measurable advantages over the single-point approach commonly used in other studies*. Roberts was able to establish by limiting boundary tests that the maximum amount of energy replacement possible with the fumigated ethanol was different at low load conditions where flame-out or misfire set the limit and at high load conditions where heavy knock was the limiting factor. Table 1, in APPDNEIX I, shows the limiting factors for the alcohol fumigation as a function of load and engine speed.

With the bounds of the fuel established, it was apparent that the port injection and dual cycle allowed the use of significantly grater amounts of alcohol than typically reported by other investigators*. thus he was able to obtained approximately 90 percent energy replacement at low loads and about 35 percent at high loads. As the rest of the operational field was examined and the emissions and computed engine parameters such as thermal efficiency were examined, it was determined that the fumigation resulted in excellent performance. Thermal efficiency was found to increase by about 3 percent at high loads. While unburned hydrocarbons increased significantly under some conditions, the levels of NO were found to decrease. Overall performance was essentially equivalent to straight diesel operation.

Examination of the pressure volume diagram showed that ignition delay was changed due to the fumigation of the ethanol. This suggested that changes in the diesel fuel injection timing may lead to further improvements in fumigated diesel engine performance. Consequently Schroeder (APPENDIX II) undertook a series of tests to establish the relation of diesel injection timing the operation with fumigation. He found that advancing pilot injection timing was not effective either low or high loads. At low loads, the amount of diesel fuel injected is so small due to the high percentage of alcohol tolerable that distribution and changes in timing leads to engine misfire. At high loads, the thermal efficiency decreased due to the shift in the peak pressure to too early in the cycle. At intermediate loads, however, changes in diesel timing lead to significant improvements. Thus at 2,000 rpm and approximately 50 percent loads, an increase in pilot injection from 18 to 29 degrees increased the thermal efficiency by 3 percent and the same change at 2,400 rpm gave an improvement of 4 percent. This indicates that the increasing use of electronic timing injection pumps where injection timing can be easily changed may allow for further improvements in the effectiveness of the fumigation method.

---

*Baranescu, R. A., "Fumigation of Alcohols in a Multicylinder Diesel Engine-Evaluation of Potential," SAE Paper No. 860308, Warrendale, PA.

Since the production of ethanol directly in the farm community, typically results in 140 to 160 proof and not the 190 to 200 proof distilled by the beverage and power alcohol industry, an examination of the effect of using lower proof in the fumigation process was undertaken. this is of additional importance due to the tendency for ethanol to absorb water while stored which degrades its proof. Hayes (APPENDIX III) consequently studied proofs of from 100 to 200 and examined all parameters including the exhaust emissions. Hayes found that the lower proofs resulted in lower rates of in-cylinder pressure rise as well as peak pressure. In some cases, the change in pressure history resulted in a pressure volume diagram similar to that of a spark ignition engine and a resultant increase in thermal efficiency. Further, the ethanol proof greatly increased the levels of unburned hydrocarbons; however, proof below 150 resulted in decreases in the NO emissions. ethanol proof did not have a significant effect on CO emissions.

Hayes concluded that the optimum type of ethanol appears to be 100 proof. Its use resulted in a measurable increase in thermal efficiency and the lowest cylinder pressure histories. This coupled with its easy and economy of manufacture make it highly attractive. The only drawbacks appear to be the large increase in unburned hydrocarbons.

The changes in pressure history and increased thermal efficiency for the low proofs suggested that fumigation results in modification of the basic engine cycle and consequently re-examination of the knock concept for this type of operation should be considered. Thus a comprehensive review of the available Data for the entire study was undertaken. This revealed that the form of knock occurring under fumigation conditions was indeed changing and that the distinct forms of knock could be identified. Savage, et al. (APPENDIX IV) have examined this in considerable detail and show that not only are there the distinct types of knock but that they are related to the alcohol injection cycle and that one form is to be preferred and one form mus be avoided.

The three knock forms are as follows:

1. Standard diesel knock with the pressure oscillations occurring early in the combustion process and typically prior to top dead center,

2. Very rapid detonation of the alcohol-air inducted charge accompanied by an extreme pressure spike, and

3. Pressure oscillations near or after top dead center and similar to spark ignition end gas detonation.

The second type causes excessive peak pressures and has a distinct knock sound which can best be described as clanging rather than knock. This type of knock can lead to serious engine damage and must be avoided when using fumigation. the results indicate that this type of knock has not occurred during the testing to date using the dual cycle and ethanol. It does occur with the other injection cycles and it is suspected of occurring with single point upstream injection leading to the consequent low tolerance levels reported for this type of fumigation.

The third type of knock is desirable in that it leads to increased thermal efficiency due to the pressure history being more similar to that occurring for the spark ignition engine. simultaneously the engine's tolerance to rate of change of pressure normally associated with heavy knock is increased allowing additional fumigation of alcohol. A complete understanding of the occurrence of the various knock form is essential to the avoidance of the type-two knock. Consequently, continued studies of the relation between diesel engine fumigation and knock would be a worthwhile contribution.

CONCLUSIONS

The current investigation has shown that ethanol fumigation of diesel engines is a viable technique for providing alternate fuel capability. Its practical application requires the understanding of the modifications of the combustion processes brought about by its use. This includes the occurrence and type of knock and the in-cylinder pressure history.

Important to the successful practical use of fumigation is the adoption of multipoint port injection. This guarantees uniform cylinder-to-cylinder fuel air distribution and provides for the capability to change both the alcohol injection timing and the cycle itself. The latter has been shown to be essential to the avoidance of potentially damaging pressure histories.

APPENDIX I

PERFORMANCE AND EMISSIONS OF A TURBOCHARGED DIESEL ENGINE FUMIGATED WITH ETHANOL

Barry Dale Roberts
B.S., University of Illinois, 1983
M.S., University of Illinois, 1986
Department of Mechanical and Industrial Engineering
University of Illinois at Urbana-Champaign
1206 West Green Street
Urbana, IL 61801

Submitted in partial fulfillment of the requirements
for the degree of Master of Science in Mechanical Engineering
in the Graduate College of the
University of Illinois at Urbana-Champaign, 1986

1. INTRODUCTION

The recent stabilization of petroleum product prices and the abundant supply of crude oil has given the consuming public the false impression of a never-ending world supply of crude petroleum reserves. Estimates made before the oil embargo of the early 1970's showed demand for petroleum products exhausting the world's economically recoverable, proven reserves of crude oil some time early in the next century [1]. The oil embargo of 1973 increased the consuming public's energy awareness, and the resulting reductions in energy consumption helped to slightly reduce demand on proven reserves, as well as providing incentives for discovering more reserves. The projected demand for petroleum, even with the reduction in petroleum demand which the oil embargo, is expected to exceed production by the middle of the twenty first century [2]. A decade after the oil embargo, the end result still remains the same, one day the oil reserves of the world will be exhausted.

At present, no suitable alternative supply of energy has been developed or identified. Of primary concern is a portable form of fuel with sufficient energy density for use in the existing engines utilized by transportation, agricultural and construction equipment. A large number of the engines existing in equipment today are diesel engines, and an increasing number of these engines are turbocharged.

While alternative fuels such as alcohols, hydrogen, solvent-refined coal fuels, and vegetable oils have been suggested, insufficient study on the effects of each fuel on engine components and the environment has left no single alternate fuel as an acceptable substitute. There remains little hope for a universally accepted alternative fuel in the near future. Federal support for research is being reduced using the assumption of increasing support and interest from the private sector [3]. There exists little or no short term economic motivation for industry to provide such support [4]. Satisfactory amounts of research cannot be conducted in the narrow time frame which would exist once economic factors compel industry to react.

A combination of political and economic demands may be required to force the identification of an accepted portable fuel for long term use in the future. Until that time, research is needed into viable methods of extending the existing reserves of crude oil, primarily though the use of fuel additives and engine design changes. As design changes take relatively longer to evolve, fuel additives and substitutes are receiving a majority of the emphasis in current research.

Agriculturally derived fuels, primarily those from grains, are receiving much interest as fuel substitutes and extenders. Much of the interest stems from the ability to renew the fuel supply each crop season. Fuel grade ethanol, derived principally from feed grain, is one renewable fuel which has great promise as a petroleum fuel substitute. Although this source is not a solution to the entire country's energy needs, each bushel of corn or wheat potentially yields over two and one-half gallons of fuel grade ethanol [5], and certain regions of the country could benefit from utilizing this local energy potential.

The characteristics which make ethanol fuels worth considering as fuel substitutes include its liquid form, energy content, and the existing tech-

nology for economical commercial production. The low cetane number and high heat of vaporization are undesirable ethanol properties which warrant further investigation with respect to their effects on combustion characteristics and engine performance when it is used a fuel component.

The majority of ethanol fuel research has been conducted using it in a blend of other fuel components and supplying it in the original fuel injection system of diesel engines. An alternate method of ethanol fueling, which allows greater flexibility in the amount of ethanol utilized, is to spray it into the air which is inducted into the cylinder for combustion. This method of fueling is called fumigation. The flexibility of fumigation was one of the primary reasons for it's use as the fueling method in this investigation.

The objectives of this investigation were:

1. To provide in-depth performance and emissions data for a testing program consisting of fixed percentages of the maximum brake torque the test engine produced at the selected engine speeds using No. 2 diesel fuel. Performance parameters of interest included brake specific fuel consumption, combustion efficiency, peak cylinder pressure, maximum rate of cylinder pressure change, and ignition delay. Emissions parameters included oxides of nitrogen, carbon monoxide, carbon dioxide, unburned hydrocarbons, and the smoke number.

2. To determine the maximum tolerable amount of ethanol which can be substituted for diesel fuel at each test point, based upon performance and emissions characteristics.

3. To gather the performance and emissions data at the same test points as the No. 2 diesel fuel testing, while substituting the maximum amount of ethanol for each test condition.

4. To investigate which engine operating parameters are the most useful for determining the maximum allowable substitutions of ethanol at each test point.

5. To provide information for the preliminary development of an aftermarket ethanol injection system which would be compatible with electronic engine control systems.

2. LITERATURE REVIEW

Methods of utilizing ethanol, as well as various other alternate fuels in diesel engines can be categorized into three general approaches according to the type of fueling system used. The fueling system types are direct injection with a single fuel, direct injection of a blended fuel, and dual injection system to allow simultaneous fueling [6].

2.1 Direct Injection

The direct injection method of ethanol fueling has two main disadvantages. The first drawback to this fueling method is the poor self-ignition characteristic which results in a low cetane number for ethanol. The poor ignition problem has been addressed through the investigation of ignition improvers [7], and the use of heated surfaces to enhance ignition [8]. While both methods provided satisfactory performance, neither appeared as an acceptable solution. Most of the ignition improvers tested were nitrates by chemical composition, which tended to increase emissions of nitrogen oxides at low to medium engine speeds, tended to be explosive as well as corrosive, and increased the cost of the fuel above the economically feasible level. The heated surface initiated ignition tests required the redesigning of the combustion chamber which is acceptable for future diesel engines, but is unacceptable for engines already in use.

Both methods investigated for overcoming the low cetane number of ethanol also fail to address the second disadvantage of direct injection, which is the requirement of sufficient lubricating properties of the fuel [9]. The low viscosity of ethanol does not provide adequate lubrication and wear protection to the many injection system components with very small tolerances which are used on existing diesel engines. Redesigning of injection system components for larger tolerances and the use of materials with greater wear resistance would accommodate the direct injection method of fueling, but is economically feasible only to future diesel engines and not existing engines. The use of viscosity improvers would accommodate existing engines, but once again economics is the decisive issue.

2.2 Blends

The direct injection of a blended ethanol fuel has received considerable investigation with mixed results. Various ethanol blends based on heavy distillate, No. 2 diesel fuel, and soybean oil as primary components have provided adequate performance, but each blend has its individual disadvantages. Two heavy distillate blends were investigated, and the blends were based upon heavy virgin distillate and a combination of No. 4 with No. 2 diesel fuel. Each petroleum base was mixed with ethanol, butanol, and cetane improver [9]. Butanol was used because of a problem with miscibility and cetane improver to raise the final cetane rating of the blend. Overall performance was acceptable, with only a slight decrease in peak power and generally higher emission of carbon monoxide with increased smoke number. The blend requirements of a high percentage of butanol and the added expense of the cetane improver, along with the fixed percentage of ethanol usage were the disadvantages of the fuel.

The blending of ethanol with No. 2 diesel fuel, soybean oil, and butanol in the right proportions was found to result in a fuel which yielded performance similar to No. 2 diesel fuel [10]. The blended fuel had slight increases in brake thermal efficiency, with emissions of nitrogen oxides and carbon monoxide also being slightly higher. A significant reduction in smoke was also noted with the blended fuel. One of the major disadvantages to the soybean oil blended with ethanol fuel was the rapid build-up of carbon in the combustion chamber [11], which results in decreased fuel efficiency and shorter engine life. Other disadvantages include the high ratio of butanol to ethanol used to control miscibility (4:1 and 2.5:1 by volume) and the mixed percentage of ethanol in the fuel blend.

lending ethanol and No. 2 diesel fuel requires the solving of a miscibility problem. Anhydrous or 100 percent ethanol forms a solution with No. 2 diesel fuel, but ethanol with a water content of greater than one-half percent will separate out of a diesel fuel mixture [12]. The normal water content of ethanol used for fuel is approximately five percent, due in part to the azeotrope formed during distillation, and the increased production cost of removing the last five percent of water. Methods of forming a combustible, stable solution utilizing the wet alcohol with No. 2 diesel fuel must be developed with economy as a prime consideration. A combustible solution can be formed by stabilizing the mixture either chemically with a surfactant or solubilizer when the components are initially mixed, or to mechanically mix and force the components together immediately before pumping to the injection system. The resulting solution is referred to as an emulsion.

Tests have been conducted on chemically stabilized emulsion fuels which use commercially available surfactants, and on emulsion fuels which use higher order alcohols as solubilizers. Although the surfactant fuel which was tested performed satisfactorily with beneficial decreases in nitrogen oxide emissions [13], the cost of surfactants proves to be inhibitive. The solubilized emulsion fuels also performed satisfactorily with noted increases in unburned hydrocarbon and carbon monoxide emissions, and reduced emissions of nitrogen oxides and smoke [14]. Disadvantages include the cost of the solubilizing agents, and conerts over their possible harmful effects on injection system materials. Both methods of forming a chemically stabilized emulsion also have the constant concentration of ethanol disadvantage.

Mechanical mixing of unstable emulsions immediately before the fuel injection system have proven to give results in performance and emissions similar to No. 2 diesel fuel [12]. While the mechanical mixing of unstable emulsion fuels does offer the flexibility of varying alcohol content according to operating conditions [15], the cost and complexity of the required equipment are the greatest problems with this method of utilizing ethanol in diesel engines.

2.3 Dual Fueling

The third method of fueling a diesel engine with ethanol is the addition of a second fuel system. Although high pressure ethanol injection systems are a possible fueling method, they are not discussed here because of their prohibitive cost and the engine design changes which must be made for such systems to be used. Low pressure supplemental fueling systems which add fuel to the intake charge of air are the most common methods used for the dual fueling

approach. Of the low pressure systems possible, carburetion and fumigation type systems are the techniques receiving the most attention.

The carburetion method has been investigated on naturally aspirated diesel engines using a simple carburetor and with a complex, dual throttling carburetor setup. The simple carburetor, which had the choke and throttle plates removed, resulted in the test engine being overfueled, with poor ethanol vaporization and increases in unburned hydrocarbons and smoke emissions [16]. The complex carburetor was equipped with dual throttling plates which were calibrated and moved simultaneously. One plate throttled air through a venturi and past the ethanol orifice, while the other plate metered bypass air to maintain a proper air to fuel ratio. This system performed satisfactorily with reductions in exhaust temperature and smoke emissions while providing up to forty-five percent ethanol (by volume) substitution [17]. The main disadvantage of this fueling system was the complexity of the carburetor design, and the resulting fixed substitution rate at a given engine speed.

The complex dual throttling carburetor has also been investigated on a turbocharged diesel engine. A system similar to that investigated on the non-turbocharged engine was field tested, resulting in a net replacement by ethanol of forty percent of the diesel fuel normally consumed. Small increases in thermal efficiency were noted with power output slightly higher than diesel fuel only, which indicates a slight overfueled condition [18]. The complexity of the system and a fixed ethanol fueling rate were also the disadvantages to this fueling system.

Fumigation refers to the method of spraying a fuel into the intake air stream of an engine. Fumigation allows the utilization of many fuels which have properties that are undesirable to diesel engines [19]. Fuel properties such as high heat of vaporization and low viscosity are compensated for by the use of fumigation as a fueling method.

Fumigation is accomplished in two ways, the first is with the use of a single spray nozzle or injector and is referred to as single point. The second method of fumigation is called multi-point and makes use of an injector or spray nozzle for each cylinder.

Single point fumigation of ethanol in turbocharged diesel engines has been attempted in two locations. Single point fumigation downstream of the turbocharger resulted in satisfactory performance with reductions in smoke and nitrogen oxide emissions while the emission of unburned hydrocarbons increased [20]. Large differences in the measured exhaust temperature from cylinder to cylinder were also noted, indicating a problem with distribution of the fumigated fuel between cylinders.

Efforts aimed at increasing the mixing of the intake air and the sprayed ethanol resulted in the second location for single point fumigation, into the compressor inlet on the turbocharger. Engine performance with this method and location of fueling were satisfactory [18], with the same emission trends as those noted for downstream single point [21,22]. No cylinder to cylinder exhaust temperature data was reported, so no information on improved distribution by using the turbocharger as a mixer was proven. Potential harm to the compressor blades due to droplet impingement is the most important drawback to the before turbocharger fumigation method.

Another method of injection designed to improve alcohol vaporization which has been investigated is called flash boiling. The temperature and supply pressure of the alcohol are increased such that after being issued from a nozzle, the pressure of the alcohol is below it's saturation pressure and it boils or vaporizes instantaneously [23]. This method improved ethanol combustion with decreases in the amount of unburned fuel which were exhausted, but the dangers of any leaks from such a fuel system make it more dangerous when compared to other fueling systems.

Research with multi-point fumigation has been conducted using gasoline type fuel injectors which resulted in ethanol supplying up to sixty percent of the fuel energy [24]. Emissions of unburned hydrocarbons and carbon monoxide were higher, and the smoke level was lower when compared to the same test conditions using diesel fuel only. Misfiring was reported as the most important factor limiting the extent of ethanol substitution.

Direct comparison of multi-point and single point fumigation systems on the same engine showed that at low loads there was no difference between systems, but at medium too high loads the multi-point system gave better performance due to more even distribution [25]. The distribution between cylinders was determined by measuring the exhaust temperature at each port.

Widespread application of electronics has led to the recent development of electronically controlled injection pumps for diesel engines [26,27], with a corresponding introduction of electronic engine controllers [28,29]. The electronic engine controllers provide computerized monitoring of all engine conditions as well as fine tuning fuel delivery and injection advance to optimize fueling. The controllers, through the use of digital control algorithms [30], also provide an excellent opportunity to fine tune an engine which is dual fueled with ethanol fumigation.

Microprocessor controlled single point fumigation systems have been developed for use on engines [31,32], with adjustment of the injection pump required to limit fueling for normal power output. Expansion of these systems to multi-point fumigation, along with coupling the fumigation system to an electronic engine controller appear to be the next steps in the utilization of dual fueling techniques.

3. EXPERIMENTAL SETUP

3.1 Engine and Control System

An International Harvester Model DT-436B, 4 stroke cycle, 6 cylinder, turbocharged engine was used for the tests. The engine bore of 109.2 mm and a stroke of 127.0 mm gave a net displacement of 7.141 liters. The compression ratio was 16:1. The turbocharger was manufactured by Airesearch for International Harvester and was Model T04B-18.

The engine had the radiator replaced by a heat exchanger which was supplied with city water, the fan was removed, and the alternator had no electrical load while being used as an idling pulley for the water pump belt.

A Midwest Dynomometer & Engineering Company type MW310 eddy current dynomometer was used to provide load for the engine. A Digalog Corporation Dynomometer Controller, Model 1022A, and companion Throttle Controller, Model TC, were used to regulate engine speed and load.

The Digalog Controllers had existing circuitry for determining engine overspeed conditions, setting the throttle position with position feedback information, measuring engine speed, measuring brake torque, and controlling the field current which provided the torque resistance to the engine (see Fig. 1). Terminal connections were also available for remote or computer input to the controllers. Hardware and software were developed which allowed an Apple IIe computer to control the test conditions through the Digalog Controllers (see APPENDIX B).

All test conditions were run using the RPM control mode of the controllers. The RPM control mode operated such that for a given throttle position and desired engine speed chosen by the operator, the controllers varied dynomometer load to maintain the desired engine speed.

3.2 Fuel Systems and Fuels

Engine consumption rates of both diesel fuel and ethanol were measured utilizing systems similar to that shown in Fig. 2. During normal operation the solenoid valve was open and the levels of fuel buret and float tube were even with the fuel level in the level tank. When the solenoid valve was open, fuel was drawn from the level tank, which maintained the fuel level by regulating flow from the supply tank with a float and needle valve combination. The solenoid valve was closed with a fuel measurement was begun and the engine drew fuel from the buret and float tube. The computer measured the time required for the engine to consume known volumes of fuel. Provisions in the fuel measuring program required the time of fuel measurement to be greater than one minute, which ensured sufficient time accuracy for the measurement.

The ethanol fumigation system which was added to bhe engine consisted of six electronic fuel injectors manufactured by Bendix, Model E-10. The supply system to the injectors consisted of Bosch 12 volt fuel pump Model 346, and a Model 344 fuel filter, with a Cash Acme pressure regulator, type FR, which was set for a 40 psia differential (see Fig. 3). Reference pressure for the pressure regulator was taken from the intake manifold so that turbocharger boost would not change the pressure differential across the injectors.

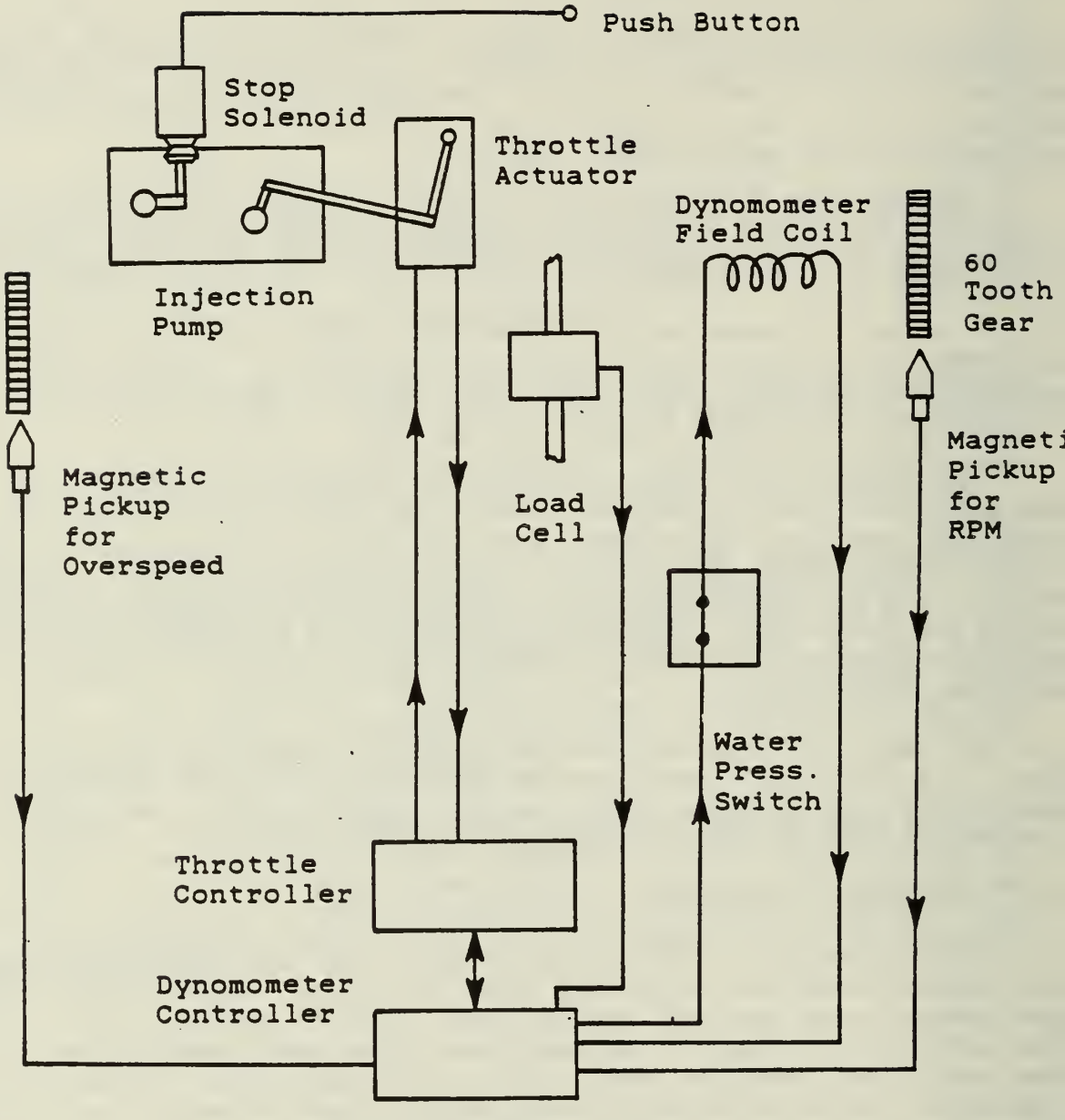

Figure 1. Digalog Throttle and Dynomometer Controller Interconnections to Engine and Dynomometer.

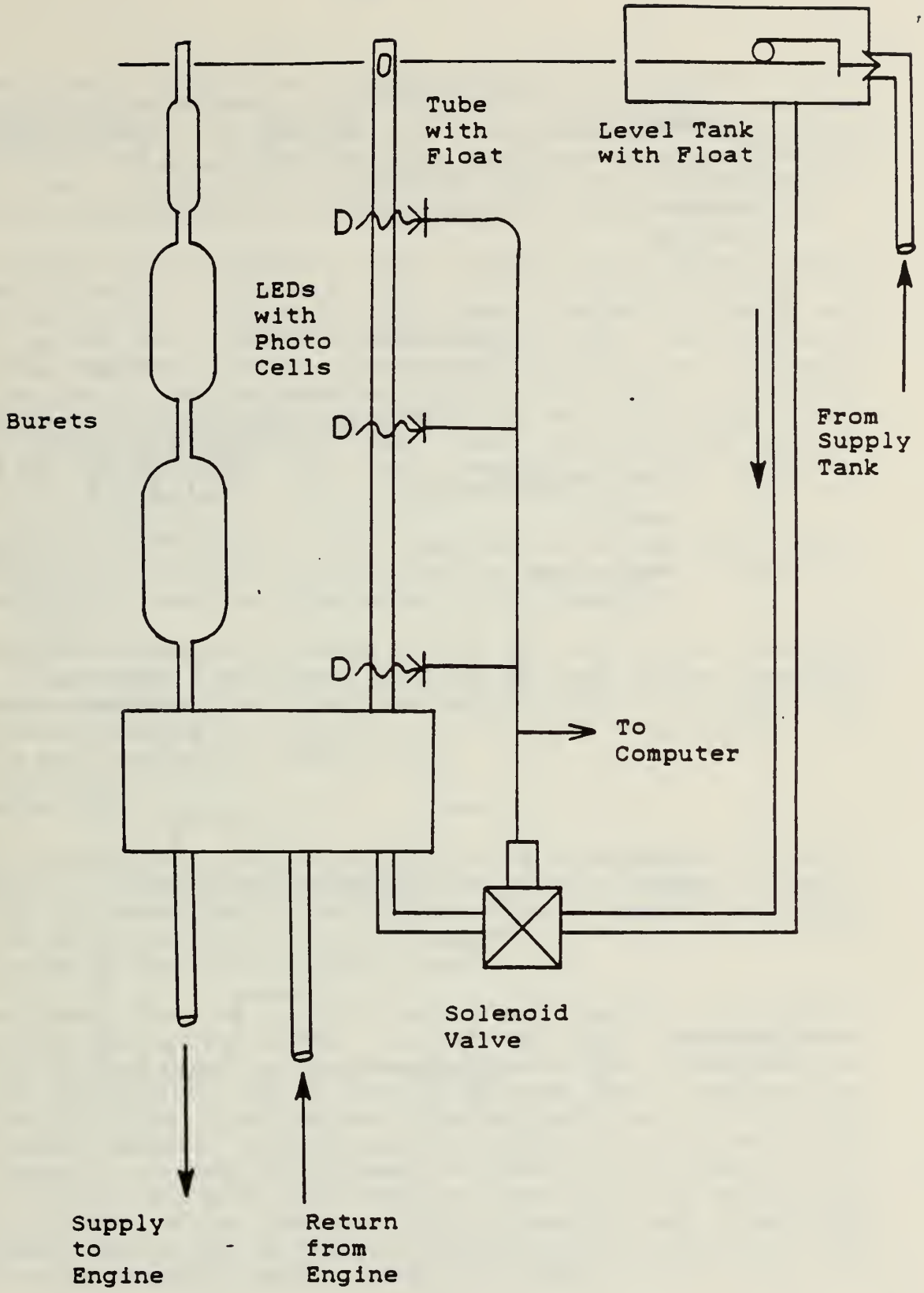

Figure 2. Electronic Fuel Measurement System

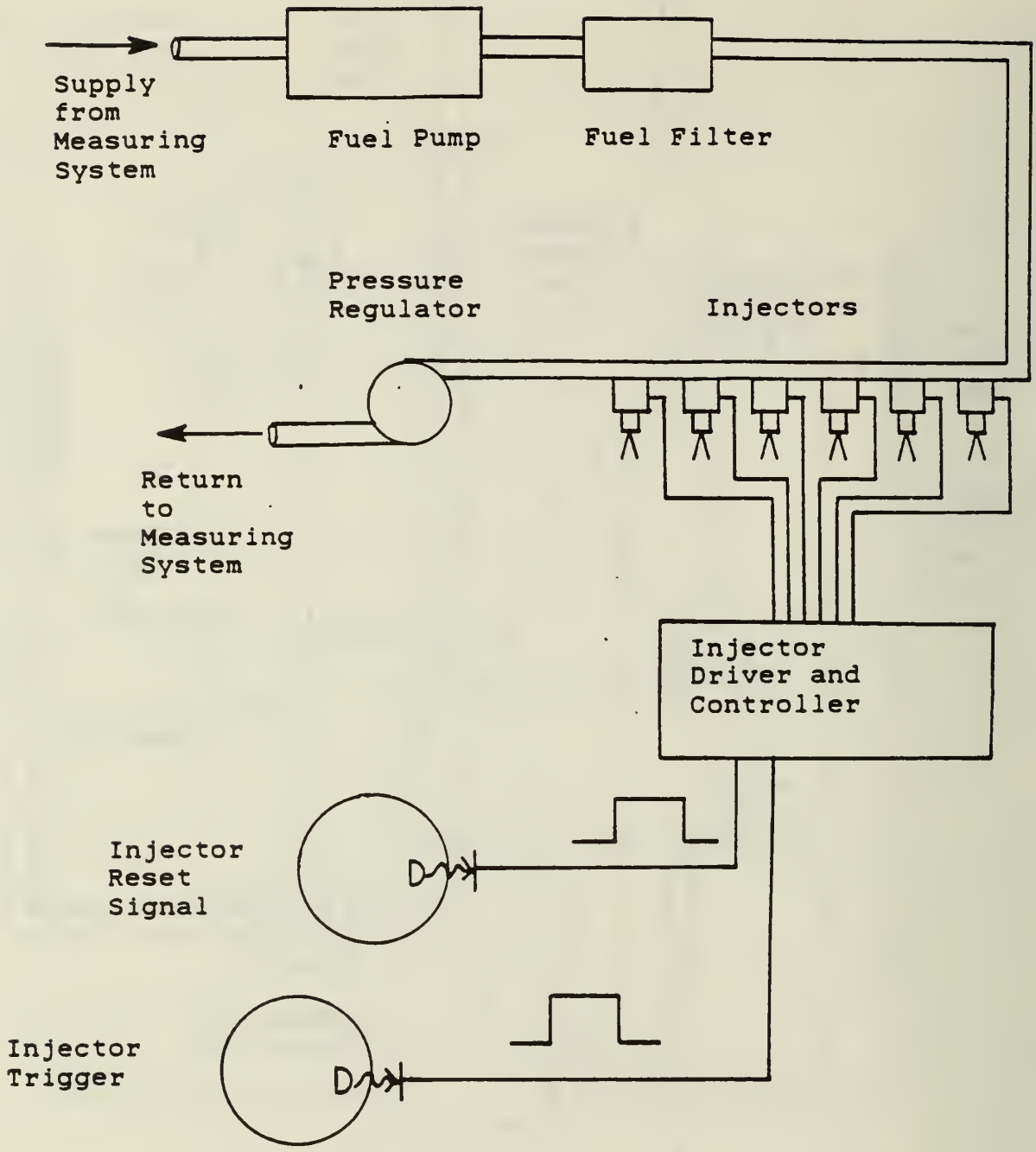

Figure 3. Ethanol Fumigation System

An injector driver circuit was necessary to utilize an injector control box which was supplied by International Harvester. The injector reset and injector trigger signals were obtained from a wheel with optical switches which was placed at the end of the dynomometer shaft opposite the engine (see APPENDIX D). The spray duration and resulting flow rate from the injectors was controlled by varying the pulse width of the signal sent to the injectors.

The estimated maximum consumption rate of ethanol by the engine required greater capacity than the electronic injectors were capable of delivering when pulsed once per cycle. This upper limit due to injector capacity was eliminated by pulsing the injectors twice per engine cycle. The first spray pulse was during the intake valve open portion of the cycle, and the second spray pulse was during the gas expansion portion of the cycle. To produce this pattern, the injector trigger wheel produced three equally spaced pulses which were timed to the opening of the intake valve for each pair of cylinders. The injector reset signal was a single pulse timed to approximately 10 crank angle degrees before top dead center for cylinder number one.

The position of an injector in the intake port of the cylinder head is shown in Fig. 4. The angle of 25° from vertical was chosen to facilitate placing as much alcohol near the intake valve as possible.

Baseline diesel data was obtained furling the engine with commercial grade No. 2 diesel fuel. The ethanol used was 200 proof ethanol denatured with 5 percent unleaded gasoline. The lower heating value of the diesel fuel was assumed to be 42781 kJ/kg. The lower heating value of the ethanol fuel was assumed by mass average to be 26900 kJ/kg.

3.3 Instrumentation

Emission sampling and analysis was done using a customized instrument bank. Instruments in the system included a Chemluminescent NO-NOx Gas Analyzer Model 10A by Thermo-Electron Corporation, a Model 402 FID hydrocarbon analyzer by Beckman, Model 315B CO2 and CO analyzers by Beckman, and a Model 715 Process Oxygen Monitor also by Beckman (see Fig. 5).

The transducers used for cylinder pressure and injection line pressure measurements were manufactured by AVL. A strain gage type transducer, Model 41 DP500K, was used for injection line pressure measurements. Location of the transducer was approximately 108 mm from the cylinder end of the injection line. A Model 8QP 500ca transducer was installed in a sleeve which passed through the water jacket of the head and the valve cover. The end of the transducer exposed to the combustion chamber was coated with RTV rubber to reduce the effects of radiation heat transfer from the flame on pressure measurements. Cooling of the pressure cylinder transducer was accomplished with the standard cooling tank and pump available from AVL. Kistler Model 504 charge amplifiers were used to amplify transducer signals.

Crank angle position was determined from a BEI Model H25D-360-ABZ-7406R-EM16 shaft encoder which was connected to an extension of the crank shaft. The shaft encoder had output signals of one pulse per revolution and 360 pulses per revolution, both TTL level signals.

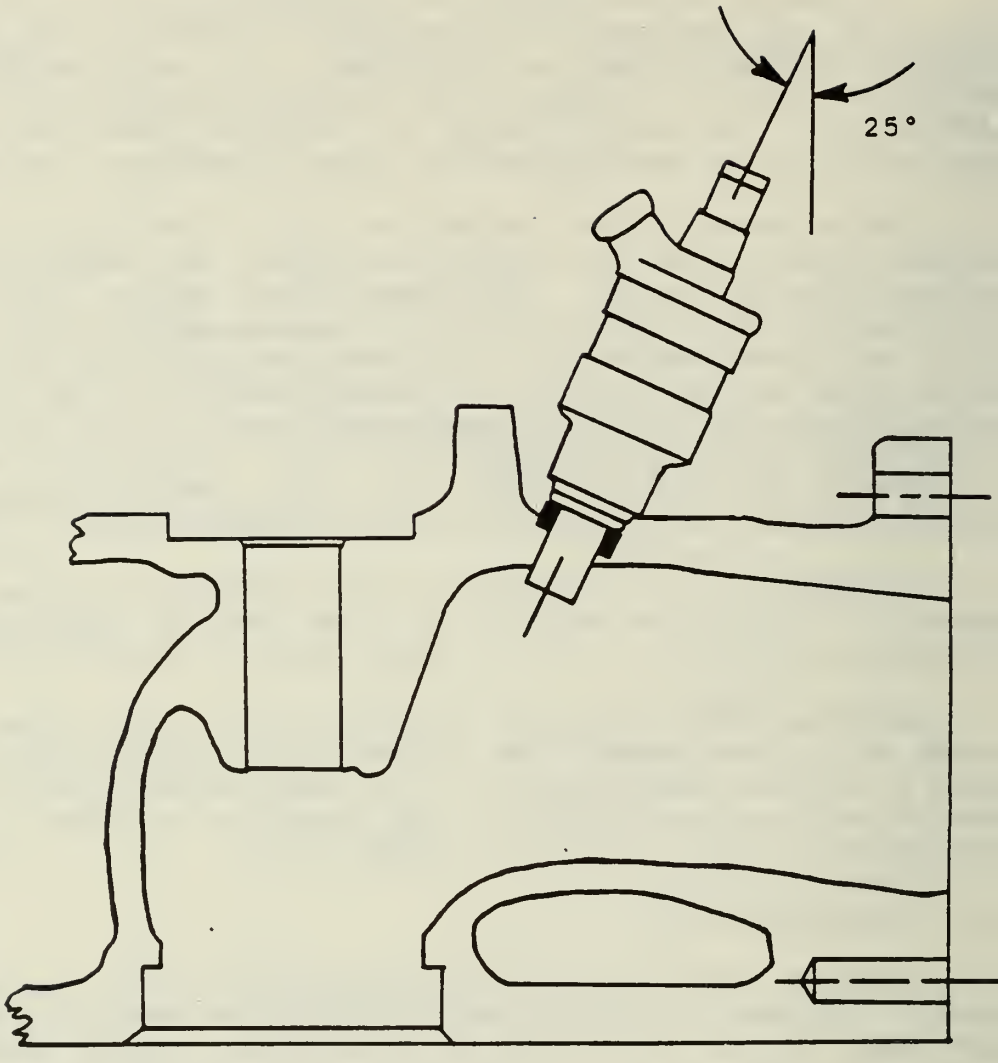

Figure 4. Cross Section of Intake Port With Position of Bendix E-10 Fuel Injector Shown.

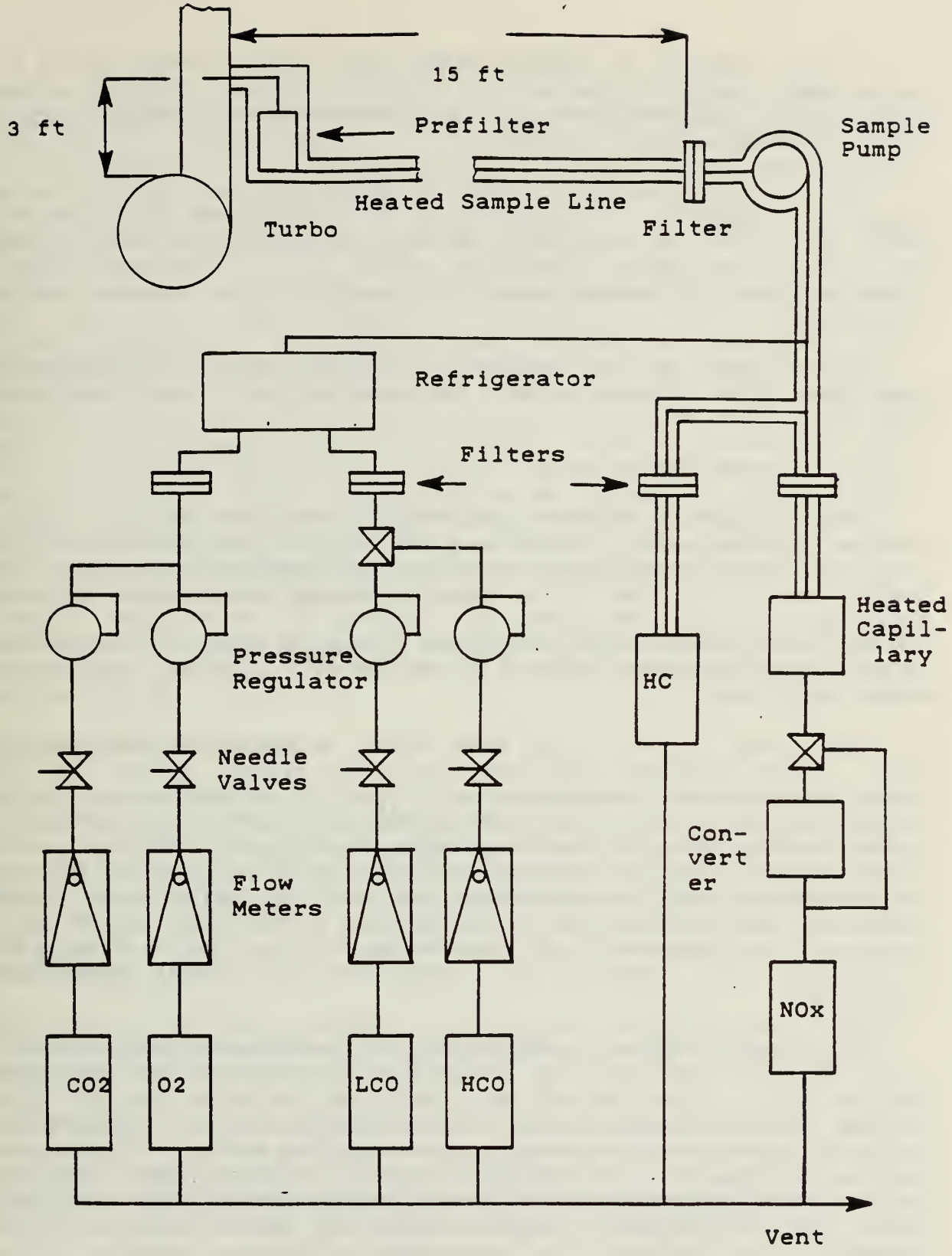

Figure 5. Emissions Sampling System

Exhaust pressure was measured using a well type manometer with a 30 inch range, Model 30eb25 FF from Merium Instrument Company. Manifold and ambient pressures were measured with a pair of calibrated Motorola MPX200A strain gage pressure transducers.

Air flow to the engine was measured through a pair of laminar flow meters connected in parallel. The flow meters were manufactured by Merium and were Models 50 MC2-4SF and 50 MC2-4F. Reading the flow meters from the computer was accomplished through interfacing a pair of D.J. Instruments Model MLR strain gage type differential pressure transducers to the pressure taps on the flow meters.

Smoke samples were drawn through filter papers with a bosch Smoke Sampler Model EFAW 65A/6. The samples were then analyzed with a Bosch smoke analyzer, Model EFAW 68A.

3.4 Experimental Procedure

The experimental procedure consisted of three main sections. The first section included warming up the emission analyzers and their heated sample line, filling the refrigerator bath with ice, checking engine coolant and oil levels (and topping them off as needed), warming up the smoke analyzer, and balancing the charge amplifiers and circuitry for the pressure transducers. The engine was then started and allowed to come to operating temperature. At an oil temperature range of 93 to 98° Celsius the engine was considered to be warmed sufficiently.

The second section of the experimental procedure was the testing section. Engine speed and load were set to the desired values. For alcohol tests the maximum allowable amount of alcohol was determined by substituting ethanol for diesel fuel in small increments until one of two conditions prevailed, either excessive knock or engine misfire and flame out. For the flame-out condition the engine was restarted on diesel fuel and then ethanol was substituted until just less than the substitution rate which caused the flame-out. Engine fueling was always adjusted to duplicate the load and speed points obtained from the diesel baseline tests. Equilibrium of the engine at a particular test condition was assumed when the exhaust temperature had stabilized.

Once equilibrium was established, fuel consumption measurements were taken, wet bulb temperature was measured and cylinder pressure data gathering was initiated. After the fuel measurement was completed, the data gathering program converted emissions data. After emissions data was completed, the exhaust was sampled for smoke using a manual sampling method. all data was then recorded on computer disk for future analysis. Once cylinder data gathering was completed and stored on disk, the engine was changed to the next test condition and the testing procedure was started again after equilibrium was reached.

The third section of the experimental procedure was the shutdown stage where the engine was idled for cooling, heated sample line turned off, filters for emissions analyzers were changed, and general pre-shutdown servicing of the equipment.

4. DATA ACQUISITION SYSTEM

The data acquisition system which was constructed consisted of two computers, an Apple II plus an Apple IIe. both computers were equipped with a Model AI-16 13-channel 12-bit analog-to-digital converter cards manufactured in Interactive Structures Corporation.

4.1 Cylinder Pressure, Injection Pressure and Crank Position

Cylinder pressure and injection line pressure measurements were desired once every crank shaft degree of rotation. To accomplish this, the BEI shaft encoder was interfaced to the Apple II plus such that the 360 pulses per revolution signal triggered an interrupt request on the Apple's central processing unit (CPU). The CPU responded to the interrupt with a machine language program which converted the analog signals representing the cylinder and injection line pressures into digital values. Once the conversions were completed, the interrupt was reset and the CPU waited for the next interrupt or crank angle position signal. The one pulse per revolution signal of the shaft encoder was used to mark top dead center of cylinder number one as a reference for the computer. To reduce the effects of any cycle to cycle variations, 128 cycles were measured consecutively and then averaged giving an "average cycle" for each test condition.

Other data measurements taken with the Apple II plus included the intake manifold pressure, air flow into the engine, ambient pressure, and exhaust pressure (see Fig. 6).

4.2 Emissions and Temperatures

Emission measurements of carbon dioxide, carbon monoxide, nitrogen oxides, unburned hydrocarbons, and oxygen were measured by the Apple IIe through the connection of analyzer output signals to the analog-to-digital conversion card. analyzer range and switch settings had to be entered into the computer manually as did the smoke number and wet bulb temperature. Calibration curves and humidity corrections were programmed into the data gathering program which allowed the emission values to be computed by the computer immediately.

Measurement of the fuel consumption rate was also controlled by the Apple IIe, with interfacing accomplished through the use of a 6522 Versatile Interface Adapter and supporting circuitry.

Various operating temperatures of the engine were interfaced to the Apple IIe and were sampled by the data gathering portion of the program. Exhaust stack, coolant, and intake manifold air temperature were available for monitoring before data gathering began so that steady state conditions could be determined. Chromel-alumel thermocouples and accompanying circuitry provided scaled voltages representing temperature to the analog-to-digital conversion card.

For more information on the data gathering such as frequency and order of measurements, see the program in APPENDIX B.

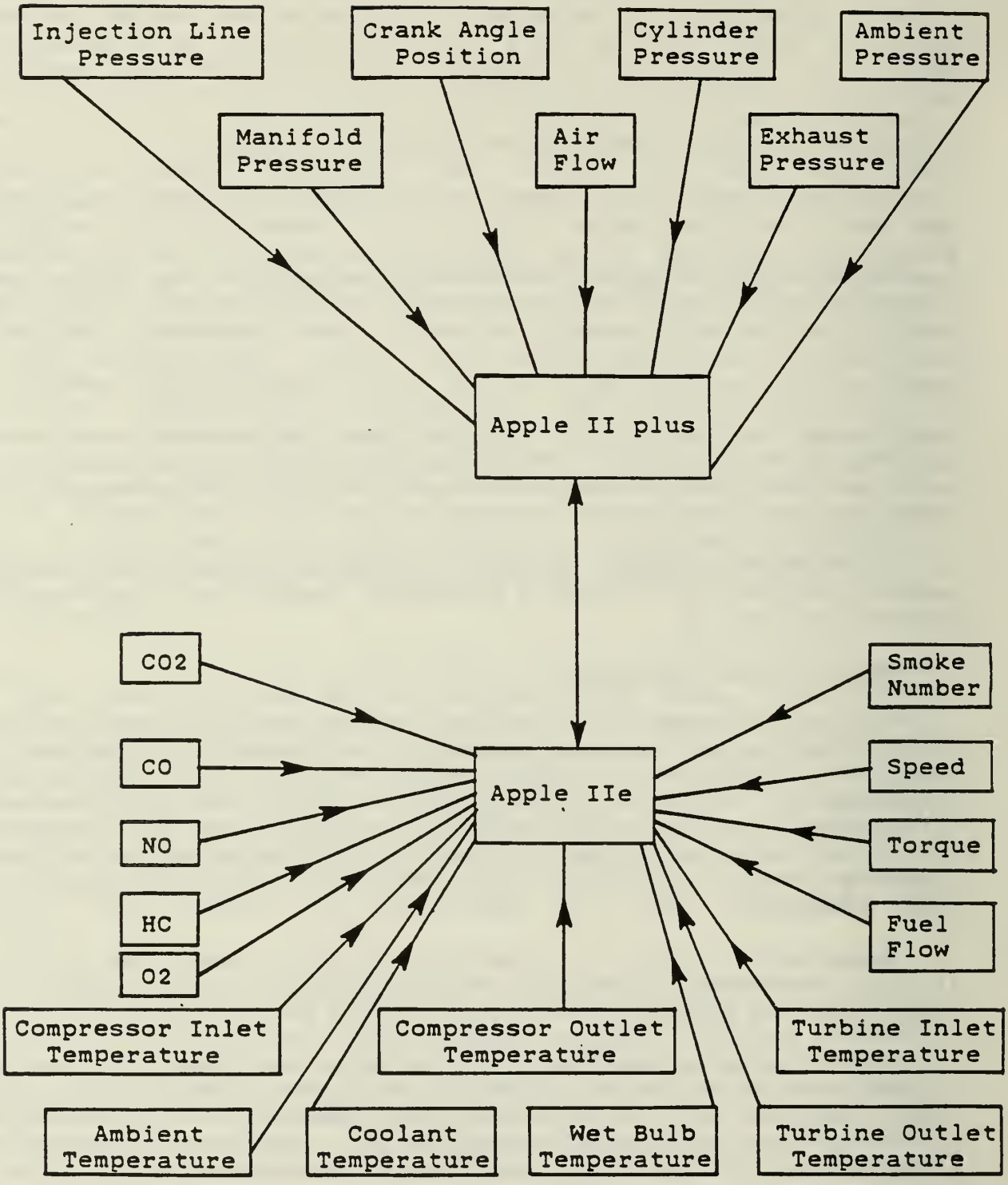

Figure 6. Data Aquisition Flow Chart

5. RESULTS

The testing schedule which was used consisted of engine speeds from 1200 rpm to 2600 rpm in 200 rpm increments, and loads at each speed which were ideal, 20, 40, 60, 80, and 100 percent of full load at each engine speed tested. The test map of 48 points was run using No. 2 diesel fuel as a baseline. The test map was rerun using the ethanol injection system to substitute the maximum amount of energy from ethanol without overfueling or causing excessive pressure rise or knocking. Tabulated data from both the diesel fuel only and the diesel fuel with ethanol tests are presented in APPENDIX A. Performance parameters used to determine the maximum amount of ethanol injection included audible knock, excessive ignition delay, misfire, and varying start of combustion. Factors which determined the maximum ethanol substitution are listed in Table 1.

The three dimensional plotting routine used to generate the surfaces contained in this section required evenly spaced grid coordinate as data inputs. Actual parameters were plotted as a function of brake mean effective pressure (BMEP) for each speed and then curve fitted for even increments of BMEP. The evenly spaced values were plotted using the surface generating program SURFACE which was written by the National Center for Atmospheric Research.

Sufficient capacity of the ethanol injection system was demonstrated by the ability at any test condition which was not limited by knock to fuel the engine with enough ethanol to cause indefinite ignition delay and engine stall. This condition occurred on several occasions until familiarity with the system was attained.

Additional testing series was conducted to investigate the effects of different percentages of ethanol substitution on engine performance parameters. An engine speed of 1800 rpm and load of 250 newton-meters was used to investigate ethanol substitutions of 57.4, 44.8, 31.9, and 19.7 percent. The tabulated data for this test series can also be found in APPENDIX A.

Engine performance parameters which were monitored during both testing series included brake thermal efficiency, brake specific diesel fuel consumption, oxygen, nitrogen oxide, carbon dioxide, carbon monoxide, Bosch smoke number, ignition delay, unburned hydrocarbons, maximum rate of cylinder pressure change, and maximum cylinder pressure. Ignition delay was defined as the number of crank angle degrees between the beginning of fuel injection and the increase in rate of pressure change, as shown in Fig. 7.

5.1 Maximum Ethanol Substitution

The maximum rate of fuel energy substitution from ethanol for the test map is shown in Fig. 8. The largest substitution rates occurred at medium speeds and no load conditions with ethanol supplying greater than 70 percent of the fuel energy at some test points. The fuel energy substitution rate by ethanol decreases for each engine speed as BMEP increases. The decrease in tolerable ethanol percentage as load increases is opposite to the trends noted by Shropshire and Goering [24] using a naturally aspirated engine, and reflects the trends resulting from a turbocharged diesel engine which were reported by Chen, et al. [20]. Energy substitution rates at low loads for all

Table 1

Factor Limiting Maximum Ethanol Substitution

	% Maximum Load at Each Speed					
RPM	0	20	40	60	80	100
1200	EID	M	AK, M	AK	AK	AK
1400	EID, M	EID, M	AK, M	AK	AK	AK
1600	EID, M	EID, M	VSC, AK	AK	AK	AK
1800	M	EID, M	M, AK	M, AK	AK	AK
2000	EID	EID, VSC	EID, AK	AK	AK	AK
2200	EID, M	EID, M	M, VSC	AK	AK	AK
2400	EID, M	EID, M	EID, M	AK	AK	AK
2600	M	M	M	M, AK	AK	AK

EID= EXCESSIVE IGNITION DELAY AK= AUDIBLE KNOCK

M= MISFIRE VSC= VARYING START OF COMBUSTION

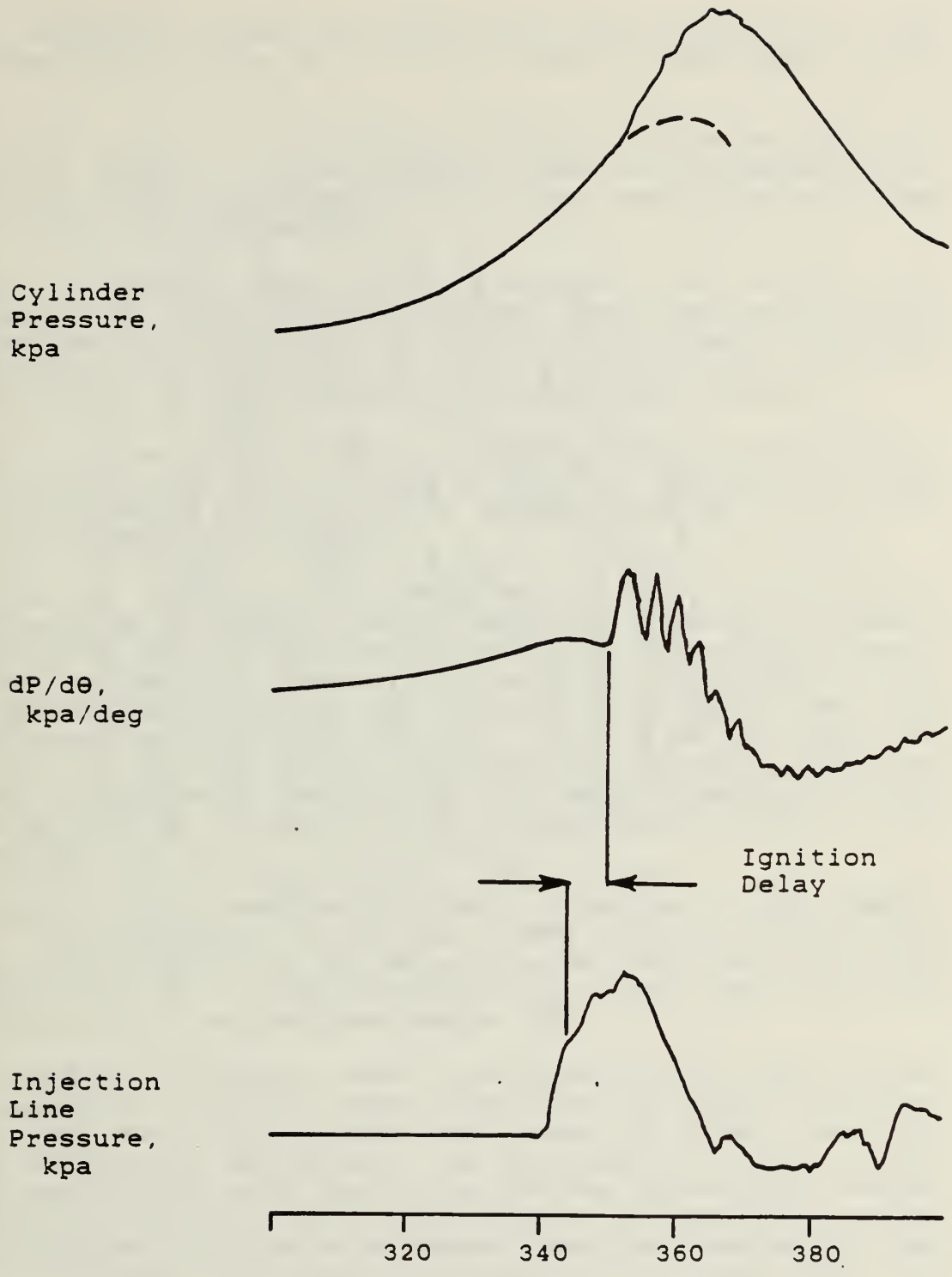

Figure 7. Cylinder Pressure, Rate of Pressure Change, and Injection Line Pressure.

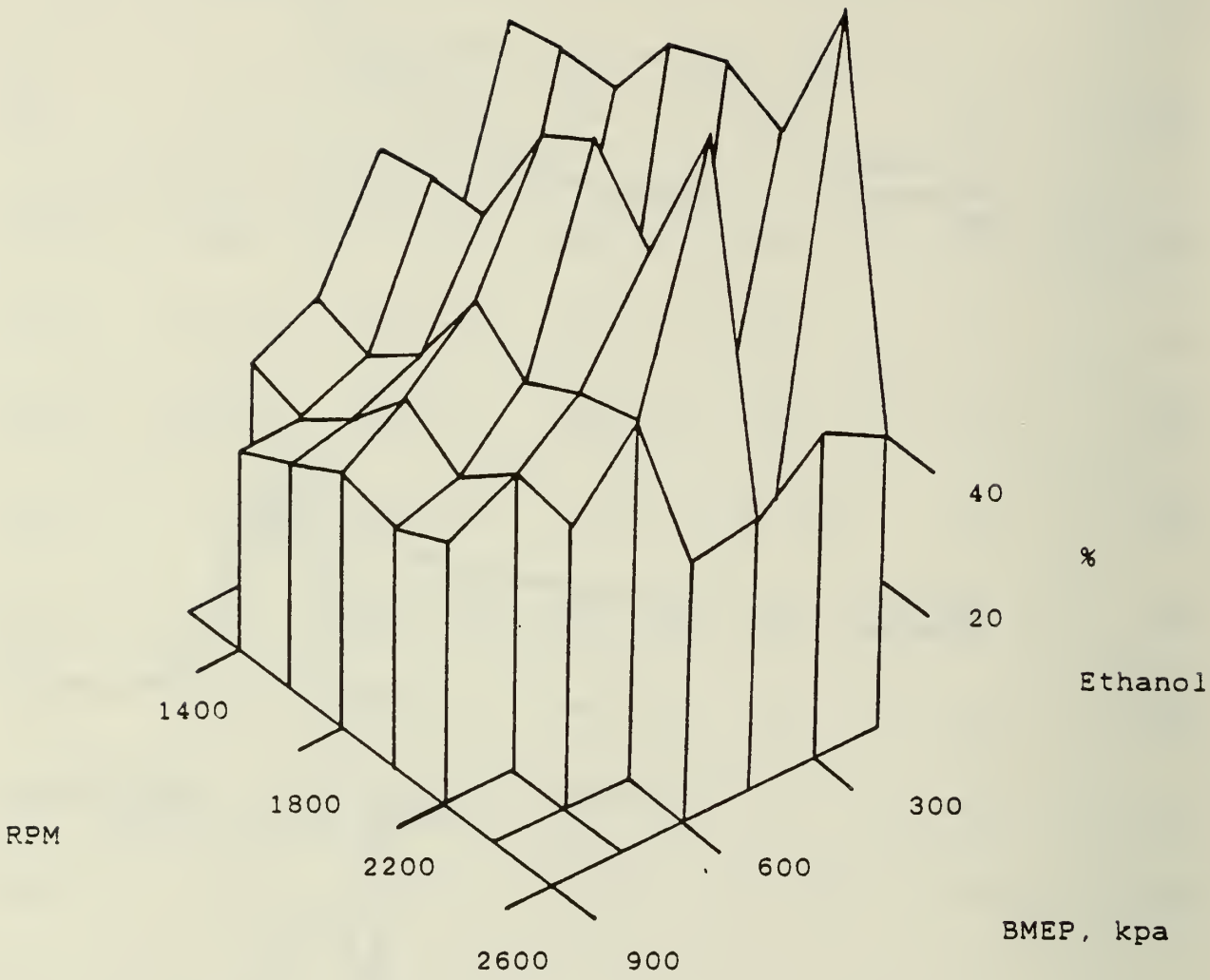

Figure 8. Percentage of Energy from Ethanol vs. Brake Mean Effective Pressure and Speed

speeds were considerably larger than those reported by Chen, et al. [20] indicating significant differences in the performance of the ethanol fueling system.

Brake specific diesel fuel consumption (BSDFC) is shown in Fig. 9 for diesel fuel only, and Fig. 10 shows BSDFC for diesel fuel and ethanol fueling. The scaling for these two figures was the same, emphasizing further the reductions in diesel fuel consumption.

A comparison of brake thermal efficiency for diesel fuel only (Fig. 11) with the brake thermal efficiency for the ethanol with diesel fuel (Fig. 12) indicates increased efficiency with ethanol fueling at high loads, and the low load conditions show efficiencies below those for diesel fuel only. The scaling for both plots are the same allowing direct comparison of the two.

A comparison of the plots of ignition delay show that the ignition delays for diesel fuel with ethanol (Fig. 13) were larger at all test conditions than the ignition delays may be attributed to the lower effective certain rating of the diesel fuel and ethanol combination.

In addition to increasing the resulting ignition delay, ethanol fueling lowered the combustion efficiency. Carbon monoxide and unburned hydrocarbons are byproducts which retain chemical energy that was not converted to thermal energy during the combustion process. The unburned hydrocarbons for the diesel fuel and ethanol combination (Fig. 15) were considerably higher than those for the diesel fuel only tests (Fig. 16). The scale for the diesel fuel and ethanol plot is one tenth that of the diesel fuel only plot, indicating that unburned hydrocarbons for some conditions of ethanol fueling are up to ten times larger than the hydrocarbons which remained unburned when the fuel is diesel fuel only.

The scales for the carbon monoxide plots are the same for both fueling test plots. High BMEP values at all speeds have similar carbon monoxide measurements for both fuels, but the carbon monoxide levels for diesel fuel and ethanol fueling (Fig. 17) were considerably higher than those for diesel fuel only (Fig. 18) at all engine speeds and low BMEP.

Carbon dioxide is a byproduct which is considered to be a result of complete fuel combustion. Levels of carbon dioxide for the diesel and ethanol fueling (Fig. 19) were slightly lower than those for diesel fuel only (Fig. 20) at the low BMEP test points. The lower levels of carbon dioxide with elevated emissions of carbon monoxide and unburned hydrocarbons indicate that the combustion efficiency, or the completeness of the combustion reaction was adversely effected by the use of the ethanol-diesel fuel combination. The lowered effective certain rating may be the cause of the lowered combustion efficiency.

A comparison of the oxygen levels in the exhaust for diesel fuel with ethanol fueling (Fig. 21) and diesel fuel only (Fig. 22) is inconclusive. Oxygen levels for the same BMEP values at different speeds for each fueling method indicate a zero offset for the meter which was not constant. The oxygen measuring device did not maintain a consistent calibration. A varied amount of offset makes trends between engine speeds impossible to detect and a comparison between fueling methods useless for this parameter.

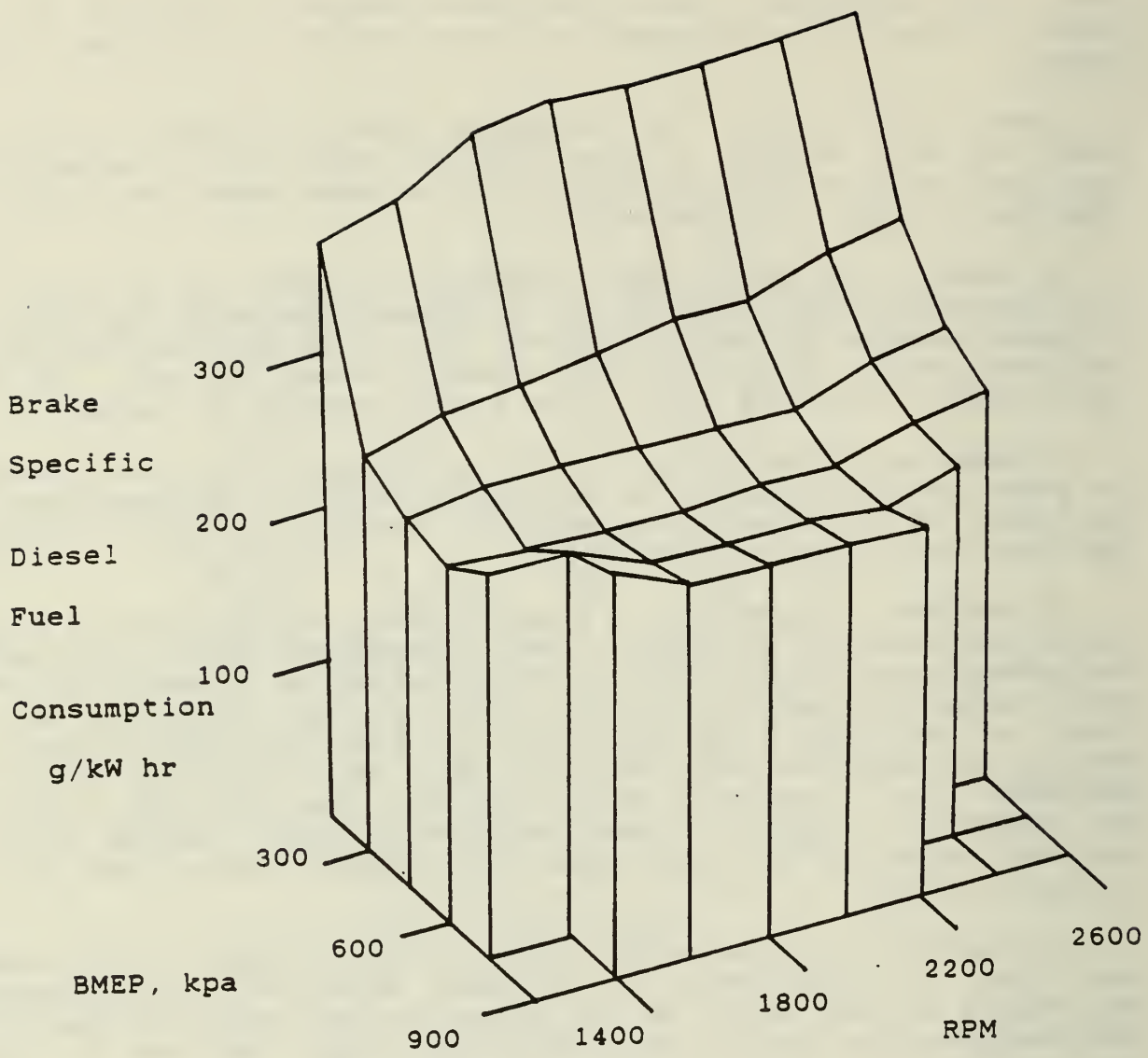

Figure 9. Brake Specific Diesel Fuel Consumption vs. Brake Mean Effective Pressure and Speed for Diesel Fuel Only.

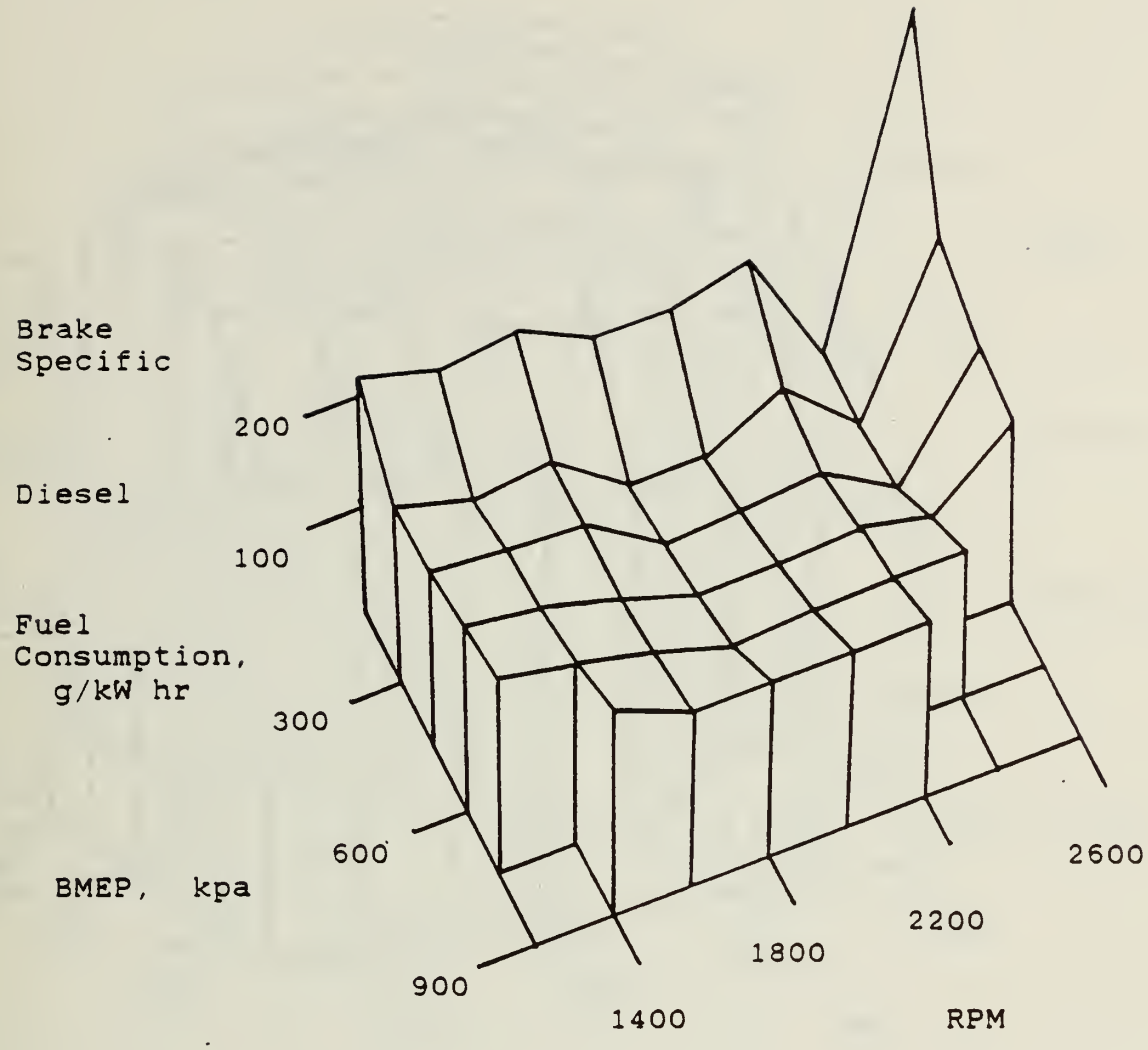

Figure 10. Brake Specific Diesel Fuel Consumption vs. Brake Mean Effective Pressure and Speed for Diesel Fuel and Ethanol.

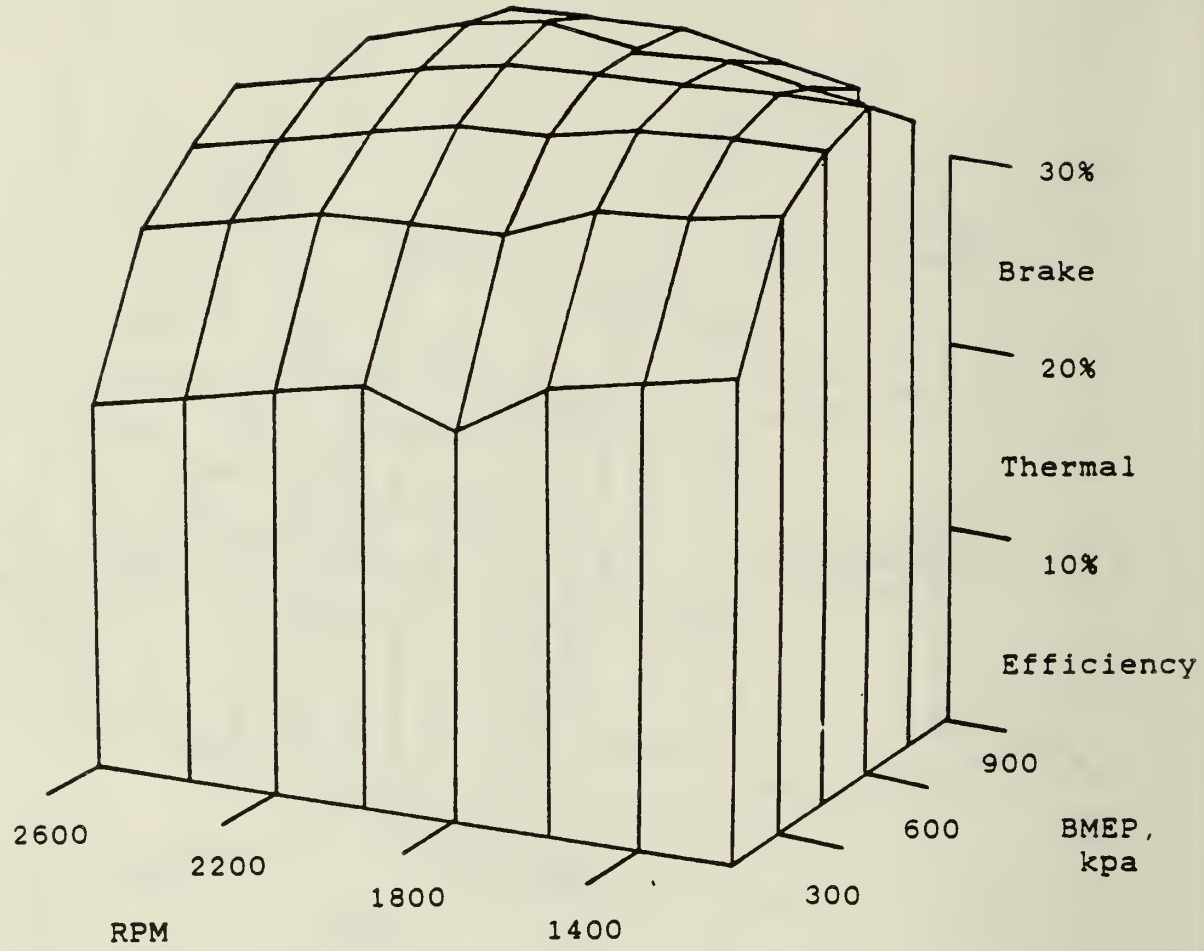

Figure 11. Brake Thermal Efficiency vs. Brake Mean Effective Pressure and Speed for Diesel Fuel Only

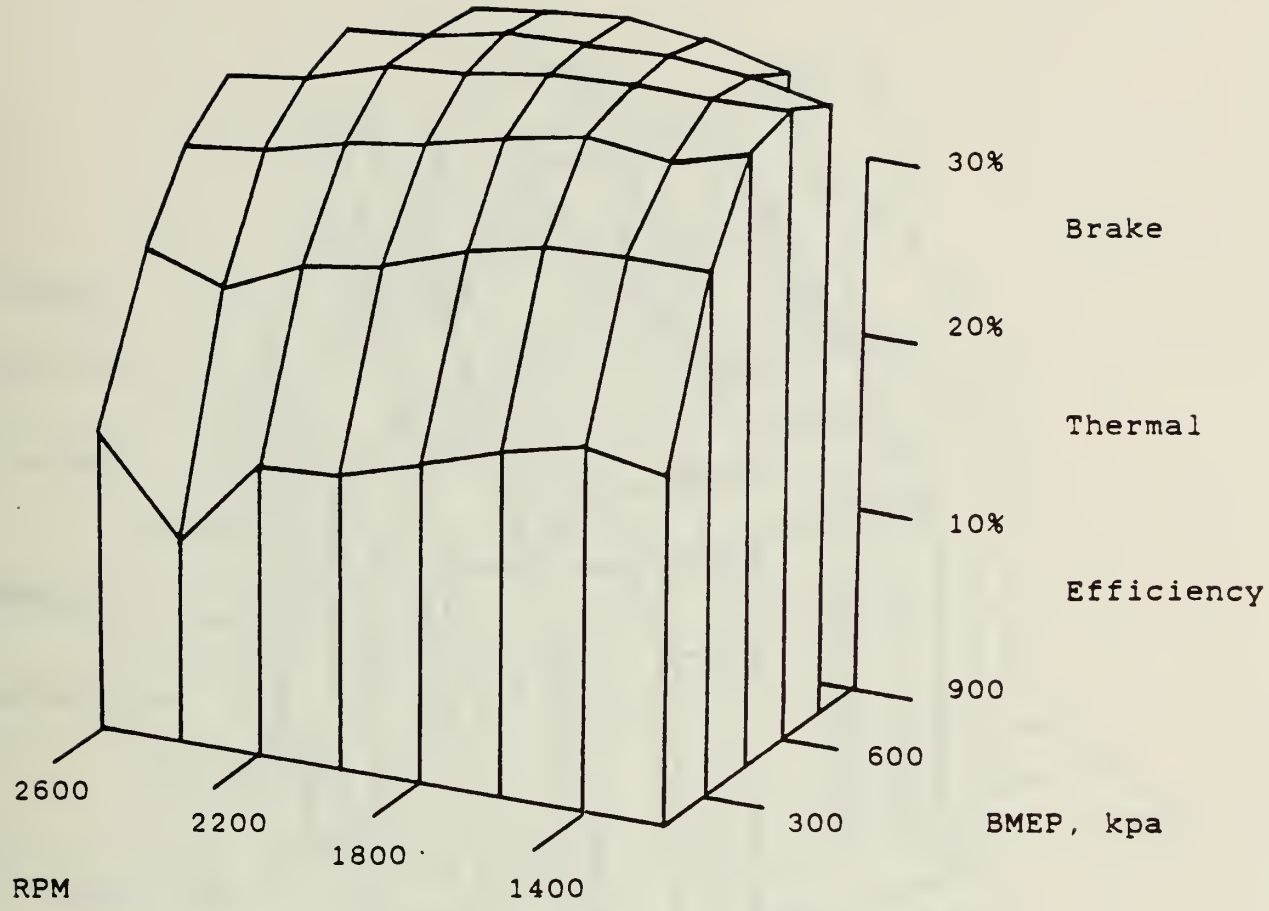

Figure 12. Brake Thermal Efficiency vs. Brake Mean Effective Pressure and Speed for Diesel Fuel and Ethanol

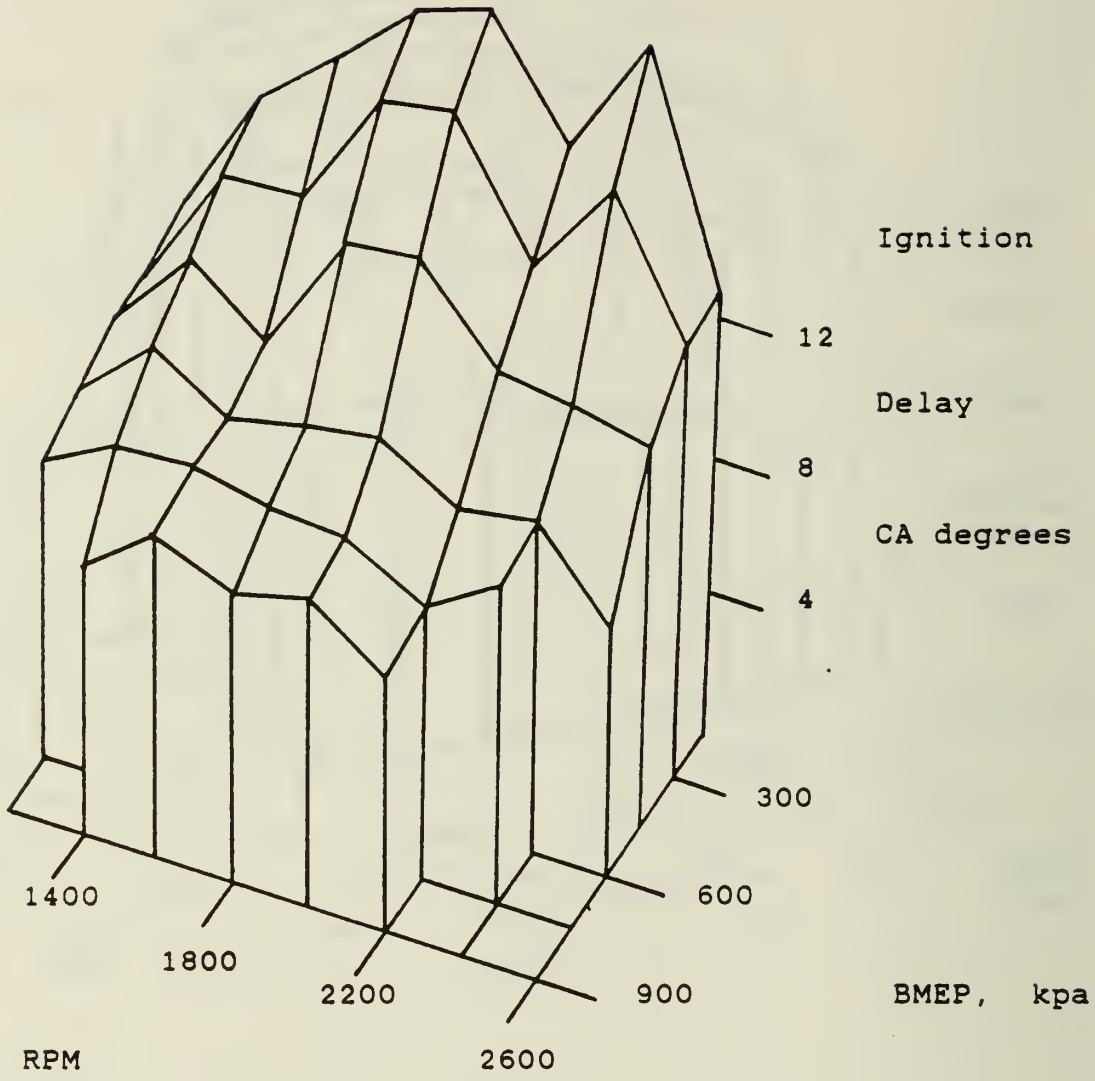

Figure 13. Ignition Delay vs. Brake Mean Effective Pressure and Speed for Diesel Fuel and Ethanol

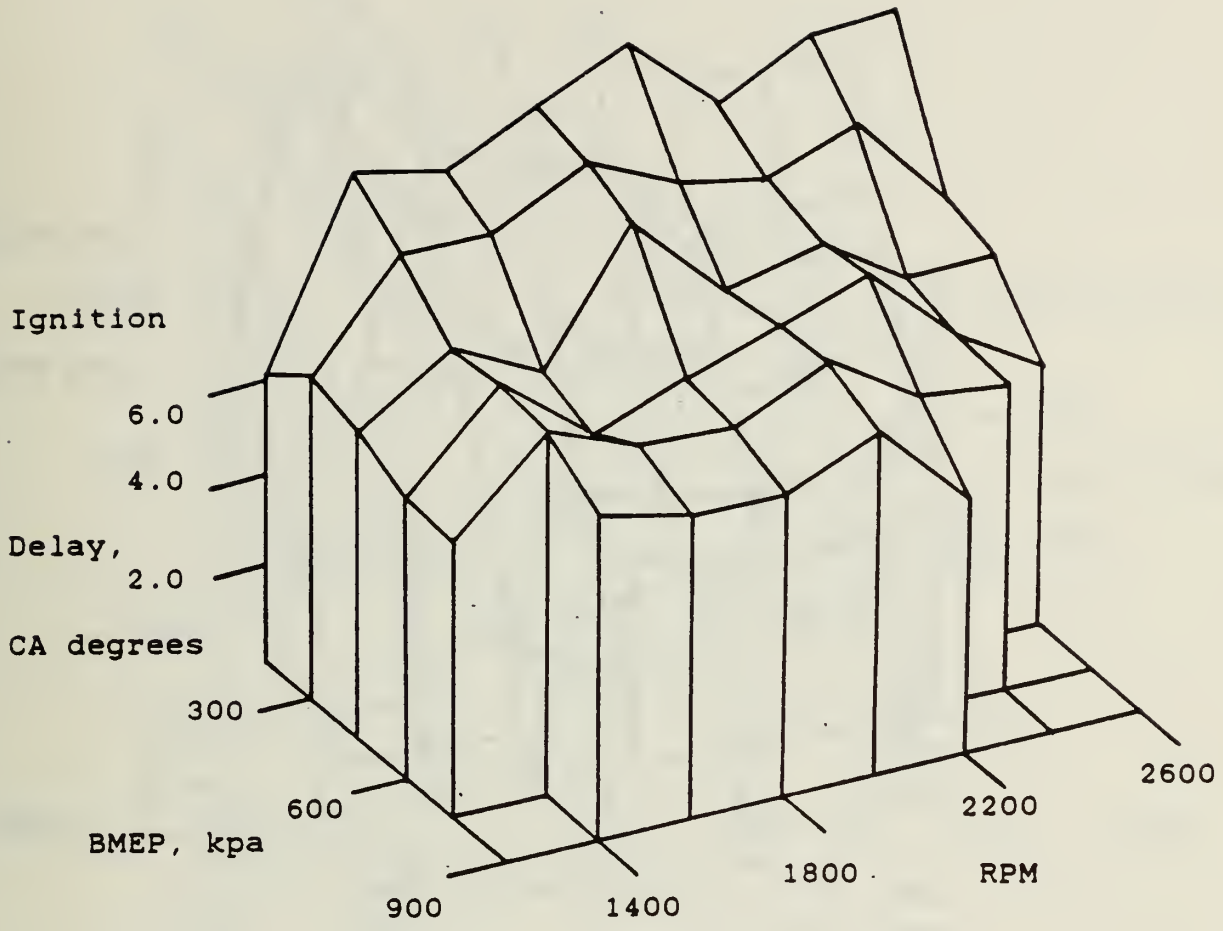

Figure 14. Ignition Delay vs. Brake Mean Effective Pressure and Speed for Diesel Fuel Only.

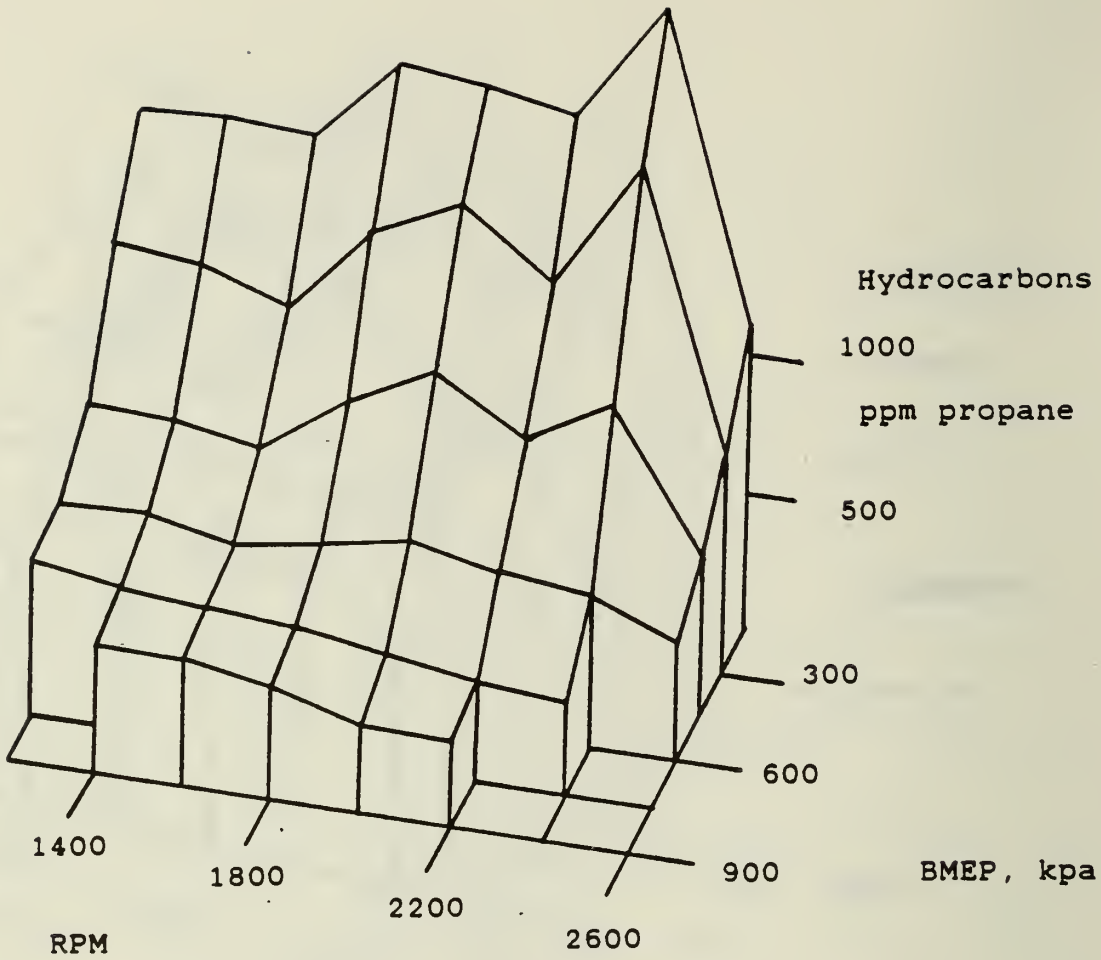

Figure 15. Hydrocarbon Emissions vs. Brake Mean Effective Pressure and Speed for Diesel Fuel and Ethanol

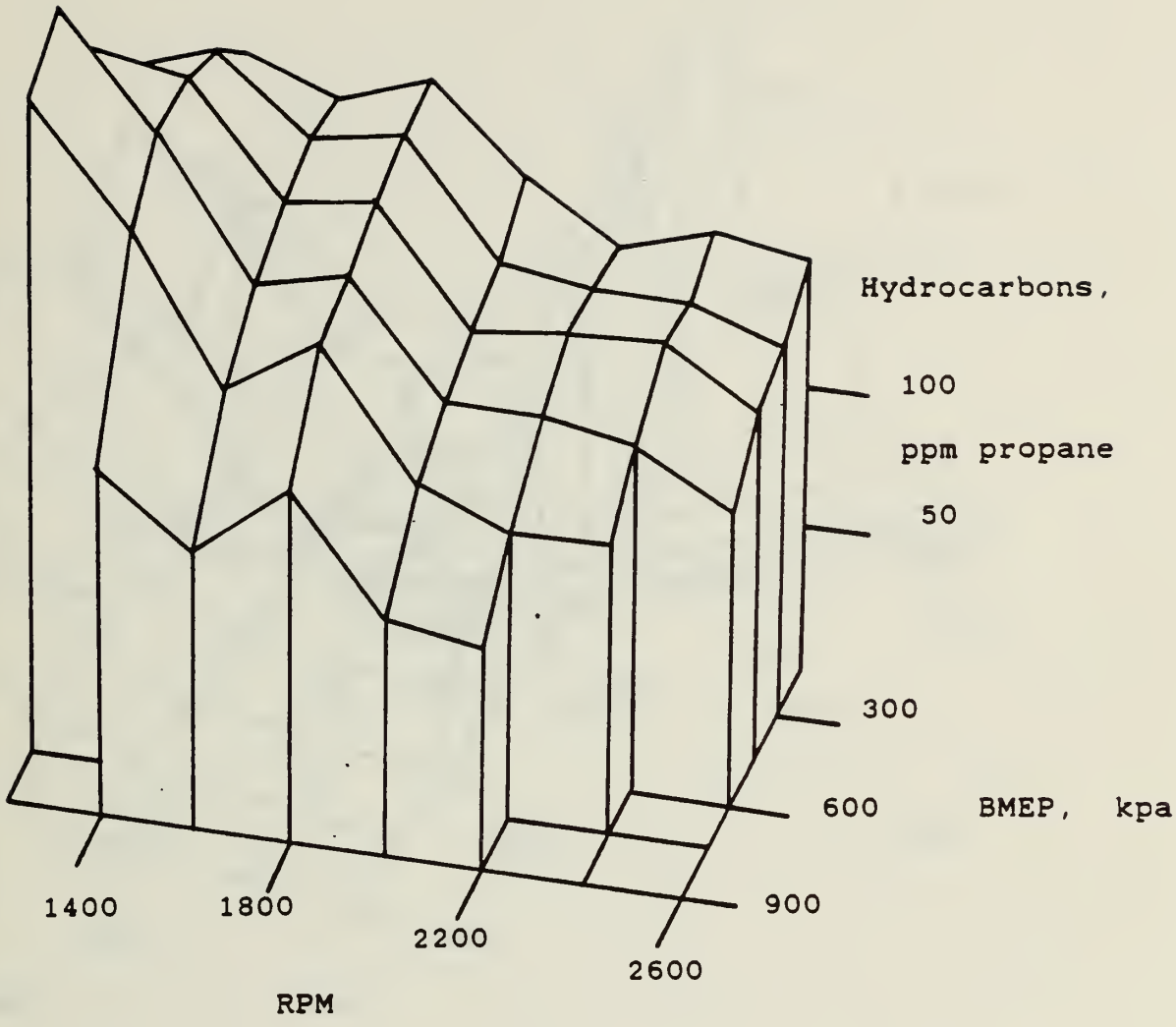

Figure 16. Hydrocarbon Emissions vs. Brake Mean Effective Pressure and Speed for Diesel Fuel Only

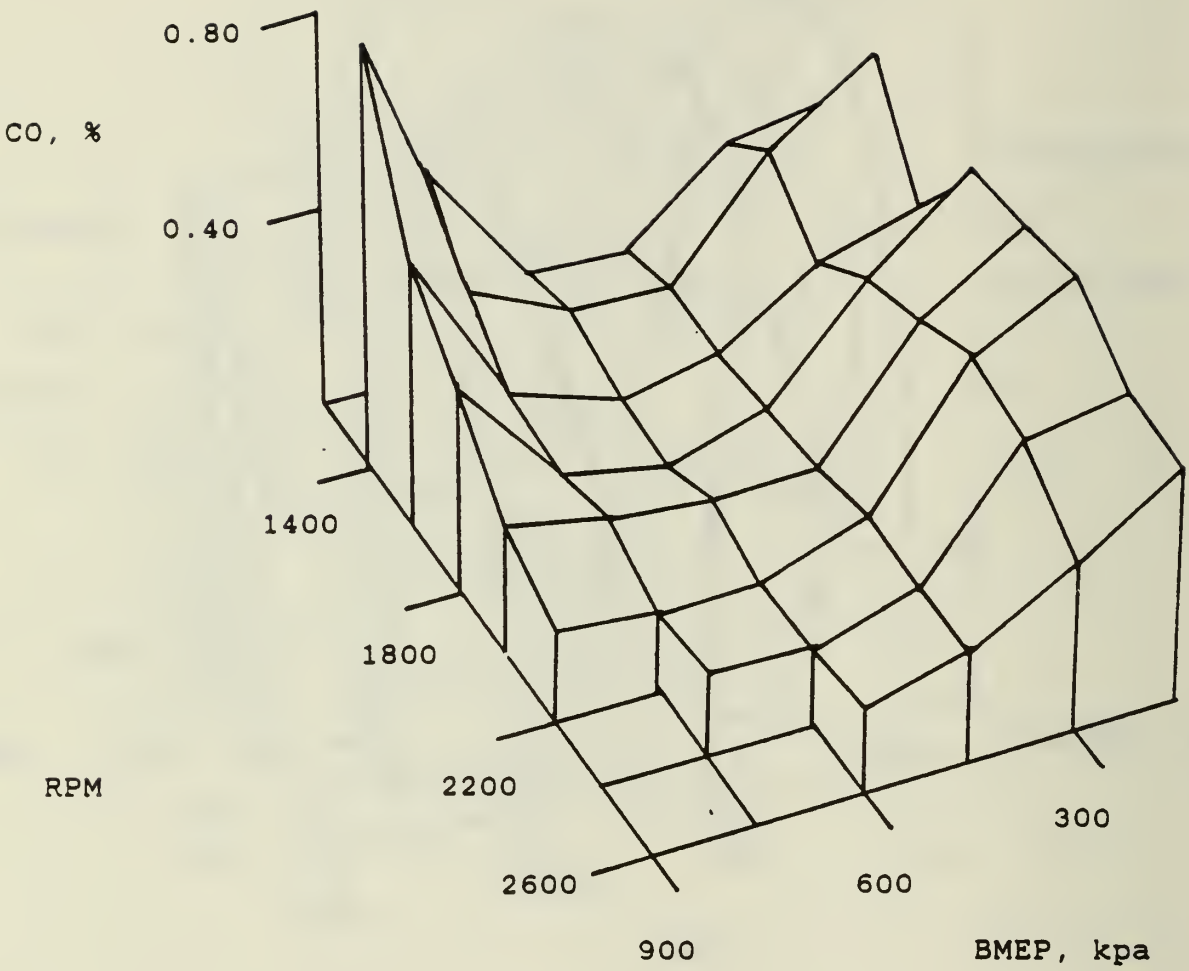

Figure 17. Carbon Monoxide Emissions vs. Brake Mean Effective Pressure and Speed for Diesel Fuel and Ethanol

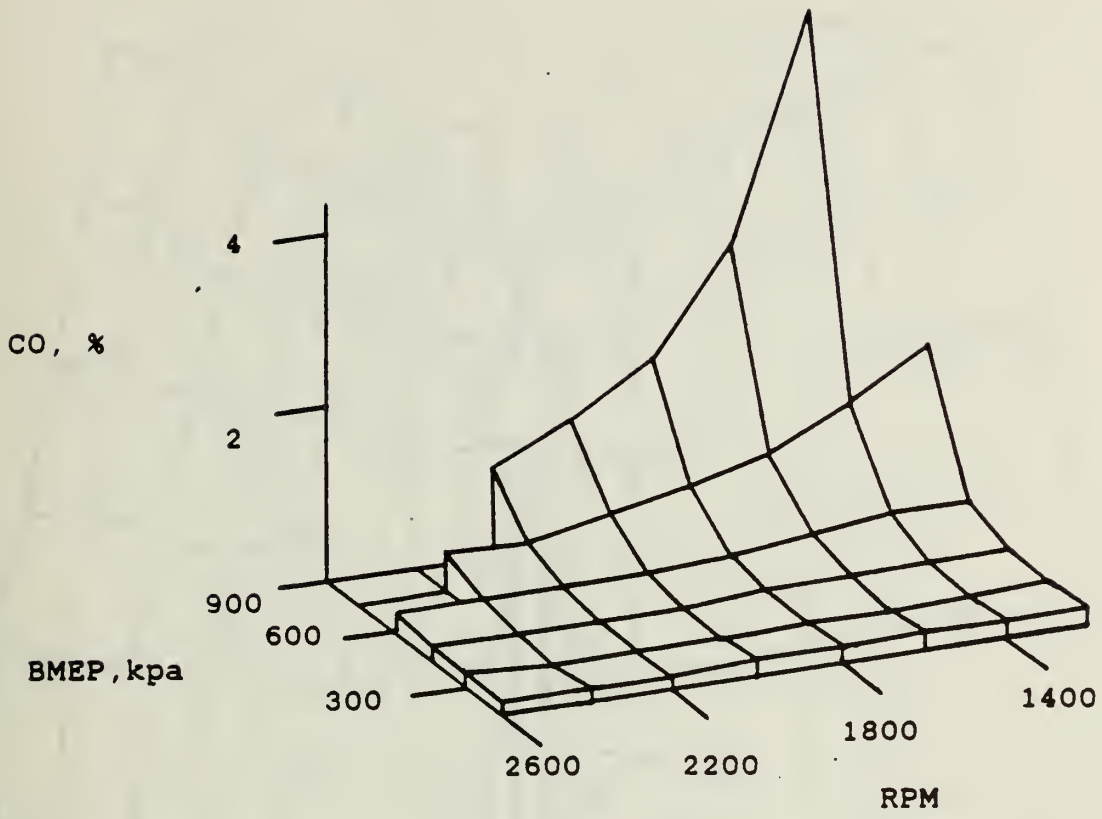

Figure 18. Carbon Monoxide Emissions vs. Brake Mean Effective Pressure and Speed for Diesel Fuel Only

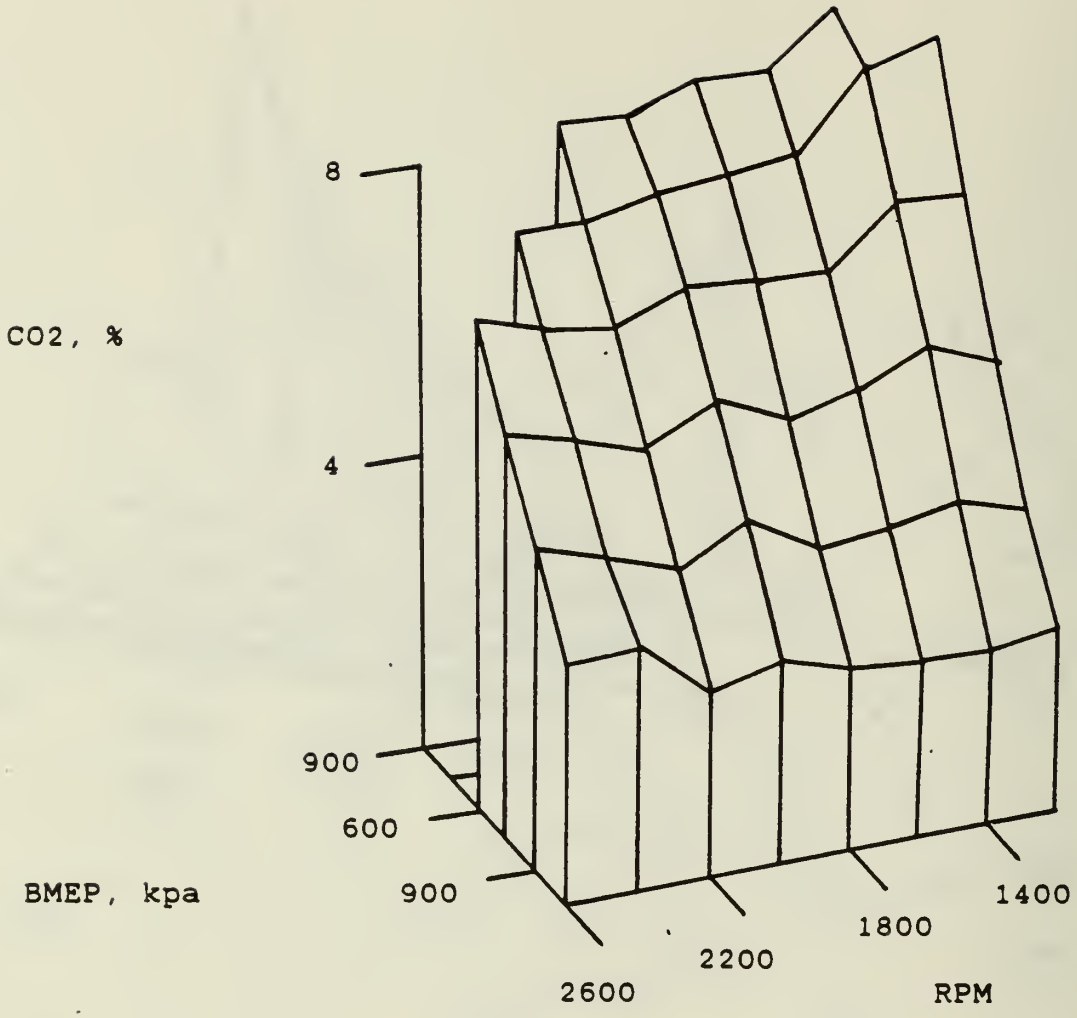

Figure 19. Carbon Dioxide Emissions vs. Brake Mean Effective Pressure and Speed for Diesel Fuel and Ethanol

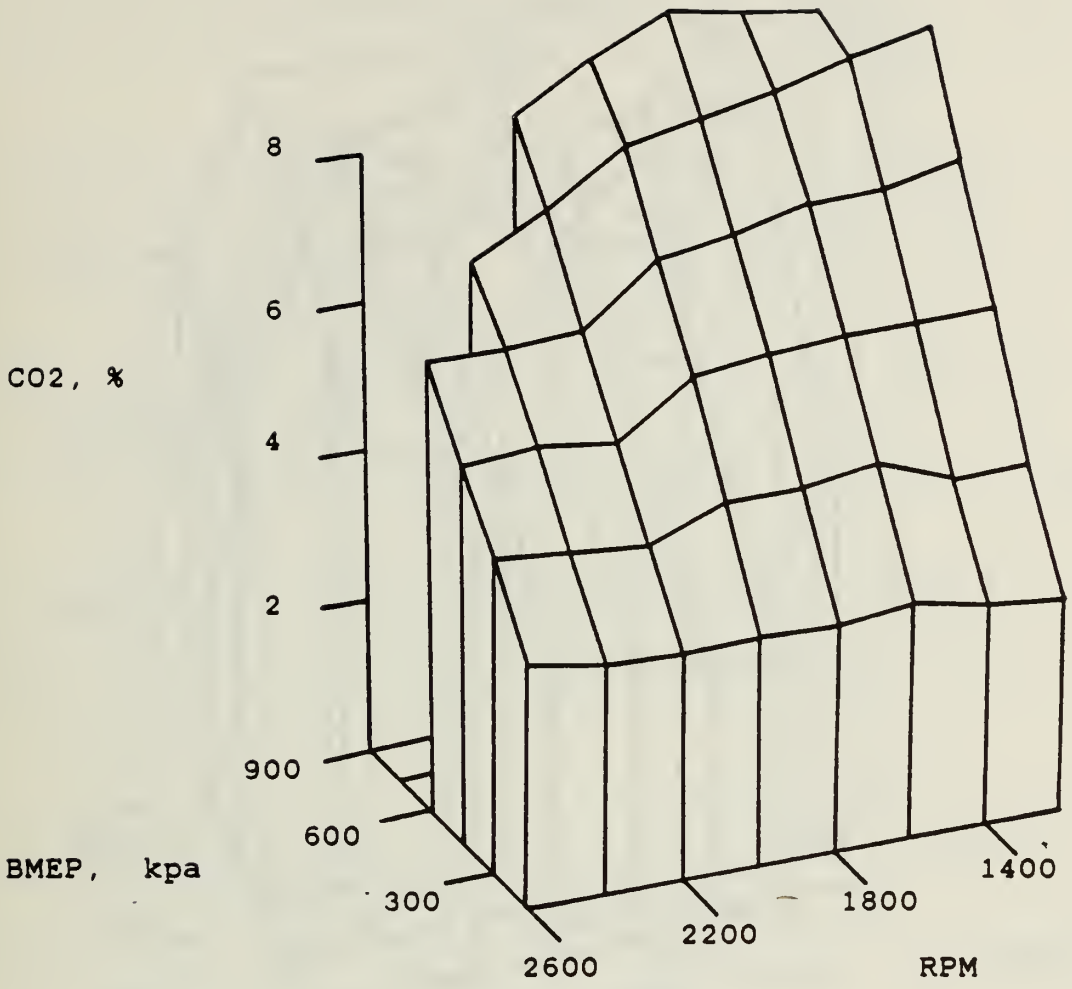

Figure 20. Carbon Dioxide Emissions vs. Brake Mean Effective Pressure and Speed for Diesel Fuel Only

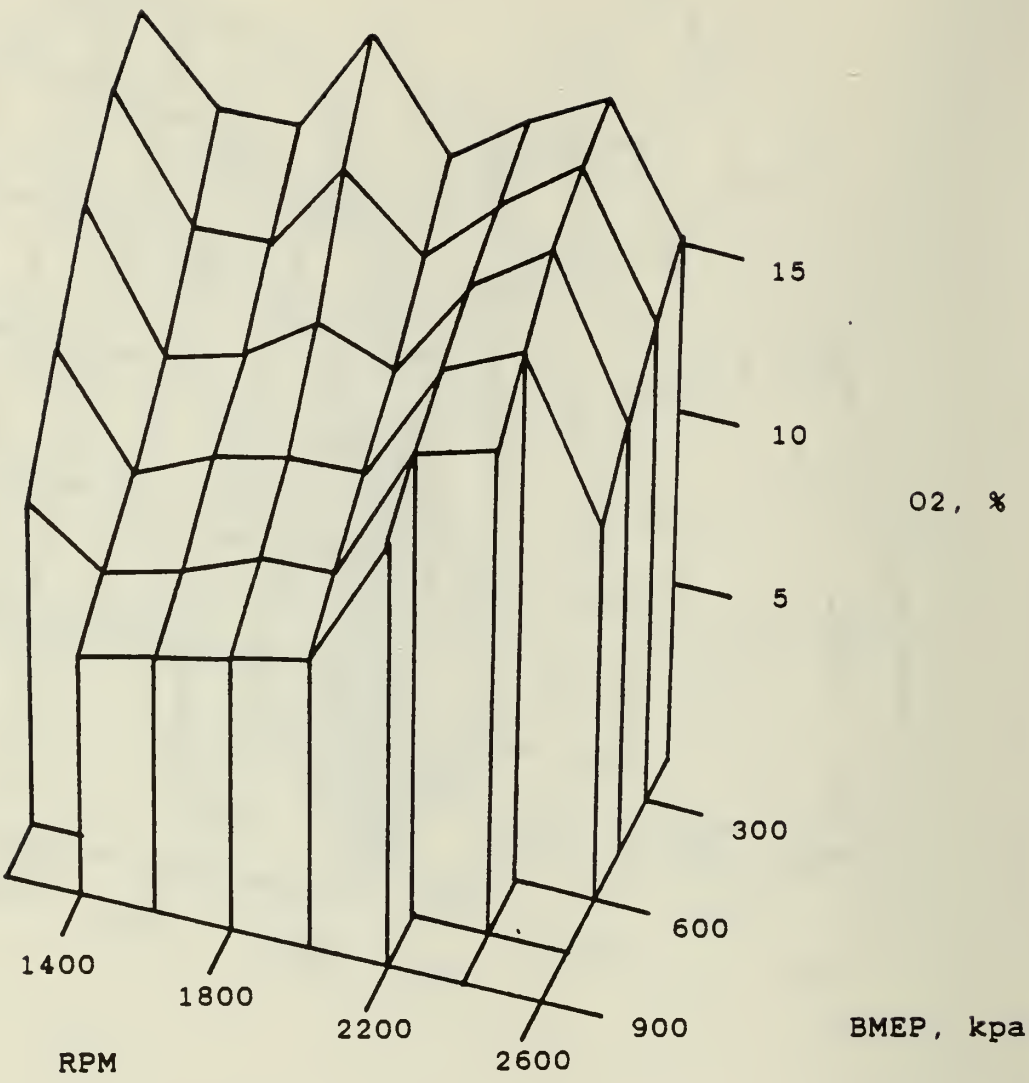

Figure 21. Oxygen Emissions vs. Brake Mean Effective Pressure and Speed for Diesel Fuel and Ethanol

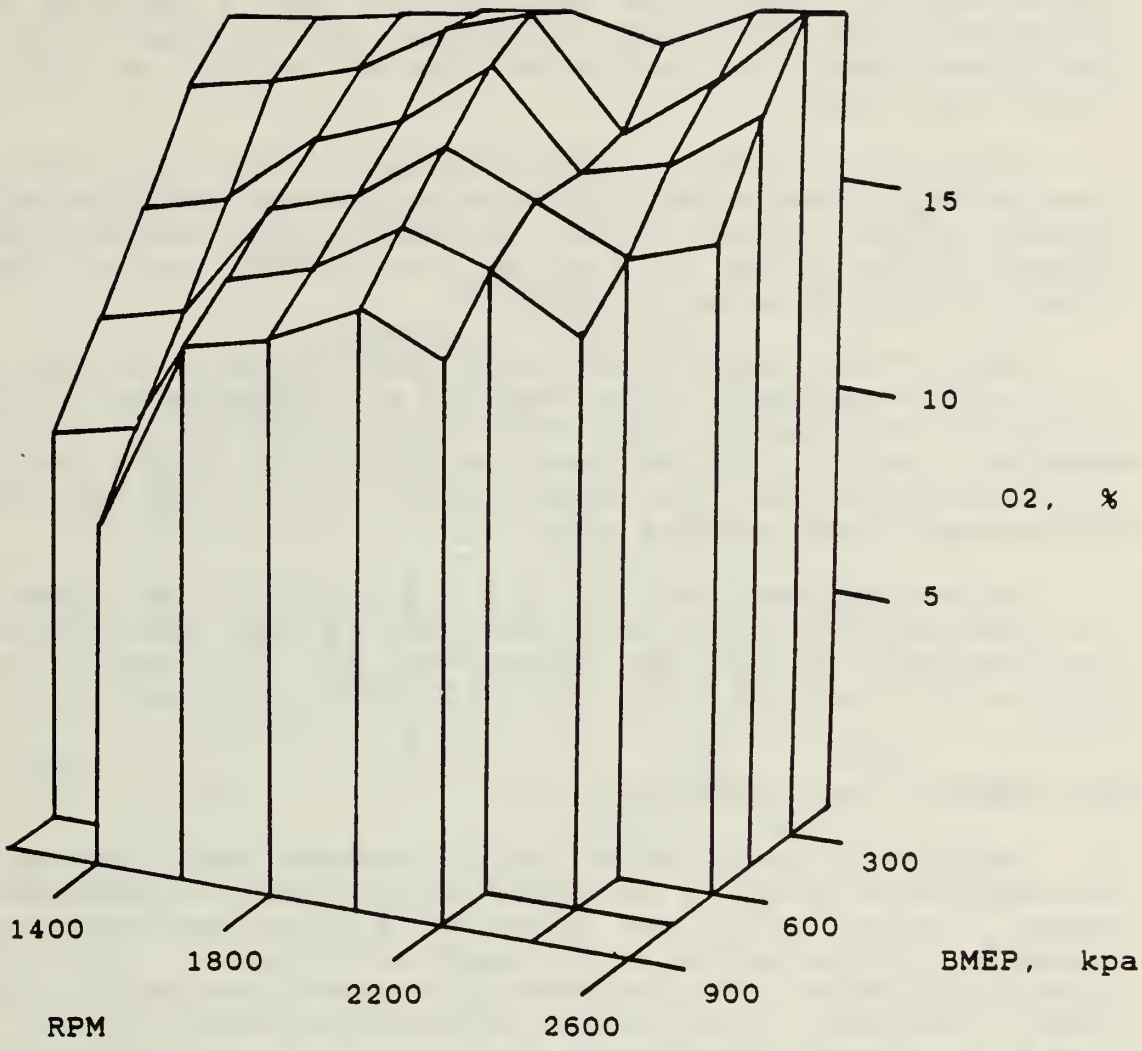

Figure 22. Oxygen Emissions vs. Brake Mean Effective Pressure and Speed for Diesel Fuel Only

The maximum rate of change for cylinder pressure per crank angle was effected to a large extent by the use of the ethanol-diesel fuel combination. Scaling for the plots are the same and allow direct comparison of the two fueling methods. Diesel fuel only (Fig. 23) shows a peak rate of change at medium BMEP values and a speed of 1800 rpm, while the peak rate of change for the ethanol-diesel fuel combination (Fig. 24) occurred at high BMEP and a higher engine speed.

The plots of maximum cylinder pressure for both fueling methods have the same scaling and show slight differences between the two fueling methods. The maximum cylinder pressure values for ethanol-diesel fueling (Fig. 25) were slightly higher at high BMEP, and lower at low BMEP than the values for the diesel only fueling method (Fig. 26).

peak cylinder pressure is directly related to peak cylinder temperature which is a driving force in the formation of nitrogen oxides. Nitrogen oxide levels for the ethanol-diesel fueling method (Fig. 27) were higher at high BMEP and lower at low BMEP than levels for the diesel fuel only tests (Fig. 28). These levels correspond to those expected from the examination of the maximum cylinder pressure plots.

The measured smoke levels for all test points with the ethanol and diesel fuel combination (Fig. 29) were lower than the Bosch smoke numbers recorded for the diesel fuel only test points (Fig. 30). This trend is in agreement with the smoke emission levels reported by other researchers utilizing ethanol fuel.

5.2 Varied Ethanol Percentages

Testing with various percentages of the input energy supplied by ethanol was conducted to determine the effects on performance and note any trends observed. Figures 31, 32, and 33 show the plots of performance and emission parameters for the varying ethanol substitution rates. Ignition delay, unburned hydrocarbons, and carbon monoxide increased considerably with increased ethanol percentage. Brake thermal efficiency increased slightly, while maximum cylinder pressure and carbon dioxide remained relatively unchanged as the percentage of the ethanol increased. Maximum rate of pressure change, nitrogen oxides, Bosch smoke number, and brake specific diesel fuel consumption decreased significantly as the percentage of ethanol increased. No conclusion was drawn from the oxygen data due to the previously suspected offset error.

Examination of the curves indicate that there is not ideal percentage of ethanol substitution when considering all performance and emission parameters. Ethanol percentages which yielded low nitrogen oxides and smoke emissions also yielded high unburned hydrocarbons and carbon monoxide emissions. The optimal percentage of ethanol substitution to be used is clearly a decision based upon a trade-off of which levels of each type of emission are the most tolerable.

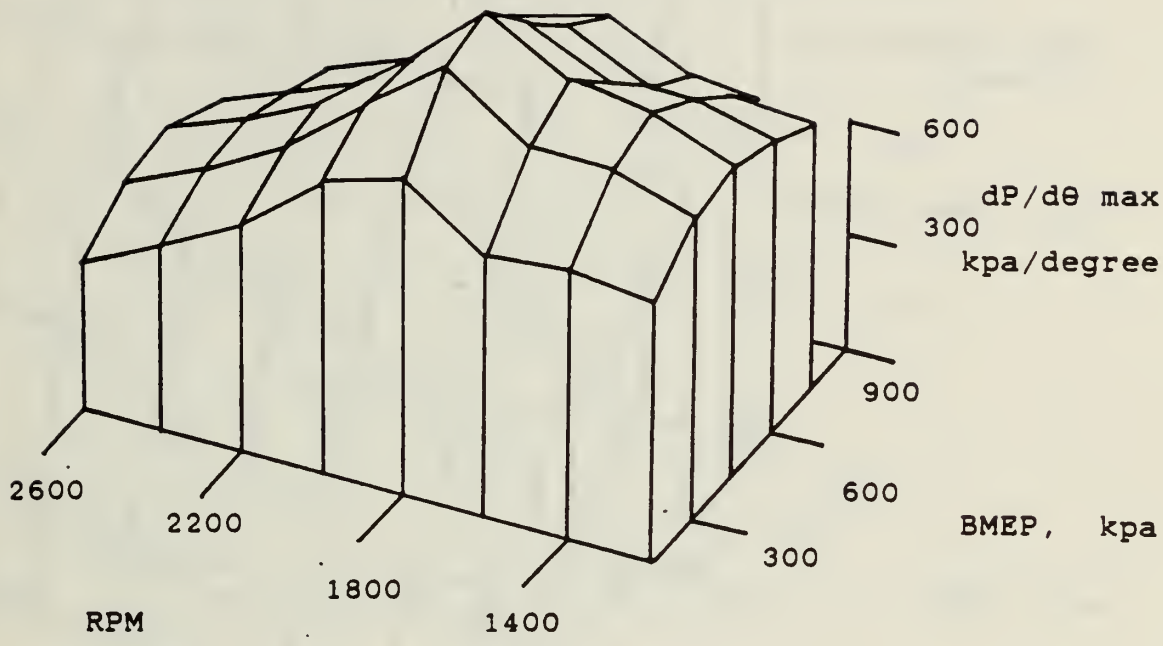

Figure 23. Maximum Rate of Cylinder Pressure Change vs. Brake Mean Effective Pressure and Speed for Diesel Fuel Only

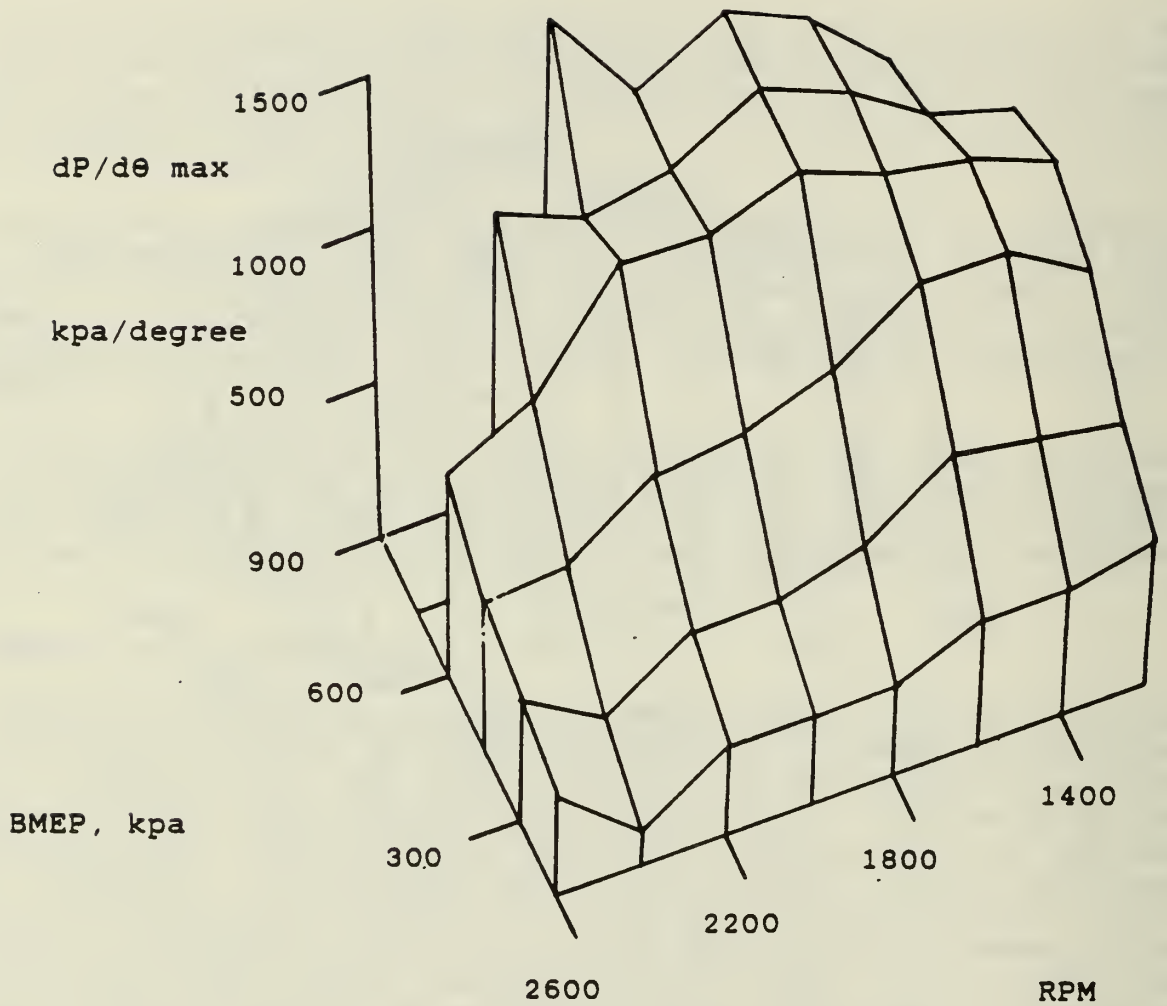

Figure 24. Maximum Rate of Cylinder Pressure Change vs. Brake Mean Effective Pressure and Speed for Diesel Fuel and Ethanol

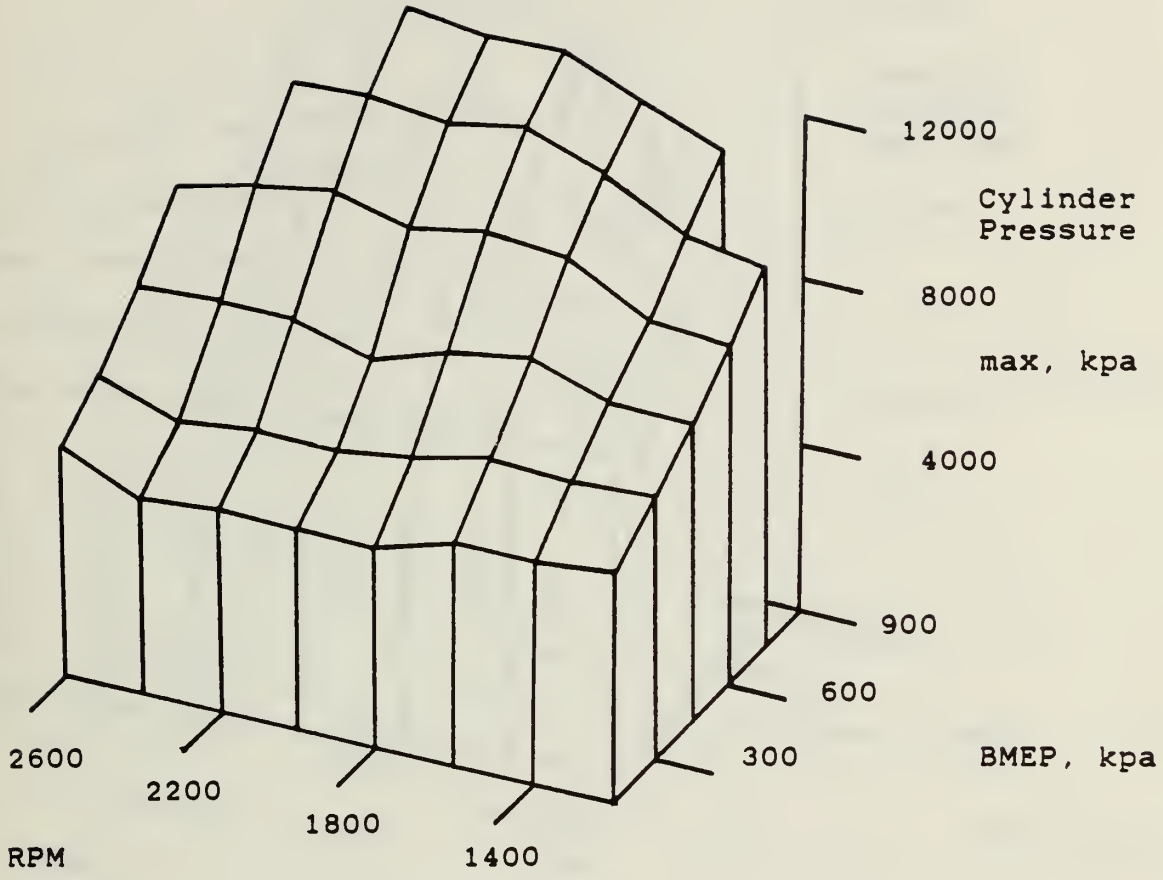

Figure 25. Maximum Cylinder Pressure vs. Brake Mean Effective Pressure and Speed for Diesel Fuel and Ethanol

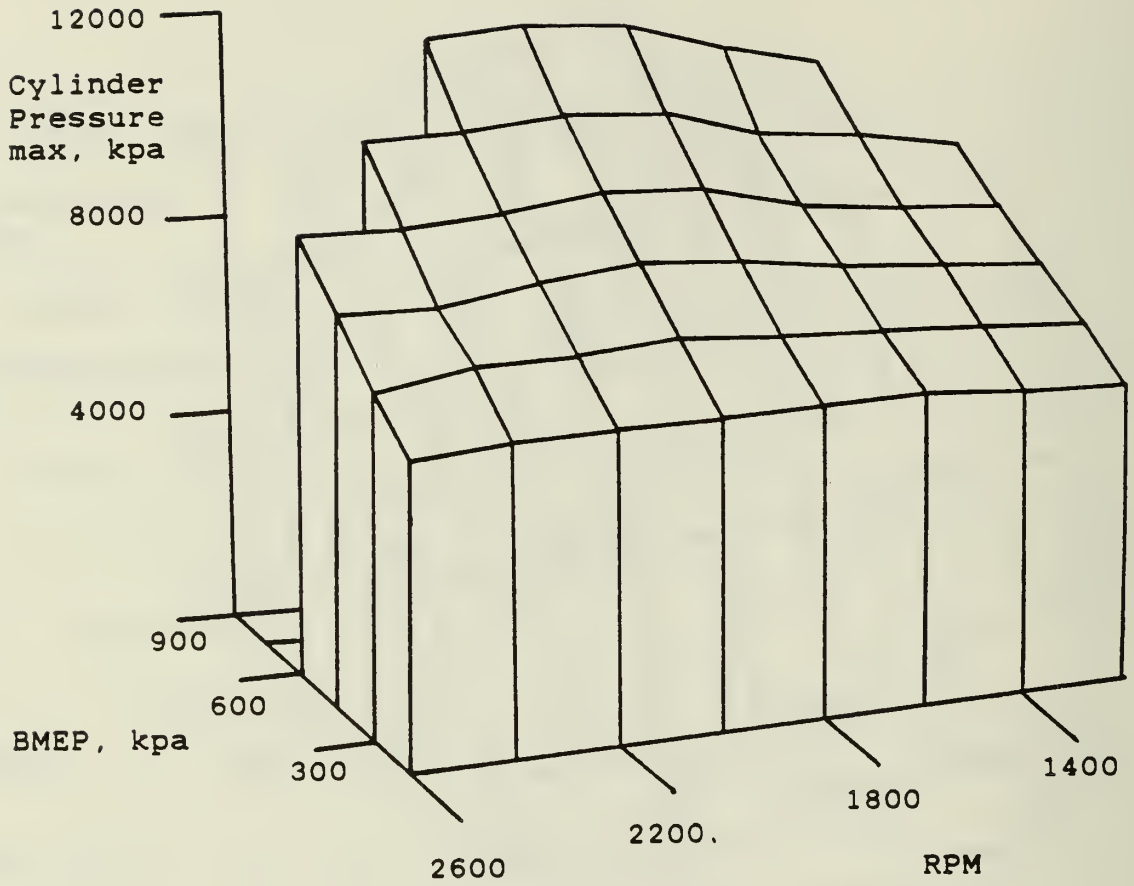

Figure 26. Maximum Cylinder Pressure vs. Brake Mean Effective Pressure and Speed for Diesel Fuel Only

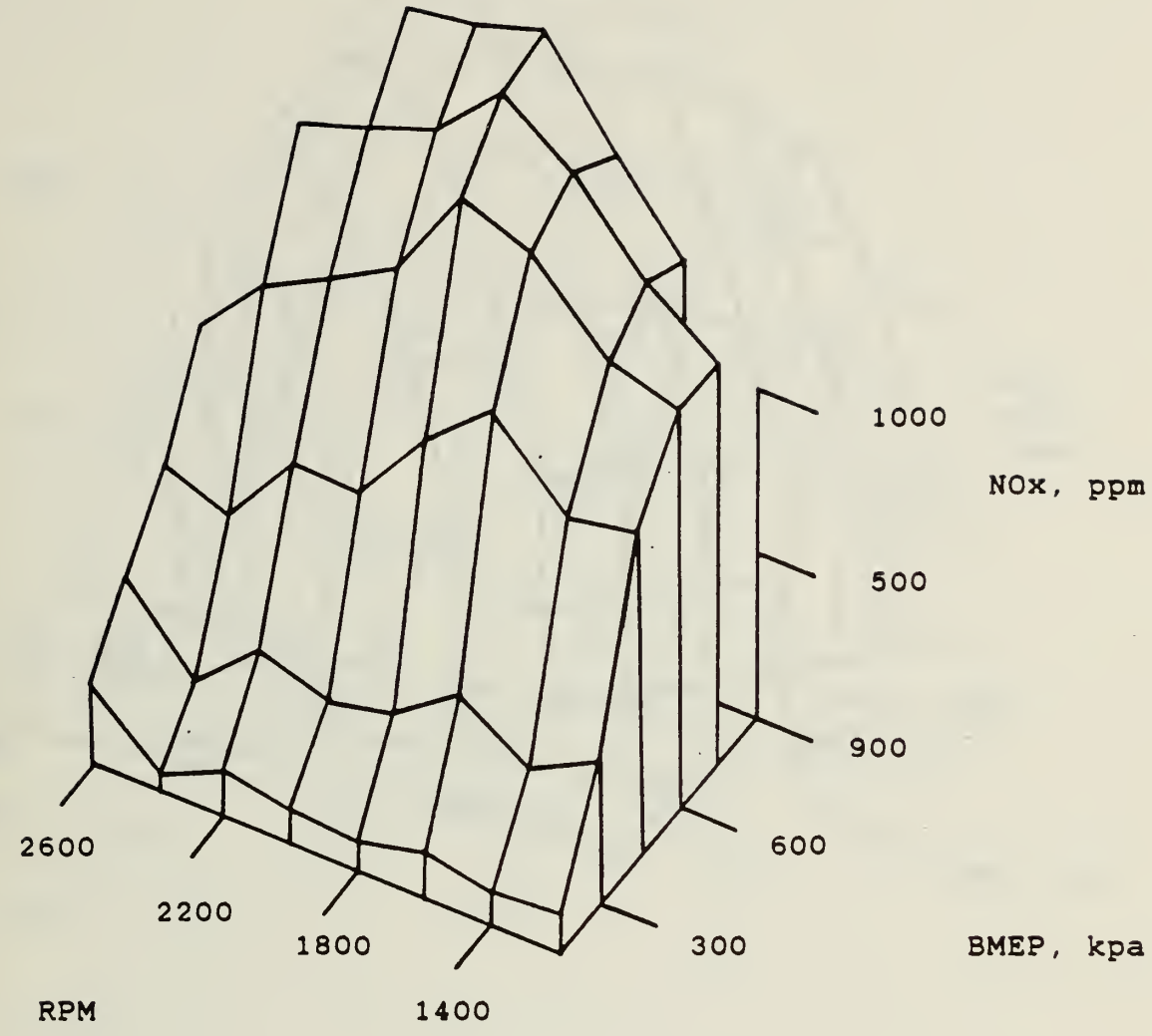

Figure 27. Nitrogen Oxide Emissions vs. Brake Mean Effective Pressure and Speed for Diesel Fuel and Ethanol

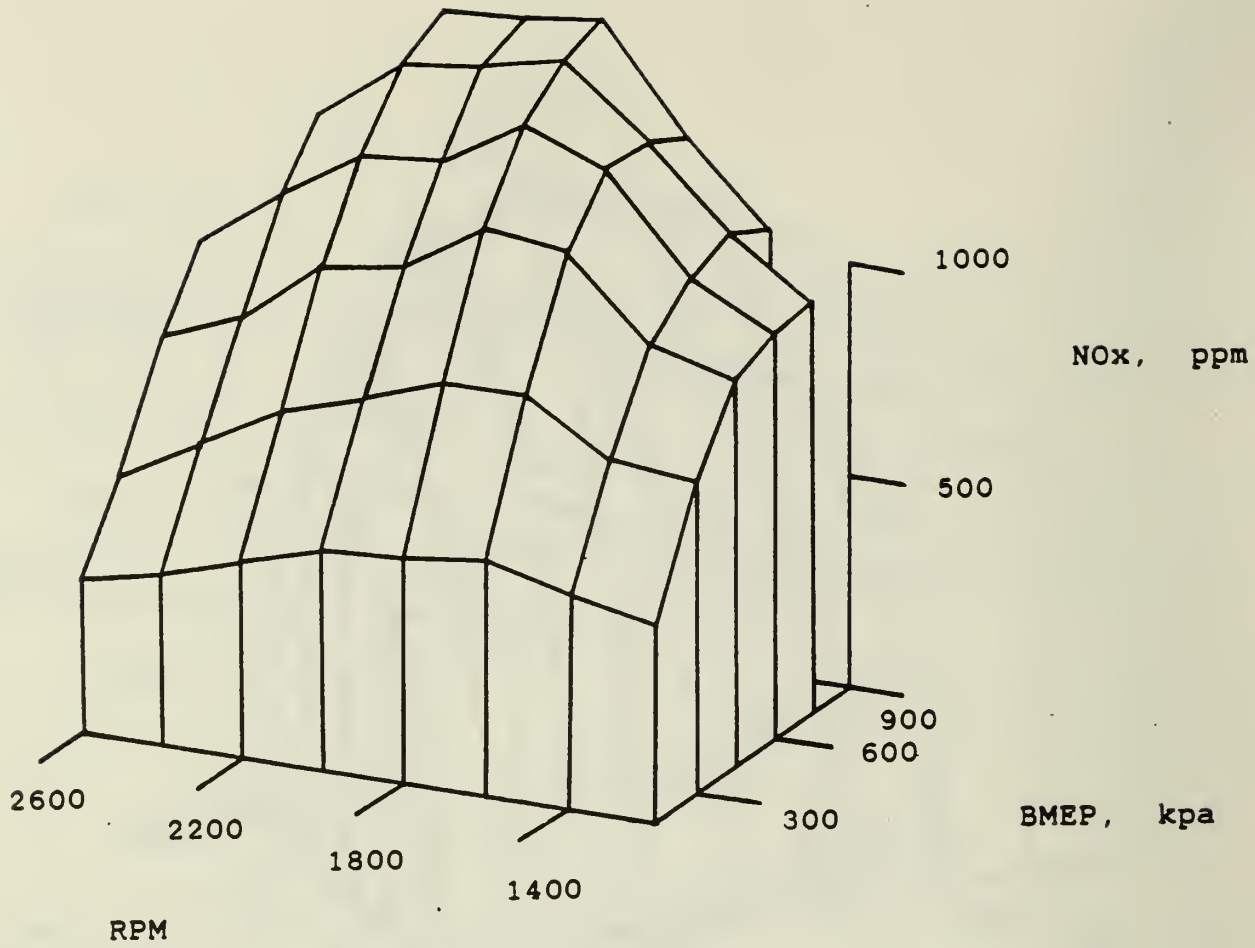

Figure 28. Nitrogen Oxide Emissions vs. Brake Mean Effective Pressure and Speed for Diesel Fuel Only

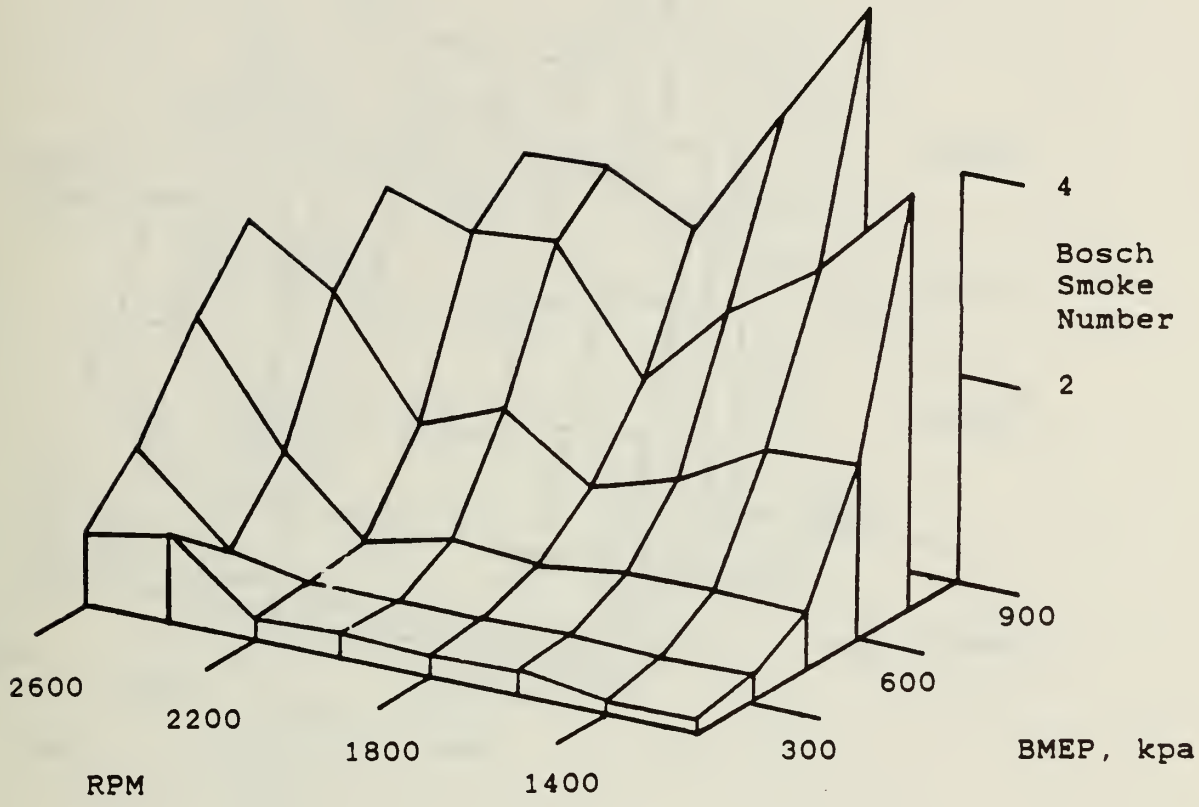

Figure 29. Bosch Smoke Number vs. Brake Mean Effective Pressure and Speed for Diesel Fuel and Ethanol

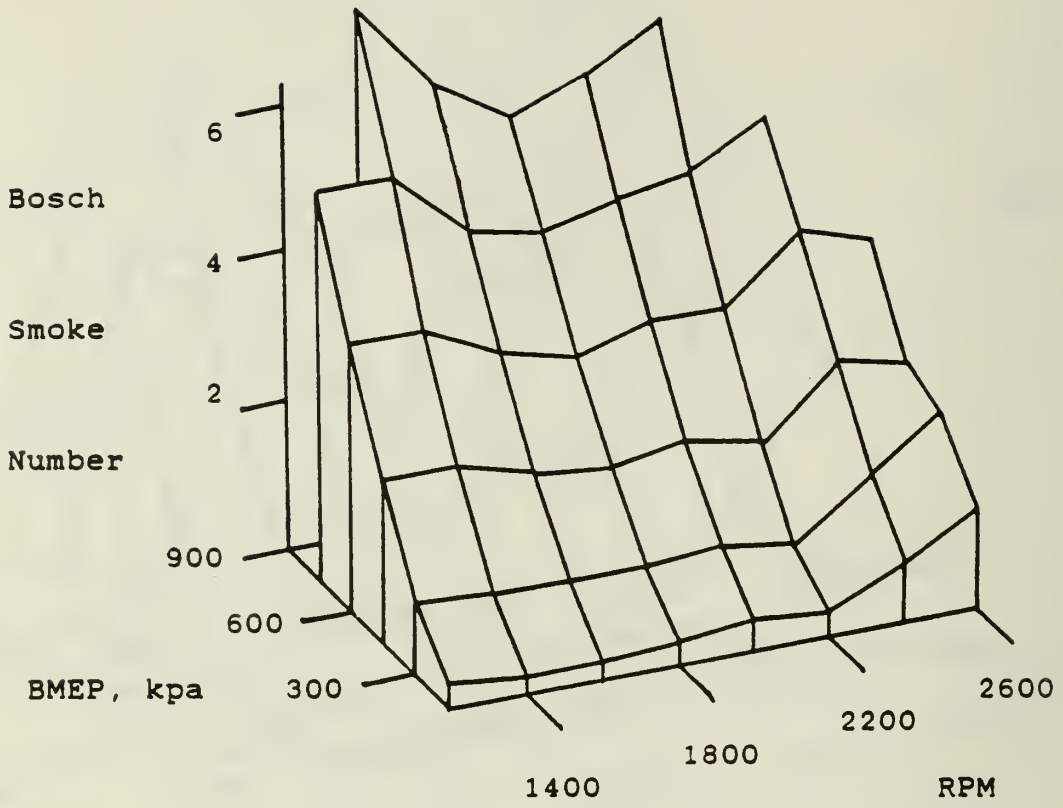

Figure 30. Bosch Smoke Number vs. Brake Mean Effective Pressure and Speed for Diesel Fuel Only

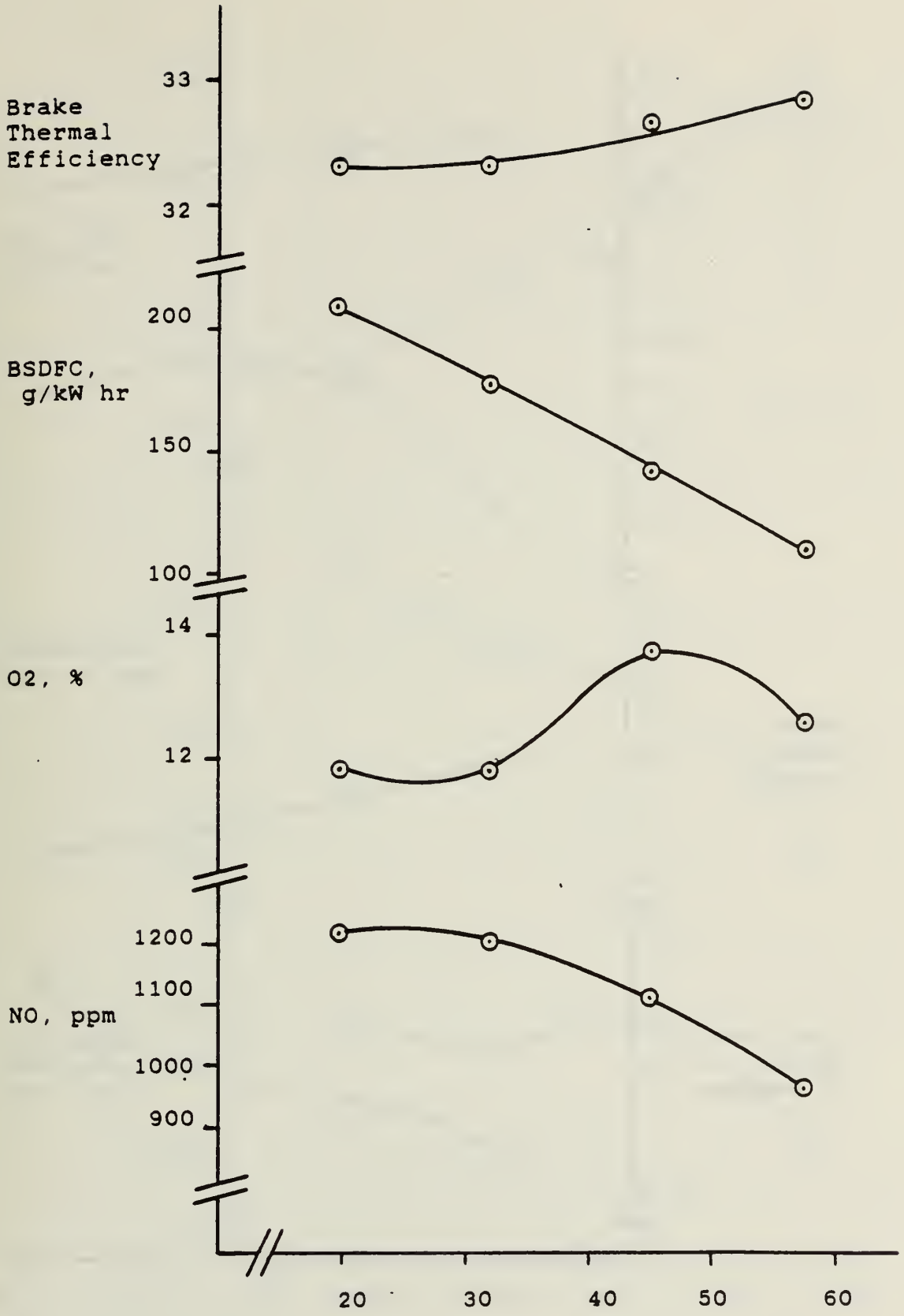

Figure 31. Brake Thermal Efficiency, Brake Specific Diesel Fuel Consumption, Oxygen and Nitrogen Oxide Emissions vs. Ethanol Percentage

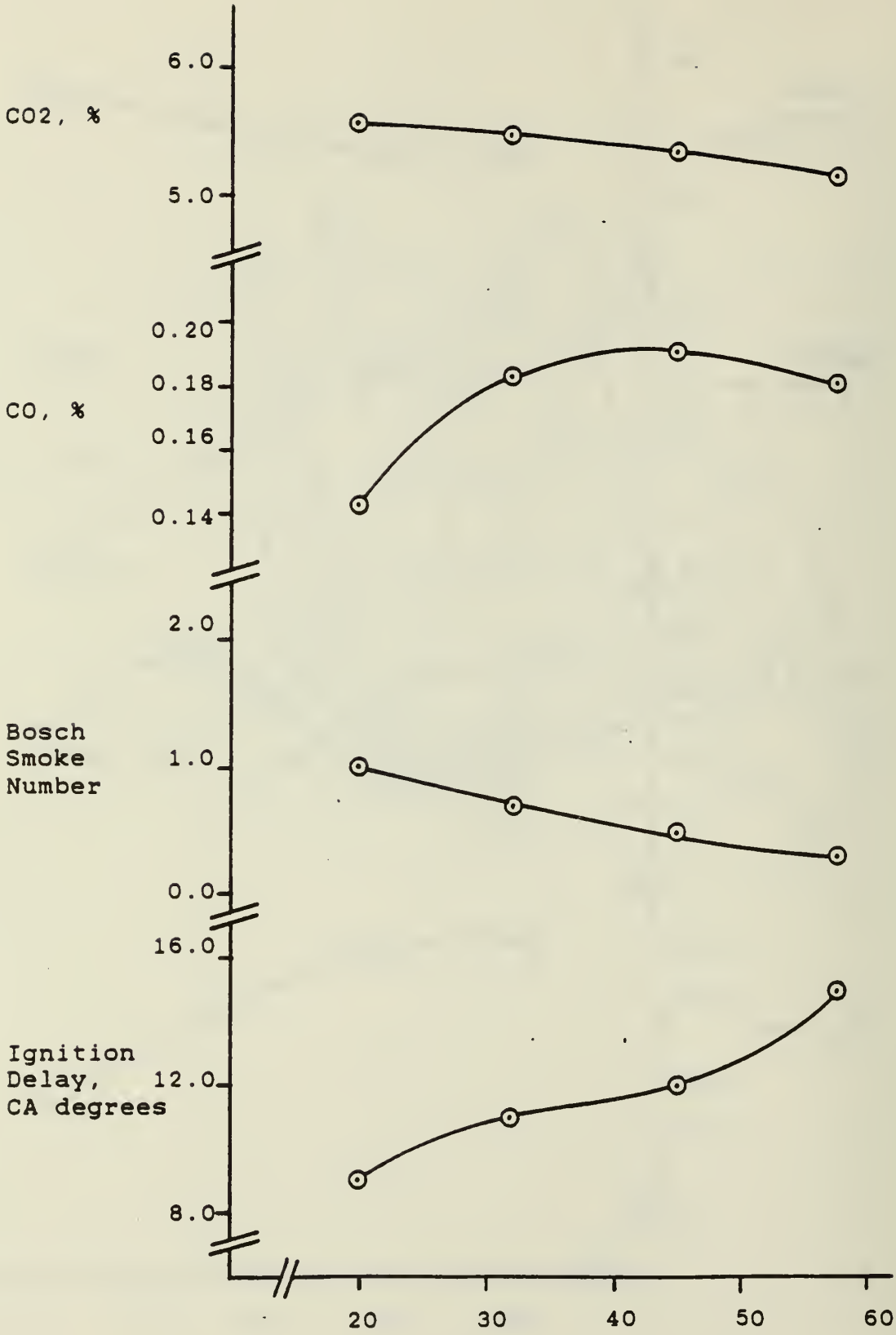

Figure 32. Carbon Dioxide, Carbon Monoxide, Bosch Smoke Number, and Ignition Delay vs. Ethanol Percentage

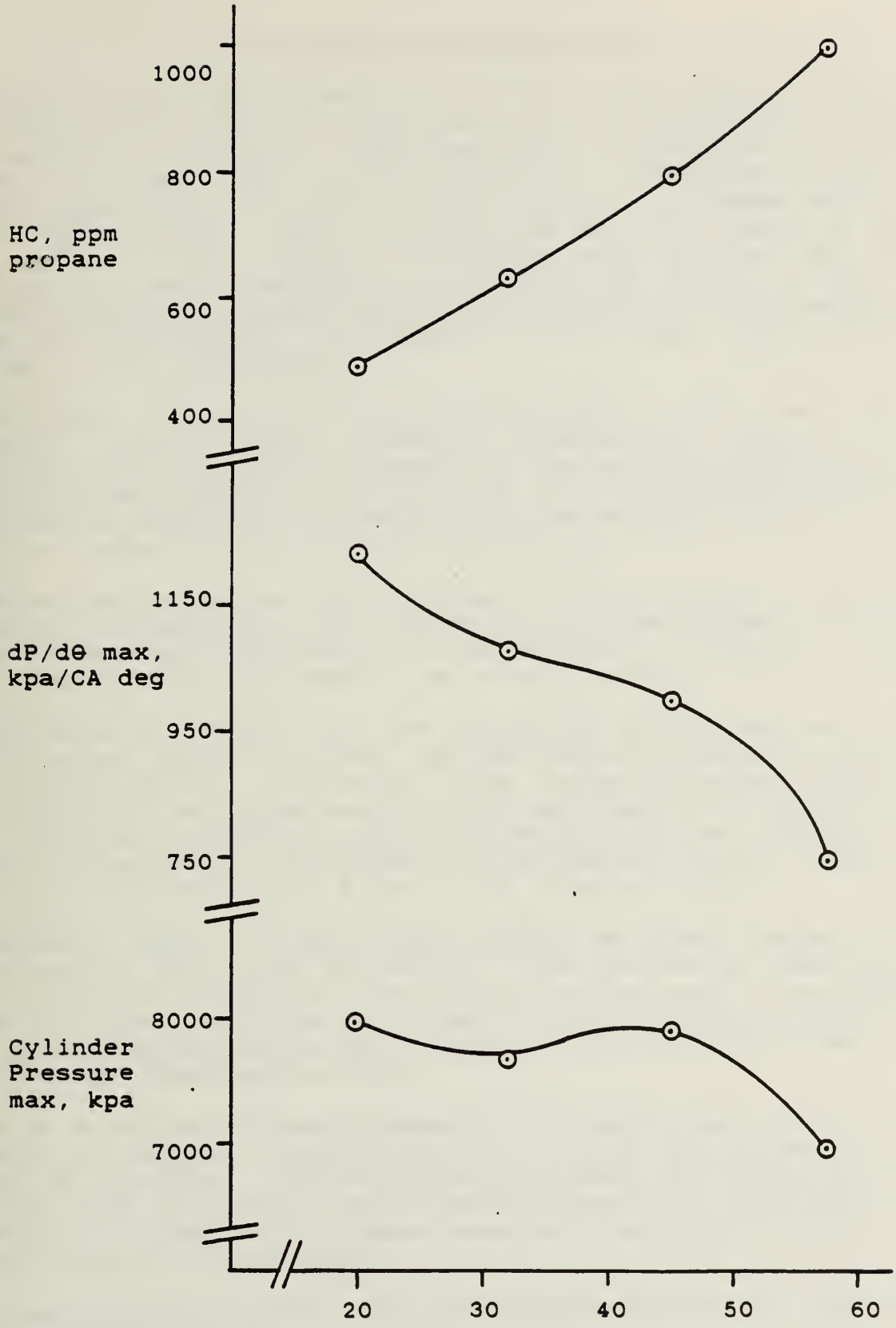

Figure 33. Hydrocarbon Emissions, Maximum Rate of Cylinder Pressure Change, and Maximum Cylinder Pressure vs. Ethanol Percentages

6. CONCLUSIONS AND RECOMMENDATIONS

The dual fueling of a turbocharged diesel engine with port injected ethanol resulted in satisfactory performance with substantial reductions in the consumption of diesel fuel. Slight increases in brake thermal efficiency were noted at high BMEP test points run with diesel fuel and ethanol when compared to similar test points run on diesel fuel only. Increases were also noted in ignition delay, unburned hydrocarbons and carbon monoxide emissions. Maximum cylinder pressure and nitrogen oxide emissions were both measured to be higher at the same test points and both lower at of the test points when compared to measured levels for diesel fuel only. Noticeable reductions in smoke emissions were measured for the diesel-ethanol fueling method used in this investigation.

The ethanol fueling system developed and tested in this investigation makes use of readily available commercial components and required slight modification of the original head assembly of the engine. The modification makes this equipment economically unattractive as an aftermarket add-on kit, but would be cost efficient if the machining of the head was carried out while the head was removed for valve system reconditioning.

Another feasible option which the ethanol fueling system allows is the machining of the head while the engine is still at the factory. suitable plugs in the machined holes would allow the engine to be operated on diesel fuel, with the ethanol system remaining as a future option.

The amounts of ethanol which were substituted at low loads were substantially greater than the amounts reported from experiments using single point injection methods. The factors which limited the maximum amount of ethanol substituted were more evenly distributed between all cylinders with the port injected, dual pulsed system. The magnitude of the difference between the best and worst case cylinders can be assumed to be much less than the differences which occur with a single point injection system.

The ethanol system developed for this research has several features which make it practical for future development. They include the commercially available components utilized for lower initial cost and ease of replacement, the ease with which the system can be adapted to microprocessor control for future optimization, and the variable rate of substitution which allows fine tuning at various operating conditions.

One of the engine performance parameters which was an important factor in determining the maximum tolerable amount of ethanol substitution was the resulting ignition delay. Unburned hydrocarbon trends were very closely related to ignition delay and may be more readily measurable in the field than ignition delay. A portable hydrocarbon sensor would be required and may need to be developed for that application.

Recommendation for further study which were suggested by the results of this investigation include:

1. Compare the effects of denatured ethanol with those of non-denatured ethanol.

2. Investigate the effects of varied diesel fuel injection timing on engine performance when fueled with ethanol and diesel fuel.

3. Investigate the effects of varied ethanol injection timing on engine performance when fueled with ethanol and diesel fuel.

4. Investigate the effects of lower ethanol proofs on engine performance when used as a fuel substitute.

5. Continue development of the computer control system for future interface with electronically controlled injection pumps currently being developed.

6. Investigate the development of a multi-point, port injected, dual pulsed ethanol system which supplies a fixed mass flow of ethanol and a varied amount of diesel fuel at all engine operating conditions. A fixed mass flow rate of ethanol would allow a simplification of the electronic controls as compared to those used for a variable ethanol flow rate system.

7. REFERENCES

1. Obert, E. F., "Internal Combustion Engines and Air Pollution," Harper and Row, New York, NY, 1973.

2. Meyer, R., "Immediate Need seen for Synfuels Industry," Automotive Engineering, Vol. 88, No. 10, Society of Automotive Engineering, Warrendale, PA, 1980.

3. The National Energy Policy Plan, DOE/S-0008, U.S. Department of Energy, Washington, D.C., 1981.

4. Fontana, C., and C. A. Rotz, "Economic Feasibility of Crop Production Using Alcohol Fuel," ASAE Paper 81-1025, presented at meeting of ASAE, Orlando, FL, 1981.

5. Hall, M. D., "Energy Alternatives and Potential," Alcohol and Vegetable Oil as Alternative Fuels, Proceedings of Region Workshops, sponsored by Purdue University, West Lafayette, IN, 1981.

6. Ryan, T. W., J. O. Storment, and B. R. Wright, "The Effects of Fuel Properties on Diesel Engine Exhaust Emissions--A Review," SAE Paper 810953, Diesel Combustion and Emissions Part III, SP-495, Warrendale, PA, 1981.

7. Schaefer, A. J., and H. O. Hardenberg, "Ignition Improvers for Ethanol Fuels," SAE Paper 810249, Alternative Fuels, SP-480, Warrendale, PA, 1981.

8. Nagalingam, B., B. L. Sridhar, N. R. Panchapakesan, K. V. Gopalakrishnan, and B. S. Murthy, "Surface Ignition Initiated Combustion of Alcohol in Diesel Engines--A New Approach," SAE Paper 800262, Warrendale, PA, 1980.

9. Goering, C. E., H. Shirvani, and S. C. Sorenson, "Alcohol-Heavy Distillate Blends as Diesel Fuel," Transactions of ASAE, Vol. 26, No. 1, pp. 2-5, 9, American Society of Agricultural Engineers, St. Joseph, MI, 1983.

10. Faletti, J. J., S. C. Sorenson, and C. E. Goering, "Energy Release Rates from Hybrid Fuels," Transactions of ASAE, Vol. 27, No. 2, pp. 322-325, St. Joseph, MI, 1984.

11. Goering, C. E., personal communication, Urbana, IL, 1985.

12. Baker, Q. A., "Use of Alcohol-in-Diesel Fuel Emulsions and Solutions in a Medium-Speed Diesel Engine," SAE Paper 810254, Alternate Fuels SP-480, Warrendale, PA, 1981.

13. Clingenpeel, J. M., "Evaluation of Alcohol in Diesel Engines in Farm Applications," Alcohol and Vegetable Oil as Alternate Fuels, Proceedings of Regional Workshops, sponsored by Purdue University, West Lafayette, IN, 1981.

14. Weidmann, K., and H. Menrad, "Fleet Test, Performance and Emissions of Diesel Engines Using Different Alcohol-Diesel Fuel Blends," SAE Paper 841331, Alternative Fuels for Compression and S.I. Engines SP-587, Warrendale, PA, 1984.

15. Lawson, A., A. J. Last, A. S. Desphande, and E. W. Simmons, "Heavy-Duty Truck Diesel Engine Operation on Unstabilized Methanol/Diesel Fuel Emulsions," SAE Paper 810346, Alternate Fuels SP-480, Warrendale, PA, 1981.

16. Goering, C. E., and D. R. Wood, "Overfueling a Diesel Engine with Carbureted Ethanol," Transactions of ASAE, Vol. 25, No. 3, pp. 576-580, St. Joseph, MI, 1982.

17. Govindarajan, S., K. R. Lakshminarayanan, L. S. Madhavan, V. Ganesan, B. Nagalingam, K. V. Gopalakrishnan, and B. S. Murthy, "Road Performance of a Diesel Vehicle with Supplementary Carburetion of Alcohol," SAE Paper 810347, Alternate Fuels SP-480, Warrendale, PA, 1981.

18. Cruz, J. M., C. A. Rotz, and D. H. Watson, "Dueling-Fueling Turbocharged Diesels with Ethanol," ASAE Paper 81-1052, St. Joseph, MI, 1981.

19. Lowi, A., "Supplementary Fueling of Four-Stroke-Cycle Automotive Diesel Engines by Propane Fumigation," SAE Paper 841398, Alternative Fuels for Compression and S.I. Engines SP-587, Warrendale, PA, 1984.

20. Chen, J., D. Gussert, X. Gao, C. Gupta, and D. Foster, "Ethanol Fumigation of a Turbocharged Diesel Engine," SAE Paper 810680, Warrendale, PA, 1981.

21. Barnes, K. D., D. B. Kittelson, and T. E. Murphy, "Effect of Alcohol as Supplemental Fuel for Turbocharged Diesel Engines," SAE Paper 750469, Warrendale, PA, 1975.

22. Walter, J. R., and K. R. Kaufman, "Dual Fueling a Farm Tractor with Ethanol," ASAE Paper 80-1050, presented at ASAE Meeting, Orlando, FL, 1981.

23. Kim, Y. K., N. Iwai, H. Suto, and T. Tsuuga, "Improvement of Alcohol Engine Performance by Flash Boiling Injection," Japanese Society of Automotive Engineers Review, pp. 81-86, 1980.

24. Shropshire, G. J., and C. E. Goering, "Ethanol Injection into a Diesel Engine," ASAE Paper 81-1051, presented at ASAE Meeting, Orlando, FL, 1981.

25. Shropshire, G. J., and L. L. Bashford, "A Comparison of Several Ethanol Fumigation Systems," ASAE Paper 83-1063, presented at ASAE Meeting, Bozeman, MT, 1983.

26. Schwarz, R., "High-Pressure Injection Pumps with Electronic Control for Heavy-Duty Diesel Engines," SAE Paper 850170, Warrendale, PA, 1985.

27. Maynard, A., "A New Electronically Controlled Injection Pump for Diesels," SAE Paper 850169, Warrendale, PA, 1985.

28. Moncelle, M. E., and G. C. Fortune, "Caterpillar 3406 PEEC (Programmable Electronic Engine Control)," SAE Paper 850173, Warrendale, PA, 1985.

29. Shiozaki, M., N. Hobo, and I. Akahori, "Development of a Fully Capable Electronic Control System for Diesel Engines," SAE Paper 850172, Warrendale, PA, 1985.

30. Garvey, D. C., "A Digital Control Algorithm for Diesel Engine Governing," SAE Paper 850174, Warrendale, PA, 1985.

31. Miller, G. L., and J. L. Smith, "Microprocessor Dual-Fuel Diesel Engine Control," Transactions of ASAE, Vol. 26, No. 1, pp. 6-9, St. Joseph, MI, 1983.

32. Walker, J. T., "Microprocessor Control for Alcohol Fuel Fumigation," Transactions of ASAE, Vol. 25, No. 6, pp. 1520-1523, 1528, St. Joseph, MI, 1982.

8. TABULAR DATA

Diesel
1200 RPM

BMEP (kpa)	24.6	189.2	355.5	522.6	682.8	848.2
Torque (Nm)	14.0	107.5	202.0	297.0	388.0	482.0
Power (kW)	1.8	13.5	25.4	37.3	48.8	60.6
BSFC (g/kW-hr)	1101.5	304.2	255.3	242.3	245.0	264.4
Therm. Eff.	0.076	0.277	0.330	0.347	0.343	0.318
F/A	0.008	0.017	0.027	0.036	0.045	0.058
Vol. Eff.	0.816	0.821	0.824	0.825	0.843	0.846
Man. Pres. (kpa)	98.4	99.5	102.0	106.3	112.0	119.9
Amb. Pres. (kpa)	99.1	99.1	99.1	99.1	99.1	99.1
Man. Temp.(C)	32.0	33.2	35.7	40.7	47.4	56.2
Exh. Temp.(C)	141.3	216.0	301.2	402.5	502.9	612.1
Cool. Temp.(C)	93.0	94.4	92.2	93.7	94.8	95.1
Oxygen (%)	18.20	16.16	14.05	11.78	9.66	7.17
NO (ppm)	177.0	503.2	840.0	945.2	999.8	929.7
HC (ppm)	165.5	181.4	202.5	228.1	246.0	151.2
CO2 (%)	1.56	3.11	4.88	6.78	8.41	10.16
CO (%)	0.04	0.04	0.04	0.07	0.22	1.27
Bosch Smoke No.	0.2	0.3	1.3	2.6	4.6	6.6
Max. Pres. (kpa)	5178.	6086.	6602.	7242.	7887.	8779.
Max. dP/dθ (kpa/deg)	491.	683.	806.	738.	737.	630.
Ign. Delay (deg)	7	6	7	6	6	6

Diesel
1400 RPM

BMEP (kpa)	32.6	208.5	383.6	557.8	733.8	894.0
Torque (Nm)	18.5	118.5	218.0	317.0	417.0	508.0
Power (kW)	2.7	17.4	32.0	46.5	61.1	74.5
BSFC (g/kW-hr)	955.9	301.1	254.6	241.5	241.4	257.9
Therm. Eff.	0.088	0.279	0.330	0.349	0.349	0.326
F/A	0.009	0.019	0.029	0.038	0.047	0.056
Vol. Eff.	0.826	0.823	0.822	0.830	0.839	0.853
Man. Pres. (kpa)	98.3	100.1	104.0	110.3	119.3	130.8
Amb. Pres. (kpa)	98.8	98.8	98.8	98.8	98.8	98.8
Man. Temp.(C)	34.6	36.3	40.5	47.4	57.2	69.9
Exh. Temp.(C)	155.9	238.1	335.5	441.6	535.6	634.1
Cool. Temp.(C)	94.5	92.5	94.1	94.3	95.4	95.6
Oxygen (%)	18.95	16.38	14.02	11.66	9.22	7.20
NO (ppm)	211.3	546.5	898.8	1001.7	1123.3	992.0
HC (ppm)	173.0	194.4	209.0	201.7	191.1	121.2
CO2 (%)	1.72	3.36	5.22	6.99	8.58	9.79
CO (%)	0.05	0.04	0.04	0.08	0.27	1.12
Bosch Smoke No.	0.1	0.3	1.6	3.4	4.9	7.2
Max. Pres. (kpa)	5250.	6077.	7021.	7663.	8564.	9589.
Max. dP/dθ (kpa/deg)	544.	755.	912.	801.	743.	605.
Ign. Delay (deg)	10	10	8	8	8	7

Diesel
1600 RPM

BMEP (kpa)	37.0	223.5	402.1	577.2	757.6	939.7
Torque (Nm)	21.0	127.0	228.5	328.0	430.5	534.0
Power (kW)	3.5	21.3	38.3	55.0	72.1	89.5
BSFC (g/kW-hr)	908.0	300.0	254.9	239.5	237.9	247.8
Therm. Eff.	0.093	0.280	0.330	0.351	0.354	0.340
F/A	0.010	0.020	0.029	0.037	0.045	0.054
Vol. Eff.	0.824	0.827	0.831	0.835	0.847	0.861
Man. Pres. (kpa)	98.8	101.6	106.8	114.9	126.1	142.6
Amb. Pres. (kpa)	98.7	98.7	98.7	98.7	98.7	98.7
Man. Temp.(C)	36.0	39.3	45.1	53.2	64.7	81.2
Exh. Temp.(C)	170.0	261.3	359.5	456.4	544.8	639.0
Cool. Temp.(C)	95.7	94.6	94.2	95.1	95.1	95.1
Oxygen (%)	17.11	15.86	14.63	13.70	12.39	11.20
NO (ppm)	269.2	721.6	1058.7	1183.7	1316.4	1213.9
HC (ppm)	176.7	180.0	175.1	157.2	133.0	80.4
CO2 (%)	1.83	3.56	5.39	7.00	8.53	9.69
CO (%)	0.05	0.04	0.04	0.08	0.23	0.87
Bosch Smoke No.	0.2	0.4	1.6	3.1	4.4	6.4
Max. Pres. (kpa)	5429.	6307.	7365.	8146.	9129.	10401.
Max. dP/dθ (kpa/deg)	535.	749.	938.	865.	671.	614.
Ign. Delay (deg)	9	10	8	6	7	6

Diesel
1800 RPM

BMEP (kpa)	43.1	238.4	429.4	615.9	800.7	962.6
Torque (Nm)	24.5	135.5	244.0	350.0	455.0	547.0
Power (kW)	4.6	25.5	46.0	66.0	85.8	103.1
BSFC (g/kW-hr)	863.1	305.7	255.8	240.2	238.0	244.6
Therm. Eff.	0.097	0.275	0.329	0.350	0.354	0.344
F/A	0.011	0.021	0.030	0.038	0.045	0.050
Vol. Eff.	0.833	0.835	0.841	0.856	0.874	0.892
Man. Pres. (kpa)	99.1	103.1	110.8	121.7	135.8	152.4
Amb. Pres. (kpa)	98.7	98.7	98.7	98.7	98.7	98.7
Man. Temp.(C)	37.7	41.7	49.9	61.2	75.1	91.5
Exh. Temp.(C)	183.0	276.3	383.6	480.1	560.8	640.3
Cool. Temp.(C)	95.5	93.5	93.6	94.2	95.0	95.9
Oxygen (%)	18.93	17.02	15.54	14.22	12.50	11.64
NO (ppm)	273.0	744.6	1140.6	1355.9	1527.5	1467.1
HC (ppm)	196.1	188.3	181.4	166.9	152.5	89.7
CO2 (%)	1.98	3.79	5.53	7.02	8.81	9.68
CO (%)	0.05	0.04	0.04	0.08	0.23	0.70
Bosch Smoke No.	0.1	0.4	1.8	3.4	4.5	6.2
Max. Pres. (kpa)	5439.	6628.	7719.	8725.	10012.	11355.
Max. dP/dθ (kpa/deg)	577.	942.	1051.	856.	786.	695.
Ign. Delay (deg)	12	10	10	7	7	6

Diesel
2000 RPM

BMEP (kpa)	49.3	232.3	409.1	582.5	756.7	937.1
Torque (Nm)	28.0	132.0	232.5	331.0	430.0	532.5
Power (kW)	5.9	27.6	48.7	69.3	90.1	111.5
BSFC (g/kW-hr)	810.1	312.6	260.5	242.8	237.6	241.7
Therm. Eff.	0.104	0.269	0.323	0.347	0.354	0.348
F/A	0.012	0.021	0.029	0.036	0.042	0.048
Vol. Eff.	0.838	0.839	0.845	0.855	0.861	0.873
Man. Pres. (kpa)	99.7	104.4	113.0	123.9	138.6	157.9
Amb. Pres. (kpa)	98.7	98.7	98.7	98.7	98.7	98.7
Man. Temp.(C)	40.3	45.0	53.7	64.8	78.5	95.7
Exh. Temp.(C)	199.7	289.6	385.2	470.4	545.6	628.5
Cool. Temp.(C)	93.5	94.1	94.9	95.3	95.4	95.2
Oxygen (%)	19.31	17.77	16.45	15.17	13.96	12.90
NO (ppm)	270.6	690.5	991.0	1229.7	1429.3	1452.8
HC (ppm)	178.3	150.3	139.6	127.4	109.0	71.4
CO2 (%)	2.12	3.76	5.34	6.75	7.84	9.04
CO (%)	0.05	0.03	0.03	0.05	0.13	0.35
Bosch Smoke No.	0.1	0.6	1.9	3.0	4.7	6.1
Max. Pres. (kpa)	5364.	6667.	7567.	8707.	9915.	11247.
Max. dP/dθ (kpa/deg)	519.	830.	862.	797.	737.	644
Ign. Delay (deg)	12	11	8	8	8	7

Diesel
2200 RPM

BMEP (kpa)	47.5	232.3	406.5	570.2	737.3	911.6
Torque (Nm)	27.0	132.0	231.0	324.0	419.0	518.0
Power (kW)	6.2	30.4	53.2	74.6	96.5	119.3
BSFC (g/kW-hr)	869.9	320.5	266.7	247.0	240.0	242.1
Therm. Eff.	0.097	0.263	0.316	0.341	0.351	0.348
F/A	0.012	0.021	0.029	0.036	0.040	0.046
Vol. Eff.	0.827	0.836	0.854	0.866	0.874	0.880
Man. Pres. (kpa)	100.9	106.9	117.0	128.8	143.3	162.6
Amb. Pres. (kpa)	99.2	99.2	99.2	99.2	99.3	99.3
Man. Temp.(C)	40.6	46.6	57.7	68.9	81.4	98.2
Exh. Temp.(C)	214.8	301.0	394.9	467.3	540.7	619.6
Cool. Temp.(C)	92.8	92.0	93.1	93.2	94.3	93.5
Oxygen (%)	17.33	15.32	14.15	14.62	13.61	12.84
NO (ppm)	246.0	628.1	904.6	1180.6	1435.2	1484.2
HC (ppm)	150.4	136.4	143.1	134.8	103.4	74.6
CO2 (%)	2.24	3.66	4.72	5.82	7.29	8.35
CO (%)	0.04	0.03	0.03	0.04	0.08	0.22
Bosch Smoke No.	0.3	0.7	2.3	2.7	4.7	6.7
Max. Pres. (kpa)	5388.	6728.	7555.	8616.	9729.	11127.
Max. dP/dθ (kpa/deg)	420.	662.	718.	656.	617.	564.
Ign. Delay (deg)	10	10	8	9	6	5

Diesel
2400 RPM

BMEP (kpa)	52.8	211.2	373.1	531.4	691.6	846.4
Torque (Nm)	30.0	120.0	212.0	302.0	393.0	481.0
Power (kW)	7.5	30.2	53.3	75.9	98.8	120.9
BSFC (g/kW-hr)	870.4	348.8	281.3	256.1	251.1	249.2
Therm. Eff.	0.097	0.241	0.299	0.329	0.335	0.338
F/A	0.014	0.021	0.027	0.033	0.039	0.043
Vol. Eff.	0.843	0.853	0.863	0.876	0.889	0.898
Man. Pres. (kpa)	101.8	107.7	118.6	130.8	145.3	164.0
Amb. Pres. (kpa)	99.2	99.2	99.2	99.2	99.2	99.2
Man. Temp.(C)	44.0	50.3	61.0	72.9	86.9	104.6
Exh. Temp.(C)	236.1	312.0	395.3	464.3	547.6	613.1
Cool. Temp.(C)	92.3	92.1	92.4	93.1	93.8	95.4
Oxygen (%)	17.95	16.47	15.18	13.95	12.59	11.80
NO (ppm)	233.8	500.4	751.0	1043.1	1249.0	1327.3
HC (ppm)	162.7	140.2	143.3	124.9	116.1	80.2
CO2 (%)	2.24	3.40	4.54	5.51	6.52	7.10
CO (%)	0.04	0.03	0.03	0.03	0.08	0.16
Bosch Smoke No.	0.5	0.9	2.5	3.3	5.0	5.8
Max. Pres. (kpa)	5435.	6382.	7400.	8233.	9283.	10364.
Max. dP/dθ (kpa/deg)	358.	549.	580.	592.	544.	465.
Ign. Delay (deg)	11	11	8	7	7	5

Diesel
2600 RPM

BMEP (kpa)	56.3	171.6	294.8	410.0	520.9	647.6
Torque (Nm)	32.0	97.5	167.5	233.0	296.0	368.0
Power (kW)	8.7	26.5	45.6	63.4	80.6	100.2
BSFC (g/kW-hr)	885.7	411.2	319.7	284.0	267.0	259.2
Therm. Eff.	0.095	0.205	0.263	0.296	0.315	0.325
F/A	0.015	0.020	0.025	0.029	0.033	0.038
Vol. Eff.	0.851	0.867	0.873	0.873	0.889	0.888
Man. Pres. (kpa)	102.9	107.7	116.2	124.9	134.3	146.4
Amb. Pres. (kpa)	99.2	99.2	99.2	99.2	99.2	99.2
Man. Temp.(C)	48.5	53.7	62.1	70.6	80.4	91.4
Exh. Temp.(C)	261.9	321.2	385.4	435.7	483.3	549.2
Cool. Temp.(C)	93.1	93.8	93.5	94.1	94.5	95.1
Oxygen (%)	19.87	18.75	17.49	16.31	15.38	13.06
NO (ppm)	240.3	400.5	545.6	745.2	924.9	1081.6
HC (ppm)	166.4	141.7	131.9	127.1	110.3	87.0
CO2 (%)	2.41	3.30	4.18	4.89	5.31	6.45
CO (%)	0.04	0.03	0.03	0.02	0.03	0.06
Bosch Smoke No.	0.8	1.2	2.2	2.4	2.7	4.7
Max. Pres. (kpa)	5399.	6015.	6754.	7458.	8161.	8984.
Max. dP/dθ (kpa/deg)	267.	394.	481.	519.	516.	457.
Ign. Delay (deg)	12	11	8	8	6	6

Ethanol
1200 RPM

BMEP (kpa)	26.4	190.1	360.7	524.4	700.4	853.5
Torque (Nm)	15.0	108.0	205.0	298.0	398.0	485.0
Power (kW)	1.9	13.6	25.7	37.3	49.8	60.9
BSDFC (g/kW-hr)	635.0	152.3	135.1	148.4	163.4	190.2
Therm. Eff.	0.045	0.223	0.318	0.346	0.347	0.322
% Ethanol	65.9	59.6	49.0	39.0	32.6	27.2
Vol. Eff.	0.849	0.847	0.842	0.827	0.840	0.854
Man. Pres. (kpa)	98.2	99.0	101.0	104.3	110.0	117.0
Amb. Pres. (kpa)	98.8	98.8	98.8	98.8	98.8	98.8
Man. Temp.(C)	32.5	33.4	35.7	34.5	46.0	54.3
Exh. Temp.(C)	145.0	218.0	291.8	381.0	486.2	584.4
Cool. Temp.(C)	95.9	94.3	96.4	96.2	97.3	97.8
Oxygen (%)	20.32	18.51	16.29	13.87	10.66	6.25
NO (ppm)	46.2	188.9	690.5	1198.0	1286.5	1111.0
HC (ppm)	1771.4	1504.1	1013.4	674.8	558.0	514.7
CO2 (%)	1.42	2.69	4.50	6.49	8.52	10.26
CO (%)	0.24	0.37	0.24	0.16	0.25	1.22
Bosch Smoke No.	0.1	0.1	0.3	0.9	3.2	6.4
Max. Pres. (kpa)	4878.	5344.	6739.	7894.	8777.	9742.
Max. dP/dθ (kpa/deg)	399.	511.	781.	1019.	1000.	970.
Ign. Delay (deg)	11	10	11	9	9	8

Ethanol
1400 RPM

BMEP (kpa)	29.0	220.0	392.4	566.6	742.6	901.0
Torque (Nm)	16.5	125.0	223.0	322.0	422.0	512.0
Power (kW)	2.4	18.3	32.7	47.2	61.9	74.8
BSDFC (g/kW-hr)	527.3	132.8	151.7	166.6	165.2	178.4
Therm. Eff.	0.045	0.246	0.318	0.342	0.351	0.339
% Ethanol	71.7	61.2	42.6	32.3	31.2	28.2
Vol. Eff.	0.816	0.822	0.826	0.831	0.838	0.851
Man. Pres. (kpa)	98.6	100.3	103.5	109.1	117.4	126.5
Amb. Pres. (kpa)	98.9	98.9	98.9	98.9	98.9	98.9
Man. Temp.(C)	32.9	34.8	38.5	44.3	53.2	64.1
Exh. Temp.(C)	154.2	232.1	316.8	417.5	511.0	593.9
Cool. Temp.(C)	96.3	93.0	93.3	95.1	96.0	97.0
Oxygen (%)	17.75	15.42	12.86	10.43	8.07	6.87
NO (ppm)	15.8	160.7	713.8	1244.4	1372.5	1322.4
HC (ppm)	1866.3	1407.0	893.7	627.6	500.0	442.6
CO2 (%)	1.49	3.03	5.04	6.99	8.70	9.89
CO (%)	0.32	0.59	0.21	0.18	0.26	0.93
Bosch Smoke No.	0.1	0.1	0.3	1.4	3.0	5.5
Max. Pres. (kpa)	4620.	5517.	7129.	8291.	9570.	10711.
Max. dP/dθ (kpa/deg)	265.	530.	959.	1172.	1055.	1007.
Ign. Delay (deg)	15	14	12	12	10	8

Ethanol
1600 RPM

BMEP (kpa)	50.0	225.2	404.7	580.7	772.5	946.7
Torque (Nm)	25.0	128.0	230.0	330.0	439.0	538.0
Power (kW)	4.1	21.4	38.5	55.3	73.6	90.1
BSDFC (g/kW-hr)	399.0	142.7	146.5	142.3	150.9	168.3
Therm. Eff.	0.061	0.244	0.324	0.350	0.353	0.347
% Ethanol	70.9	58.7	43.6	40.9	36.6	30.6
Vol. Eff.	0.842	0.841	0.834	0.834	0.842	0.865
Man. Pres. (kpa)	98.9	101.4	106.0	112.2	123.7	137.6
Amb. Pres. (kpa)	98.9	98.9	98.9	98.9	98.9	98.9
Man. Temp.(C)	34.5	36.7	41.7	48.4	60.2	74.9
Exh. Temp.(C)	170.5	246.9	333.9	420.3	518.3	600.7
Cool. Temp.(C)	94.3	93.3	94.9	95.9	96.8	96.3
Oxygen (%)	17.40	15.03	12.74	10.76	8.53	7.18
NO (ppm)	32.8	303.6	1015.9	1521.4	1627.1	1514.2
HC (ppm)	1884.0	1350.8	821.5	577.6	443.1	475.4
CO2 (%)	1.62	3.01	4.82	6.21	7.77	8.70
CO (%)	0.36	0.36	0.21	0.16	0.22	0.77
Bosch Smoke No.	0.2	0.2	0.5	1.0	2.9	5.1
Max. Pres. (kpa)	4680.	5860.	7792.	9259.	11015.	11821.
Max. dP/dθ (kpa/deg)	291.	583.	1107.	1112.	1220.	1166.
Ign. Delay (deg)	17	15	11	10	10	9

Ethanol
1800 RPM

BMEP (kpa)	44.0	239.3	431.1	621.2	807.7	960.8
Torque (Nm)	25.0	136.0	245.0	353.0	459.0	546.0
Power (kW)	4.7	25.6	46.2	66.5	86.5	102.9
BSDFC (g/kW-hr)	373.1	99.5	102.9	123.5	146.0	161.4
Therm. Eff.	0.054	0.235	0.329	0.349	0.356	0.351
% Ethanol	76.0	72.2	59.7	48.8	38.3	32.8
Vol. Eff.	0.845	0.847	0.843	0.834	0.855	0.877
Man. Pres. (kpa)	99.6	103.2	108.4	117.6	131.9	146.3
Amb. Pres. (kpa)	98.9	98.9	98.9	98.9	98.9	98.9
Man. Temp.(C)	36.9	40.5	45.8	55.0	69.8	83.2
Exh. Temp.(C)	183.2	266.3	345.3	439.1	533.7	596.2
Cool. Temp.(C)	96.1	94.2	95.3	96.2	97.4	97.6
Oxygen (%)	20.44	17.69	13.87	10.94	8.90	7.67
NO (ppm)	39.3	232.4	910.8	1677.3	1828.5	1809.1
HC (ppm)	2023.0	1615.0	1020.3	536.9	409.4	397.4
CO2 (%)	1.68	3.07	4.78	6.73	7.95	8.65
CO (%)	0.57	0.58	0.19	0.13	0.22	0.61
Bosch Smoke No.	0.1	0.3	0.4	0.7	2.7	3.8
Max. Pres. (kpa)	4265.	5318.	7247.	10422.	11681.	12971.
Max. dP/dθ (kpa/deg)	141.	414.	762.	1348.	1292.	1409.
Ign. Delay (deg)	19	17	15	10	9	8

Ethanol
2000 RPM

BMEP (kpa)	45.8	244.6	417.9	601.8	762.0	936.2
Torque (Nm)	26.0	139.0	237.5	342.0	433.0	532.0
Power (kW)	5.4	29.1	49.7	71.6	90.7	111.4
BSDFC (g/kW-hr)	393.3	100.9	87.3	158.5	158.9	159.2
Therm. Eff.	0.058	0.228	0.316	0.343	0.354	0.357
% Ethanol	72.8	72.6	67.3	35.5	33.1	32.4
Vol. Eff.	0.822	0.833	0.836	0.844	0.863	0.876
Man. Pres. (kpa)	100.7	105.2	111.0	123.8	136.2	151.7
Amb. Pres. (kpa)	98.9	98.9	98.9	98.9	98.9	98.9
Man. Temp.(C)	38.7	43.6	49.1	61.7	73.7	88.4
Exh. Temp.(C)	196.5	283.7	349.4	452.8	519.8	582.0
Cool. Temp.(C)	92.5	92.5	93.6	94.3	95.4	96.5
Oxygen (%)	17.34	14.94	13.08	10.66	9.26	8.01
NO (ppm)	26.3	181.0	622.9	1352.4	1610.1	1852.7
HC (ppm)	1920.6	1626.4	1235.7	562.9	435.9	341.4
CO2 (%)	1.85	3.34	4.76	6.62	7.62	8.31
CO (%)	0.57	0.58	0.20	0.19	0.19	0.28
Bosch Smoke No.	0.4	0.2	0.4	1.6	3.1	3.5
Max. Pres. (kpa)	4510.	5402.	6696.	9731.	11273.	12755.
Max. dP/dθ (kpa/deg)	225.	407.	581.	1181.	1138.	1231.
Ign. Delay (deg)	19	18	15	11	9	9

Ethanol
2200 RPM

BMEP (kpa)	56.3	232.3	412.7	571.9	742.6	920.4
Torque (Nm)	32.0	132.0	234.5	325.0	422.0	523.0
Power (kW)	7.4	30.4	54.0	74.9	97.2	120.5
BSDFC (g/kW-hr)	298.5	140.4	113.5	126.3	148.3	157.7
Therm. Eff.	0.061	0.221	0.308	0.340	0.350	0.349
% Ethanol	78.4	63.1	58.4	48.9	38.2	34.5
Vol. Eff.	0.849	0.852	0.860	0.860	0.871	0.879
Man. Pres. (kpa)	101.9	107.1	114.7	124.3	139.7	157.2
Amb. Pres. (kpa)	99.4	99.4	99.4	99.4	99.4	99.4
Man. Temp.(C)	41.0	46.1	53.7	62.9	78.2	94.6
Exh. Temp.(C)	222.1	296.8	368.5	430.8	511.6	578.0
Cool. Temp.(C)	93.2	93.9	93.7	93.9	96.6	96.9
Oxygen (%)	18.92	17.48	16.00	14.72	13.50	12.40
NO (ppm)	48.5	279.3	650.0	1207.8	1497.8	1861.1
HC (ppm)	2052.9	1488.4	1077.1	619.4	378.1	277.5
CO2 (%)	1.92	3.06	4.33	5.79	7.23	8.32
CO (%)	0.58	0.58	0.25	0.16	0.15	0.20
Bosch Smoke No.	0.1	0.2	0.4	0.9	2.8	3.5
Max. Pres. (kpa)	4567.	5757.	6430.	10308.	11278.	12685.
Max. dP/dθ (kpa/deg)	181.	434.	584.	1217.	1049.	1625.
Ign. Delay (deg)	18	14	13	9	9	7

Ethanol
2400 RPM

BMEP (kpa)	53.7	204.1	381.9	543.8	696.9	850.0
Torque (Nm)	30.5	116.0	217.0	309.0	396.0	483.0
Power (kW)	7.7	29.2	54.5	77.7	99.5	121.4
BSDFC (g/kW-hr)	110.2	60.2	62.4	160.2	144.6	156.0
Therm. Eff.	0.034	0.156	0.281	0.324	0.342	0.345
% Ethanol	95.5	88.8	79.2	38.3	41.2	36.1
Vol. Eff.	0.848	0.854	0.860	0.865	0.870	0.875
Man. Pres. (kpa)	113.0	110.7	116.6	129.6	141.5	158.1
Amb. Pres. (kpa)	99.4	99.4	99.4	99.4	99.4	99.4
Man. Temp.(C)	53.5	52.0	57.4	70.2	81.6	96.4
Exh. Temp.(C)	290.2	323.0	366.5	447.4	500.0	562.0
Cool. Temp.(C)	90.9	92.8	92.6	94.0	94.1	95.6
Oxygen (%)	18.56	18.40	17.37	15.87	13.63	12.77
NO (ppm)	20.3	72.9	354.7	1034.4	1401.1	1691.1
HC (ppm)	2353.8	2017.0	1476.8	585.0	455.9	319.9
CO2 (%)	2.82	3.31	4.48	6.01	7.08	7.95
CO (%)	0.20	0.56	0.24	0.19	0.14	0.17
Bosch Smoke No.	1.3	0.7	0.4	2.2	2.9	3.7
Max. Pres. (kpa)	4414.	4697.	6420.	9291.	10882.	12463.
Max. dP/dθ (kpa/deg)	129.	129.	406.	745.	1022.	1748.
Ign. Delay (deg)	**	18	14	10	10	8

Ethanol
2600 RPM

BMEP (kpa)	56.3	183.0	302.7	418.8	550.8	649.3
Torque (Nm)	32.0	104.0	172.0	238.0	313.0	369.0
Power (kW)	8.7	28.3	46.8	64.8	85.2	100.5
BSDFC (g/kW-hr)	606.3	278.4	207.8	176.9	170.4	169.2
Therm. Eff.	0.074	0.190	0.254	0.291	0.320	0.334
% Ethanol	46.8	37.2	37.3	38.7	35.2	32.9
Vol. Eff.	0.850	0.869	0.868	0.889	0.885	0.900
Man. Pres. (kpa)	103.1	108.5	115.1	122.5	134.5	143.1
Amb. Pres. (kpa)	98.8	98.8	98.8	98.8	98.8	98.8
Man. Temp.(C)	47.2	53.4	59.7	69.0	80.4	87.8
Exh. Temp.(C)	261.2	328.3	377.0	425.2	476.8	508.2
Cool. Temp.(C)	94.5	95.6	95.4	95.9	95.6	93.1
Oxygen (%)	15.93	14.89	13.47	12.54	11.52	10.72
NO (ppm)	147.7	316.1	451.1	624.1	838.3	1038.8
HC (ppm)	1472.5	997.3	792.5	615.5	452.8	369.0
CO2 (%)	2.45	3.55	4.34	5.42	6.31	6.91
CO (%)	0.28	0.49	0.31	0.26	0.18	0.16
Bosch Smoke No.	0.3	0.8	1.2	2.4	2.7	3.5
Max. Pres. (kpa)	5216.	5685.	6501.	7538.	8836.	9845.
Max. dP/dθ (kpa/deg)	310.	374.	475.	504.	603.	838.
Ign. Delay (deg)	15	12	13	12	8	7

Ethanol
1800 RPM, BMEP= 439.9 kpa

% Ethanol	57.4	44.8	31.9	19.7
BSDFC (g/kW-hr)	109.2	142.1	177.5	209.0
Therm. Eff.	0.328	0.327	0.323	0.323
Vol. Eff.	0.843	0.840	0.835	0.840
Man. Pres. (kpa)	108.9	109.6	110.1	111.0
Amb. Pres. (kpa)	98.8	98.8	98.8	98.8
Man. Temp.(C)	45.7	46.3	46.8	47.5
Exh. Temp.(C)	350.7	359.8	369.4	380.4
Cool. Temp.(C)	95.1	94.7	95.1	94.6
Oxygen (%)	12.57	13.79	11.82	11.85
NO (ppm)	967.0	1112.1	1204.1	1215.9
HC (ppm)	992.0	791.8	628.9	483.4
CO2 (%)	5.16	5.35	5.47	5.56
CO (%)	0.18	0.19	0.18	0.14
Bosch Smoke No.	0.3	0.5	0.7	1.0
Max. Pres. (kpa)	6968.	7915.	7694.	7968.
Max. dP/dθ (kpa/deg)	741.	999.	1078.	1232.
Ign. Delay (deg)	15	12	11	9

9. DEVELOPMENT OF COMPUTER CONTROL AND PROGRAM LISTING

Communication between the real world and the Apple computer was accomplished through the use of an interface board which was designed by Professor L.D. Savage of the Mechanical and Industrial Engineering Department, and utilized a 6522 Versatile Interface Adapter (VIA). The VIA features used here included two eight bit bi-directional ports, four programable interupt requests, and two timer/counter options. Port A was utilized as an eight bit data bus, while port B was used as a control bus. The output of the 6522 was buffered on the Multiplexing board, then connected to other circuits as required. The eight bits of data (port A, 0-7) and five control lines (port B, 0-4) were buffered through the 74LS244 bus drivers on the Multiplexing board. The buffered data signals then exited the Multiplexing board and connected to the DAC board. The buffered control signals PB0 through PB3 were connected to the two 74154 multiplexing chips on the board. One multiplexing chip was used for the DAC controls and was selected/deselected by the connection of PB4 to the enable pin. The resulting configuration had one multiplexer following all control sequences and one multiplexer changing only when selected through the use of PB4. The selectable multiplexer output was connected to the DAC Control Logic board, while the other multiplexer was available for other applications.

An understanding of the Digital to Analog device used is necessary before the description of the DAC Control Logic board

becomes meaningful. Digital to Analog converters, model DAC0830 manufactured by National Semiconductor, were used in combination to brovide a zero to ten volt analog signal to the Digalog controllers. Updating of the DAC0830 required a combination of CS, WR1, and WR2 low signals while valid data was latched from the eight input data bits, and then a combination of WR1, WR2, and XFER low signals to change the analog output to reflect the new eight bit word. Two DAC0830's were combined to provide each analog signal of the two signals required for computer control of the Digalog setpoints. The DAC Control Logic board provides the hard wired logic, using a 74LS27 triple three-input NOR gate, which provides the WR1 and WR2 signals for each of the four CS and two XFER sequences required to update the analog output signal. All chips receive the WR1 and WR2 signals regardless of the chip select or transfer operation being conducted.

The DAC0830's provided faster switching and better response when operated at the CMOS voltage level of approximately fifteen volts for a high level. All data and control signals were level shifted by connecting to an open collector buffer/driver input. Each output of the 7417 driver was connected to positive fifteen volts through a 10 K ohm resistor as well as to the required pins on the DAC0830's. The ten volt reference for the DAC0830's was taken from the ten volt VREF output on the Digalogs.

The analog voltage resolution which was necessary for adequate control of the Digalogs required the compounding of two

DAC0830's for each analog signal. Using one full eight bit DAC coupled to a DAC using only five bits allowed the system to provide resolution similar to a thirteen bit DAC. The fifth bit of the five bit DAC was the most significant bit while the first bit of the eight bit DAC was the least significant bit. The output of both DAC's were buffered through operational amplifier voltage followers, scaled to proper levels (five bit value scaled up, eight bit value scaled down in magnitude), then "added" to result in a zero to ten volt analog signal from a thirteen bit word. Updates of the analog signal were achieved by selecting the eight bit DAC and latching the eight bits, then selecting the five bit DAC and latching the five bits, finally transferring the new data to each analog output simultaneously using a common XFER command.

Speed measurement was accomplished through connection of the TTL level speed signal from the Digalog to the PB6 pin of the 6522. The using of the Timer 1 function and software to count one second of real time while Timer 2 decremented with speed pulses from PB6 resulted in a count value which was the compliment of the engine speed in revolutions per minute.

The Interrupt board was designed to use external sensors to provide the computer with emergency monitoring capability. Murphy switch guages for temperature and pressure were used as the external sensors. Problems with the emergency monitoring resulted in the running of all test conditions in the manual mode. The Interrupt board sent a five volt signal to all

sensors and monitors the return signal. An interupt condition signaled the computer through one of the interrupt requset lines, which the latched the status of all four interrupt signals onto the PA0-PA3 data lines and stored them in memory for evaluation at a later time. Erratic and false interrupts which crashed the program were not eliminatedto the extent which allowed a smooth and continuous operation of the automatic computer program.

The Analog Multiplexing board was developed for use in expanding the capabilities of the sixteen channel, twelve bit analog to digital conversion card which was installed in the computer. National Semiconductor analog switches, model LF13202, were used to select between multiple analog signals. Two LF13202's controlled eight analog signals which could be selected for an analog to digital conversion on a single channel of the ADC card. Two channels of the ADC card were wired into such a circuit and selection logic was provided from the continuously updating multiplexer on the Multiplexing board. Thirty seperate analog signals could be converted from within a software routine, the fourteen hardwired analog signals and the two sets of eight signals which were multiplexed.

Applesoft Program Listing

Boot-up Program: `Hello'

Written by B.D. Roberts

```
10   PRINT "          APPLE II"
15   PRINT "       DOS VERSION 3.3"
20   PRINT "          COPYRIGHT"
25   PRINT "      APPLE COMPUTER, INC."
30   PRINT "         1980, 1982"
35   PRINT " "
40   PRINT " "
45   PRINT " "
50   PRINT "          MAIN DISK FOR"
55   PRINT "      I.H. ENGINE OPERATION"
56   PRINT "            VOLUME 199"
60   PRINT " "
65   PRINT " "
70   PRINT " "
75   PRINT "    TYPE 'LOAD AID' WITH RETURN"
76   PRINT " "
77   PRINT "       THEN 'RUN' WITH RETURN"
78   PRINT " "
80   PRINT "       FOR STARTUP PROCEDURE"
85   END
```

Applesoft Program Listing

Startup Procedure: `Aid'

Written by B.D. Roberts

```
5    CALL - 936
10   PRINT "THIS PROGRAM LOADS THE APPLESOFT"
11   PRINT " "
15   PRINT " AND MACHINE LANGUAGE PROGRAMS"
16   PRINT " "
20   PRINT "WHICH ARE USED TO TEST THE ENGINE"
21   PRINT " "
25   PRINT " FROM AN INITIAL CONDITION OF "
26   PRINT " "
30   PRINT "RUNNING AT LOW IDLE WITH NO LOAD"
31   PRINT " "
32   PRINT " "
33   PRINT " "
34   PRINT " "
40   PRINT "TYPE 'L' TO BEGIN LOADING PROGRAMS"
41   INPUT K1$
42   IF K1$ = "L" THEN GOTO 45
43   PRINT " INPUT INCORRECT, TRY AGAIN"
44   GOTO 31
45   D$ = CHR$(4)
48   PRINT D$;"BLOAD HERTZ"
49   HIMEM: 32752
50   LOMEM: 8192
51   PRINT " "
52   PRINT " "
60   PRINT "PROGRAM LOADING COMPLETE"
61   PRINT " "
62   PRINT " "
65   PRINT "ENGINE MUST BE AT LOW IDLE AND NO LOAD"
66   PRINT "  TO REACH THIS POINT:"
67   PRINT " "
68   PRINT " "
70   PRINT "ALL PUSHBUTTONS ON THE DYNO CONTROLLER SHOULD BE IN
          THE OUT POSITION"
71   PRINT " "
72   PRINT " "
73   PRINT " "
75   PRINT "CHECK FOR THE FOLLOWING:"
76   PRINT " "
80   PRINT "LEFT TURNPOT FULL COUNTERCLOCKWISE"
81   PRINT "****                ****************"
```

```
82   PRINT " "
83   PRINT "RIGHT TURNPOT FULL CLOCKWISE"
84   PRINT "*****                *********"
85   PRINT " "
90   PRINT "TYPE ANY KEY WHEN SETTINGS ARE CORRECT"
91   INPUT K2$
100  PRINT " "
101  PRINT " "
102  PRINT " "
103  PRINT "AT THIS POINT THE ENGINE SHOULD"
104  PRINT " "
105  PRINT "BE STARTED IF NOT ALREADY RUNNING"
106  PRINT " "
107  PRINT "TYPE ANY KEY WHEN READY TO CONTINUE"
108  INPUT K3$
115  CALL -936
116  PRINT "SYSTEM SHOULD NOW BE READY FOR "
117  PRINT " RUNNING OF TESTS"
120  PRINT " "
121  PRINT " "
122  PRINT "TYPE 'B' TO BEGIN TESTS"
123  INPUT K4$
124  IF K4$ = "B" THEN GOTO 130
125  PRINT " INPUT INCORRECT, TRY AGAIN"
126  GOTO 120
130  CALL - 936
132  D$ = CHR(4)
133  PRINT D$;"RUN MAIN"
134  END
```

Applesoft Program Listing

Engine Control:`Main'

Written by B.D. Roberts

```
1     HIMEM: 32752
2     CS = 0
3     CT = 0
4     UF = 0
5     CALL 34144
6     POKE 49374,3
7     CALL 34240
10    POKE 32960,0
11    POKE 33231,0
12    POKE 33842,2
14    CC = 0
15    POKE 32961,0
16    PRINT "TYPE IN DESIRED RPM"
17    INPUT DS
18    PRINT "TYPE IN DESIRED LOAD, IN Nm"
19    INPUT DL
20    PRINT "TYPE IN SCALING FACTOR FOR SPEED CHANGES"
21    HS% = 09
22    LS% = 00
25    PRINT "1 FOR FAST CHANGES, 5 FOR SLOW CHANGES"
30    INPUT " ";FACT%
31    POKE 33794,FACT%
32    POKE 33230,1
35    CALL 32764
40    LSB = PEEK (32976)
45    MSB = PEEK (32977)
49    SP = (MSB * 256.0) + LSB
50    IF SP > DS THEN GOTO 55
51    SF = DS +10.
52    NM = SF / 1000.0 / 0.00122
53    HS% = NM / 256.0
54    LS% = NM - (HS% * 256.0)
55    POKE 33801, HS%
56    POKE 33800, LS%
57    CALL 33802
58    PRINT "RPM SETPOINT= ";SF
60    PRINT "ENGINE RPM= ";SP
61    PRINT " "
62    PRINT "TYPE 'S' FOR STATUS "
63    PRINT " "
64    PRINT "TYPE 'C' FOR CHANGES "
65    PRINT " "
66    PRINT "TYPE 'F' FOR FUEL MEASUREMENT"
67    PRINT "    WITH EMISSIONS SAMPLING"
68    CALL 34192
70    IV = PEEK (32960)
```

```
80   KY = PEEK (32961)
81   POKE -16368,0
90   IF KY = 0 THEN GOTO 500
91   KY = KY - 128
95   IF KY = 67 THEN GOTO 124
96   IF KY = 83 THEN GOTO 800
97   IF KY = 70 THEN GOTO 1050
98   PRINT " "
99   PRINT "INPUT CHARACTER NOT RECOGNIZED
100  GOTO 61
124  CALL -936
125  CALL 32764
126  LSB = PEEK (32976)
127  MSB = PEEK (32977)
128  SP = (MSB * 256.0) + LSB
129  PRINT "ENGINE RPM= ";SP
132  L2 = 0.0
133  FOR X = 1 TO 10
134  POKE 49392,0
135  L1 = PEEK (49393) * 256.0 + PEEK (49392)
136  L2 = L1 + L2
137  NEXT
138  LD = L2 * 4.9988 / 4095. / 10.0
144  L3 = 0
145  PRINT " "
146  PRINT "VREF ON ADC CARD= ";LD
147  PRINT " "
148  FOR X = 1 TO 10
149  POKE 49392,01
150  L4 = PEEK (49393) * 256.0 + PEEK (49392)
151  L3 = L4 + L3
152  NEXT
153  L5 = L3 / 10.0 * 4.9988 * 2.0 / 4095. * 100.0
160  L6 =0
161  FOR X = 1 TO 10
162  POKE 49392,2
163  L7 = PEEK (49393) * 256.0 + PEEK (49392)
164  L6 = L7 + L6
165  NEXT
166  L8 = L6 / 10.0 * 4.9988 / 4095. * 4.0
170  CV = L5
171  PRINT " "
172  PRINT " "
173  PRINT " "
174  PRINT "LOAD= ";CV;" Nm"
175  PRINT " "
176  PRINT " "
177  PRINT " "
178  PRINT " "
179  PRINT " "
180  PRINT " "
181  PRINT "TYPE 'T' TO CHANGE THROTTLE"
```

```
182  PRINT " "
183  PRINT "TYPE 'S' TO CHANGE RPM SETPOINT"
184  PRINT " "
185  PRINT "TYPE 'E' TO EXIT"
186  INPUT S2$
187  IF S2$ = "S" THEN GOTO 193
188  IF S2$ = "T" THEN GOTO 193
189  IF S2$ = "E" THEN GOTO 61
190  IF S2$ = "A" THEN GOTO 500
191  PRINT " INPUT CHARACTER INCORRECT"
192  GOTO 178
193  PRINT " "
194  PRINT " "
195  PRINT " "
196  PRINT " TYPE 'I' FOR INCREASE"
197  PRINT " "
198  PRINT " TYPE 'D' FOR DECREASE"
199  INPUT S3$
205  IF S3$ = "I" THEN GOTO 210
206  IF S3$ = "D" THEN GOTO 210
207  IF S3$ = "A" THEN GOTO 500
208  PRINT "TRY AGAIN"
209  GOTO 193
210  PRINT " "
211  PRINT "TYPE 'L' FOR LARGE CHANGES"
212  PRINT "(250 STEPS OR MORE)"
213  PRINT " "
214  PRINT "TYPE 'M' FOR MEDIUM CHANGES"
215  PRINT " "
216  PRINT " TYPE 'S' FOR SINGLE STEP CHANGES"
217  INPUT S4$
218  IF S4$ = "L" THEN GOTO 230
219  IF S4$ = "M" THEN GOTO 235
220  IF S4$ = "S" THEN GOTO 239
221  IF S4$ = "A" THEN GOTO 500
222  PRINT " INPUT CHARACTER INCORRECT"
223  PRINT "TRY AGAIN"
224  GOTO 210
230  POKE 33528,255
231  POKE 33842,255
232  GOTO 241
235  POKE 33528,20
236  POKE 33842,20
237  GOTO 241
239  POKE 33842,02
240  POKE 33528,02
241  PRINT " "
245  PRINT "TYPE 'Y' TO CHANGE SCALING FACTOR"
246  PRINT "TYPE 'N' TO USE EXISTING FACTOR"
247  INPUT S5$
250  IF S5$ = "N" THEN GOTO 265
251  IF S5$ = "Y" THEN GOTO 260
```

```
252  IF S5$ = "A" THEN GOTO 500
253  PRINT "INCORRECT INPUT TRY AGAIN"
254  GOTO 241
260  PRINT "TYPE IN SCALING FACTOR, FROM 1 TO 5"
261  PRINT "WHERE 1 IS FAST CHANGES"
262  INPUT FACT%
265  IF S3$ = "I" THEN GOTO 268
266  POKE 33230,0
267  GOTO 270
268  POKE 33230,1
270  IF S2$ = "S" THEN GOTO 370
271  IF CT = 0 THEN GOTO 285
272  POKE 33226,FACT%
273  CALL 33498
274  VE = PEEK (33224)
280  IF VE = 255 THEN GOTO 300
281  IF VE = 15 THEN GOTO 310
282  CALL - 936
283  PRINT "CHANGES IN THROTTLE SETTING YIELD:"
284  GOTO 125
285  POKE 33228,1
286  POKE 33229,0
287  POKE 33226,FACT%
288  POKE 33230,1
289  CALL 33498
290  CT = 1.0
295  PRINT "CHANGES IN THROTTLE SETTING YIELD:"
296  GOTO 125
300  PRINT "MAXIMUM THROTTLE SETTING"
301  PRINT "MAX THROTTLE SETTING YIELDS:"
302  GOTO 125
310  PRINT "MINIMUM THROTTLE SETTING"
311  PRINT "MIN THROTTLE SETTING YIELDS:"
312  GOTO 125
370  POKE 33794,FACT%
375  CALL 33802
380  V2 = PEEK (33797)
385  IF V2 = 255 THEN GOTO 410
386  IF V2 = 15 THEN GOTO 430
387  CALL - 936
388  PRINT " "
389  PRINT "CHANGE IN SETPOINT YIELDS:"
390  GOTO 125
410  CALL -936
411  PRINT "MAXIMUM SETPOINT SETTING"
412  PRINT " "
413  PRINT "MAX SETPOINT YIELDS:"
414  GOTO 125
430  CALL -936
431  PRINT "MINIMUM SETPOINT SETTING"
432  PRINT " "
433  PRINT "MIN SETPOINT YIELDS:"
```

```
434  GOTO 125
500  IC = PEEK (33486)
501  IF IC = 15 THEN GOTO 600
505  IF IC = 12 THEN GOTO 620
510  IF IC = 10 THEN GOTO 640
515  IF IC = 6 THEN GOTO 660
520  PRINT "INTERRUPT ERROR"
525  END
600  PRINT " ";"DYNO COOLANT PRESS TOO LOW"
605  GOTO 700
620  PRINT " ";"ENGINE OIL PRESS TOO LOW"
625  GOTO 700
640  PRINT " ";"ENGINE COOLANT TEMP TOO HIGH"
645  GOTO 700
660  PRINT " ";"DYNO COOLANT TEMP TOO HIGH"
700  PRINT " ";"INTERRUPT ENABLE REGISTER= ";FG
705  F1 = PEEK (32963)
710  PRINT "INTERRUPT FLAG REGISTER= ";F1
715  END
800  CALL - 936
801  CALL 32764
802  LSB = PEEK (32976)
803  MSB = PEEK (32977)
805  SP = (MSB * 256.0) + LSB
810  HS% = PEEK (33801)
811  LS% = PEEK (33800)
812  PRINT "ENGINE RPM= ";SP
814  PRINT " "
815  NM = (HS% * 256.0) + LS%
816  SF = NM * 1000.0 * 0.00122
817  PRINT "SETPOINT FOR RPM CONTROL= ";SF
822  L2 = 0
823  FOR X = 1 TO 10
824  POKE 49392,0
825  L1 = PEEK (49393) * 256.0 + PEEK(49392)
826  L2 = L2 + L1
827  NEXT
828  LD = L2 / 10.0 * 4.9988/ 4095.
829  L3 = 0
832  FOR X = 1 TO 10
833  POKE 49392,01
834  L4 = PEEK (49393) * 256.0 + PEEK (49392)
835  L3 = L3 + L4
836  NEXT
837  L5 = L3 / 10.0 * 4.9988 * 2.0 / 4095. * 100.0
838  L6 = 0
841  FOR X = 1 TO 10
842  POKE 49392,2
843  L7 = PEEK (49393) * 256.0 + PEEK (49392)
844  L6 = L6 + L7
845  NEXT
846  L8 = L6 / 10.0 * 4.9988 / 4095. * 4.0
```

```
848  CV = L5
849  PRINT " "
855  PRINT "ENGINE LOAD, IN Nm= ";CV
856  PRINT " "
857  PRINT " "
858  PRINT " "
859  PRINT " "
899  PRINT " "
900  PRINT "TYPE 'Y' TO SAVE THIS DATA"
901  PRINT " "
902  PRINT "TYPE 'N' TO EXIT"
903  INPUT S7$
904  IF S7$ = "Y" THEN GOTO 930
905  IF S7$ = "N" THEN GOTO 61
906  IF S7$ = "A" THEN GOTO 500
907  PRINT "INPUT INCORRECT TRY AGAIN"
908  GOTO 899
930  PRINT " "
931  PRINT " "
932  PRINT "TYPE IN FILENAME"
933  PRINT "DATA IS TO BE STORED IN"
934  INPUT FILE$
935  IF UF = 0 THEN GOTO 980
936  D$ = CHR(4)
937  PRINT D$;"APPEND";FILE$
938  PRINT D$;"WRITE";FILE$
939  PRINT SP
940  PRINT SF
941  PRINT CV
970  PRINT D$;"CLOSE";FILE$
972  PRINT "STATUS UPDATE AND DATA STORAGE COMPLETE"
973  GOTO 61
980  D$ = CHR$ (4)
981  PRINT D$;"OPEN";FILE$;",D2"
982  PRINT D$;"WRITE";FILE$
983  PRINT SP
984  PRINT SF
985  PRINT CV
1020 PRINT D$;"CLOSE";FILE$
1021 UF = 1.0
1022 GOTO 972
1023 END
1050 CALL - 936
1051 IF CC = 1 THEN GOTO 1115
1052 CC = 1
1053 PRINT " "
1054 PRINT "    FUEL + EMISSIONS MEASUREMENT"
1055 PRINT "             IN PROGRESS"
1065 PRINT " "
1066 PRINT " "
1067 CALL 36864
1075 PRINT " FUEL MEASUREMENT COMPLETE"
```

```
1076 PRINT " "
1077 PRINT " "
1080 PRINT "TYPE IN RANGE FOR EMISSIONS CHANNEL 3"
1081 INPUT E3
1082 PRINT " "
1085 PRINT "TYPE IN RANGE FOR EMISSIONS CHANNEL 4"
1086 INPUT E4
1087 PRINT " "
1090 PRINT "TYPE IN RANGE FOR EMISSIONS CHANNEL 5"
1091 INPUT E5
1092 PRINT " "
1095 PRINT "TYPE IN RANGE FOR EMISSIONS CHANNEL 6"
1096 INPUT E6
1097 PRINT " "
1100 PRINT "TYPE IN RANGE FOR EMISSIONS CHANNEL 7"
1101 INPUT E7
1102 PRINT " "
1105 PRINT "TYPE IN RANGE FOR EMISSIONS CHANNEL 8"
1106 INPUT E8
1107 PRINT " "
1110 CALL - 936
1115 PRINT " THE FOLLOWING RANGE VALUES HAVE BEEN SELECTED: "
1116 PRINT " "
1117 PRINT "CHANNEL 3: ";E3
1118 PRINT "CHANNEL 4: ";E4
1119 PRINT "CHANNEL 5: ";E5
1120 PRINT "CHANNEL 6: ";E6
1121 PRINT "CHANNEL 7: ";E7
1122 PRINT "CHANNEL 8: ";E8
1130 PRINT " "
1131 PRINT " "
1135 PRINT " TYPE 'Y' TO CHANGE"
1136 PRINT " TYPE 'N' TO CONTINUE"
1137 INPUT CR$
1140 IF CR$ = "Y" THEN GOTO 1076
1141 IF CR$ = "N" THEN GOTO 1150
1142 PRINT " "
1143 PRINT "INPUT INCORRECT TRY AGAIN"
1144 GOTO 1115
1150 PRINT "EMISSIONS AND FUEL COMPLETE"
1151 PRINT "RETURN TO MAIN PROGRAM"
1153 GOTO 61
1154 END
```

MACHINE LANGUAGE PROGRAM LISTING

MAIN

WRITTEN BY B.D. ROBERTS

```
7FFC    08          PHP
7FFD    EA          NOP
7FFE    48          PHA
7FFF    EA          NOP
8000    A9 00       LDA   #$00
8002    8D 36 80    STA   $8036
8005    A9 50       LDA   #$50
8007    EA          NOP
8008    EA          NOP
8009    EA          NOP
800A    EA          NOP
800B    EA          NOP
800C    EA          NOP
800D    EA          NOP
800E    EA          NOP
800F    A9 20       LDA   #$20
8011    8D DB C0    STA   $C0DB
8014    EA          NOP
8015    EA          NOP
8016    EA          NOP
8017    EA          NOP
8018    EA          NOP
8019    A9 C0       LDA   #$C0
801B    8D DE C0    STA   $C0DE
801E    A9 FF       LDA   #$FF
8020    8D D4 C0    STA   $C0D4
8023    A9 FF       LDA   #$FF
8025    8D D8 C0    STA   $C0D8
8028    A9 FF       LDA   #$FF
802A    8D D5 C0    STA   $C0D5
802D    A9 FF       LDA   #$FF
802F    8D D9 C0    STA   $C0D9
8032    4C 3A 80    JMP   $803A


803A    A9 10       LDA   #$10
803C    4D 36 80    EOR   $8036
803F    F0 03       BEQ   $8044
8041    4C 3A 80    JMP   $803A
8044    EA          NOP
8045    68          PLA
8046    28          PLP
8047    EA          NOP
8048    EA          NOP
8049    60          RTS
```

```
8050    08          PHP
8051    48          PHA
8052    EE 36 80    INC   $8036
8055    A9 0F       LDA   #$0F
8057    4D 36 80    EOR   $8036
805A    F0 1A       BEQ   $8076
805C    A9 C0       LDA   #$C0
805E    8D DE C0    STA   $C0DE
8061    A9 FF       LDA   #$FF
8063    8D D4 C0    STA   $C0D4
8066    A9 FF       LDA   #$FF
8068    8D D5 C0    STA   $C0D5
806B    68          PLA
806C    28          PLP
806D    40          RTI
806E    EA          NOP
806F    EA          NOP
8070    EA          NOP
8071    EA          NOP
8072    EA          NOP
8073    EA          NOP
8074    EA          NOP
8075    EA          NOP
8076    A9 80       LDA   #$80
8078    8D D4 C0    STA   $C0D4
807B    A9 8D       LDA   #$8D
807D    8D D5 C0    STA   $C0D5
8080    A9 90       LDA   #$90
8082    8D 22 81    STA   $8122
8085    A9 80       LDA   #$80
8087    8D 23 81    STA   $8123
808A    68          PLA
808B    28          PLP
808C    40          RTI
808D    EA          NOP
808E    EA          NOP
808F    EA          NOP
8090    48          PHA
8091    8A          TXA
8092    48          PHA
8093    EE 36 80    INC   $8036
8096    AD D8 C0    LDA   $C0D8
8099    8D D0 80    STA   $80D0
809C    AD D9 C0    LDA   $C0D9
809F    8D D1 80    STA   $80D1
80A2    A9 FF       LDA   #$FF
80A4    4D D0 80    EOR   $80D0
80A7    8D D0 80    STA   $80D0
80AA    A9 FF       LDA   #$FF
80AC    4D D1 80    EOR   $80D1
80AF    8D D1 80    STA   $80D1
```

```
80B2    20 DD FB    JSR   $FBDD
80B5    AD D4 C0    LDA   $C0D4
80B8    A9 50       LDA   #$50
80BA    8D 22 81    STA   $8122
80BD    4C C5 80    JMP   $80C5

80C5    68          PLA
80C6    AA          TAX
80C7    68          PLA
80C8    40          RTI

80DB    48          PHA
80DC    8A          TXA
80DD    48          PHA
80DE    98          TYA
80DF    48          PHA
80E0    A9 7F       LDA   #$7F
80E2    8D DE C0    STA   $C0DE
80E5    AD DD C0    LDA   $C0DD
80E8    8D D4 80    STA   $80D4
80EB    EA          NOP
80EC    EA          NOP
80ED    EA          NOP
80EE    EA          NOP
80EF    A9 03       LDA   #$03
80F1    2D DD C0    AND   $C0DD
80F4    F0 03       BEQ   $80F9
80F6    AD D1 C0    LDA   $C0D1
80F9    AD 91 C0    LDA   $C091
80FC    4C 01 81    JMP   $8101

8101    A9 40       LDA   #$40
8103    2D DD C0    AND   $C0DD
8106    F0 1C       BEQ   $8124
8108    EA          NOP
8109    EA          NOP
810A    EA          NOP
810B    EA          NOP
810C    EA          NOP
810D    EA          NOP
810E    EA          NOP
810F    EA          NOP
8110    EA          NOP
8111    EA          NOP
8112    A9 D0       LDA   #$D0
8114    8D DE C0    STA   $C0DE
8117    A9 0F       LDA   #$0F
8119    8D DE C0    STA   $C0DE
811C    68          PLA
```

```
811D    A8          TAY
811E    68          PLA
811F    AA          TAX
8120    68          PLA
8121    4C 50 80    JMP   $8050
8124    A9 10       LDA   #$10
8126    2D DD C0    AND   $C0DD
8129    D0 0D       BNE   $8138
812B    4C F0 85    JMP   $85F0
812E    EA          NOP
812F    EA          NOP
8130    EA          NOP
8131    EA          NOP
8132    EA          NOP
8133    EA          NOP
8134    EA          NOP
8135    EA          NOP
8136    EA          NOP
8137    EA          NOP
8138    A9 DE       LDA   #$DE
813A    8D DC C0    STA   $C0DC
813D    A9 F0       LDA   #$F0
813F    8D D3 C0    STA   $C0D3
8142    AD DF C0    LDA   $C0DF
8145    29 0F       AND   #$0F
8147    49 0E       EOR   #$0E
8149    D0 26       BNE   $8171
814B    AD DF C0    LDA   $C0DF
814E    29 0F       AND   #$0F
8150    49 0E       EOR   #$0E
8152    D0 1D       BNE   $8171
8154    A9 FE       LDA   #$FE
8156    8D DC C0    STA   $C0DC
8159    A9 FF       LDA   #$FF
815B    8D D3 C0    STA   $C0D3
815E    AD D1 C0    LDA   $C0D1
8161    A9 D0       LDA   #$D0
8163    8D DE C0    STA   $C0DE
8166    A9 0F       LDA   #$0F
8168    8D DE C0    STA   $C0DE
816B    4C 20 86    JMP   $8620
816E    00          BRK
816F    00          BRK
8170    00          BRK
8171    AD DF C0    LDA   $C0DF
8174    8D D9 82    STA   $82D9
8177    A9 FE       LDA   #$FE
8179    8D DC C0    STA   $C0DC
817C    A9 FF       LDA   #$FF
817E    8D D3 C0    STA   $C0D3
8181    A9 C8       LDA   #$C8
8183    20 ED FD    JSR   $FDED
```

```
8186    A9 C9       LDA   #$C9
8188    20 ED FD    JSR   $FDED
818B    A9 D4       LDA   #$D4
818D    20 ED FD    JSR   $FDED
8190    A9 A0       LDA   #$A0
8192    20 ED FD    JSR   $FDED
8195    A9 A7       LDA   #$A7
8197    20 ED FD    JSR   $FDED
819A    A9 40       LDA   #$40
819C    8D C0 80    STA   $80C0
819F    A9 10       LDA   #$10
81A1    8D 6E 83    STA   $836E
81A4    8D 92 83    STA   $8392
81A7    8D B6 83    STA   $83B6
81AA    A9 10       LDA   #$10
81AC    8D C0 84    STA   $84C0
81AF    8D E4 84    STA   $84E4
81B2    8D 08 85    STA   $8508
81B5    AD D1 C0    LDA   $C0D1
81B8    4C E2 81    JMP   $81E2


81E2    A9 1F       LDA   #$1F
81E4    8D D2 C0    STA   $C0D2
81E7    A9 FF       LDA   #$FF
81E9    8D D3 C0    STA   $C0D3
81EC    EA          NOP
81ED    EA          NOP
81EE    EA          NOP
81EF    EA          NOP
81F0    A9 03       LDA   #$03
81F2    8D D0 C0    STA   $C0D0
81F5    A9 FF       LDA   #$FF
81F7    8D DF C0    STA   $C0DF
81FA    48          PHA
81FB    08          PHP
81FC    A9 00       LDA   #$00
81FE    20 A8 FC    JSR   $FCA8
8201    28          PLP
8202    68          PLA
8203    A9 10       LDA   #$10
8205    8D D0 C0    STA   $C0D0
8208    48          PHA
8209    08          PHP
820A    A9 00       LDA   #$00
820C    20 A8 FC    JSR   $FCA8
820F    28          PLP
8210    68          PLA
8211    A9 04       LDA   #$04
8213    8D D0 C0    STA   $C0D0
8216    A9 FF       LDA   #$FF
8218    8D DF C0    STA   $C0DF
```

```
821B    48          PHA
821C    08          PHP
821D    A9 00       LDA   #$00
821F    20 A8 FC    JSR   $FCA8
8222    28          PLP
8223    68          PLA
8224    A9 10       LDA   #$10
8226    8D D0 C0    STA   $C0D0
8229    48          PHA
822A    08          PHP
822B    A9 00       LDA   #$00
822D    20 A8 FC    JSR   $FCA8
8230    28          PLP
8231    68          PLA
8232    A9 05       LDA   #$05
8234    8D D0 C0    STA   $C0D0
8237    48          PHA
8238    08          PHP
8239    A9 00       LDA   #$00
823B    20 A8 FC    JSR   $FCA8
823E    28          PLP
823F    68          PLA
8240    A9 10       LDA   #$10
8242    8D D0 C0    STA   $C0D0
8245    48          PHA
8246    08          PHP
8247    A9 00       LDA   #$00
8249    20 A8 FC    JSR   $FCA8
824C    28          PLP
824D    68          PLA
824E    A9 00       LDA   #$00
8250    8D D0 C0    STA   $C0D0
8253    A9 00       LDA   #$00
8255    8D DF C0    STA   $C0DF
8258    48          PHA
8259    08          PHP
825A    A9 00       LDA   #$00
825C    20 A8 FC    JSR   $FCA8
825F    28          PLP
8260    68          PLA
8261    A9 10       LDA   #$10
8263    8D D0 C0    STA   $C0D0
8266    48          PHA
8267    08          PHP
8268    A9 00       LDA   #$00
826A    20 A8 FC    JSR   $FCA8
826D    28          PLP
826E    68          PLA
826F    A9 01       LDA   #$01
8271    8D D0 C0    STA   $C0D0
8274    A9 00       LDA   #$00
8276    8D DF C0    STA   $C0DF
```

```
8279    48          PHA
827A    08          PHP
827B    A9 00       LDA   #$00
827D    20 A8 FC    JSR   $FCA8
8280    28          PLP
8281    68          PLA
8282    A9 10       LDA   #$10
8284    8D D0 C0    STA   $C0D0
8287    48          PHA
8288    08          PHP
8289    A9 00       LDA   #$00
828B    20 A8 FC    JSR   $FCA8
828E    28          PLP
828F    68          PLA
8290    A9 02       LDA   #$02
8292    8D D0 C0    STA   $C0D0
8295    48          PHA
8296    08          PHP
8297    A9 00       LDA   #$00
8299    20 A8 FC    JSR   $FCA8
829C    28          PLP
829D    68          PLA
829E    A9 C1       LDA   #$C1
82A0    20 ED FD    JSR   $FDED
82A3    A9 A7       LDA   #$A7
82A5    20 ED FD    JSR   $FDED
82A8    A9 A0       LDA   #$A0
82AA    20 ED FD    JSR   $FDED
82AD    A9 CB       LDA   #$CB
82AF    20 ED FD    JSR   $FDED
82B2    A9 C5       LDA   #$C5
82B4    20 ED FD    JSR   $FDED
82B7    A9 D9       LDA   #$D9
82B9    20 ED FD    JSR   $FDED
82BC    A9 C0       LDA   #$C0
82BE    8D DE C0    STA   $C0DE
82C1    AD D1 C0    LDA   $C0D1
82C4    68          PLA
82C5    A8          TAY
82C6    68          PLA
82C7    AA          TAX
82C8    68          PLA
82C9    40          RTI


82DA    48          PHA
82DB    08          PHP
82DC    8A          TXA
82DD    48          PHA
82DE    98          TYA
82DF    48          PHA
82E0    A9 00       LDA   #$00
```

```
82E2    8D CB 81    STA   $81CB
82E5    A9 00       LDA   #$00
82E7    8D C8 81    STA   $81C8
82EA    A9 1F       LDA   #$1F
82EC    8D D2 C0    STA   $C0D2
82EF    A9 FF       LDA   #$FF
82F1    8D D3 C0    STA   $C0D3
82F4    EE CB 81    INC   $81CB
82F7    A9 14       LDA   #$14
82F9    4D CB 81    EOR   $81CB
82FC    D0 07       BNE   $8305
82FE    68          PLA
82FF    A8          TAY
8300    68          PLA
8301    AA          TAX
8302    28          PLP
8303    68          PLA
8304    60          RTS
8305    A9 01       LDA   #$01
8307    2D CE 81    AND   $81CE
830A    F0 27       BEQ   $8333
830C    A9 FF       LDA   #$FF
830E    4D CC 81    EOR   $81CC
8311    F0 06       BEQ   $8319
8313    EE CC 81    INC   $81CC
8316    4C 5A 83    JMP   $835A
8319    A9 1F       LDA   #$1F
831B    4D CD 81    EOR   $81CD
831E    F0 0B       BEQ   $832B
8320    EE CD 81    INC   $81CD
8323    A9 00       LDA   #$00
8325    8D CC 81    STA   $81CC
8328    4C 5A 83    JMP   $835A
832B    A9 FF       LDA   #$FF
832D    8D C8 81    STA   $81C8
8330    4C FE 82    JMP   $82FE
8333    A9 00       LDA   #$00
8335    4D CC 81    EOR   $81CC
8338    F0 06       BEQ   $8340
833A    CE CC 81    DEC   $81CC
833D    4C 5A 83    JMP   $835A
8340    A9 00       LDA   #$00
8342    4D CD 81    EOR   $81CD
8345    F0 0B       BEQ   $8352
8347    CE CD 81    DEC   $81CD
834A    A9 FF       LDA   #$FF
834C    8D CC 81    STA   $81CC
834F    4C 5A 83    JMP   $835A
8352    A9 0F       LDA   #$0F
8354    8D C8 81    STA   $81C8
8357    4C FE 82    JMP   $82FE
835A    EE FA 83    INC   $83FA
```

```
835D    A9 18       LDA   #$18
835F    4D FA 83    EOR   $83FA
8362    D0 A1       BNE   $8305
8364    A9 00       LDA   #$00
8366    8D FA 83    STA   $83FA
8369    EA          NOP
836A    EA          NOP
836B    EA          NOP
836C    EA          NOP
836D    A9 00       LDA   #$00
836F    8D D0 C0    STA   $C0D0
8372    AD CC 81    LDA   $81CC
8375    8D DF C0    STA   $C0DF
8378    48          PHA
8379    08          PHP
837A    AD CF 81    LDA   $81CF
837D    20 A8 FC    JSR   $FCA8
8380    28          PLP
8381    68          PLA
8382    A9 10       LDA   #$10
8384    8D D0 C0    STA   $C0D0
8387    48          PHA
8388    08          PHP
8389    AD CF 81    LDA   $81CF
838C    20 A8 FC    JSR   $FCA8
838F    28          PLP
8390    68          PLA
8391    A9 01       LDA   #$01
8393    8D D0 C0    STA   $C0D0
8396    AD CD 81    LDA   $81CD
8399    8D DF C0    STA   $C0DF
839C    48          PHA
839D    08          PHP
839E    AD CF 81    LDA   $81CF
83A1    20 A8 FC    JSR   $FCA8
83A4    28          PLP
83A5    68          PLA
83A6    A9 10       LDA   #$10
83A8    8D D0 C0    STA   $C0D0
83AB    48          PHA
83AC    08          PHP
83AD    AD CF 81    LDA   $81CF
83B0    20 A8 FC    JSR   $FCA8
83B3    28          PLP
83B4    68          PLA
83B5    A9 02       LDA   #$02
83B7    8D D0 C0    STA   $C0D0
83BA    48          PHA
83BB    08          PHP
83BC    AD CF 81    LDA   $81CF
83BF    20 A8 FC    JSR   $FCA8
83C2    28          PLP
```

```
83C3    68          PLA
83C4    A9 10       LDA   #$10
83C6    8D D0 C0    STA   $C0D0
83C9    48          PHA
83CA    08          PHP
83CB    AD CF 81    LDA   $81CF
83CE    20 A8 FC    JSR   $FCA8
83D1    28          PLP
83D2    68          PLA
83D3    A9 00       LDA   #$00
83D5    8D C9 81    STA   $81C9
83D8    EE C9 81    INC   $81C9
83DB    48          PHA
83DC    08          PHP
83DD    A9 00       LDA   #$00
83DF    20 A8 FC    JSR   $FCA8
83E2    28          PLP
83E3    68          PLA
83E4    AD C9 81    LDA   $81C9
83E7    4D CA 81    EOR   $81CA
83EA    F0 03       BEQ   $83EF
83EC    4C D8 83    JMP   $83D8
83EF    4C F4 82    JMP   $82F4

840B    08          PHP
840C    8A          TXA
840D    48          PHA
840E    98          TYA
840F    48          PHA
8410    A9 00       LDA   #$00
8412    8D 06 84    STA   $8406
8415    A9 00       LDA   #$00
8417    8D 07 84    STA   $8407
841A    A9 00       LDA   #$00
841C    8D 05 84    STA   $8405
841F    EA          NOP
8420    EA          NOP
8421    EA          NOP
8422    EA          NOP
8423    EA          NOP
8424    A9 1F       LDA   #$1F
8426    8D D2 C0    STA   $C0D2
8429    A9 FF       LDA   #$FF
842B    8D D3 C0    STA   $C0D3
842E    EE 06 84    INC   $8406
8431    A9 02       LDA   #$02
8433    EA          NOP
8434    EA          NOP
8435    EA          NOP
8436    EA          NOP
8437    EA          NOP
```

```
8438    EA          NOP
8439    EA          NOP
843A    EA          NOP
843B    EA          NOP
843C    EA          NOP
843D    4D 06 84    EOR   $8406
8440    D0 07       BNE   $8449
8442    68          PLA
8443    A8          TAY
8444    68          PLA
8445    AA          TAX
8446    28          PLP
8447    68          PLA
8448    60          RTS
8449    A9 01       LDA   #$01
844B    2D CE 81    AND   $81CE
844E    F0 27       BEQ   $8477
8450    A9 FF       LDA   #$FF
8452    4D 08 84    EOR   $8408
8455    F0 06       BEQ   $845D
8457    EE 08 84    INC   $8408
845A    4C AB 84    JMP   $84AB
845D    A9 09       LDA   #$09
845F    4D 09 84    EOR   $8409
8462    F0 0B       BEQ   $846F
8464    EE 09 84    INC   $8409
8467    A9 00       LDA   #$00
8469    8D 08 84    STA   $8408
846C    4C AB 84    JMP   $84AB
846F    A9 FF       LDA   #$FF
8471    8D 05 84    STA   $8405
8474    4C 42 84    JMP   $8442
8477    A9 E0       LDA   #$E0
8479    4D 08 84    EOR   $8408
847C    F0 18       BEQ   $8496
847E    A9 00       LDA   #$00
8480    4D 08 84    EOR   $8408
8483    F0 06       BEQ   $848B
8485    CE 08 84    DEC   $8408
8488    4C AB 84    JMP   $84AB
848B    CE 09 84    DEC   $8409
848E    A9 FF       LDA   #$FF
8490    8D 08 84    STA   $8408
8493    4C AB 84    JMP   $84AB
8496    A9 03       LDA   #$03
8498    4D 09 84    EOR   $8409
849B    F0 06       BEQ   $84A3
849D    CE 08 84    DEC   $8408
84A0    4C AB 84    JMP   $84AB
84A3    A9 0F       LDA   #$0F
84A5    8D 05 84    STA   $8405
84A8    4C 42 84    JMP   $8442
```

```
84AB    EE 07 84    INC   $8407
84AE    A9 06       LDA   #$06
84B0    4D 07 84    EOR   $8407
84B3    D0 94       BNE   $8449
84B5    A9 00       LDA   #$00
84B7    8D 07 84    STA   $84 07
84BA    EA          NOP
84BB    EA          NOP
84BC    EA          NOP
84BD    EA          NOP
84BE    EA          NOP
84BF    A9 03       LDA   #$03
84C1    8D D0 C0    STA   $C0D0
84C4    AD 08 84    LDA   $8408
84C7    8D DF C0    STA   $C0DF
84CA    48          PHA
84CB    08          PHP
84CC    AD 04 84    LDA   $8404
84CF    20 A8 FC    JSR   $FCA8
84D2    28          PLP
84D3    68          PLA
84D4    A9 10       LDA   #$10
84D6    8D D0 C0    STA   $C0D0
84D9    48          PHA
84DA    08          PHP
84DB    AD 04 84    LDA   $8404
84DE    20 A8 FC    JSR   $FCA8
84E1    28          PLP
84E2    68          PLA
84E3    A9 04       LDA   #$04
84E5    8D D0 C0    STA   $C0D0
84E8    AD 09 84    LDA   $8409
84EB    8D DF C0    STA   $C0DF
84EE    48          PHA
84EF    08          PHP
84F0    AD 04 84    LDA   $8404
84F3    20 A8 FC    JSR   $FCA8
84F6    28          PLP
84F7    68          PLA
84F8    A9 10       LDA   #$10
84FA    8D D0 C0    STA   $C0D0
84FD    48          PHA
84FE    08          PHP
84FF    AD 04 84    LDA   $8404
8502    20 A8 FC    JSR   $FCA8
8505    28          PLP
8506    68          PLA
8507    A9 05       LDA   #$05
8509    8D D0 C0    STA   $C0D0
850C    48          PHA
850D    08          PHP
850E    AD 04 84    LDA   $8404
```

```
8511    20 A8 FC    JSR   $FCA8
8514    28          PLP
8515    68          PLA
8516    A9 10       LDA   #$10
8518    8D D0 C0    STA   $C0D0
851B    48          PHA
851C    08          PHP
851D    AD 04 84    LDA   $8404
8520    20 A8 FC    JSR   $FCA8
8523    28          PLP
8524    68          PLA
8525    A9 00       LDA   #$00
8527    8D 03 84    STA   $8403
852A    EE 03 84    INC   $8403
852D    48          PHA
852E    08          PHP
852F    A9 00       LDA   #$00
8531    20 A8 FC    JSR   $FCA8
8534    28          PLP
8535    68          PLA
8536    AD 03 84    LDA   $8403
8539    4D 02 84    EOR   $8402
853C    F0 03       BEQ   $8541
853E    4C 2A 85    JMP   $852A
8541    4C 2E 84    JMP   $842E
8560    08          PHP
8561    48          PHA
8562    A9 FE       LDA   #$FE
8564    8D DC C0    STA   $C0DC
8567    A9 90       LDA   #$90
8569    8D DE C0    STA   $C0DE
856C    A9 0F       LDA   #$0F
856E    8D DE C0    STA   $C0DE
8571    A9 DB       LDA   #$DB
8573    8D FE 03    STA   $03FE
8576    A9 80       LDA   #$80
8578    8D FF 03    STA   $03FF
857B    68          PLA
857C    28          PLP
857D    60          RTS


8590    48          PHA
8591    08          PHP
8592    8A          TXA
8593    48          PHA
8594    98          TYA
8595    48          PHA
8596    A9 80       LDA   #$80
8598    2D 00 C0    AND   $C000
859B    F0 0D       BEQ   $85AA
859D    AD 00 C0    LDA   $C000
```

```
85A0    8D C1 80    STA   $80C1
85A3    68          PLA
85A4    A8          TAY
85A5    68          PLA
85A6    AA          TAX
85A7    28          PLP
85A8    68          PLA
85A9    60          RTS
85AA    A9 40       LDA   #$40
85AC    2D C0 80    AND   $80C0
85AF    F0 07       BEQ   $85B8
85B1    68          PLA
85B2    A8          TAY
85B3    68          PLA
85B4    AA          TAX
85B5    28          PLP
85B6    68          PLA
85B7    60          RTS
85B8    4C 96 85    JMP   $8596

85C0    48          PHA
85C1    08          PHP
85C2    8A          TXA
85C3    48          PHA
85C4    98          TYA
85C5    48          PHA
85C6    AD D1 C0    LDA   $C0D1
85C9    AD D0 C0    LDA   $C0D0
85CC    AD D8 C0    LDA   $C0D8
85CF    AD D4 C0    LDA   $C0D4
85D2    AD DA C0    LDA   $C0DA
85D5    58          CLI
85D6    68          PLA
85D7    A8          TAY
85D8    68          PLA
85D9    AA          TAX
85DA    28          PLP
85DB    68          PLA
85DC    60          RTS

85F0    AD 91 C0    LDA   $C091
85F3    AD 90 C0    LDA   $C090
85F6    AD 98 C0    LDA   $C098
85F9    AD 94 C0    LDA   $C094
85FC    AD 9A C0    LDA   $C09A
85FF    AD D1 C0    LDA   $C0D1
8602    AD D0 C0    LDA   $C0D0
8605    AD D8 C0    LDA   $C0D8
8608    AD DA C0    LDA   $C0DA
860B    4C 38 81    JMP   $8138
```

```
8620    AD 91 C0    LDA   $C091
8623    AD 90 C0    LDA   $C090
8626    AD 98 C0    LDA   $C098
8629    AD 94 C0    LDA   $C094
862C    AD 9A C0    LDA   $C09A
862F    AD D1 C0    LDA   $C0D1
8632    AD D0 C0    LDA   $C0D0
8635    AD D8 C0    LDA   $C0D8
8638    AD DA C0    LDA   $C0DA
863B    68          PLA
863C    A8          TAY
863D    68          PLA
863E    AA          TAX
863F    68          PLA
8640    40          RTI


9000    8D FF 8F    LDA   $8FFF
9003    49 01       EOR   #$01
9005    F0 08       BEQ   $900F
9007    A9 01       LDA   #$01
9009    8D FF 8F    STA   $8FFF
900C    20 15 92    JSR   $9215
900F    A9 00       LDA   #$00
9011    8D FE 8F    STA   $8FFE
9014    EA          NOP
9015    EA          NOP
9016    EA          NOP
9017    A9 01       LDA   #$01
9019    2D FD 8F    AND   $8FFD
901C    D0 1E       BNE   $903C
901E    EE FE 8F    INC   $8FFE
9021    48          PHA
9022    08          PHP
9023    A9 FF       LDA   #$FF
9025    20 A8 FC    JSR   $FCA8
9028    28          PLP
9029    68          PLA
902A    A9 3C       LDA   #$3C
902C    4D FE 8F    EOR   $8FFE
902F    F0 03       BEQ   $9034
9031    4C 17 90    JMP   $9017
9034    A9 AB       LDA   #$AB
9036    20 ED FD    JSR   $FDED
9039    4C 0F 90    JMP   $900F
903C    A9 00       LDA   #$00
903E    8D FD 8F    STA   $8FFD
9041    A9 00       LDA   #$00
9043    8D FE 8F    STA   $8FFE
9046    A9 00       LDA   #$00
```

```
9048    8D FF 8F    STA   $8FFF
904B    60          RTS
```

FUEL WEIGHING

WRITTEN BY A.R. SCHROEDER

```
9200    A9 55       LDA   #$55
9202    8D 9C C0    STA   $C09C
9205    A9 03       LDA   #$03
9207    8D 9B C0    LDA   $C09B
920A    A9 FF       LDA   #$FF
920C    8D 92 C0    STA   $C092
920F    A9 04       LDA   #$04
9211    8D 90 C0    STA   $C090
9214    60          RTS
9215    A9 01       LDA   #$01
9217    8D 90 C0    STA   $C090
921A    A9 FF       LDA   #$FF
921C    8D 94 C0    STA   $C094
921F    8D 95 C0    STA   $C095
9222    8D 9D C0    STA   $C09D
9225    A9 D0       LDA   #$D0
9227    8D 9E C0    STA   $C09E
922A    A9 00       LDA   #$00
922C    8D A1 92    STA   $92A1
922F    8D A2 92    STA   $92A2
9232    8D A3 92    STA   $92A3
9235    60          RTS
9236    48          PHA
9237    8A          TXA
9238    48          PHA
9239    98          TYA
923A    48          PHA
923B    A9 40       LDA   #$40
923D    2C 9D C0    BIT   $C09D
9240    D0 03       BNE   $9245
9242    4C 60 92    JMP   $9260
9245    A9 FF       LDA   #$FF
9247    8D 94 C0    STA   $C094
924A    8D 95 C0    STA   $C095
924D    A9 C0       LDA   #4C0
924F    8D 9E C0    STA   $C09E
9252    EE A1 92    INC   $92A1
9255    D0 03       BNE   $925A
9257    EE A2 92    INC   $92A2
925A    68          PLA
925B    A8          TAY
925C    68          PLA
925D    AA          TAX
```

```
925E    68          PLA
925F    40          RTI
9260    EE A3 92    INC   $92A3
9263    AD A2 92    LDA   $92A2
9266    C9 03       CMP   #$03
9268    90 07       BCC   $9271
926A    D0 05       BNE   $9271
926C    AD A1 92    LDA   $92A1
926F    C9 A9       CMP   #$A9
9271    90 03       BCC   $9276
9273    4C 91 92    JMP   $9291
9276    AD 90 C0    LDA   $C090
9279    09 02       ORA   #$02
927B    8D 90 C0    STA   $C090
927E    AD 90 C0    LDA   $C090
9281    29 FD       AND   #$FD
9283    8D 90 C0    STA   $C090
9286    A9 90       LDA   #$90
9288    8D 9E C0    STA   $C09E
928B    68          PLA
928C    A8          TAY
928D    68          PLA
928E    AA          TAX
928F    68          PLA
9290    40          RTI
9291    A9 40       LDA   #$40
9293    8D 9E C0    STA   $C09E
9296    A9 04       LDA   #$04
9298    8D 90 C0    STA   $C090
929B    68          PLA
929C    A8          TAY
929D    68          PLA
929E    AA          TAX
929F    68          PLA
92A0    40          RTI
```

Applesoft Program Listing

Data Acquisition

Written by A.R. Schroeder

```
10   HIMEM: 36864
20   DIM A(15)
30   D$ =  CHR$(4)
40   PRINT D$;"BLOAD FWR,D1"
50   POKE 1022,203
60   POKE 1023,146
70   CALL 37376
80   HOME : VTAB 10: HTAB 15
90   PRINT " START ENGINE"
100  VTAB 20: HTAB 11
110  PRINT "ANY KEY TO CONTINUE"
120  GET K$: HOME
130  VTAB 10: INPUT "  ENTER TODAY'S DATE:";DA$
140  AP=38.3
150  HOME
160  HTAB 12 : PRINT "HIT 'R' TO READ" : PRINT
170  HTAB 9: PRINT "HIT 'D' TO TAKE DATA" : PRINT
180  PRINT : HTAB 12
190  PRINT "TEMP. (CELSIUS)" : PRINT
200  HTAB 29: PRINT "INTAKE"
210  PRINT "     STACK      COOLANT    MANIFOLD"
220  POKE 34,10
230  HOME
240  GET K$
250  IF ASC(K$) = 68 THEN 630
260  IF ASC(K$) = 82 THEN 280
270  GOTO 240
280  ST=0:CO=0:OI=0:AM=0
290  FOR I=1 TO 10
300  POKE -16144, (7+16)
310  RESULT = PEEK(-16143)*256 + PEEK (-16144)
320  V = RESULT/4096
330  ST = ST + V * 996.512
340  POKE -16144,(8 + 16)
350  RESULT = PEEK (-16143) * 256 + PEEK (-16144)
360  V = RESULT/4096
370  CO = CO + V*195.791
380  POKE -16144,(6+16)
390  RESULT = PEEK(-16143) *256 + PEEK (-16144)
400  V = RESULT/ 4096
410  OI=OI+V*198.61
420  POKE -16144,(3+16)
430  RESULT = PEEK(-16143) *256 +PEEK (-16144)
440  V=RESULT/ 4096
450  AM = AM + V * 96.386
460  NEXT I
```

```
470  ST = ST/10
480  CO = CO/10
490  OI = OI/10
500  AM = AM/10
510  ST$ = STR$ (ST)
520  CO$ = STR$ (CO)
530  OI$ = STR$ (OI)
540  AM$ = STR$ (AM)
550  AM$ = LEFT$ (AM$,5)
560  ST$ = LEFT$ (ST$,6)
570  CO$ = LEFT$ (CO$,5)
580  OI$ = LEFT$ (OI$,5)
590  HTAB 6: PRINT ST$;
600  HTAB 18: PRINT CO$;
610  HTAB 30: PRINT OI$
620  GOTO 240
630  TEXT : HOME : VTAB 10
640  INPUT "  ENTER TIME:. "; TM$
650  PRINT : INPUT "  ENTER HOURS : ";HR$
655  PRINT : INPUT " ENTER DIES. FUEL TEMP. (F):";TZ
656  TZ = (TZ-32) / 1.8
660  HOME : VTAB 10
670  PRINT " AMBIENT TEMP.= ";AM$;: PRINT "  (C)"
675  VTAB 15: HTAB 10: PRINT "ANY KEY TO CONTINUE": GET K$
680  HOME : VTAB 4
690  INPUT "  ENTER SPEED  (RPM): ";RPM
700  PRINT : INPUT "  ENTER TORQUE  (Nm): ";TQ
710  HOME : VTAB4: HTAB 14: PRINT "TAKING DATA"
720  POKE 34,7: HOME
730  J=0
740  POKE 37571,0
750  CALL 37551
760  TI= PEEK (37569) * 256 +PEEK (37568)
770  TI = TI * 0.06408
780  VO = PEEK (37570)
790  PRINT " DIES. FUEL TIME= "; TI;: PRINT " (SEC)"
800  PRINT : PRINT "  VOLUMES= "; VO
810  PRINT : PRINT : PRINT : HTAB 10
820  PRINT "ANY KEY TO CONTINUE"
830  GET K$
831  HOME : INPUT " ETHANOL TIME (SEC)?  ";TE
832  PRINT : INPUT " # OF VOLUMES? ";VE
833  IF VE = 1 THEN VE=215
834  IF VE = 2 THEN VE=425
835  IF VE = 3 THEN VE=635
840  IF VO = 1 THEN VF=90
850  IF VO = 2 THEN VF=258
860  IF VO = 3 THEN VF=740
870  HOME :BP = 6.2832 * TQ *RPM / 60000
880  BMEP = BP * 120 / (RPM * 7.141E - 3)
890  DFU = 141.5 / (AP + 131.5)
891  DFU = DFU - .00063 * (TZ - 15)
```

```
892  DFU = DFU *997
893  DE = 783
894  ME = (VE / TE) * DE / 1E6
895  MF = (VF / TI) * DFU / 1E6
896  PE = ME * 26900 * 100 / (MF * 42781 + ME * 26900)
901  MS = RPM * 127 / 30000
902  FMEP = 136.6 + 0.1371 * (MS - 3)^3 -0.8488 * (MS-3)^2 +
            17.553 * (MS - 3)
903  IMEP = BMEP + FMEP
904  IP = IMEP * RPM * 7.141 / 120000
910  PRINT "  SPEED= ";RPM;: PRINT "  (RPM)"
920  PRINT "  TORQUE= ";TQ;: PRINT "  (Nm)"
925  PRINT "  IND. POWER= ";IP;: PRINT "  (KW)"
930  PRINT "  BRAKE POWER= ";BP;: PRINT "  (KW)"
935  PRINT "  IMEP= ";IMEP;: PRINT "  (KPA)"
940  PRINT "  BMEP= ";BMEP;: PRINT "  (KPA)"
955  PRINT "  % ETHANOL BY ENERGY = ";PE
960  PRINT : PRINT : PRINT
970  HTAB 10: PRINT "ANY KEY TO CONTINUE"
980  GET K$
990  HOME
1000 FOR I=1 TO 14
1010 A(I) = 0
1020 NEXT I
1030 POKE 49362,15
1040 FOR I=1 TO 100
1050 FOR K=1 TO 8
1060 POKE - 16144,(K + 18)
1070 RESULT =PEEK ( - 16143) * 256 + PEEK ( - 16144)
1080 V = RESULT / 4096
1090 A(K) = A(K) + V
1100 NEXT K
1110 FOR K=9 TO 11
1120 POKE - 16144,(K + 2)
1130 RESULT = PEEK ( - 16143) * 256 + PEEK( - 16144)
1140 V = RESULT * 5 / 4096
1150 A(K) = A(K) + V
1160 NEXT K
1170 L = 7
1180 FOR K = 12 TO 14
1190 POKE 49360,L
1200 POKE - 16144,15
1210 RESULT = PEEK ( -16143) * 256 + PEEK ( - 16144)
1220 V = RESULT * 5 / 4096
1230 A(K) = A(K) + V
1240 L = L - 1
1250 NEXT K
1260 NEXT I
1270 FOR I = 1 TO 14
1280 A(I) = A(I) / 100
1290 NEXT I
1300 TEXT : HOME : POKE 34,7: HOME
```

```
1310 INPUT "  ENTER WET BULB  (F): ";TW: PRINT
1320 INPUT "  ENTER AIR FLOW  (E-3 m^3/s): ";MA: PRINT
1330 TW = (TW - 32) / 1.8
1340 MA = MA * 0.001
1350 INPUT "  ENTER AMB. PRESS. (KPA): ";PAMB: PRINT
1360 INPUT "  ENTER MAN. PRESS. (KPA): ";PMAN: HOME
1365 A(1) = A(1) * 96.386
1366 A(4) = A(4) * 198.61
1370 DMAN = PMAN / (.287 * (A(4) + 273.15))
1380 DAMP = PAMB / (.287 * (A(1) + 273.15))
1390 MA = MA * DAMB
1400 MT = DMAN * RPM * 7.141E-3 / 120
1410 NV = MA / MT
1425 BTH = BP / (MF * 42781 + ME * 26900)
1426 ITH = IP / (MF * 42781 + ME * 26900)
1430 PRINT "  VOLUMETRIC EFF.= ";NV
1435 PRINT : PRINT "  IND. THERM. EFF.= ";ITH
1436 PRINT : PRINT "  BRAKE THERM. EFF.= ";BTH
1450 VTAB 17: HTAB 10
1460 PRINT "ANY KEY TO CONTINUE"
1470 GET K$: HOME
1480 HTAB 15: PRINT "TEMP. (C)": PRINT
1500 PRINT "  AMBIENT= ";A(1)
1510 A(2) = A(2) * 100.523
1520 PRINT "  COMP. INLET= ";A(2)
1530 A(3) = A(3) * 978.953
1540 PRINT "  TURB. INLET= ";A(3)
1560 PRINT "  COMP. OUTLET= ";A(4)
1570 A(5) = A(5) * 996.512
1580 PRINT "  TURB. OUTLET= ";A(5)
1590 A(6) = A(6) * 195.791
1600 PRINT "  COOLANT= ";A(6)
1610 PRINT : PRINT
1620 HTAB 10: PRINT "ANY KEY TO CONTINUE"
1630 GET K$
1640 HOME
1650 INPUT "  ENTER 'O2' RANGE (%): ";O2: PRINT
1660 INPUT "  ENTER 'NO' RANGE (ppm): ";NO: PRINT
1670 INPUT "  ENTER 'FID' MULTIPLIER: ";FID: PRINT
1680 INPUT " LCO (L) OR HCO (H)? ";CM$
1684 PRINT
1685 INPUT "  ENTER SMOKE #: ";SM$
1690 HOME
1700 CD = 0.1484 * (A(12)^3)-0.3936 * (A(12)^2) + 1.2 * A(12)
1710 A(12)=CD
1720 HCO = 0.0913 * (A(14)^3) - 0.306 * (A(14)^2) + 1.1892 *
          A(14)
1730 A(14) = HCO
1740 LCO = 0.0019 * (A(13)^3) - 0.0035 * (A(13)^2) + 0.0499 *
          A(13)
1750 A(13) = LCO
1760 A(9) = A(9) * O2 / 5
```

```
1770 A(10) = A(10) * NO / 5
1780 A(11) = A(11) * FID * (1039 / 5)/ 100
1790 HTAB 15: PRINT "EMISSIONS": PRINT
1800 PRINT "  OXYGEN= ";A(9);: PRINT " %"
1810 PRINT "  NO= ";A(10);: PRINT " (ppm)"
1820 PRINT "  FID= ";A(11);:PRINT " (ppm)"
1830 PRINT "  CO2= ";A(12);: PRINT " %"
1840 PRINT "  LCO= ";A(13);: PRINT " %"
1850 PRINT "  HCO= ";A(14);: PRINT " %"
1860 PRINT : PRINT
1870 HTAB 10: PRINT "ANY KEY TO CONTINUE"
1880 GET K$
1890 HOME
1900 PRINT "  WRITE DATA TO DISK ?  (Y/N)";
1910 GET K$
1920 IF K$ = "N" THEN 2250
1930 IF K$ = "Y" THEN 1950
1940 GOTO 1910
1950 PRINT : PRINT
1960 INPUT "  ENTER NAME OF DATA FILE: ";NA$
1970 HOME
1980 PRINT D$;"OPEN ";NA$;",D2"
1990 PRINT D$; "WRITE ";NA$
2000 PRINT DA$
2010 PRINT TM$
2020 PRINT HR$
2025 PRINT SM$
2030 PRINT RPM
2040 PRINT TQ
2050 PRINT BP
2060 PRINT BMEP
2080 PRINT NV
2091 PRINT PMAN
2092 PRINT PAMB
2093 PRINT MA
2094 PRINT BTH
2095 PRINT TW
2100 FOR I = 1 TO 6
2110 PRINT A(I)
2120 NEXT I
2130 FOR I = 9 TO 12
2140 PRINT A(I)
2150 NEXT I
2160 IF CM$ = "L" THEN 2190
2170 PRINT A(14)
2180 GOTO 2200
2190 PRINT A(13)
2200 PRINT IMEP
2210 PRINT IP
2230 PRINT ITH
2235 PRINT PE
2236 PRINT MF
```

```
2237 PRINT ME
2240 PRINT D$;"CLOSE ";NA$
2250 TEXT
2260 GOTO 150
```

APPLESOFT PROGRAM LISTING

DATA DISK CONVERSION

WRITTEN BY B.D. ROBERTS

```
5    D$ = CHR$ (4)
10   PRINT "TYPE IN FILE NAME"
15   INPUT FI$
20   PRINT "DATA DISK SHOULD BE IN DRIVE"
25   PRINT " "
30   PRINT "TYPE ANY KEY WHEN READY"
35   INPUT K$
40   PRINT D$;"OPEN";FI$
45   PRINT D$;"READ";FI$
46   INPUT CS$
50   INPUT CT$
55   INPUT CU$
60   INPUT CV$
65   INPUT D1
70   INPUT D2
75   INPUT D3
80   INPUT D4
85   INPUT D5
90   INPUT D6
95   INPUT D7
100  INPUT D8
105  INPUT D9
110  INPUT E1
115  INPUT E2
120  INPUT E3
125  INPUT E4
130  INPUT E5
135  INPUT E6
140  INPUT E7
145  INPUT E8
150  INPUT E9
155  INPUT F1
160  INPUT F2
165  INPUT F3
170  INPUT F4
175  INPUT F5
```

```
180  INPUT F6
185  INPUT F7
190  INPUT F8
195  INPUT F9
200  PRINT D$;"CLOSE";FI$
201  PRINT D$;"PR#3"
205  PRINT "DATE:";CS$;"    HR:";CV$;"    TIME:";CT$
210  PRINT "RPM= ";D1
215  PRINT "TORQUE= ";D2;"  (NM)"
220  PRINT "IND. POWER= ";F5;"  (KW)"
225  PRINT "BRAKE POWER= ";D3;"  (KW)"
230  PRINT "IMEP= ";F4;"  (KPA)"
235  PRINT "BMEP= ";D4;"  (KPA)"
240  PRINT "IND. THERM. EFF.= ";F6
245  PRINT "BRAKE THERM. EFF.= ";D9
250  PRINT "VOL. EFF.= ";D5
255  PRINT "MASS AIR= ";D8;"  (KG/S)"
260  PRINT "MAN. PRESS.= ";D6;"  (KPA)"
265  PRINT "AMB. PRESS.= ";D7;"  (KPA)"
270  PRINT "WET BULB TEMP.= ";E1;"  (C)"
275  PRINT "AMB. TEMP.= ";E2;"  (C)"
280  PRINT "COMP. INLET TEMP.= ";E3;"  (C)"
285  PRINT "COMP. OUTLET TEMP.= ";E5;"  (C)"
290  PRINT "TURB. INLET TEMP.= ";E4;"  (C)"
295  PRINT "TURB. OUTLET TEMP.= ";E6;"  (C)"
300  PRINT "COOLANT TEMP.= ";E7;"  (C)"
305  PRINT "OXYGEN= ";E8;"  (%)"
310  PRINT "NO= ";E9;"  (PPM)"
315  PRINT "HC= ";F1;"  (PPM PROPANE EQUIV.)"
320  PRINT "CO2= ";F2;"  (%)"
325  PRINT "CO= ";F3;"  (%)"
330  PRINT "SMOKE # = ";CV$
335  PRINT "% ENERGY FROM ETHANOL = ";F7
340  PRINT "MASS FLOW DIESEL= ";F8;"  (KG/S)"
345  PRINT "MASS FLOW ETHANOL= ";F9;"  (KG/S)"
350  BB = F8 / D3 * 3600.0 * 1000.0
355  PRINT "BSDFC= ";BB;"  (G/KW-HR)"
360  END
```

10. CIRCUITS FOR INTERFACING DIGALOG CONTROLLERS AND COMPUTER

INTERUPT BOARD

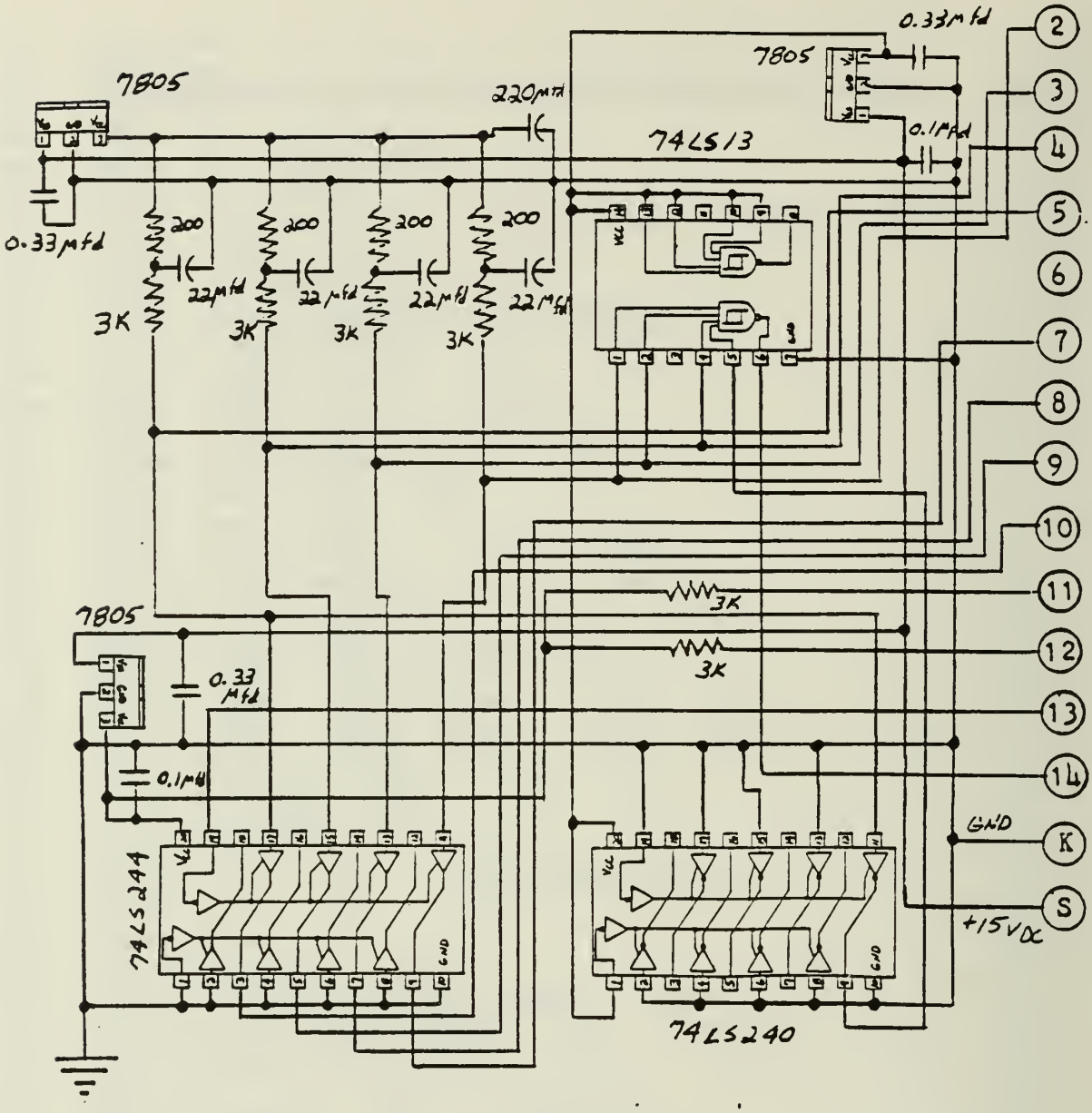

○ -- CINCH CONNECTER PIN

DAC CONTROL LOGIC BOARD

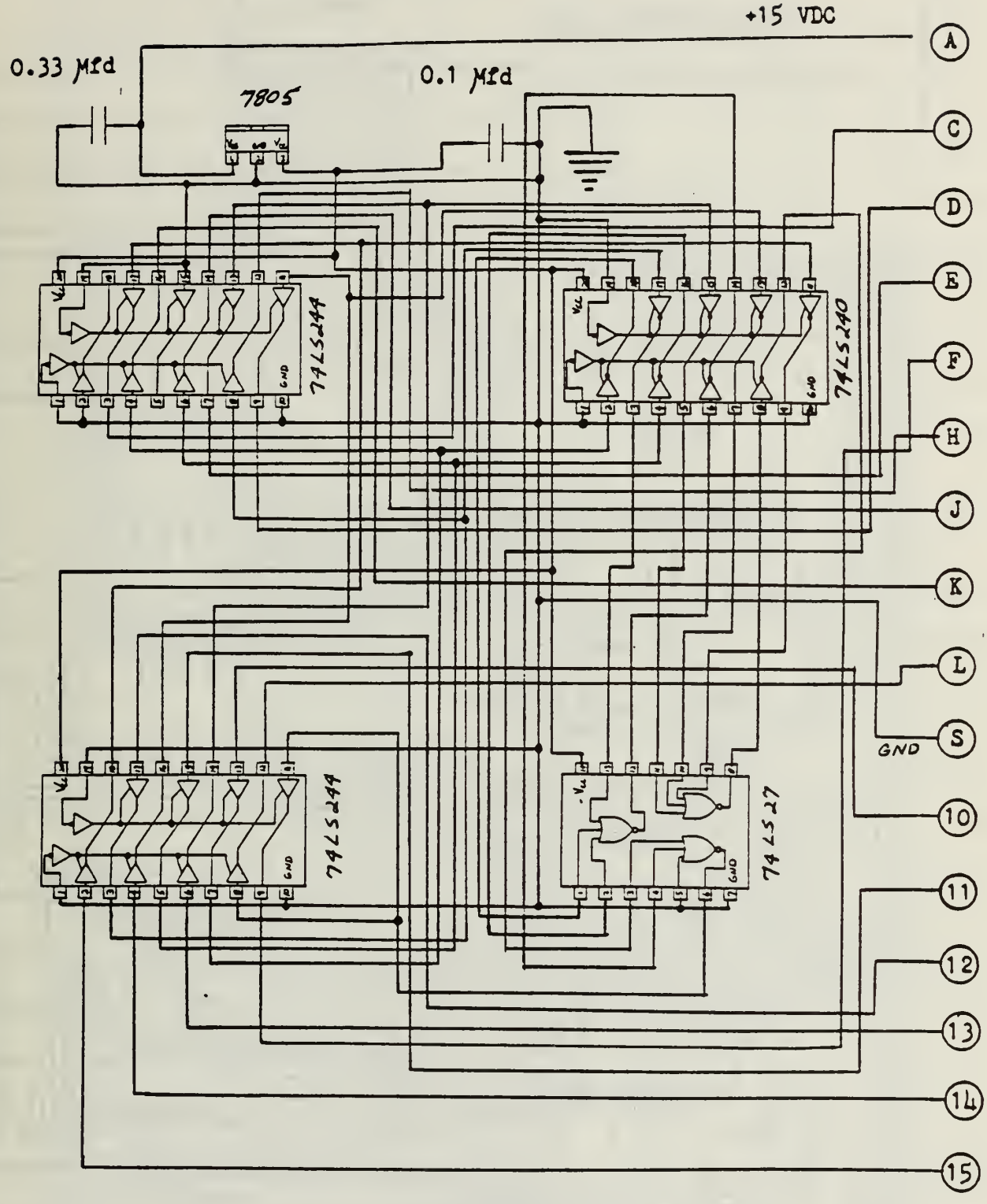

○ -- CINCH CONNECTER PIN

MULTIPLEXING BOARD

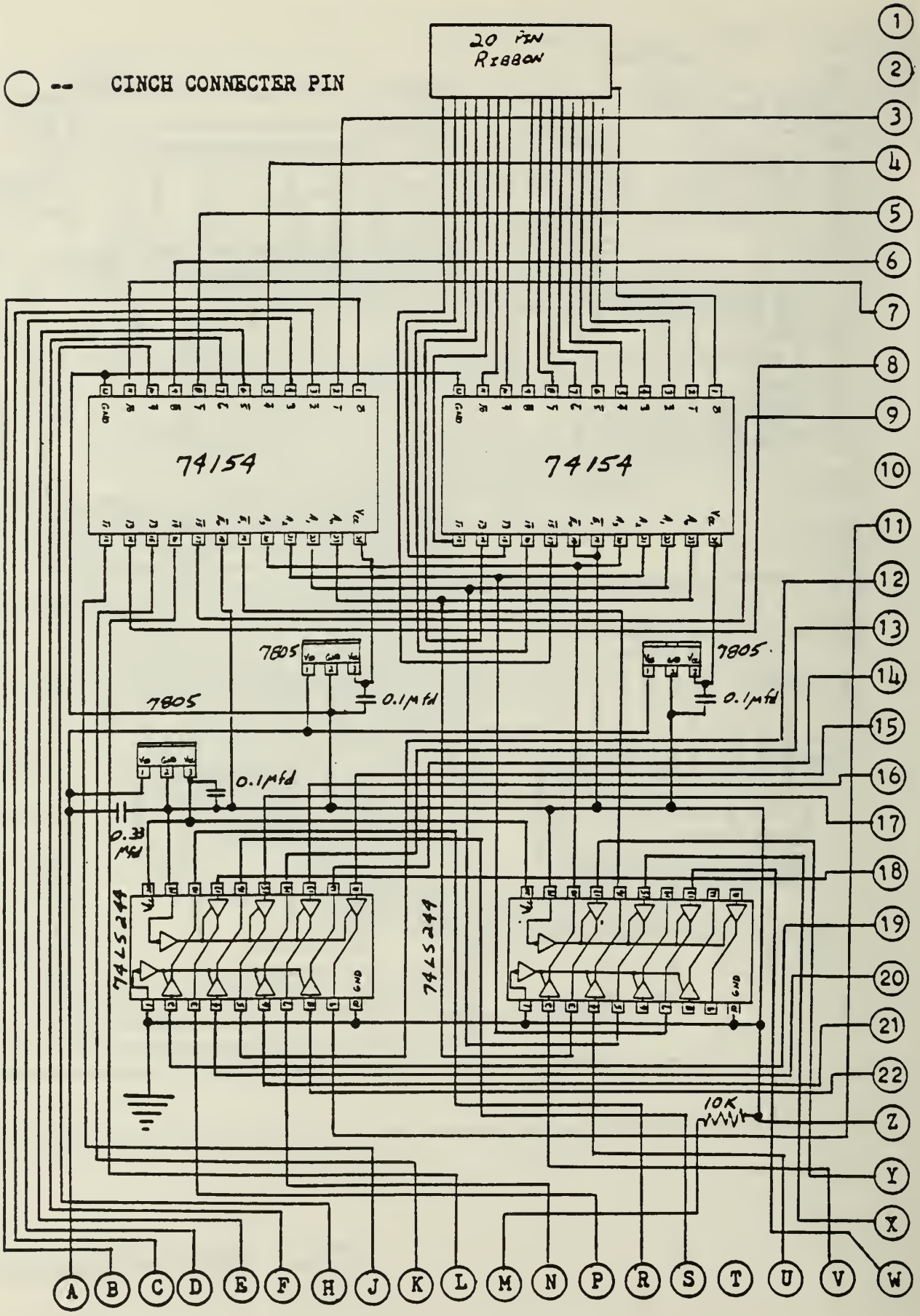

DAC BOARD

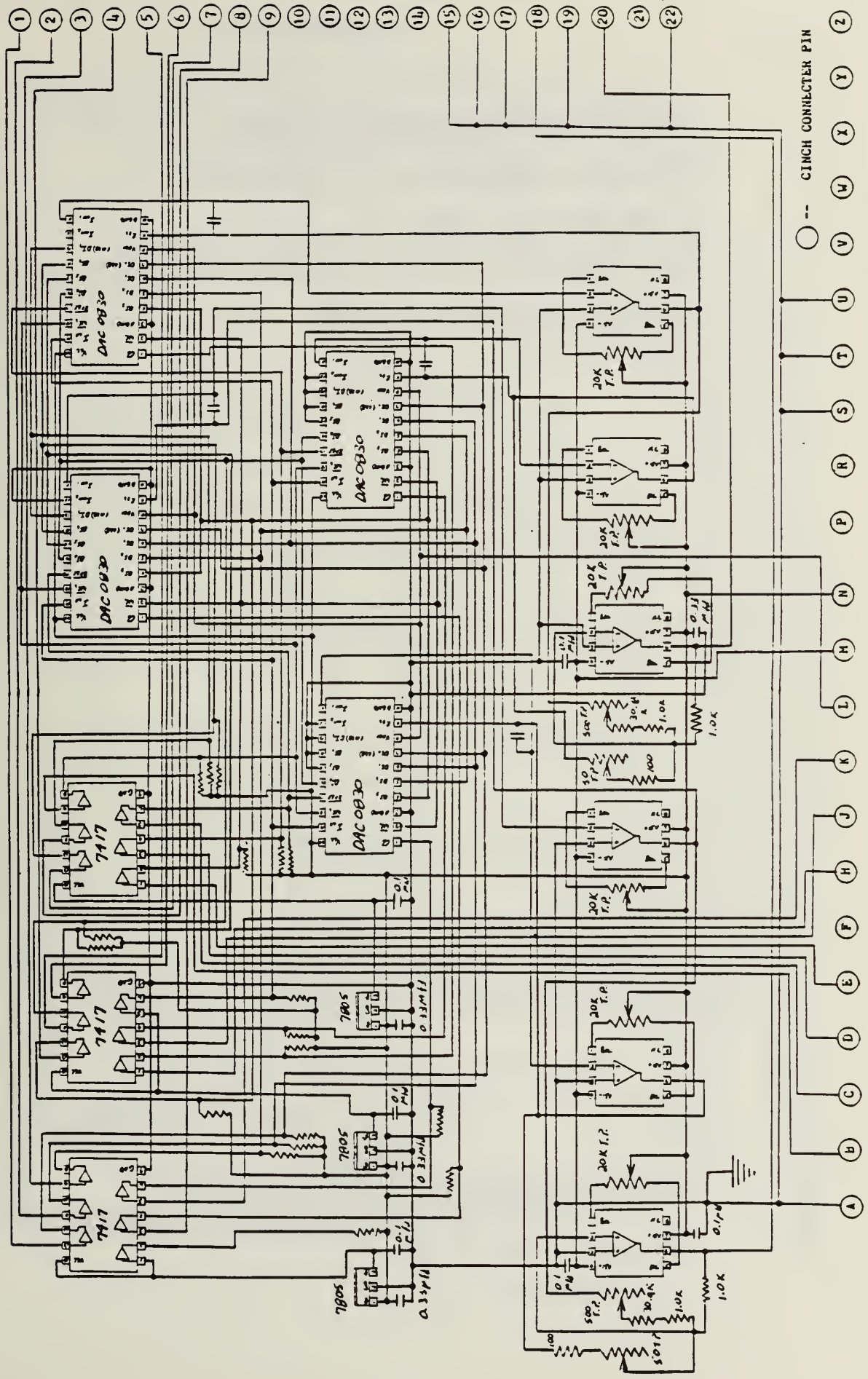

DAC BOARD NOTES

- ALL UNLABLED RESISTORS ARE 10.0 K VALUES
- ALL UNLABLED CAPACITORS ARE 5.0 pfd VALUES
- OP AMPS ARE LF 356 TYPE
- T.P. = TRIM POT
- ALL RESISTORS HAVE VALUES IN OHMS

ANALOG MULTIPLEXING BOARD

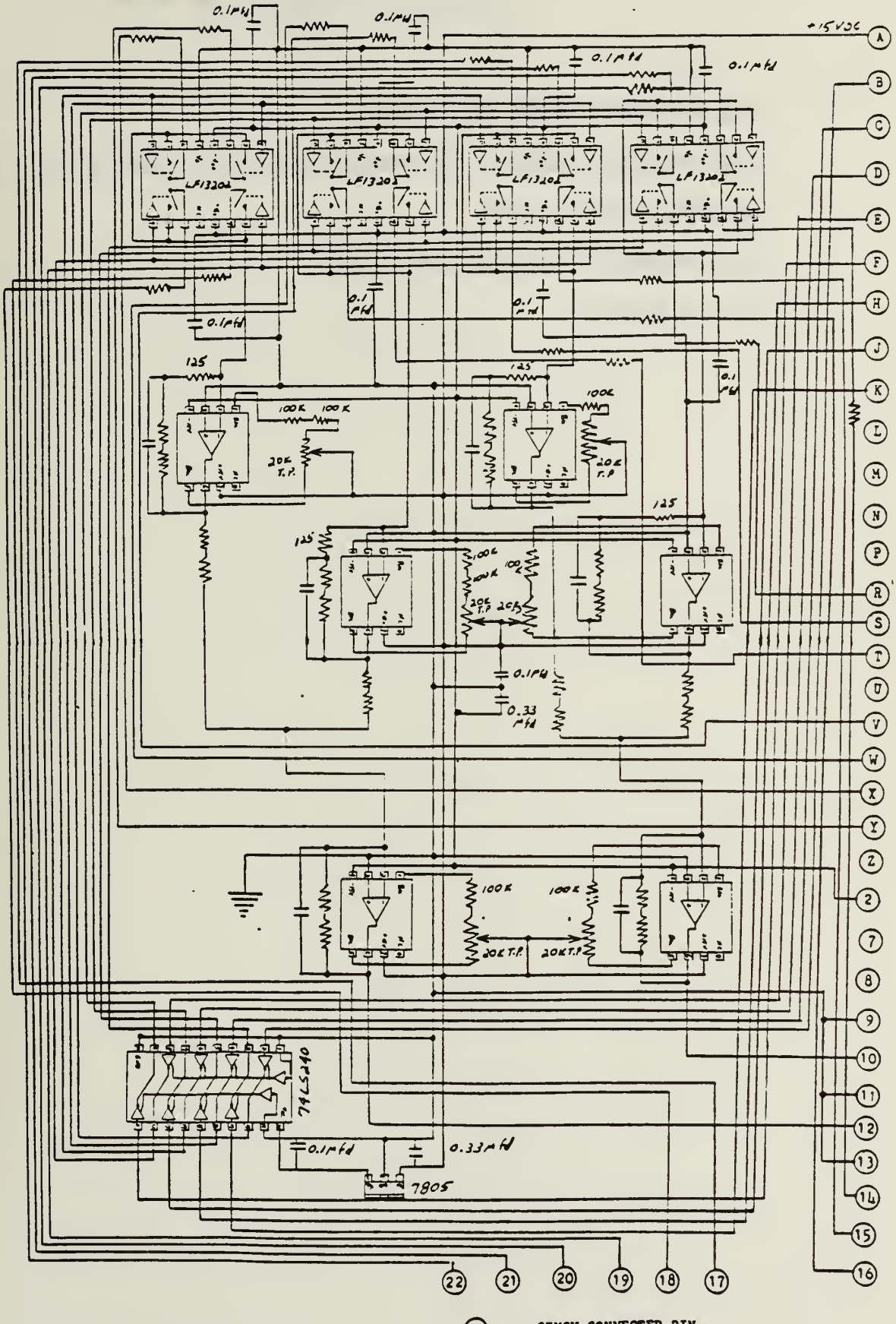

○ — CINCH CONNECTER PIN

ANALOG MULTIPLEXING BOARD NOTES

- ALL RESISTOR VALUES ARE IN OHMS
- ALL UNMARKED RESISTORS ARE PRECISION MATCHED PAIRS OF 15.61 K ($\pm$ 5)
- OP AMPS ARE LF356 TYPE
- ALL UNMARKED CAPACITORS ARE 5 pfd
- T.P. = TRIM POT

11. ETHANOL TRIGGER CIRCUIT

ETHANOL TRIGGER

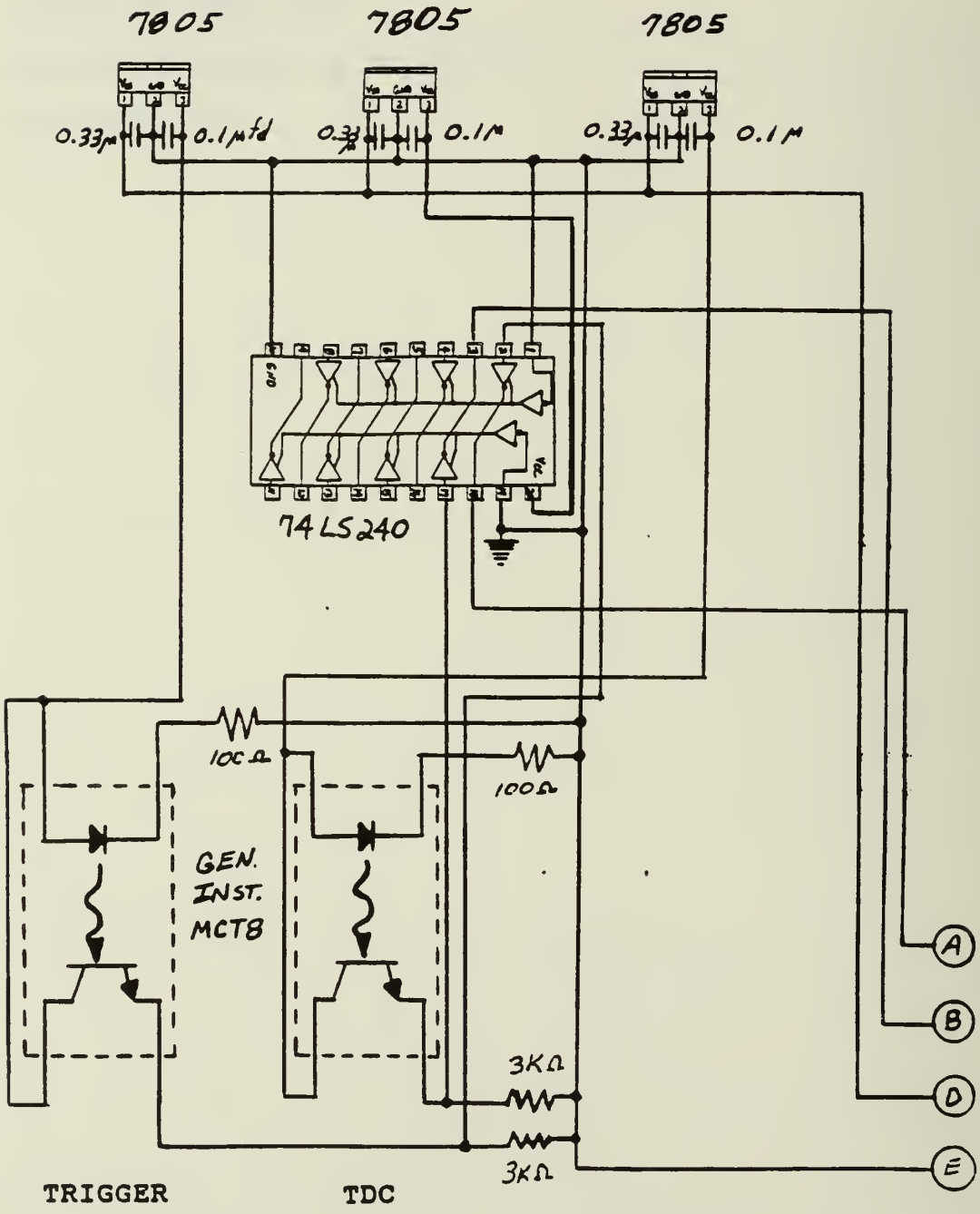

APPENDIX II

THE EFFECT OF DIESEL INJECTION TIMING ON A TURBOCHARGED DIESEL ENGINE FUMIGATED WITH ETHANOL

Alan Robert Schroeder
B.S., University of Illinois, 1983
M.S., University of Illinois, 1986
Department of Mechanical and Industrial Engineering
University of Illinois at Urbana-Champaign
1206 West Green Street
Urbana, IL 61801

Submitted in partial fulfillment of the requirements
for the degree of Master of Science in Mechanical Engineering
in the Graduate College of the
University of Illinois at Urbana-Champaign, 1986

1. INTRODUCTIONS

High prices and the short-term interruptions in supply of petroleum fuels which have occurred in the past, has led to an increased awareness of the need for alternative fuels. Ethanol, in particular, is a promising alternative fuel since it can be derived from agricultural products. Ethanol also has a high octane rating which makes it a suitable replacement for high octane petroleum fuels. However, ethanol can also be used as a partial replacement for low octane fuels. An example of this is the fumigation of a diesel engine with ethanol. With this technique, ethanol is premixed with the intake air outside of the combustion chamber. The mixture is than inducted into the cylinder and compressed. Diesel fuel is injected in the normal manner and acts as an ignition source for the ethanol-air mixture. Using this method, significant levels of diesel fuel can be replaced by ethanol (approximately 40% by energy at high loads and as much as 80% by energy at low loads [1]).

One problem with this technique, however, is that the addition of ethanol results in longer ignition delays. This is primarily due to the low cetane number of ethanol and the lower mixture temperatures at the time of diesel fuel injection which result from the lower specific heat ratio of the ethanol-air mixture. The longer ignition delays result in a shift of peak pressure to a point later in the engine cycle. This causes lower thermal efficiencies, especially at low to medium loads. One way to compensate for the longer ignition delays is to advance the diesel fuel injection timing.

The purpose of this investigation is to determine the effect of changes in pilot fuel injection timing on engine performance and the conditions at which these changes are most effective.

2. LITERATURE REVIEW

2.1 Feasibility of Fumigation

The basic methods used to dual fuel a diesel engine with ethanol are (1) direct injection, (2) direct injection of blended fuel, and (3) fumigation. A detailed review of each of these methods is given by Roberts [1]. The techniques are briefly described here. With direct injection, ethanol is injected directly into the combustion chamber immediately after the injection os a small charge of diesel fuel. The diesel fuel acts as an ignition source for the ethanol. The main disadvantage of this technique is that two accurately controlled, high pressure injection systems are required. Thus, modification of an existing diesel engine is expensive. An alternate method is to blend the ethanol with the diesel fuel and use the existing diesel fuel injection system. The problem with this method, however, is that ethanol containing small amounts of water will not remain in solution with diesel fuel. Thus, this method involves the added cost of using higher ethanol proofs and chemicals to stabilize the ethanol-diesel mixture. The third alternative is fumigation. With this method, ethanol is premixed with the intake air using a low pressure injection system. The mixture is inducted into the cylinder and ignited by a reduced charge of diesel fuel. Fumigation alleviates the problems which occur for the other two methods of dual fueling. For example, the water content of the alcohol is not critical. In fact, the use of lower proof ethanol may actually improve engine performance at certain operating conditions [2]. Also, fumigation does not require major modifications of the existing engine. Thus, fumigation is the most practical method of dual fueling a diesel engine with ethanol.

2.2 Effect of Pilot Fuel Injection Timing

One of the problems associated with the fumigation of a diesel engine with ethanol is the increase in ignition delay. Data obtained by Roberts [1] with the same engine used for the current investigation showed that ignition delay could be increased by as much as 75% when a large percentage of the fuel energy was supplied as ethanol. Ignition delay increased with there addition of ethanol due to the low cetane number of ethanol and the lower charge temperatures at the time of diesel injection which were a result of the lower specific heat ratio of the ethanol-air mixture. The longer ignition delays resulted in significant decreases in thermal efficiency (as much as 15%) at low to medium loads where relatively large percentages of the fuel energy were supplied as ethanol. The decrease in thermal efficiency was due to the shift of peak pressure to a point later in the cycle.

One way to compensate for the increased ignition delay is to advance the diesel fuel injection timing. Studies done with a single-cylinder diesel engine [3] have shown that advancing the pilot fuel injection timing can result in considerable improvement of performance at engine conditions where the percentage of fuel energy supplied as ethanol is large (low to medium loads). The data suggested that to achieve optimum combustion, advance of the pilot fuel injection timing was required as the ethanol flow was increased. There has not been many detailed studies on the effect of pilot fuel injection timing on the performance of multicylinder diesel engines. Thus, the purpose of the current investigation is to use a multicylinder diesel engine to determine the effect of changes in pilot fuel injection timing on engine performance and the conditions at which these changes are most effective.

2.3 Control of Diesel Injection Timing

Methods to accurately control pilot fuel injection timing must exist in order for the investigation of the effect of pilot fuel timing on engine performance to have practical significance. Fortunately, systems have been developed and tested which allow accurate control of diesel fuel quantity and injection timing. Stanadyne has developed an electronically controlled rotor-type diesel fuel injection pump [4]. A microcomputer is used to schedule diesel fuel flow and timing via actuators. Adjustments are made based on information received from sensors which monitor engine operating conditions. Tests done on a 4.3 liter V-6 and a 6.2 liter V-8 showed that significant improvements in engine performance resulted with the use of the electronically controlled fuel system. This type of control system would be suitable for sue with a dual fuel engine. The microcomputer could be programmed to adjust the timing to the optimum value for a particular operating condition.

3. EQUIPMENT AND EXPERIMENTAL METHOD

3.1 Engine and Dynamometer

An International Harvester model DT-436B four stroke, six cylinder, turbocharged, direct injection diesel engine was used for the test program. The bore was 109 mm and the stroke 127 mm which gave a total displacement volume of 7.14 liters. The compression ratio was 16:1. The engine was equipped with an American Bosch single-plunger distributor fuel pump. Rated power for the engine was 170 bhp at 2500 rpm. The engine was operated without a fan and cooled by an auxiliary heat exchanger. The alternator was turning but not charging. A type MW310 eddy current dynamometer manufactured by Midwest Dynamometer and Engineering Company was used to load the engine. Engine speed and load were maintained by a set of controllers manufactured by Digalog Corporation. A schematic of the control system is shown in Fig. 3.1. A model 1022A dynamometer controller was used to control the field current which provided load on the engine. Inputs to the controller included a load cell to measure brake torque and a magnetic pickup to measure engine speed. Digital readings of torque and speed were provided by the controller. A model TC throttle controller was used to control throttle position via a throttle actuator.

3.2 Ethanol Injection System

Ethanol was injected directly into the intake ports to assure even distribution among the cylinders. Six Bendix type E-10 electronic fuel injectors were used (one for each cylinder). Each injector was mounted in the cylinder head as shown in Fig. 3.2. The injector was oriented so that most of the spray would hit the intake valve.

The complete ethanol fumigation system is shown in Fig. 3.3. A Bosch 12 VDC fuel pump provided the required fuel pressure at the injectors. Following the pump was a Bosch fuel filter. Based on earlier testing of the injector spray pattern with ethanol, 40 psi was chosen for the pressure differential across the fuel injector. The pressure regulator was referenced to the intake manifold pressure so that the pressure differential across the injector was not affected by the amount of turbocharger boost.

Based on results given in the literature, it was expected that approximately fifty percent of the fuel energy at high load could be supplied by ethanol [3,5,6]. The ethanol injection system had to be capable of delivering enough fuel to the cylinders to achieve this. Approximate calculations showed that if the injector being utilized was only as long as the intake valve was open, the required flow rate of ethanol would not be reached. To avoid this problem, the injector was pulsed twice per engine cycle, once during the intake stroke and once during the power stroke. A possible advantage of this method is that half of the ethanol charge is preheated since it sits on the relatively hot intake valve until it is inducted on the intake stroke.

An injector driver and control unit built by Bendix was supplied with the injectors. Two digital input signals were required to operate the unit. One signal was a reset or starting point for the firing order of the injectors and the other was a trigger to pulse each individual injector sequentially. Since the injectors were to be pulsed twice per cycle, they could be pulsed in

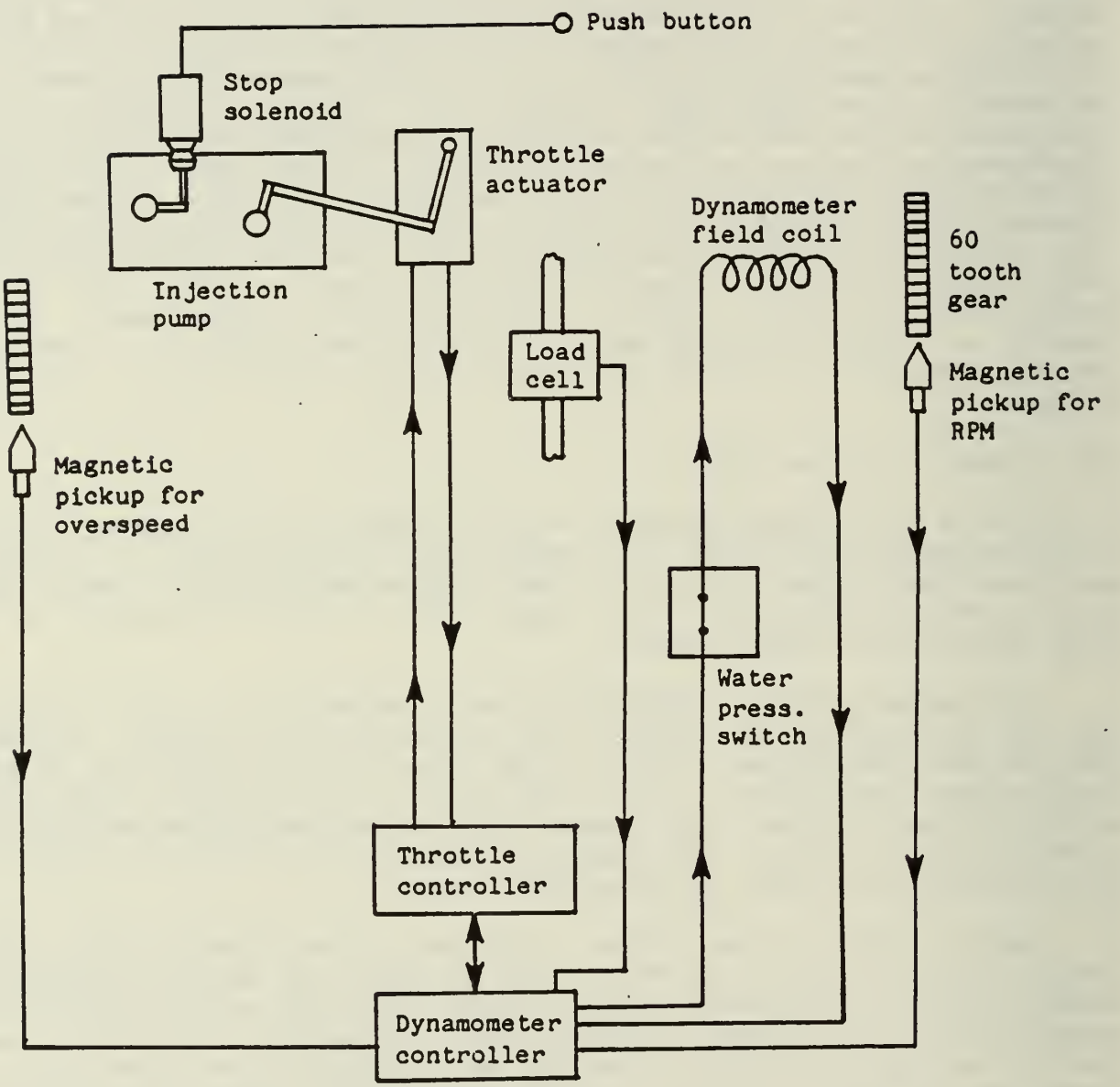

Figure 3.1 Engine and dynamometer control system.

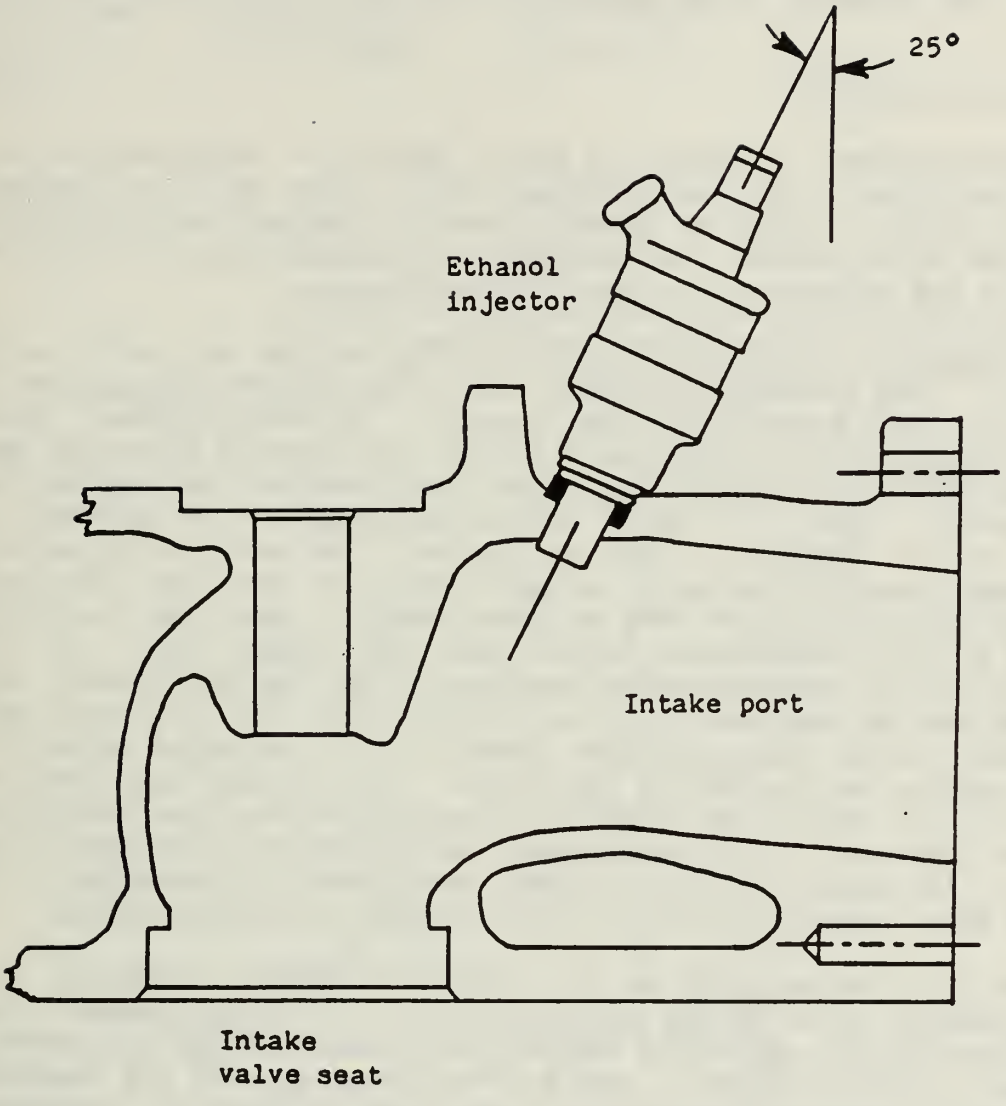

Figure 3.2 Cross section of cylinder head showing position of ethanol injector with respect to intake valve.

pairs. Thus, three pulses per revolution were required to trigger the injectors and one pulse per revolution was required to reset the circuit. These signals were obtained by mounting two discs, one having one hole and one having three holes, on the dynamometer shaft. Optical switches were then used to generate the required pulses. The output of the injector control unit was a pulse of variable duration. Thus, the ethanol flow rate was controlled by varying the injector pulse duration with the potentiometer on the control unit.

3.3 Instrumentation

Two computers, an Apple IIe and an Apple II+, were used for most of the data acquisition. Eqch was equipped with a model AI-13 16 channel, 12 bit analog-to-digital converter manufactured by Interactive Structures Corporation. The Apple IIe was also equipped with a 6522 Versatile Interface Adapter to enable the computer to be used for control.

A computer controlled fuel measuring system was built as shown in Fig. 3.4. The solenoid valve was controlled by the computer and the photo transistors were connected to the computer's interrupt system. During normal operation, when data was not being taken, the solenoid valve was open. Thus, the fuel level in the glass buret and float tube was the same as that in the level control tank. To begin a fuel measurement, the solenoid valve was closed and the computer's timer was started. The level in the buret and fload tube then dropped. The buret volumes were sized such that the fuel measurement was over a period of one to three minutes. When the fload triggered an optical switch, the computer would check the elapsed time. If it was less than one minute, the measurement continued using the next volume. Knowing the total volume of fuel used and the elapsed time, the flow rate could be determined. It was found that the diesel fuel in the buret became fairly warm as the engine was run due to the return line carrying heat from the engine. To account for density variation with temperature, the fuel temperature in the buret was measured with a thermocouple and a correction for the API number was applied. The fuels used for all tests were commercial grade no. 2 diesel fuel and 200 proof ethanol denatured with 5 percent unleaded gasoline.

Air flow was measured by two laminar flowmeters connected in parallel. The flowmeters were Meriam models 50 MC2. A plenum chamber sized to SAE specifications [7] was placed between the flowmeters and the compressor inlet to dampen pressure pulses. Two D.J. Instruments model MLR strain gage type differential pressure transducers were used to measure the pressure drop across the laminar elements. The transducer signals were read by the computer.

Temperature data was taken using six type K thermocouple amplifier circuits with electronic reference junction compensation. The amplifier outputs were read by the computer. Ambient, coolant, compressor inlet, intake and exhaust manifold, and exhaust stack temperatures were measured. The wet bulb temperature was measured using a sling psychrometer.

Motorola model MPX strain gage type absolute pressure transducers were used to measure ambient and intake manifold pressures. The transducer outputs were read by the computer. The same type of pressure transducer was initially used to exhaust manifold pressure, but it was damaged by prolonged exposure to

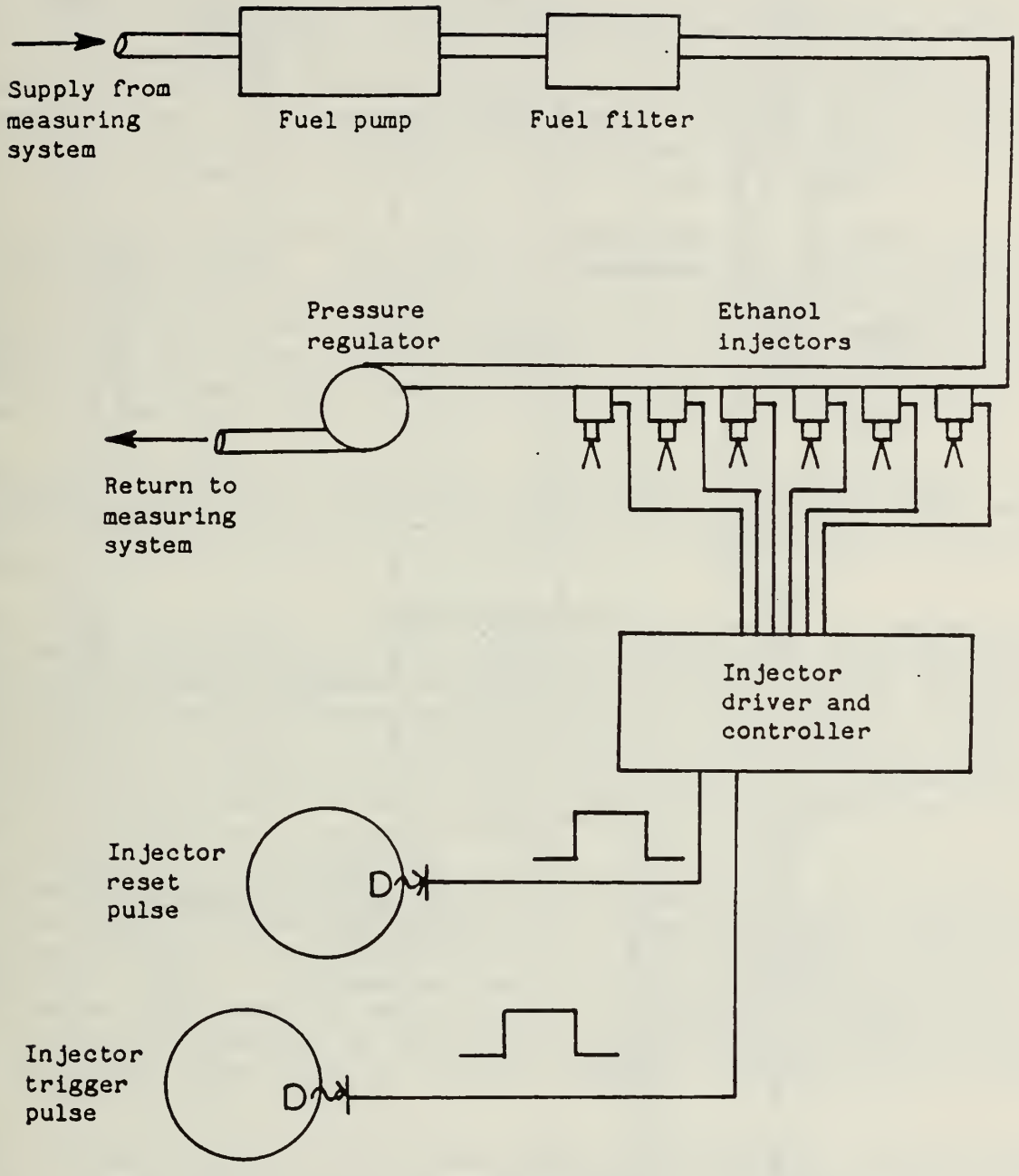

Figure 3.3 Ethanol fumigation system.

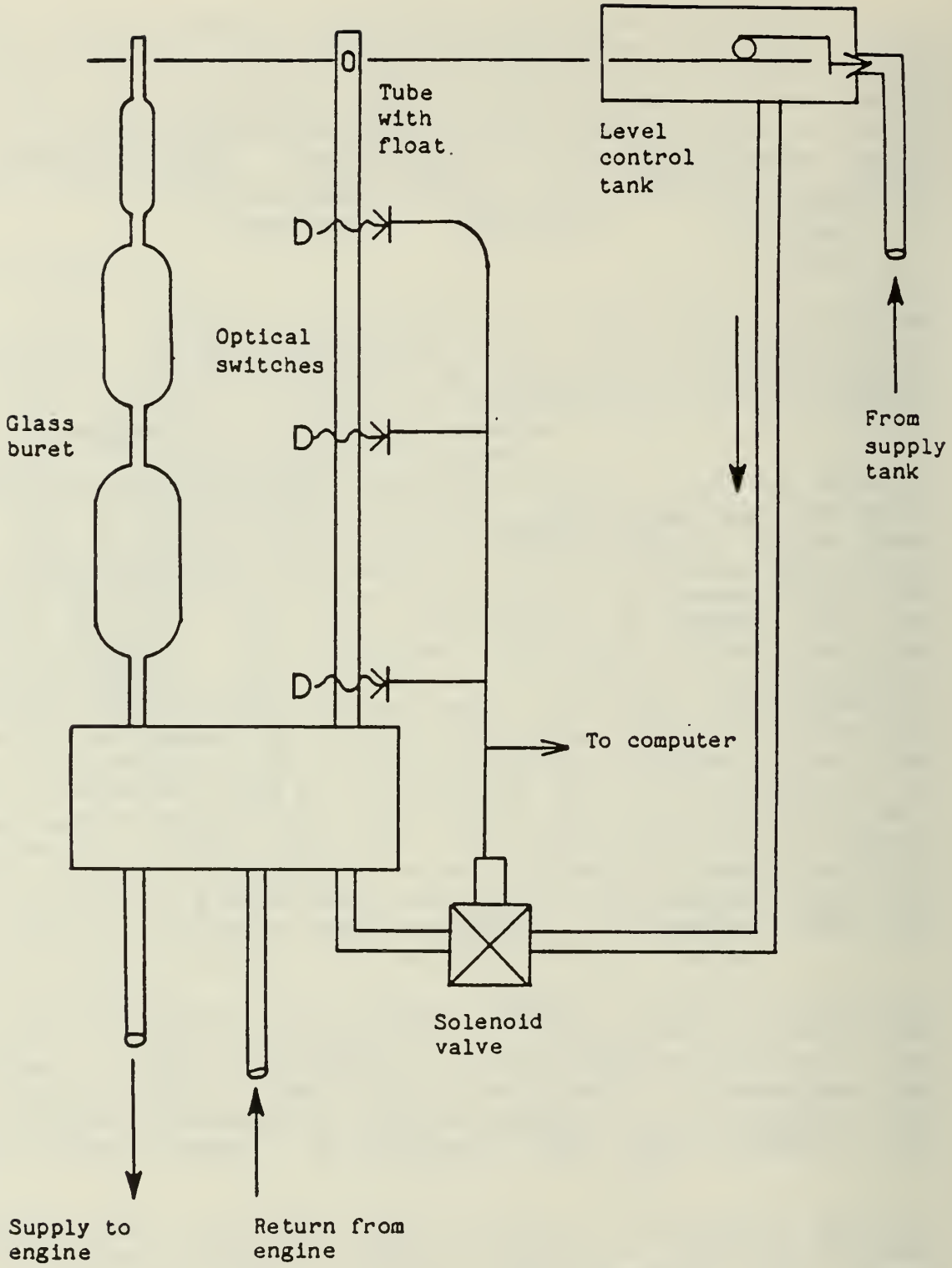

Figure 3.4 Computer controlled fuel measuring system.

exhaust gas. This led to the use of a Meriam well type manometer to measure exhaust manifold pressure.

An AVL model 8QP500 piezoelectric pressure transducer was used to measure the pressure in cylinder number one. The transducer was watercooled using a tank and pump system available from AVL. The face of the transducer was coated with silicone rubber to reduce signal noise caused by thermal stress. A Kistler model 504 charge amplifier was used to amplify the transducer signal. The amplifier output was read by the computer. The cylinder pressure trace was also displayed on an oscilloscope for diagnostic purposes.

A shaft encoder manufactured by BEI was coupled to the crankshaft to indicate crank angle position. The shaft encoder output consisted of two TTL signals: a single pulse per revolution and a single pulse per crank angle degree. Both signals were read by the computer. The pulse per revolution signal indicated top dead center and was used to initiate the reading of cylinder pressure data. Cylinder pressure was recorded for every crank angle degree by using the pulse per degree signal from the shaft encoder as a trigger.

Injection line pressure for cylinder number one was measured using an AVL model 41DP500K strain gage type pressure transducer. The transducer was mounted 7.6 cm from the injector. The output from the transducer was read by the computer.

The exhaust gas analysis system is shown in Fig. 3.5. The system was built and operated according to SAE recommended practice [8]. Beckman model 315 NDIR analyzers were used to measure carbon dioxide and carbon monoxide concentrations. Oxides of nitrogen were measured by a Thermo-Electron model 10A chemiluminescent analyzer. A Beckman model 402 FID analyzer was used to measure hydrocarbons. Oxygen concentration was measured using a Beckman model 715 process oxygen monitor. The data obtained with the oxygen analyzer, however, was not reliable and is not presented.

The sampling probe was located four feet downstream of the turbocharger. The sample line was maintained at 350 degrees Fahrenheit. Soot was removed from the sample by a pyrex wool filter. A pump was used to maintain the sample flow rate. Before the sample entered the NDIR and oxygen analyzers, water was removed using an ice bath condenser. Rotameters were used to indicate the flowrates in these analyzers. The sample passed through a heated capillary before entering the NOX analyzer. Outputs of all the analyzers were read by the computer.

Smoke samples were taken just downstream of the exhaust gas sampling prove using a Bosch model EFAW 65A-6 smoke sampler. The samples were then analyzed using a Bosch model EFAW 68A smoke analyzer.

3.4 Data Reduction

The Apple computers were used to reduce the raw data into its final form. The reduced data was then stored on disc. Data which was taken manually had to be entered into the computer. Steady state analog voltages from the exhaust analyzers, thermocouple amplifiers, and pressure transducers were read several times by the computer and then averaged. The voltages were then converted to the appropriate units using equations for the calibration curves of the devices.

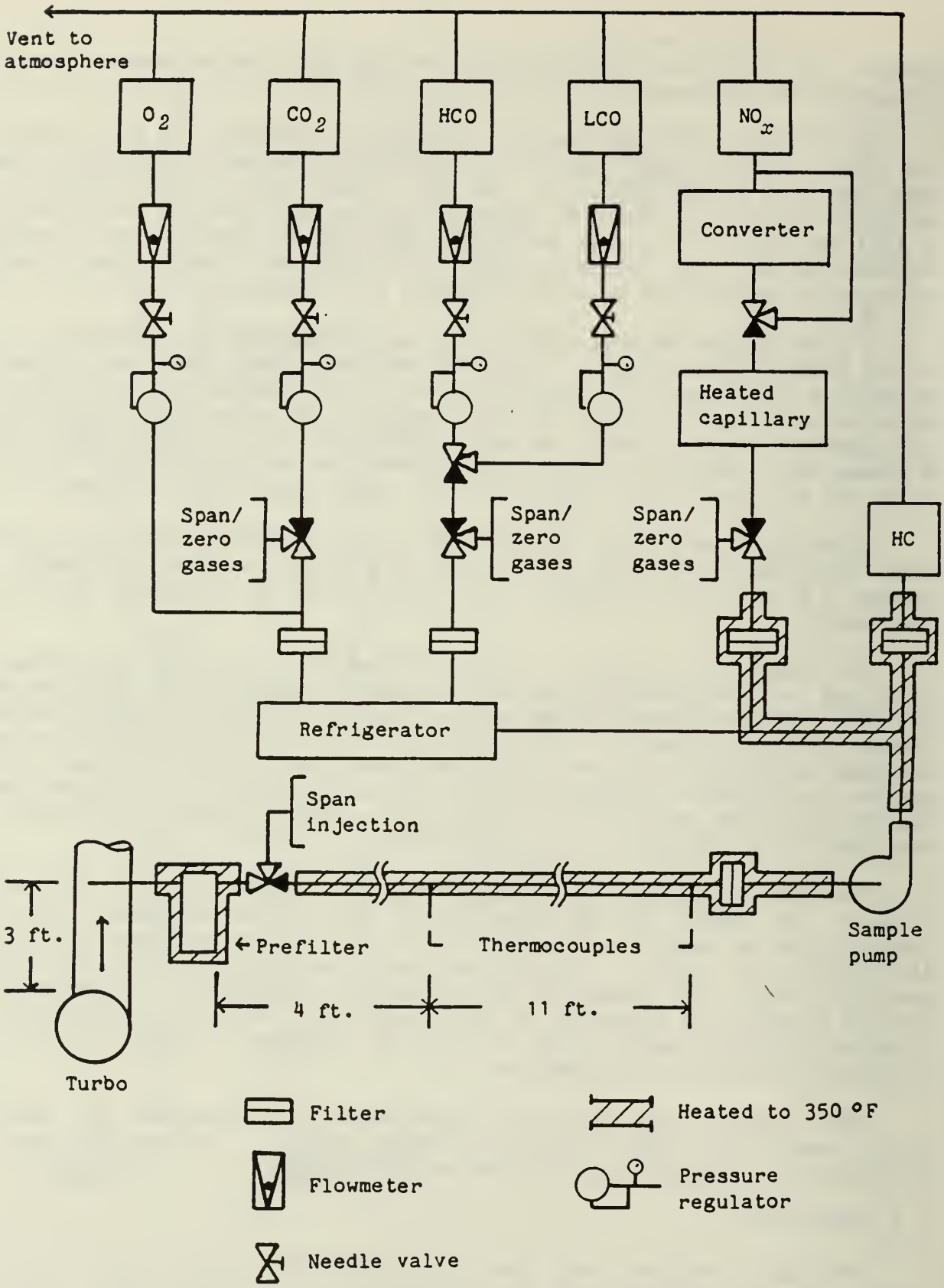

Figure 3.5 Exhaust gas analysis system.

Injection line pressure and cylinder pressure data were taken for each crank angle degree. Only one engine cycle of injection line pressure data was taken. However, 128 consecutive engine cycles of cylinder pressure data were taken and averaged to account for cycle to cycle variation. A reference pressure was needed to determine cylinder pressure since a piezoelectric transducer only measures relative pressure changes. In this case, intake manifold pressure was used as the reference pressure. Before the cylinder pressure data was stored on disc, a simplified heat release analysis was done on the Apple computer to assure that the pressure data was properly phased [9].

The method used to determine ignition delay is illustrated in Fig. 3.6. The crank angle at which the diesel injector opened was determined from the injection line pressure data. The crank angle at which combustion started was determined by examining the derivative of cylinder pressure. This point was defined by a marked deviation of the derivative of cylinder pressure from a value representation of the motoring curve.

3.5 Experimental Procedure

The exhaust gas analyzers were left on continuously to minimize instrument drift. The heated sample line and sample pump were turned on and the condenser filled with ice approximately two hours before testing to allow the exhaust gas analysis system to reach equilibrium.

Before starting the engine, the diesel fuel pump static timing was set to the value specified for the test. The engine was then started and allowed to warm up. Once the oil and coolant temperatures reached equilibrium, the engine speed and load were set to the values specified for the test using the Digalog controllers. The ethanol injectors were then turned on and the ethanol flow rate slowly increased while the controllers were adjusted to hold load constant (the diesel flow rate was decreased by the throttle actuator). After setting the ethanol flow rate to the specified test value, the engine was allowed to come to equilibrium. During this time, the exhaust gas analyzers were calibrated with the span gases. Coolant, intake manifold, and exhaust manifold temperatures were displayed on the computer to indicate when the engine was at equilibrium. Data was taken when the exhaust temperature reached a steady value. After taking data, the engine was set to the next test pont and the process repeated.

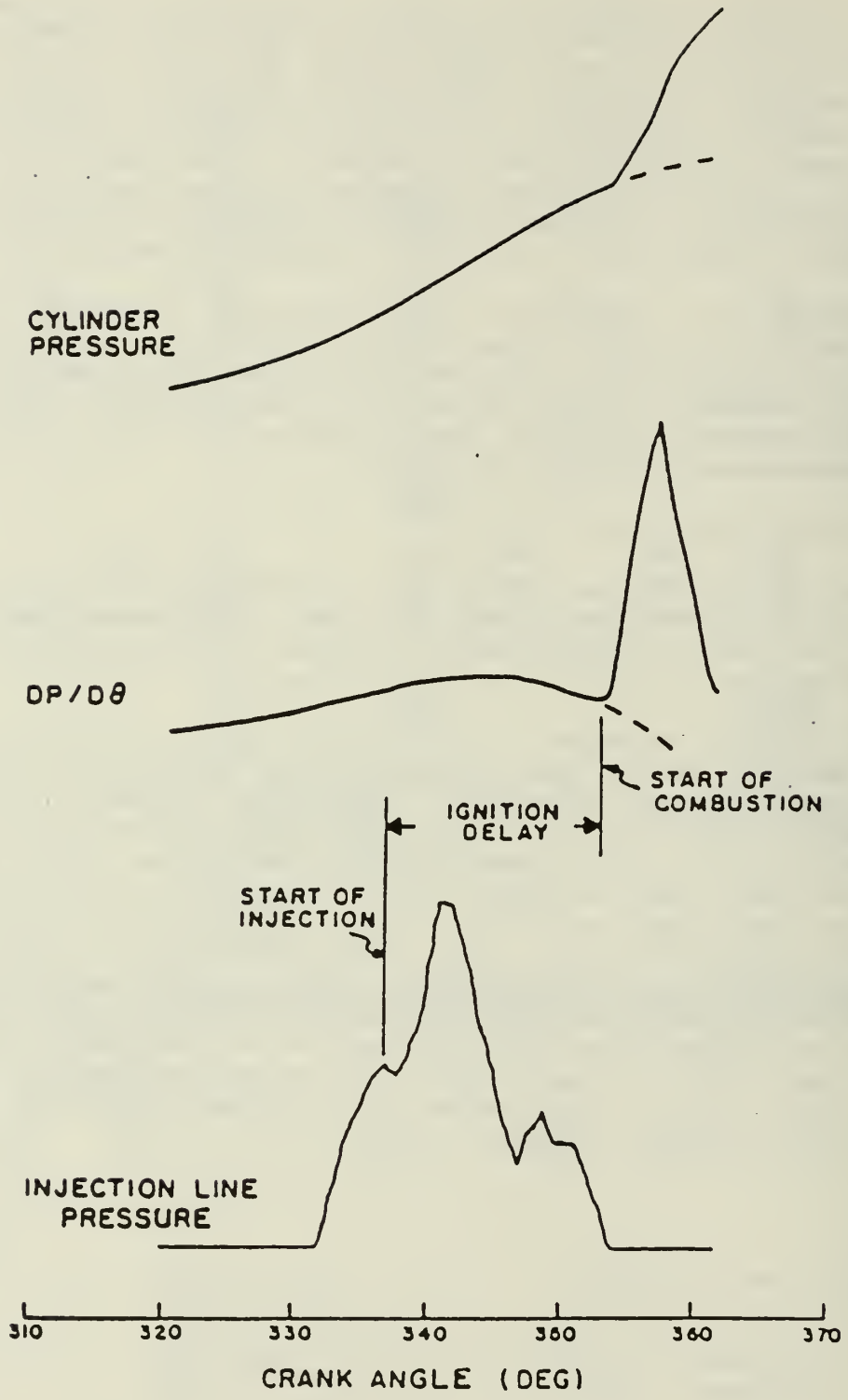

Figure 3.6 Representative curves of cylinder pressure, derivative of cylinder pressure and injection line pressure versus crank angle.

4. TEST SCHEDULE

It was first necessary to determine the engine conditions at which changes in pilot fuel injection timing would be most effective. For this test, the engine was operated at 2000 rpm with five different loads. The loads gave brake mean effective pressures of 100, 300, 500, 700, and 900 kPa. Baseline diesel data was taken at each load with the diesel fuel pump static timing at the factory setting of 18 degrees before top dead center. The engine was then operated in the dual fuel mode for the same loads. Data was taken at each load with diesel pump timings of 14, 22, 26, and 29 degrees before top dead center. One or two tests were performed at each setting of load and timing using ethanol flow rates near the maximum limit. This limit was due to misfire at low loads and knock at high loads. Engine misfire was determined by observing the cylinder pressure trace on the oscilloscope. The ethanol flow rate was increased until there was a stable and significant rise in pressure due to combustion for each cycle. The oscilloscope was not used to determine the knock limit since audible knock occurred before the trace on the oscilloscope indicated knock. The knock limit was determined by listening for excessive knock based on subjective experience. High ethanol flow rates were used in order to get maximum ignition delays. It was expected that changes in pilot timing would be most effective for such conditions. The pump timing was then set back to the factory setting of 18 degrees BTDC and the ethanol flow rates previously used for the pump timings of 14, 22, 26, and 29 degrees BTDC were repeated at the corresponding loads.

The results of this test indicated that changes in pilot fuel injection timing were likely to be most effective at a brake mean effective pressure between 300 and 500 kPa. Thus, a more detailed test was carried out at 2000 rpm and a brake mean effective pressure of 400 kPa, which was slightly less than fifty percent load. Baseline diesel data was taken for fuel pump timings of 18, 22, 26, and 29 degrees BTDC. Data was also obtained for four different ethanol flow rates at each pump timing. For comparison, a similar test was done at 2400 rpm and a brake mean effective pressure of 400 kPa using the same ethanol flow rates. An extra pump timing (14 degrees BTDC) was also tested t 2400 rpm for completeness.

The 2000 rpm test at various loads was completed in one day in order to minimize variation in the results due to atmospheric changes. Similarly, the 2000 rpm and 2400 rpm tests at a brake mean effective pressure of 400 kPa were each completed in one day.

5. RESULTS AND DISCUSSION

5.1 Results of Test at 2000 RPM and Various Loads

The mass flow rate of ethanol was held constant as diesel injection timing was varied. Note that this did not mean that the percentage of fuel energy supplied as ethanol remained constant. For a given speed, load, and mass flow rate of ethanol the controllers adjusted the flow rate of diesel to hold load constant. Changes in the diesel fuel injection timing resulted in changes in thermal efficiency, thus the diesel flow rate required to hold load constant varied with pilot timing. Rather than refer to the actual values of ethanol mass flow rate in the following discussion and figures, the flow rates are represented by the potentiometer settings on the ethanol injector control unit. An increase in the potentiometer setting corresponds to an increase in the ethanol flow rate. Table 5.1 lists the controller settings and corresponding percentages of fuel energy supplied as ethanol for the test at 2000 rpm and various loads. The actual values of ethanol mass flow rate for each controller setting can be found in the data tables in the appendix.

5.1.1 Results for BMEP of 100 kPa

Figures 5.1 and 5.2 show plots of cylinder pressure versus crank angle degree for four different ethanol flow rates. Each figure has three curves: one for diesel and one for dual fuel at a pilot timing of 18 degrees BTDC, and one for dual fuel at the maximum advanced timing used for that particular ethanol flow rate. Figure 5.1(a) shows that for an ethanol flow of 5, advancing the pilot timing for the dual fuel resulted in an earlier start of combustion. The peak pressure, however, was not as high for the advanced timing. Figure 5.1(b) shows a similar result for an ethanol flow of 6. Note that in this case, the maximum advanced pilot timing was less than that for an ethanol flow of 5. At this load, misfire became worse as the timing was advanced for a particular ethanol flow rate. Table 5.2 shows the approximate maximum ethanol flows at each timing. The table shows that as pilot fuel timing was advanced, the maximum flow rate of ethanol had to be decreased in order to avoid misfire. Figures 5.2(a) and 5.2(b) show cylinder pressure diagrams for ethanol flows of 7 and 8. The trends are similar to those for the lower ethanol flow rates. Figure 5.2(b) shows that at an ethanol flow of 8, the maximum timing advance was again decreased. Note that Figs. 5.1 and 5.2 also show that cylinder pressures during the compression stroke for the dual fuel were below those for diesel. This was primarily due to the lower specific heat ratio of the ethanol-air mixture [10].

Figure 5.3 is a plot of maximum cylinder pressure versus pilot timing for the four ethanol flow rates. The general trend was a decrease in peak pressure with an advance in pilot timing above 18 degrees BTDC. This indicates that timing advance failed to result in better ignition of the mixture. Peak pressure also decreased as more ethanol was added. This was due to the increased ignition delays and slower burning rates that occurred with the addition of ethanol.

Figure 5.4 shows the maximum rate of pressure rise as a function of pilot timing. For all of the ethanol flow rates, the maximum rate of pressure rise decreased as timing was advanced. Again, this indicates that advancing the timing led to slower initial burning rates. Also, the maximum rate of pres-

BMEP (kpa)	Controller setting	Timing (°BTDC)	% Ethanol by energy
100	5	18	57.5
100	5	29	57.9
100	6	18	65.8
100	6	26	66.7
100	7	18	72.3
100	7	22	72.4
100	7	26	72.7
100	8	14	75.1
100	8	18	77.1
100	8	22	77.3
300	6	18	48.7
300	6	26	49.2
300	6	29	48.9
300	8	18	64.6
300	8	26	65.9
300	8	29	66.2
300	10	18	78.1
300	10	22	78.9
300	11.5	14	82.4
300	11.5	18	84.5
300	11.5	22	84.0
500	11.5	14	70.6
500	11.5	18	71.6
500	11.5	26	68.3
500	11.5	29	67.3
500	12.5	18	77.9
500	12.5	22	75.5
700	10.5	14	49.1
700	10.5	18	49.1
700	10.5	22	47.8
700	10.5	26	46.4
900	9	14	32.2
900	9	18	32.9
900	9	22	32.3
900	9	26	31.1

Table 5.1 Listing of ethanol controller settings and corresponding percentages of ethanol by energy for test at 2000 rpm and various loads.

BMEP (kpa)	Timing (°BTDC)	Maximum Eth. flow	Limiting condition
100	14	8	Misfire
100	18	8	Misfire
100	22	7	Misfire
100	26	6	Misfire
100	29	5	Misfire
300	14	11.5	Misfire
300	18	11.5	Misfire
300	22	10	Misfire
300	26	8	Misfire
300	29	8	Misfire
500	14	11.5	Knock
500	18	12.5	Knock
500	22	12.5	Knock
500	26	11.5	Knock
500	29	11.5	Knock
700	14	10.5	Knock
700	18	10.5	Knock
700	22	10.5	Knock
700	26	10.5	Knock
900	14	9	Knock
900	18	9	Knock
900	22	9	Knock
900	26	9	Knock

Table 5.2 Listing of maximum ethanol flow settings at different pilot fuel timings for test at 2000 rpm and various loads.

Test conditions: RPM = 2000
BMEP = 400 kpa

Timing (°BTDC)	Controller setting	% Ethanol by energy
18	8	56.1
18	9	63.6
18	10	71.2
18	11	77.6
22	8	56.6
22	9	64.4
22	10	72.5
22	11	79.2
26	8	56.4
26	9	64.6
26	10	73.3
26	11	79.5
29	8	56.5
29	9	65.0
29	10	73.7
29	11	79.4

Test conditions: RPM = 2400
BMEP = 400 kpa

Timing (°BTDC)	Controller setting	% Ethanol by energy
18	8	55.0
18	9	61.8
18	10	67.4
18	11	73.9
22	8	55.2
22	9	62.4
22	10	69.0
22	11	75.8
26	8	54.8
26	9	62.5
26	10	69.7
26	11	76.4
29	8	54.2
29	9	62.1
29	10	69.5
29	11	76.8
14	8	53.1
14	9	59.6
14	10	65.2
14	11	70.5

Table 5.3 Listing of ethanol controller settings and corresponding percentages of ethanol by energy for tests at 2000 and 2400 rpm with a BMEP of 400 kpa.

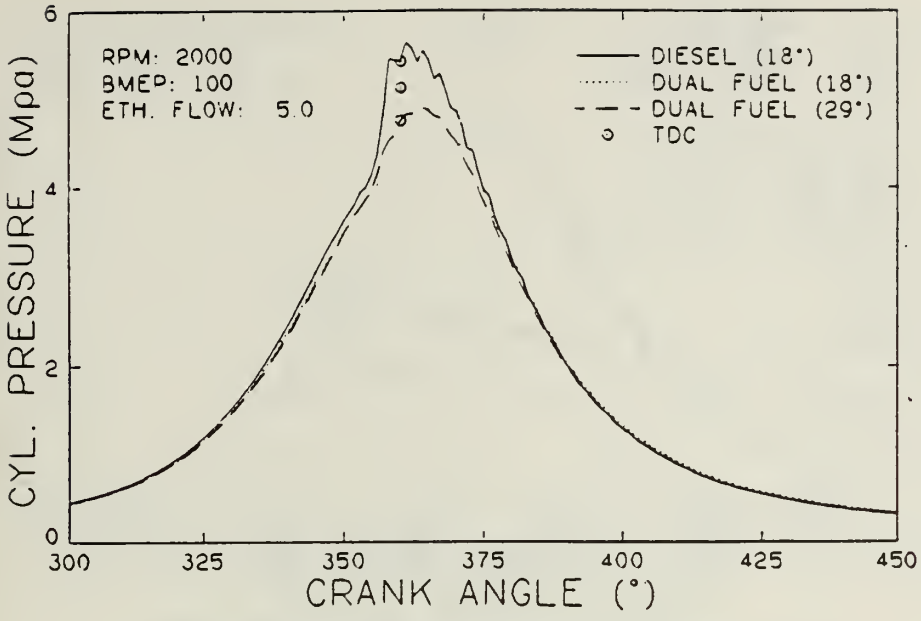

(a) RPM = 2000, BMEP = 100 kpa.
Ethanol flow setting = 5.

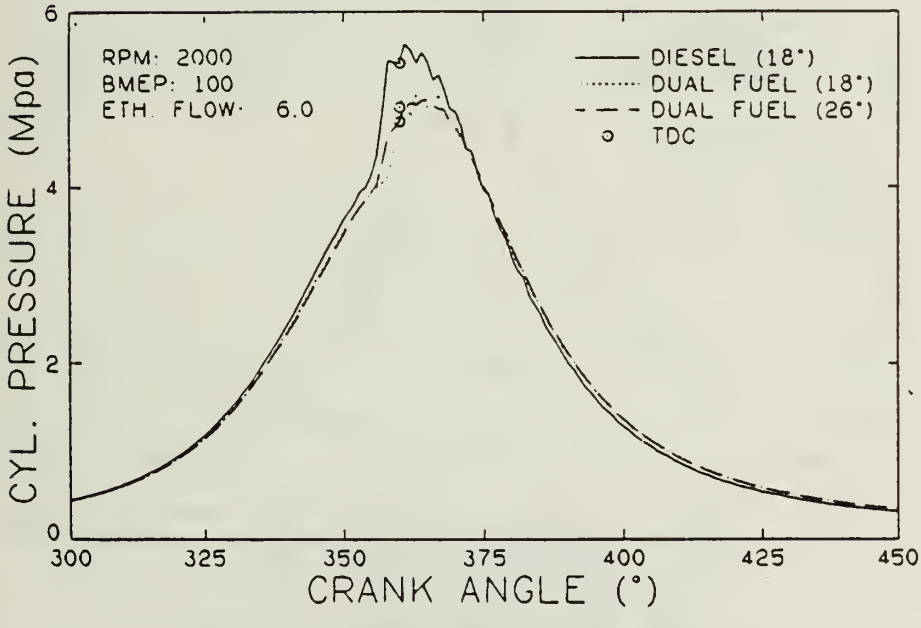

(b) RPM = 2000, BMEP = 100 kpa.
Ethanol flow setting = 6.

Figure 5.1 Effect of pilot timing advance on cylinder pressure for different flow rates of ethanol.

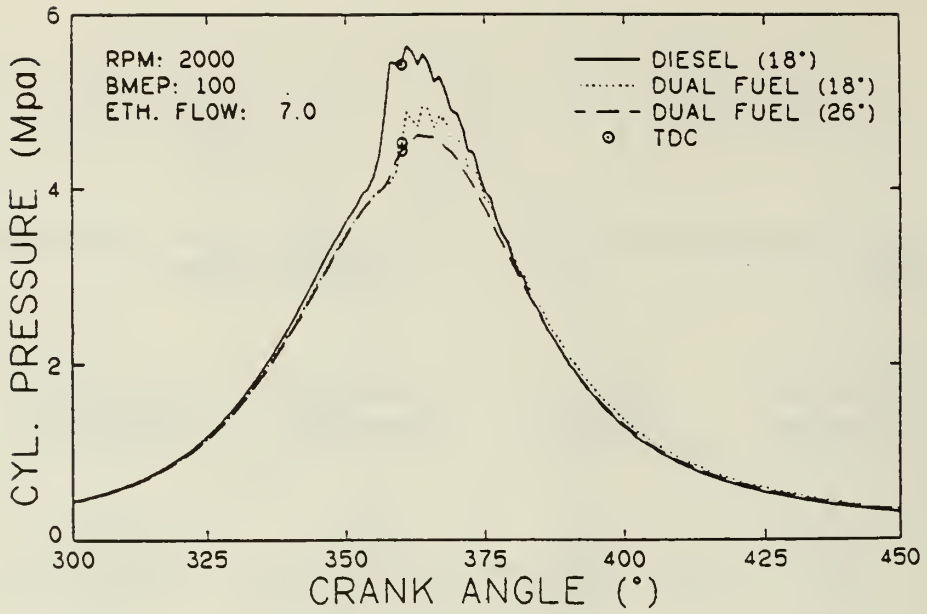

(a) RPM = 2000, BMEP = 100 kpa.
Ethanol flow setting = 7.

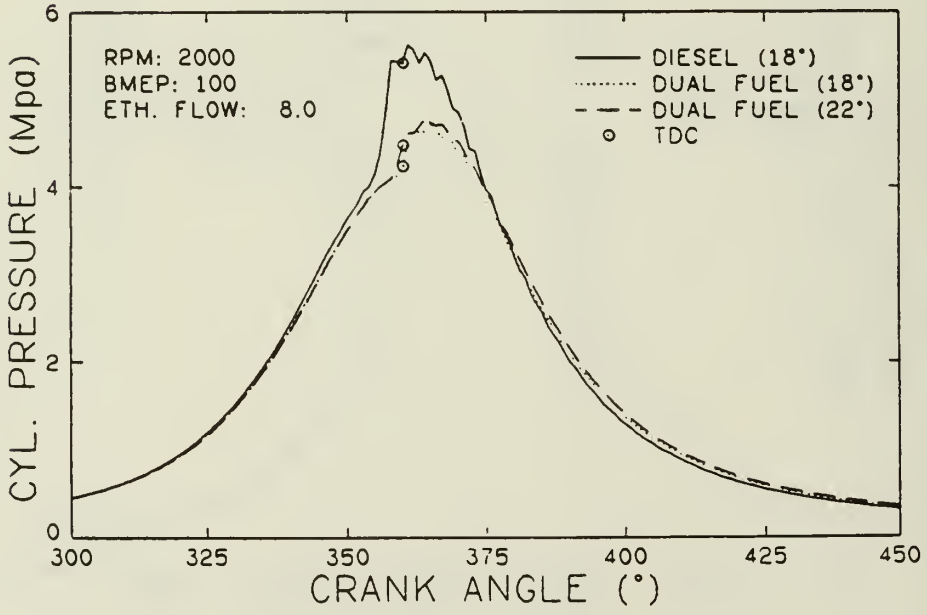

(b) RPM = 2000, BMEP = 100 kpa.
Ethanol flow setting = 8.

Figure 5.2 Effect of pilot timing advance on cylinder pressure for different flow rates of ethanol.

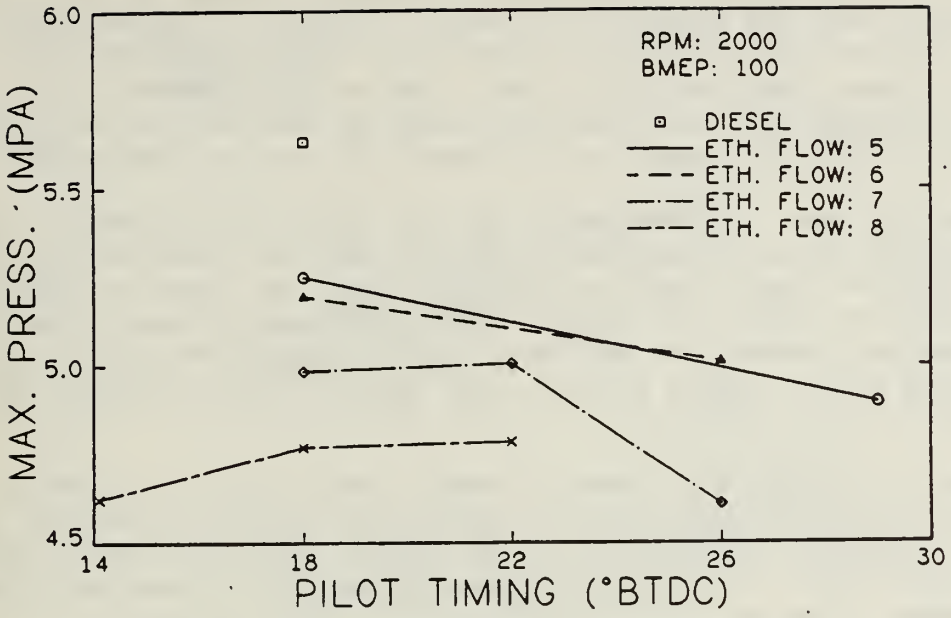

Figure 5.3 Effect of pilot fuel timing on maximum pressure for different flow rates of ethanol.

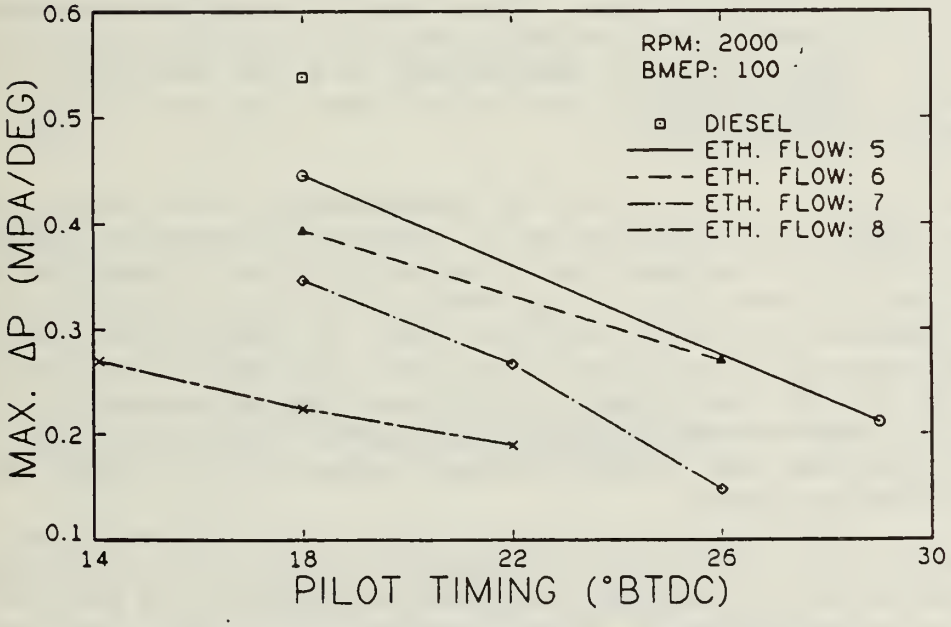

Figure 5.4 Effect of pilot fuel timing on maximum rate of pressure rise for different flow rates of ethanol.

sure rise for the ethanol flow rates was never as high as baseline diesel. This indicates that the addition of ethanol resulted in poorer ignition of the mixture. This may have been due to the lower charge temperatures at the time of injection which resulted with larger flow rates of ethanol. Also, ignition of the pilot charge may have been inhibited by the addition of ethanol since the diesel fuel was surrounded by an ethanol-air mixture rather than just air.

Figure 5.5 shows an increase in ignition delay with advance in pilot timing. As timing was advanced, the pilot fuel was injected into cooler charges which resulted in longer ignition delays. Also, the ignition delay generally increased with an increase in ethanol flow. This was primarily due to the low cetane number of ethanol and the lower charge temperatures at the time of injection which were a result of the lower specific heat ratio of the ethanol-air mixture.

Figure 5.6 is a plot of exhaust temperature versus pilot timing. Exhaust temperature did not change much with pilot timing for the ethanol flows of 5 and 6. The exhaust temperature for an ethanol flow of 8 at 14 degrees BTDC was high due to late burning on the power stroke. The same was probably true for the ethanol flow of 7 at 26 degrees BTDC since advancing the timing resulted in slower burning rates.

Figure 5.7 is a plot of nitric oxide concentration versus pilot timing. Adding ethanol resulted in concentrations of NO well below that of baseline diesel. NO is a strong function of peak temperature. Adding ethanol resulted in lower peak pressures and temperatures due to the increased ignition delays and slower initial burning rates. Thus, the NO concentration decreased with the addition of ethanol. NO concentration did not change much as timing was advanced. This shows that peak temperatures were not increased as timing was advanced which again indicates that pilot timing advance did not result in better ignition of the mixture.

Figure 5.8 is a plot of unburned hydrocarbons versus pilot timing. As ethanol was added, the concentration of unburned hydrocarbons increased significantly. This may have been due to the effect of wall quenching which prevented the complete combustion of the premixed ethanol-air mixture. Also, the ethanol-air mixture may have been too lean in some regions to burn completely. Hydrocarbons might also increase with the addition of ethanol due to the escape of some of the ethanol-air mixture into the exhaust as a result of valve overlap. Hydrocarbon concentration did not change much with timing advance which indicates that temperatures and combustion efficiency were not increased with timing advance.

Figure 5.9 shows carbon monoxide concentration versus pilot timing. The CO concentration for the dual fuel mode was much higher than that for baseline diesel. The concentration of CO for baseline diesel was approximately 0.05 percent and is not shown on the graph since it was so small. The increase in CO concentration with ethanol addition was due to the burning characteristics of the homogeneous ethanol-air mixture. The combustion of a homogeneous charge is controlled by a flame front rather than by diffusion. A characteristic of this type of combustion is that the CO produced is not readily oxidized to CO2 [6]. The concentration of CO is also increased slightly with timing advance which tends to indicate combustion became more inefficient.

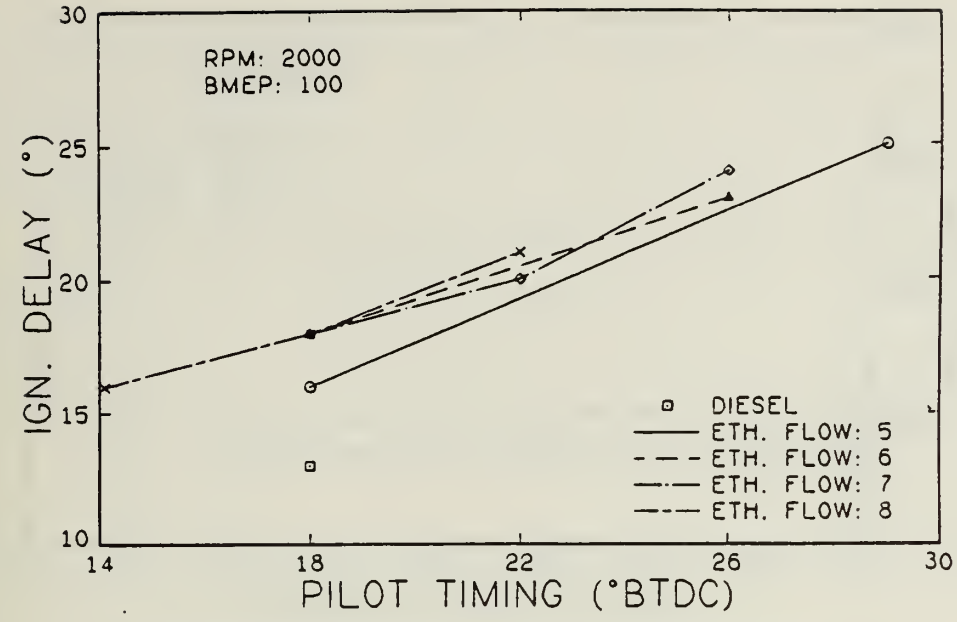

Figure 5.5 Effect of pilot fuel timing on ignition delay for different flow rates of ethanol.

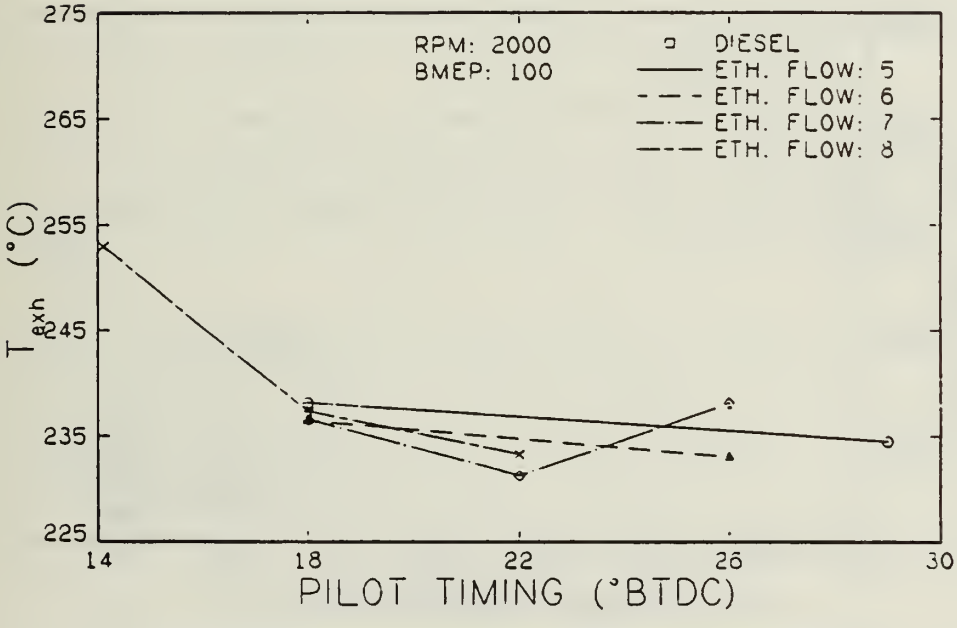

Figure 5.6 Effect of pilot fuel timing on exhaust temperature for different flow rates of ethanol.

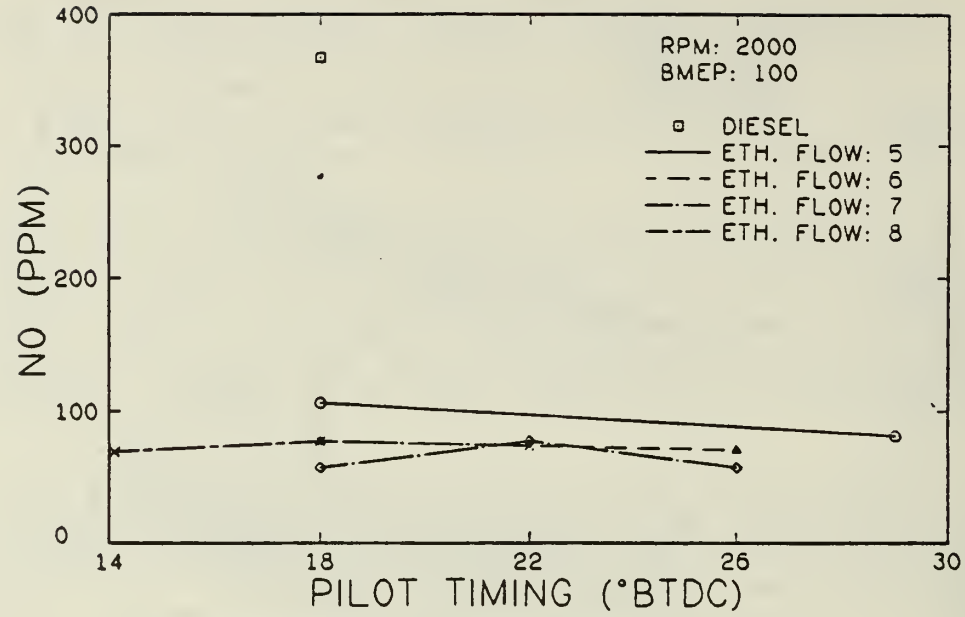

Figure 5.7 Effect of pilot fuel timing on nitric oxide concentration for different flow rates of ethanol.

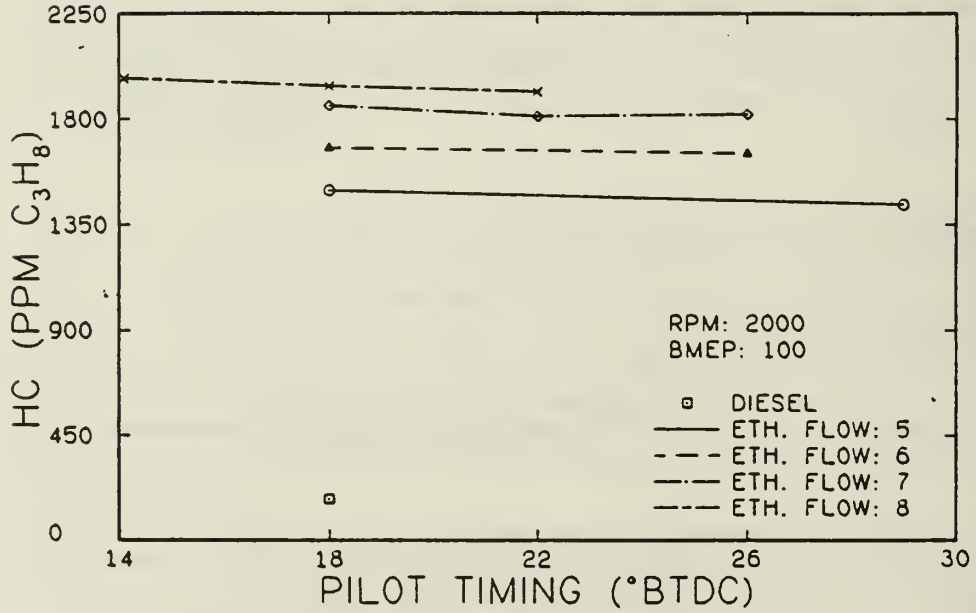

Figure 5.8 Effect of pilot fuel timing on hydrocarbon concentration for different flow rates of ethanol.

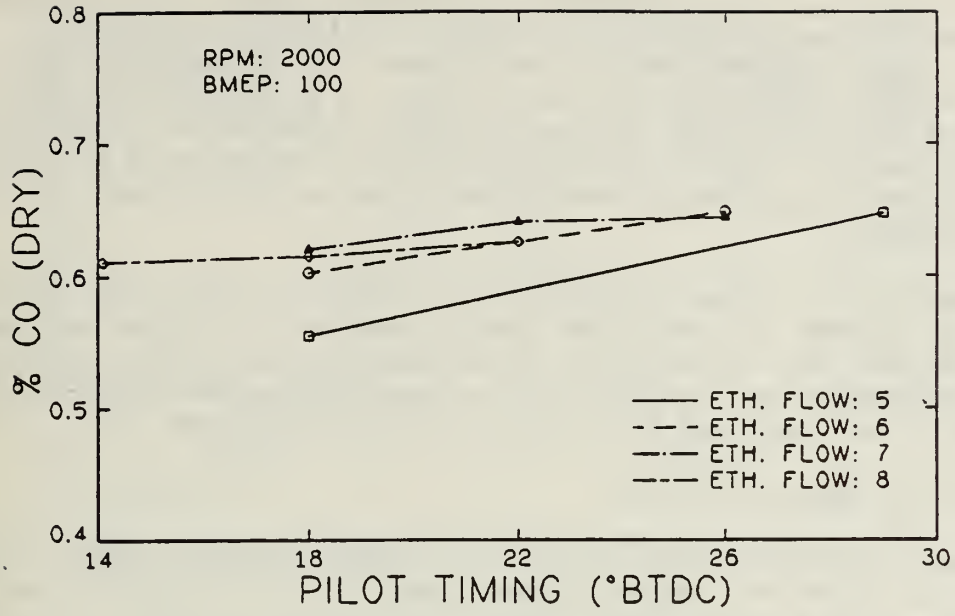

Figure 5.9 Effect of pilot fuel timing on carbon monoxide concentration for different flow rates of ethanol.

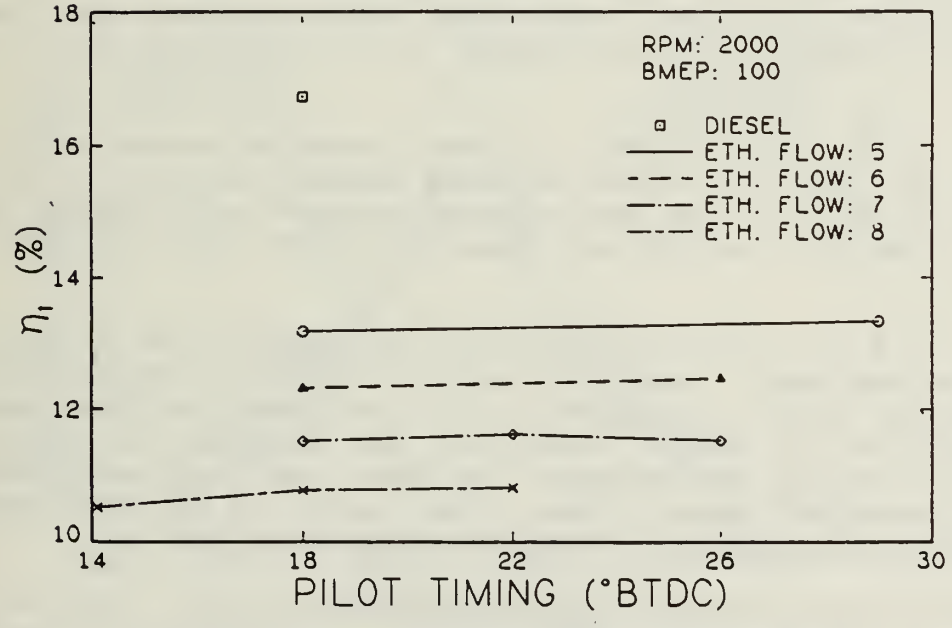

Figure 5.10 Effect of pilot fuel timing on thermal efficiency for different flow rates of ethanol.

Figure 5.10 is a plot of thermal efficiency versus pilot timing. As the ethanol flow rate was increased, the thermal efficiency decreased. This was due to the longer ignition delays and slower initial burning rates shifting the peak cylinder pressures to a point later in the cycle. Also, incomplete combustion of the ethanol-air mixture may have contributed to the decrease in thermal efficiency. Thermal efficiency did not change much with timing advance. This indicates that timing advance had no significant effect on the combustion process.

In summary, at a brake mean effective pressure of 100 kPa, advancing the timing in an attempt to shift the peak pressure to a point earlier in the engine cycle was not successful. There was little change in thermal efficiency. Advancing the timing actually increased engine misfire which meant lower ethanol flow rates had to be used at advanced timings.

5.2 Results for BMEP of 300 kPa

Figures 5.11 and 5.12 show plots of cylinder pressure versus crank angle degree for four different ethanol flow rates. As Fig. 5.11(a) shows, advancing the timing had a significant effect on cylinder pressure for an ethanol flow of 6. The dual fuel cylinder pressures at a pilot timing of 29 degrees BTDC follow those for baseline diesel. As Fig. 5.11(b) shows, however, advancing the pilot timing was not effective when the ethanol flow was increased to 8. Advancing the pilot timing for the dual fuel led to an earlier start of combustion, but peak pressure was not significantly increased. Figures 5.12(a) and (b) also show that advancing the timing was not effective for higher ethanol flow rates. For ethanol flows of 10 and 11.5, the maximum advanced pilot timing had to be decreased to avoid misfire. This is shown in Table 5.2.

Figure 5.13 shows maximum cylinder pressure versus pilot timing. Increasing the ethanol flow rate decreased maximum pressure, as was the case for a BMEP of 100 kPa. The peak pressure increased with advanced timing for an ethanol flow of 6, but did not change much with timing at higher ethanol flow rates.

Figure 5.14 is a plot of maximum rate of pressure rise versus pilot timing. The maximum rate of pressure rise for all ethanol flows was never above that of baseline diesel. The maximum rate of pressure rise increased with advanced timing for an ethanol flow of 6, but decreased for higher ethanol flows. This indicates that advancing the timing led to poorer ignition of the mixture at the higher ethanol flows. Thus, advancing the timing meant a decrease in the maximum amount of ethanol that could be used.

Figure 5.15 shows ignition delay versus pilot timing. The trends are the same as those discussed for a BMEP of 100 kPa. There was an increase in ignition delay as timing was advanced and ethanol flow rate was increased.

Figure 5.16 is a plot of exhaust temperature versus pilot timing. Again, the trends are similar to those for a BMEP of 100 kPa. As ethanol flow rate increased, the exhaust temperature decreased. At the higher ethanol flow rates, advancing the pilot timing reduced the exhaust temperature which means that timing advance succeeded in reducing some of the late burning on the power stroke.

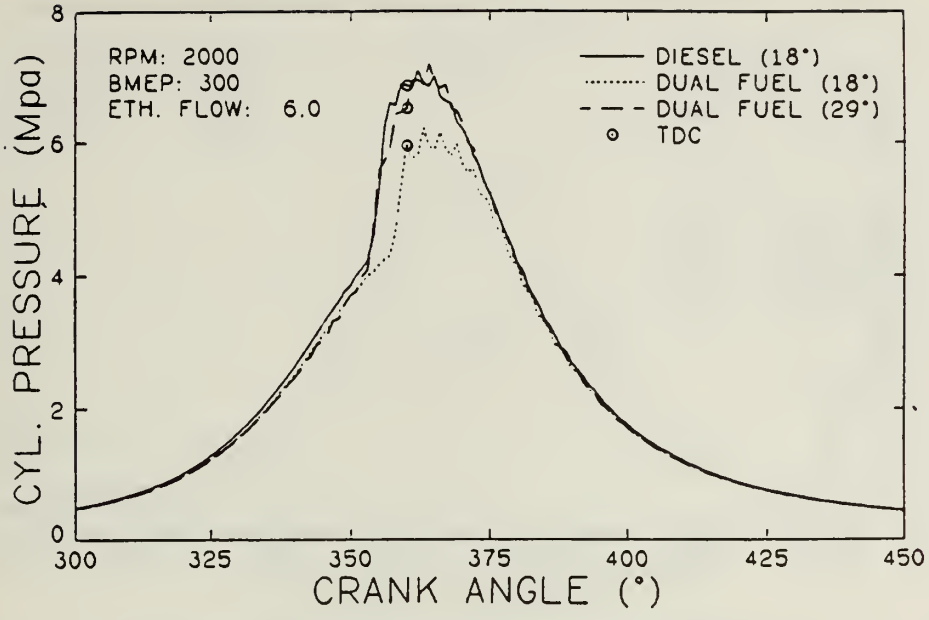

(a) RPM = 2000, BMEP = 300 kpa.
Ethanol flow setting = 6.

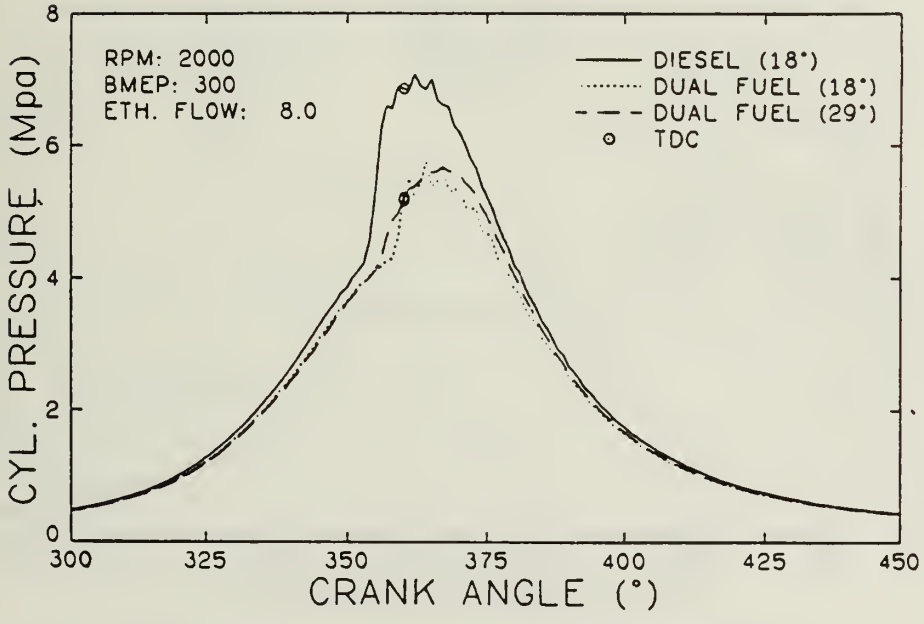

(b) RPM = 2000, BMEP = 300 kpa.
Ethanol flow setting = 8.

Figure 5.11 Effect of pilot timing advance on cylinder pressure for different flow rates of ethanol.

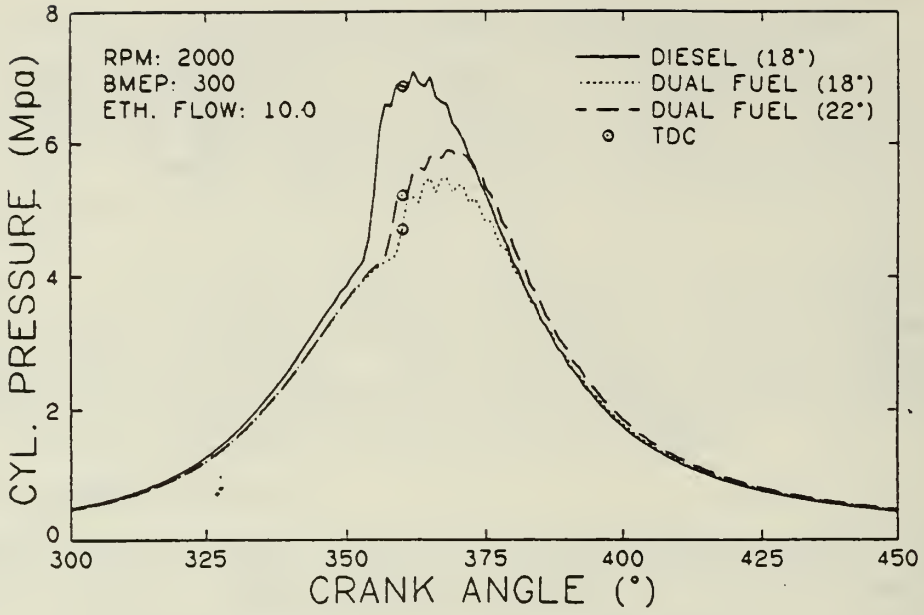

(a) RPM = 2000, BMEP = 300 kpa.
Ethanol flow setting = 10.

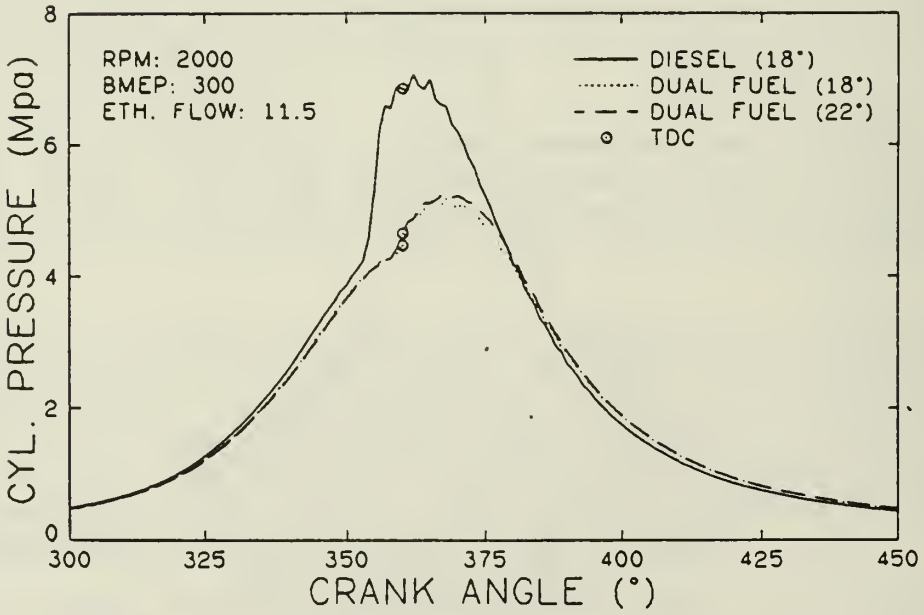

(b) RPM = 2000, BMEP = 300 kpa.
Ethanol flow setting = 11.5

Figure 5.12 Effect of pilot timing advance on cylinder pressure for different flow rates of ethanol.

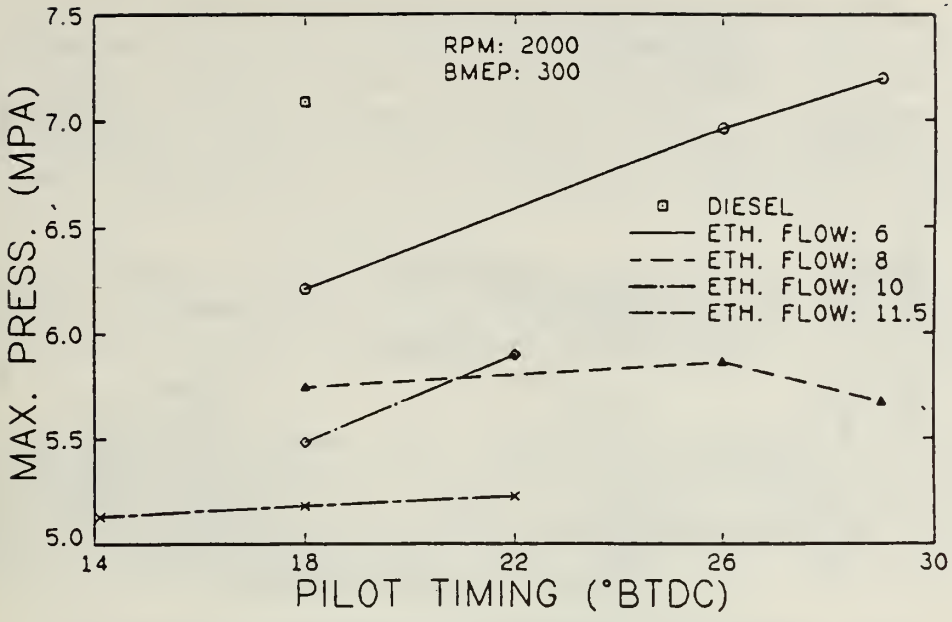

Figure 5.13 Effect of pilot fuel timing on maximum pressure for different flow rates of ethanol.

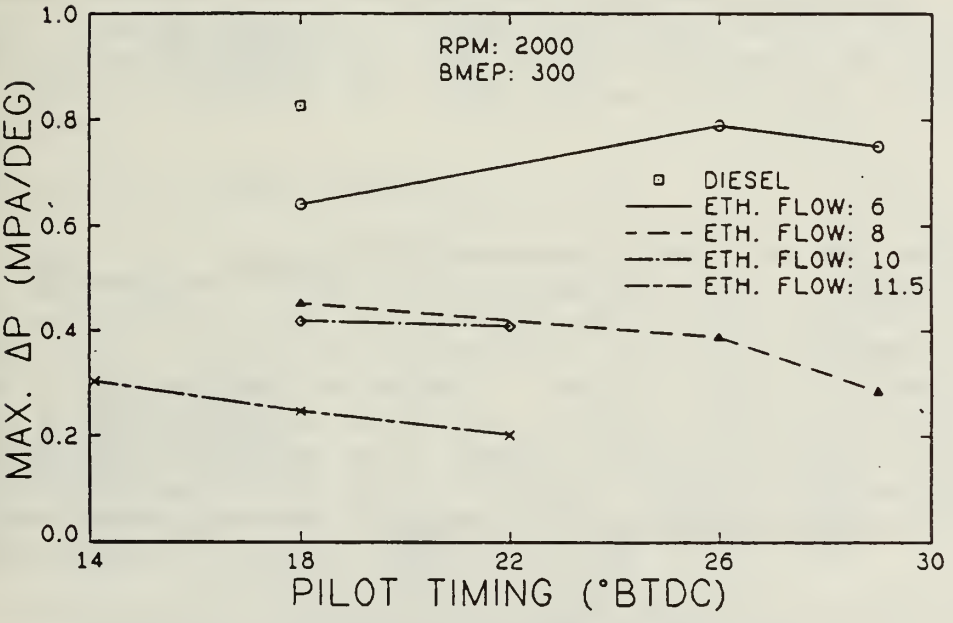

Figure 5.14 Effect of pilot fuel timing on maximum rate of pressure rise for different flow rates of ethanol.

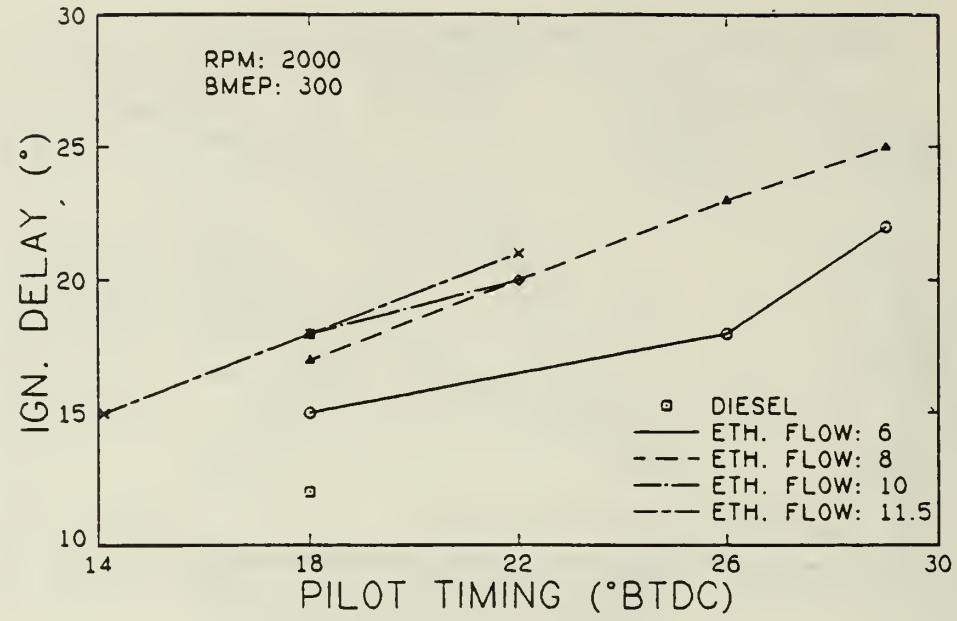

Figure 5.15 Effect of pilot fuel timing on ignition delay for different flow rates of ethanol.

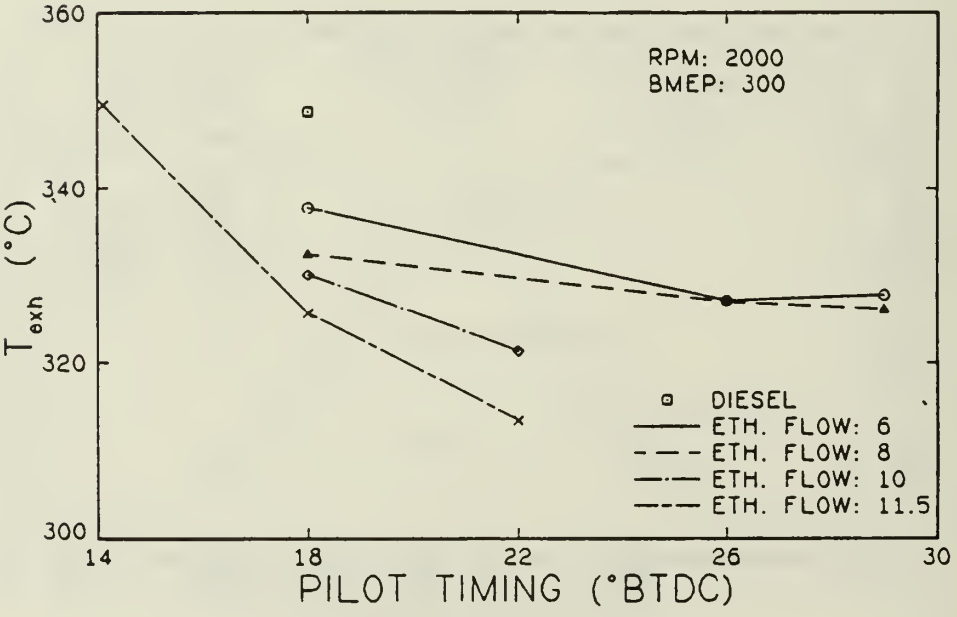

Figure 5.16 Effect of pilot fuel timing on exhaust temperature for different flow rates of ethanol.

Figure 5.17 is a plot of NO concentration versus pilot timing. NO concentration decreased as ethanol flow increased due to lower peak temperatures. for ethanol flows of 6 and 8 there was a general increase in NO as timing was advanced while for ethanol flows of 10 and 11.5 there was not much change. The increase in NO with timing advance at lower ethanol flows tends to indicate that changing the timing led to higher temperatures and better combustion.

Figure 5.18 shows unburned hydrocarbons versus pilot timing. As expected, hydrocarbon concentration increased as ethanol flow increased. There was no significant decrease in hydrocarbon concentration as timing was advanced.

Figure 5.19 shows that there was a significant decrease in CO concentration as pilot timing was advanced. This indicates that combustion became more efficient with timing advance. At a BMEP of 100 kPa, however, CO concentration increased slightly with timing. Thus, advancing the timing seems to be more effective at a BMEP of 300 kPa.

Figure 5.20 is a plot of thermal efficiency versus pilot timing. As was the case for a BMEP of 100 kPa, the thermal efficiency was lower for the dual fuel than for baseline diesel. But timing advance increased thermal efficiency for the ethanol flows of 6, 8 and 10. The relative increase in thermal efficiency for an ethanol flow of 8 was 3.7 percent.

In summary, advancing the timing seemed to be more effective at a BMEP of 300 kPa than it was at 100 kPa. Thermal efficiency was increased significantly by advancing the timing for some ethanol flow rates. At the maximum flow rates, however, advancing the timing had no significant effect on the combustion process.

5.2.3 Results for a BMEP of 500 kPa

Figure 5.21 shows cylinder pressure versus crank angle degree for two ethanol flow rates. Figure 5.21(a) shows that for an ethanol flow of 11.5, advancing the timing for the dual fuel had a major effect on cylinder pressure. The start of combustion for the dual fuel at an advanced timing was earlier than it was for baseline diesel. The dual fuel at advanced timing also achieved a higher peak pressure than baseline diesel. Figure 5.21(b) shows that advancing the timing at an ethanol flow of 12.5 also significantly changed cylinder pressure. But at this ethanol flow rate, the maximum timing advance which could be used was 22 degrees BTDC. Further advance resulted in excessive engine knock.

Figure 5.22 shows that the maximum cylinder pressure was much higher for the dual fuel at advanced timings than for baseline diesel. This was due to the rapid burning of the ethanol-air mixture once it was ignited. In contrast to the case of a BMEP of 300 kPa, advancing the pilot timing at 500 kPa resulted in a significant increase in peak pressure.

Figure 5.23 shows that the maximum rate of cylinder pressure rise increased significantly for the dual fuel as pilot timing was advanced. Thus, advancing the timing at high ethanol flows did not lead to poorer combustion as it did at the lower loads. One reason for this may be the increased

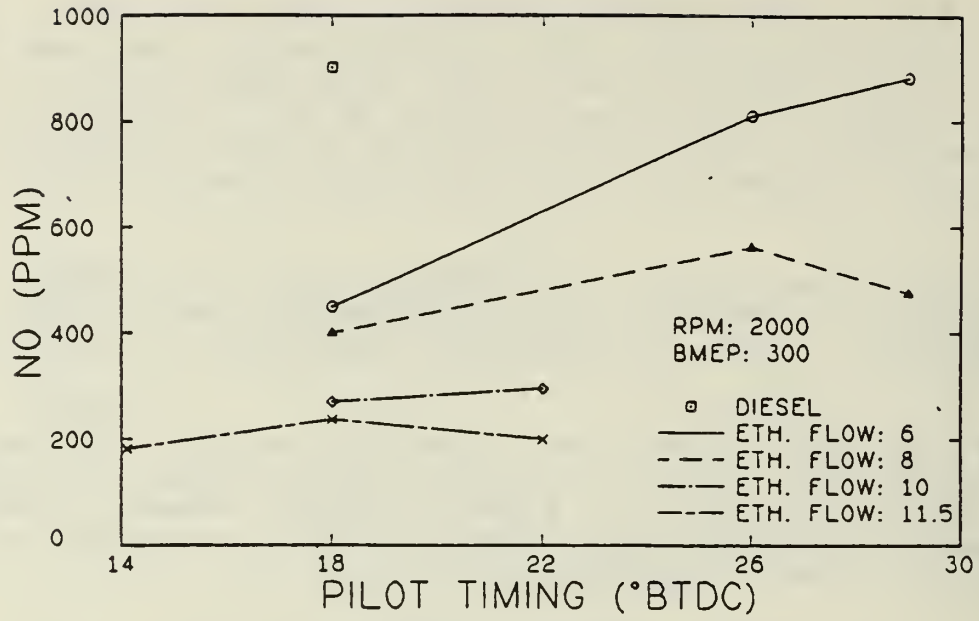

Figure 5.17 Effect of pilot fuel timing on nitric oxide concentration for different flow rates of ethanol.

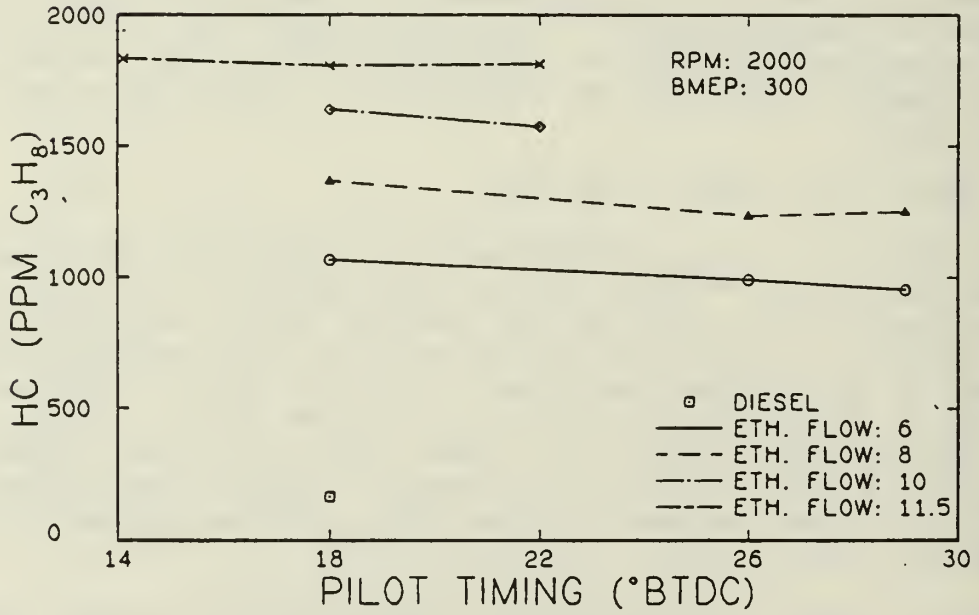

Figure 5.18 Effect of pilot fuel timing on hydrocarbon concentration for different flow rates of ethanol.

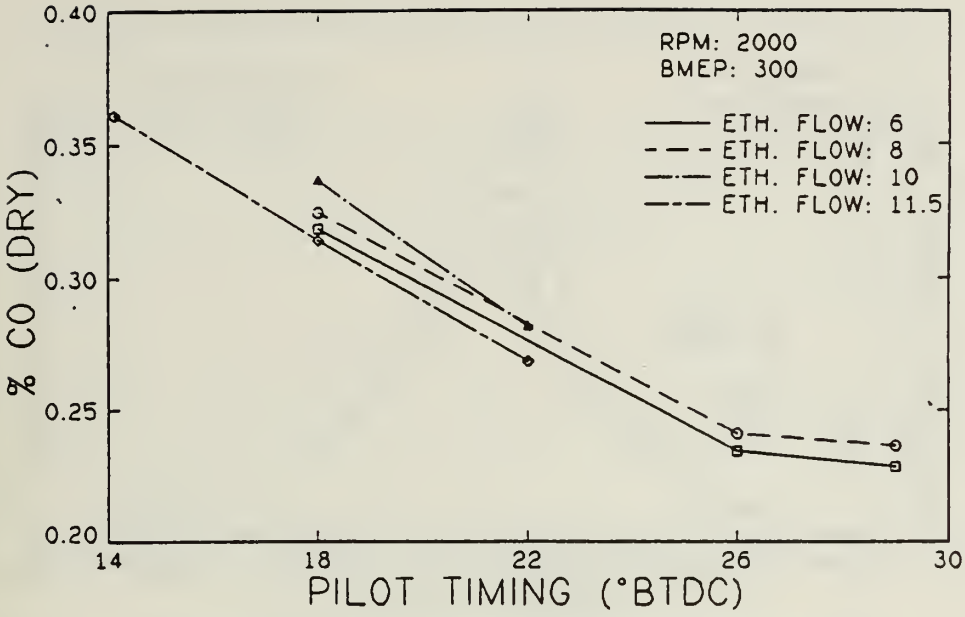

Figure 5.19 Effect of pilot fuel timing on carbon monoxide concentration for different flow rates of ethanol.

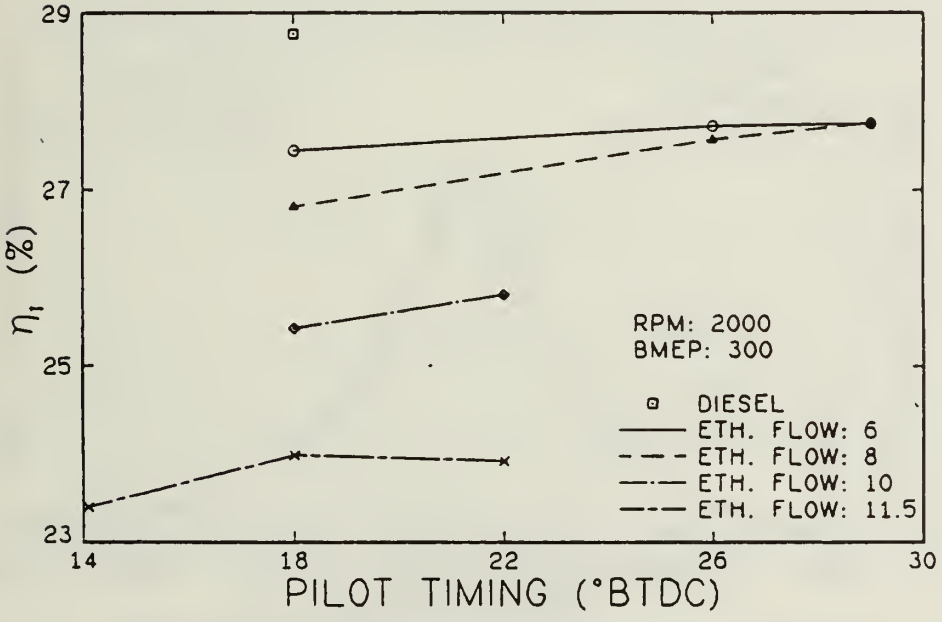

Figure 5.20 Effect of pilot fuel timing on thermal efficiency for different flow rates of ethanol.

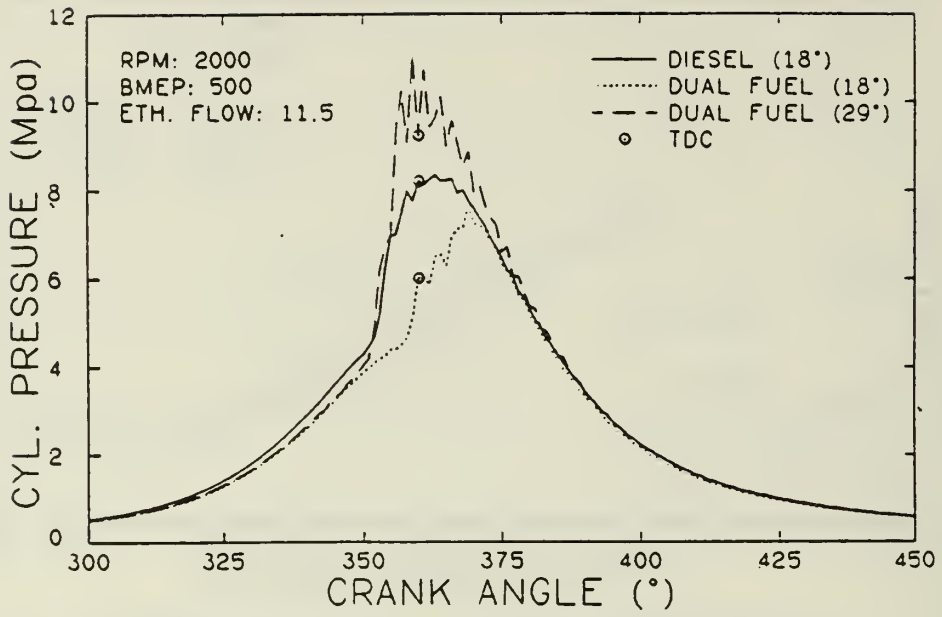

(a) RPM = 2000, BMEP = 500 kpa.
Ethanol flow setting = 11.5

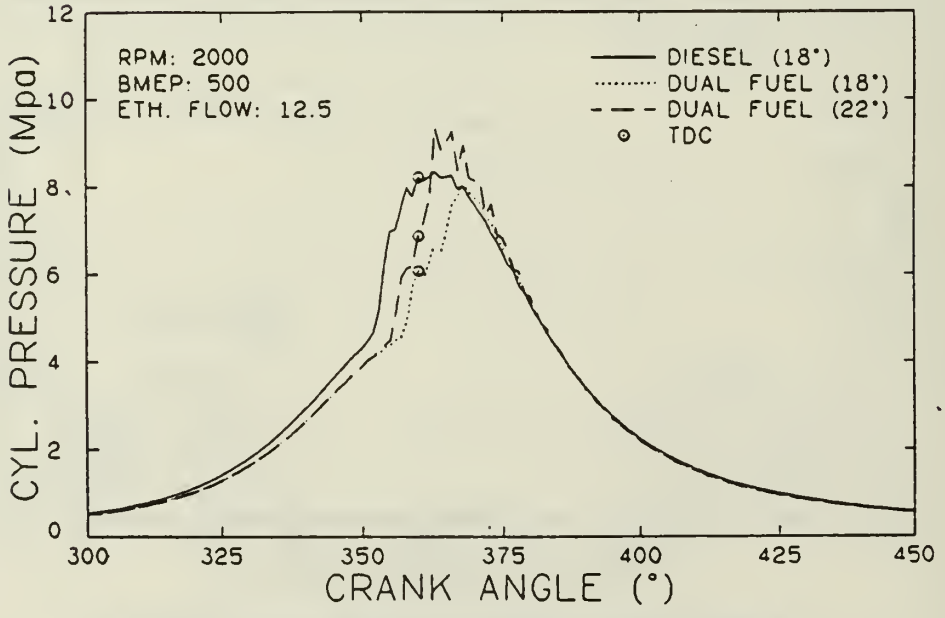

(b) RPM = 2000, BMEP = 500 kpa.
Ethanol flow setting = 12.5

Figure 5.21 Effect of pilot timing advance on cylinder pressure for different flow rates of ethanol.

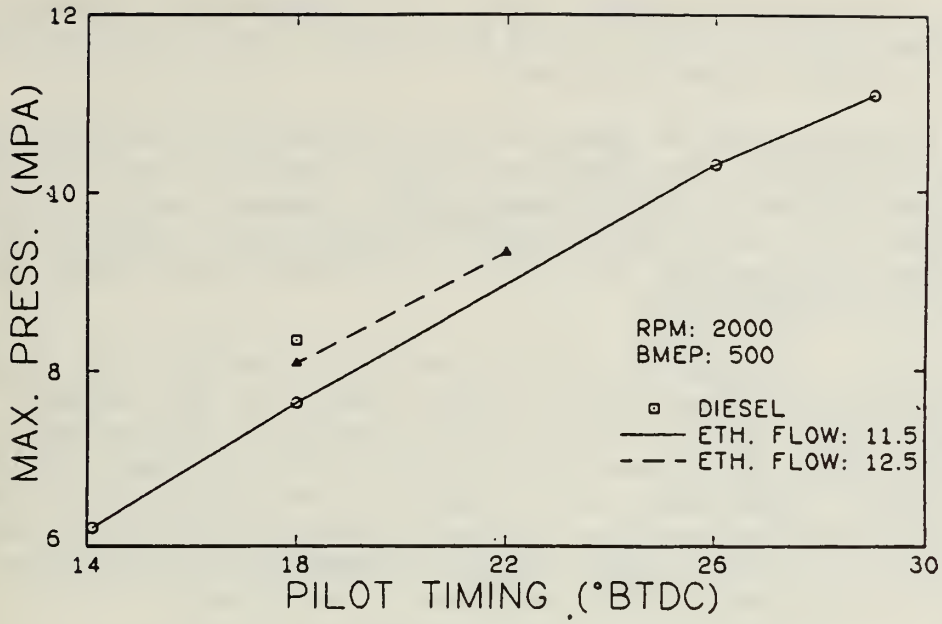

Figure 5.22 Effect of pilot fuel timing on maximum pressure for different flow rates of ethanol.

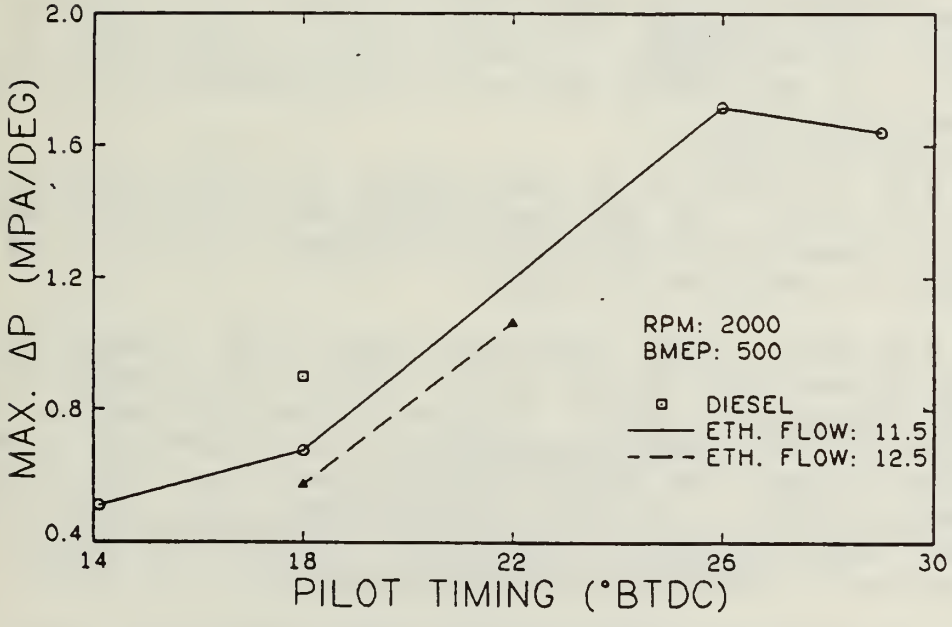

Figure 5.23 Effect of pilot fuel timing on maximum rate of pressure rise for different flow rates of ethanol.

temperatures at the time of diesel injection for the higher load case. At 500 kPa, the maximum rate of pressure rise for the dual fuel at an advanced timing was well above that for baseline diesel.

Figure 5.24 is a plot of ignition delay versus pilot timing. Trends with pilot timing and ethanol flow were the same as those discussed for the lower loads. The magnitudes of the ignition delays, however, were less than those at lower loads for similar percentages of fuel energy supplied as ethanol. This was probably because the pilot fuel was injected into higher charge temperatures at the higher load.

Figure 5.25 is a plot of exhaust temperature versus pilot timing. Exhaust temperature was lower for the fuel fuel than for diesel. This was probably due to the rapid burning of the ethanol-air mixture near top dead center as compared to the slower diffusion burn for the baseline diesel. The change in exhaust temperature as a result of the addition of ethanol was higher at this load than for lower loads. Again, this indicates that the addition of ethanol resulted in more complete combustion of the mixture near top dead center for the higher load as compared to lower loads.

Figure 5.26 shows NO concentration versus pilot timing. There was a large increase in the concentration of NO when timing was advanced. Levels for the dual fuel at advanced timings were much higher than for baseline diesel due to higher peak temperatures.

Figure 5.27 shows unburned hydrocarbons versus pilot timing. As was the case at lower loads, the dual fuels had a higher concentration of unburned hydrocarbons. But the advance of timing led to a significant decrease in hydrocarbons. This was probably due to the higher temperatures achieved when timing was advanced.

Figure 5.28 is a plot of CO concentration as a function of pilot timing. CO levels at this load were approximately half those at a BMEP of 300 kPa. Also, CO concentration decreased with advances in pilot timing indicating an increase in combustion efficiency.

Figure 5.29 shows thermal efficiency versus pilot timing. At a pilot timing of 18 degrees BTDC, the use of dual fuel led to a higher thermal efficiency than for baseline diesel. This was because the addition of ethanol resulted in more of the combustion process occurring at constant volume. However, at other timings, the thermal efficiency was lower for the dual fuel than for baseline diesel. This was because advancing the timing resulted in peak pressures occurring early in the cycle. The lower efficiency at 14 degrees BTDC was due to the peak pressure occurring late in the cycle.

In summary, changes in pilot timing had more effect on cylinder pressure at a BMEP of 500 kPa than for lower loads. However, the use of timings other than the stock timing of 18 degrees BTDC was not beneficial since peak pressures were shifted in such a way as to lower thermal efficiency.

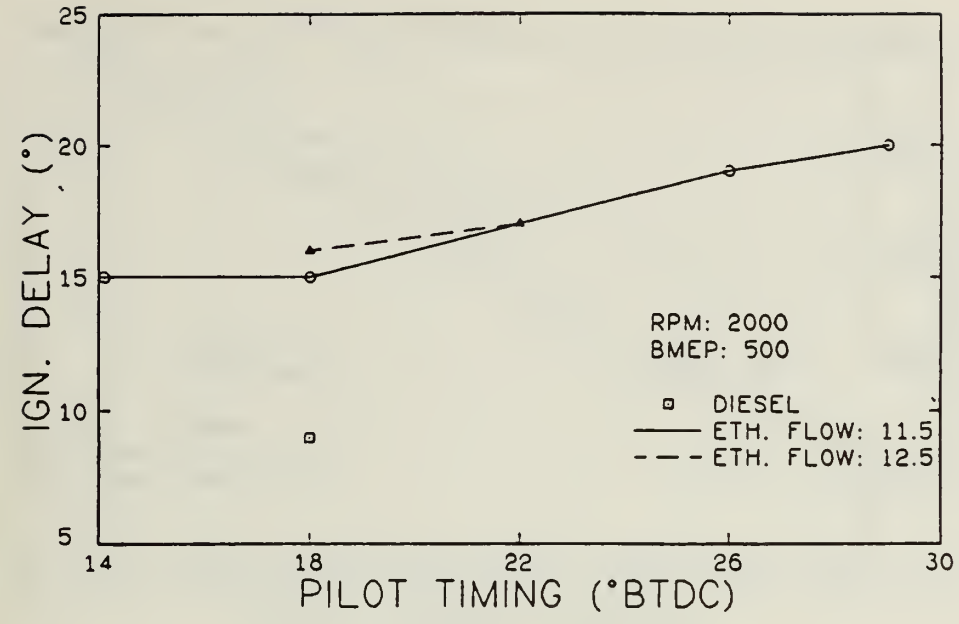

Figure 5.24 Effect of pilot fuel timing on ignition delay for different flow rates of ethanol.

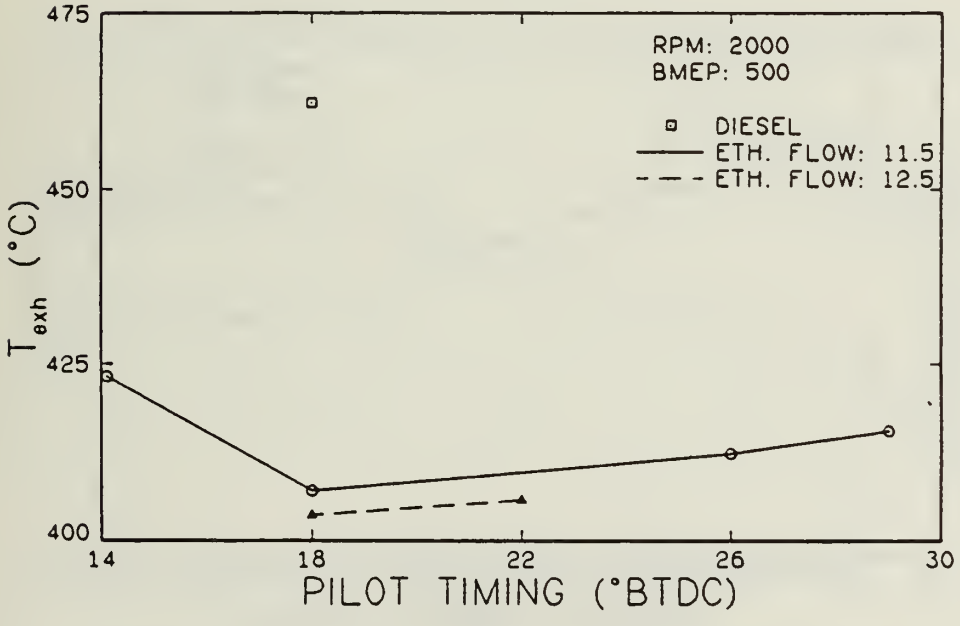

Figure 5.25 Effect of pilot fuel timing on exhaust temperature for different flow rates of ethanol.

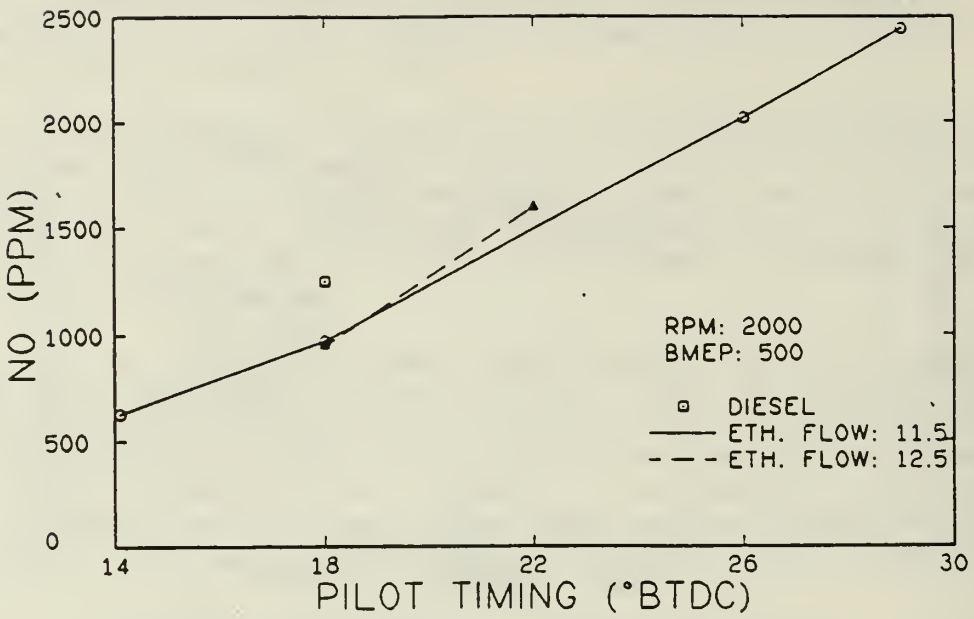

Figure 5.26 Effect of pilot fuel timing on nitric oxide concentration for different flow rates of ethanol.

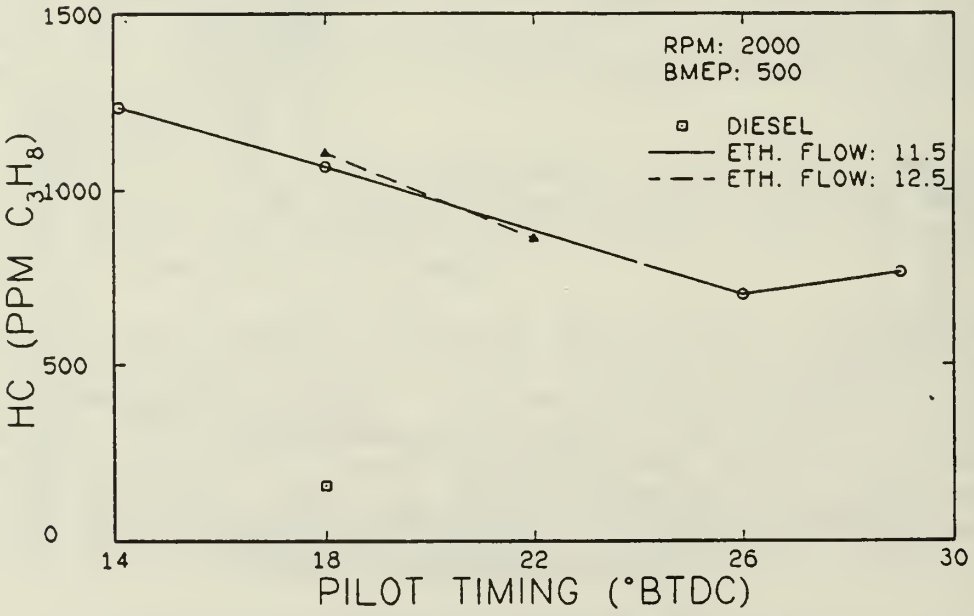

Figure 5.27 Effect of pilot fuel timing on hydrocarbon concentration for different flow rates of ethanol.

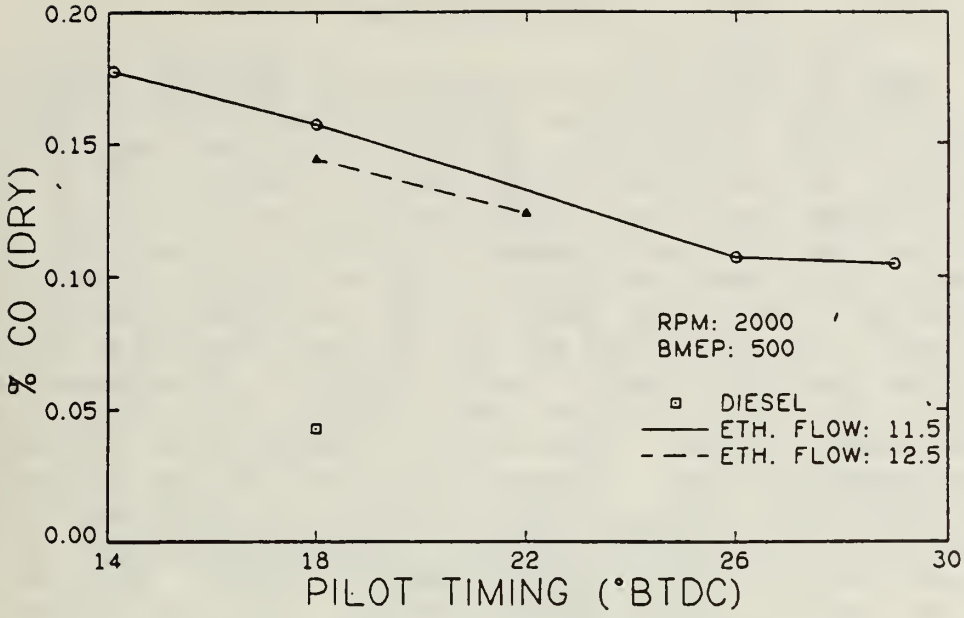

Figure 5.28 Effect of pilot fuel timing on carbon monoxide concentration for different flow rates of ethanol.

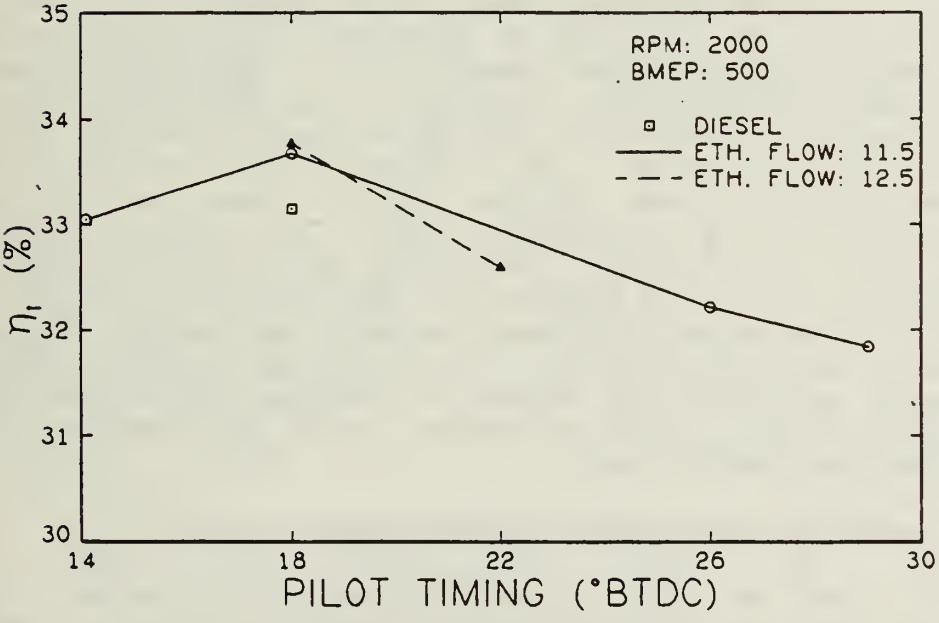

Figure 5.29 Effect of pilot fuel timing on thermal efficiency for different flow rates of ethanol.

5.2.4 Results for BMEP's of 700 and 900 kPa

These two loads are discussed together since the trends were similar. Figures 5.20(a) and (b) show cylinder pressure versus crank angle degree for the two loads. Basically, the results were the same as those at a BMEP of 500 kPa. At the higher loads, however, the dual fuel at 18 degrees BTDC reached a higher peak pressure than the baseline diesel case. As timing was advanced for the dual fuel, combustion started much earlier. It can be seen from the cylinder pressure diagrams that the advanced timing shifted the peak pressure to a point too early in the cycle resulting in increased compression work. Figures 5.31(a) and (b) show peak pressure as a function of pilot timing for the higher loads. Peak pressures at 18 degrees BTDC for the dual fuel were significantly higher than baseline diesel due to the rapid pressure rise after ignition. There was also the expected increase in peak pressure with advanced timing. Figures 5.32(a) and (b) show the maximum rate of pressure rise versus timing. Values for dual fuel at 18 degrees BTDC were roughly twice as high as baseline diesel. Figures 5.33(a) and (b) show the expected trends for ignition delay with the pilot timing. Also, as load was increased, the ignition delay became shorter. This was because a lower percentage of ethanol had to be used at higher load to avoid excessive knock. At 18 degrees BTDC the ignition delay for dual fuel was close to that of diesel. Figures 5.34(a) and (b) show exhaust temperature versus pilot timing. The plots show that exhaust temperature was a minimum at a pilot timing of 18 degrees BTDC. This tends to indicate that thermal efficiency was highest at this timing. As will be shown later, this was the case. Figures 5.35(a) and (b) show the expected trends for NO concentration. Note that the concentrations of NO fur dual fuel at 18 degrees BTDC were higher than baseline diesel due to the higher peak temperatures. Figures 5.36(a) and (b) show that the levels of unburned hydrocarbons were lower at high loads than at low loads. This was mostly a result of the use of lower percentages of ethanol at high loads to avoid excessive knock. Figures 5.37(a) and (b) show CO concentration versus pilot timing. Fur dual fuels at these loads, CO levels were minimum at a pilot timing of 18 degrees BTDC. This suggests that combustion was most efficient at that timing. For a BMEP of 900 kPa, the level of CO was lower for the dual fuel at 18 degrees BTDC that for baseline diesel. Figures 5.38(a) and (b) show thermal efficiency versus pilot timing. for both loads, efficiency was a maximum for the dual fuels at 18 degrees BTDC. for a BMEP of 900 kPa, thermal efficiency was higher for the dual fuel at 18 degrees BTDC than for baseline diesel. This was because more of the combustion occurred at constant volume for the dual fuel.

5.2.5 Summary of Test at 2000 RPM and Various Loads

At a BMEP of 100 kPa, advancing the pilot timing was ineffective. Higher timings actually led to increased engine misfire. At a BMEP of 300 kPa, advancing the pilot timing effectively increased the thermal efficiency at some ethanol flow rates, but still increased engine misfire at maximum ethanol flows. At a BMEP of 500 kPa, pilot timing had a major effect on cylinder pressure. Advances in timing no longer increased engine misfire, but instead resulted in increased knock. Thermal efficiency was a maximum at the stock timing of 18 degrees BTDC for the dual fuel. Similar results were obtained for BMEP's of 700 and 900 kPa. Advanced timing caused peak pressures to occur too early in the cycle which lowered thermal efficiency. An optimum timing of 18 degrees BTDC was expected for dual fuel at these loads since low

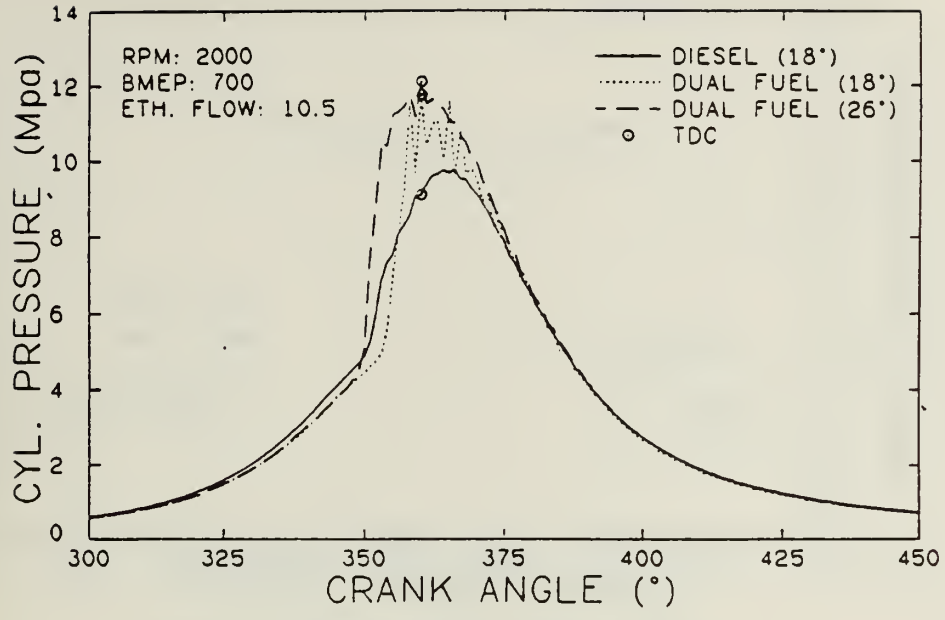

(a) RPM = 2000, BMEP = 700 kpa.
Ethanol flow setting = 10.5

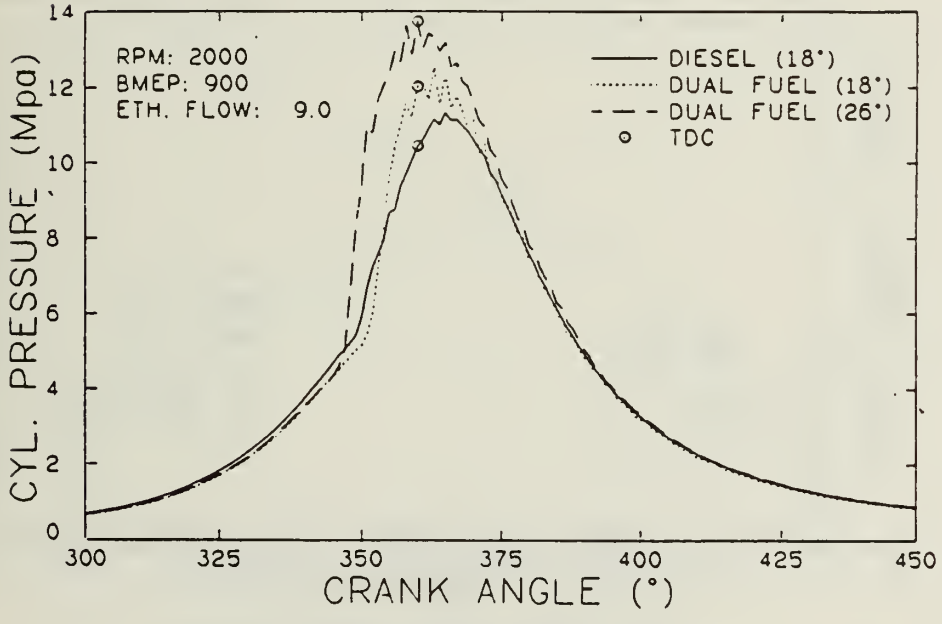

(b) RPM = 2000, BMEP = 900 kpa.
Ethanol flow setting = 9.

Figure 5.30 Effect of pilot timing advance on cylinder pressure.

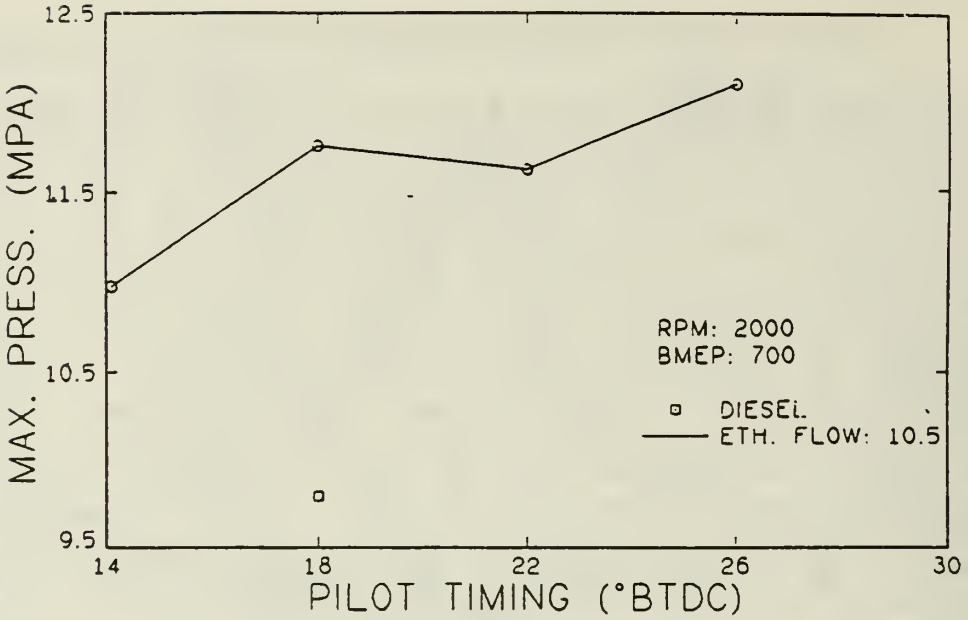

(a) RPM = 2000, BMEP = 700 kpa.
Ethanol flow setting = 10.5

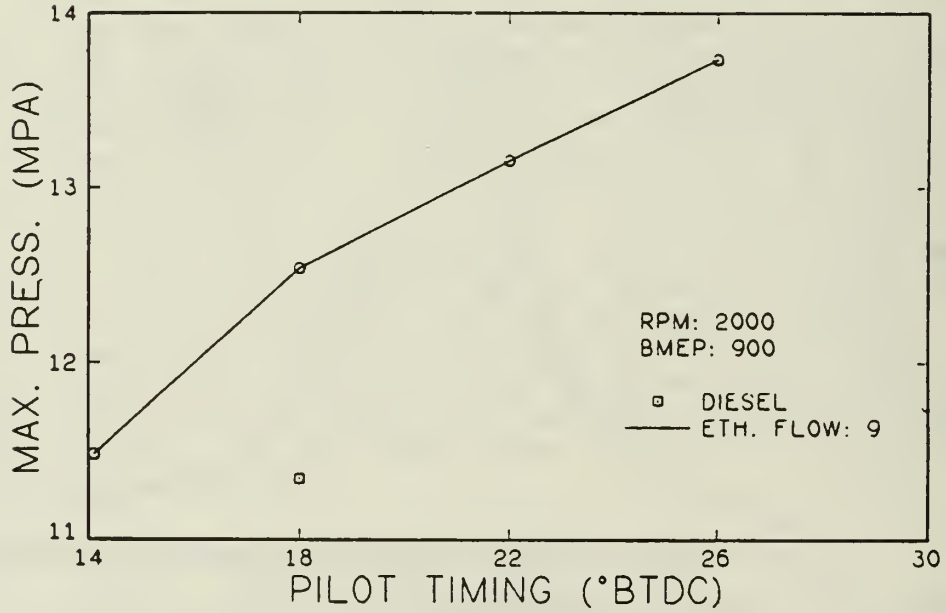

(b) RPM = 2000, BMEP = 900 kpa.
Ethanol flow setting = 9.

Figure 5.31 Effect of pilot fuel timing on maximum pressure.

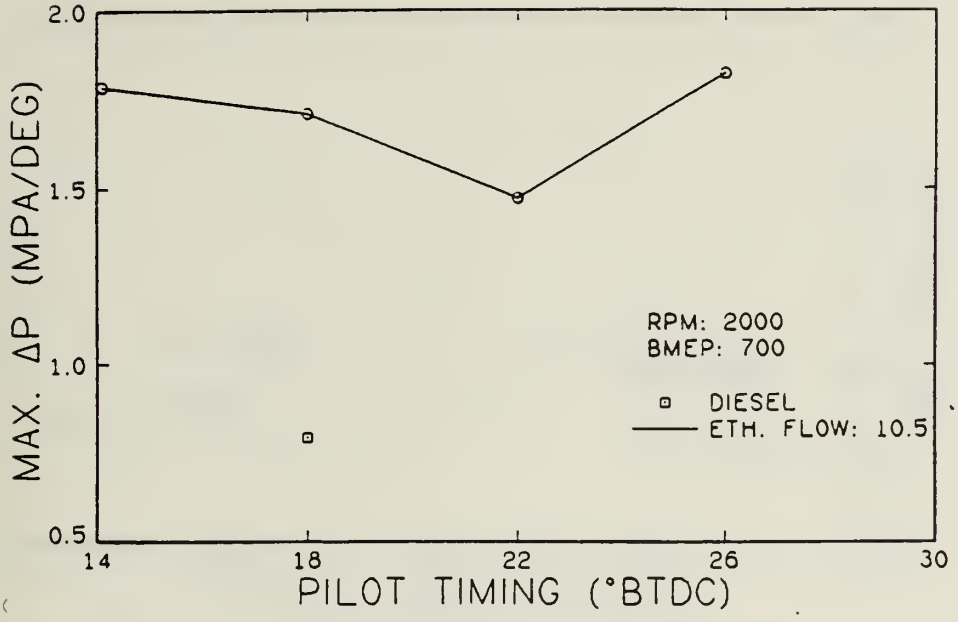

(a) RPM = 2000, BMEP = 700 kpa.
Ethanol flow setting = 10.5

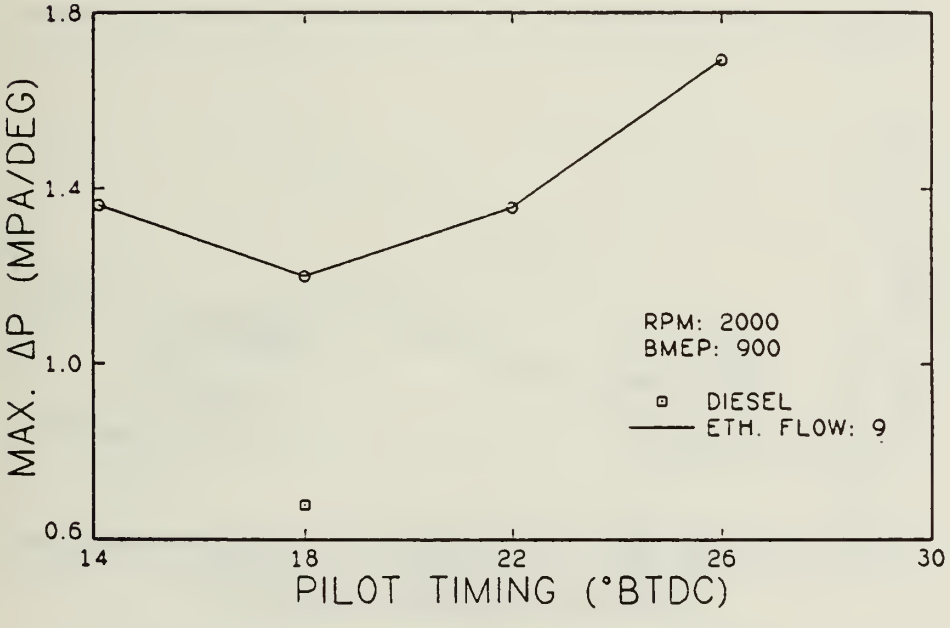

(b) RPM = 2000, BMEP = 900 kpa.
Ethanol flow setting = 9.

Figure 5.32 Effect of pilot fuel timing on maximum rate of pressure rise.

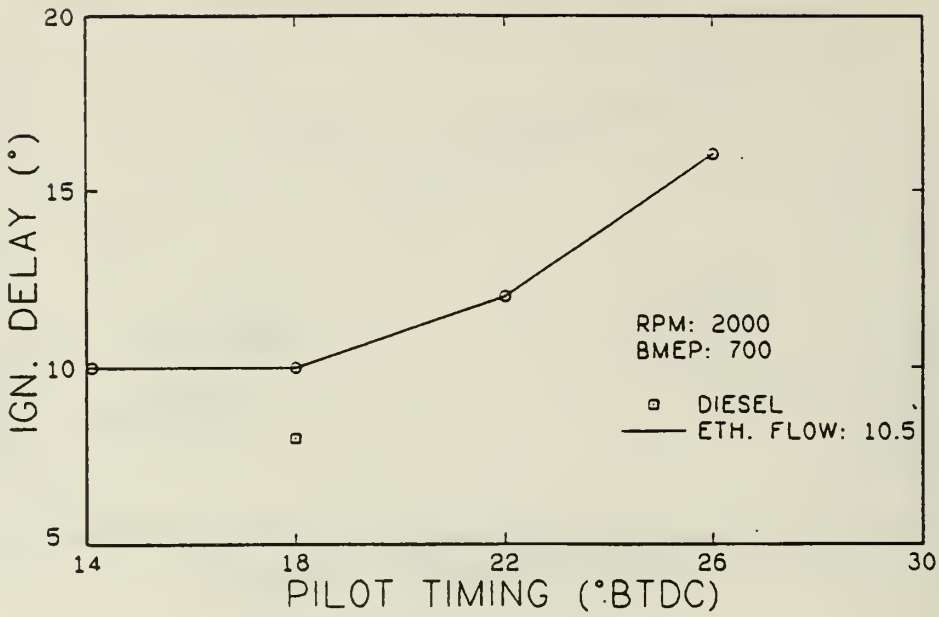

(a) RPM = 2000, BMEP = 700 kpa.
Ethanol flow setting = 10.5

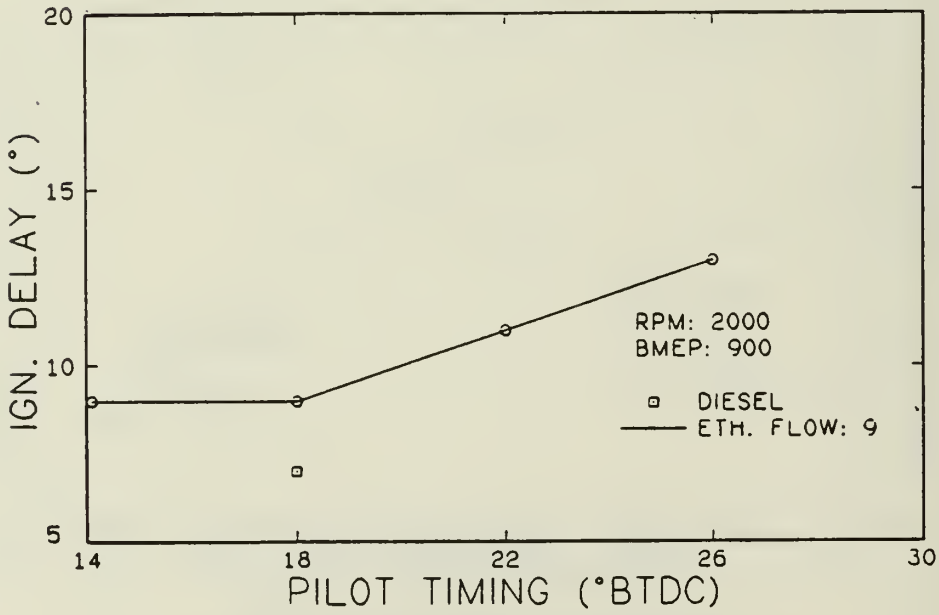

(b) RPM = 2000, BMEP = 900 kpa.
Ethanol flow setting = 9.

Figure 5.33 Effect of pilot fuel timing on ignition delay.

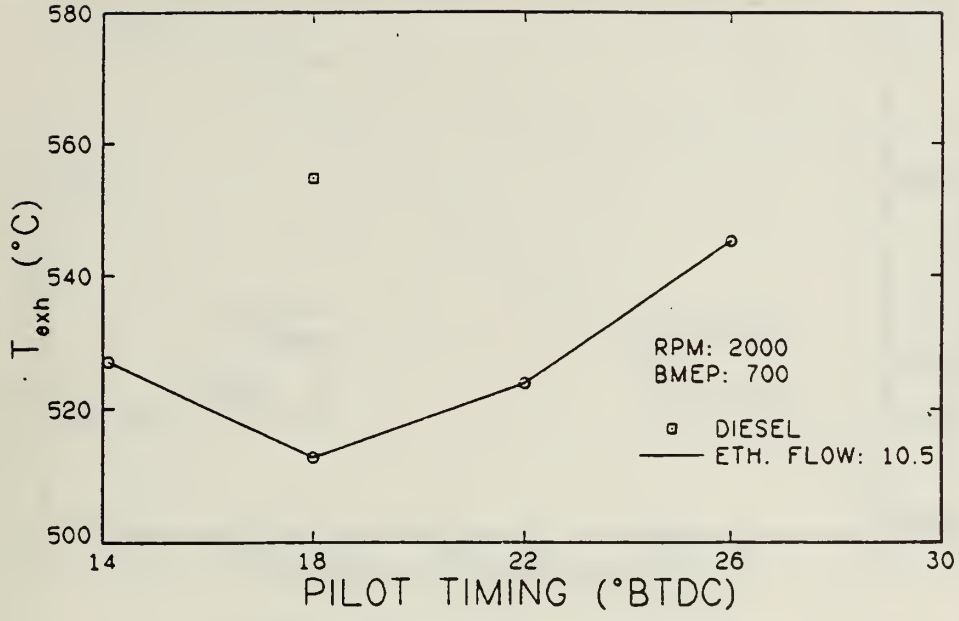

(a) RPM = 2000, BMEP = 700 kpa.
Ethanol flow setting = 10.5

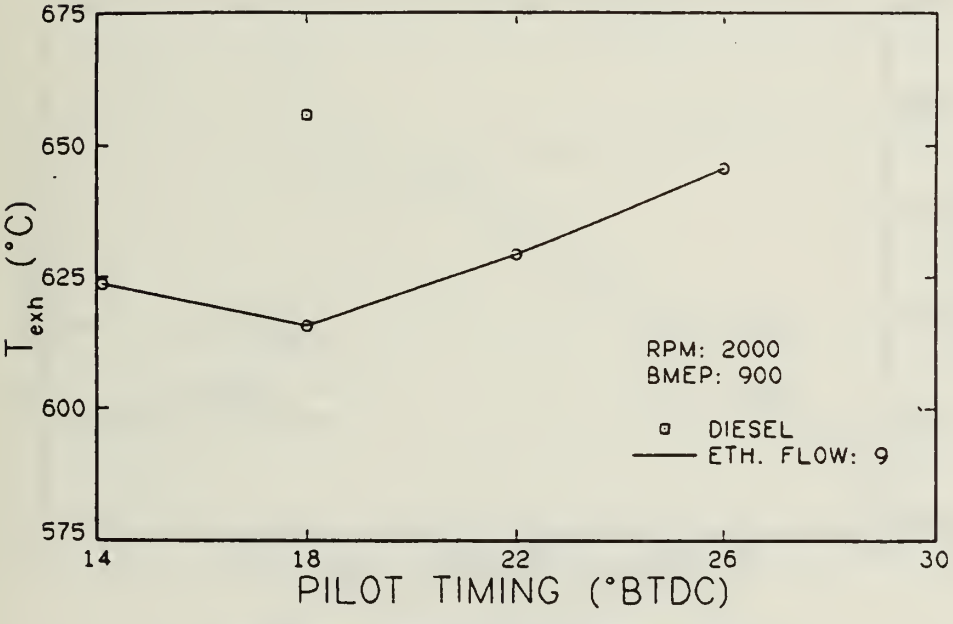

(b) RPM = 2000, BMEP = 900 kpa.
Ethanol flow setting = 9.

Figure 5.34 Effect of pilot fuel timing on exhaust temperature.

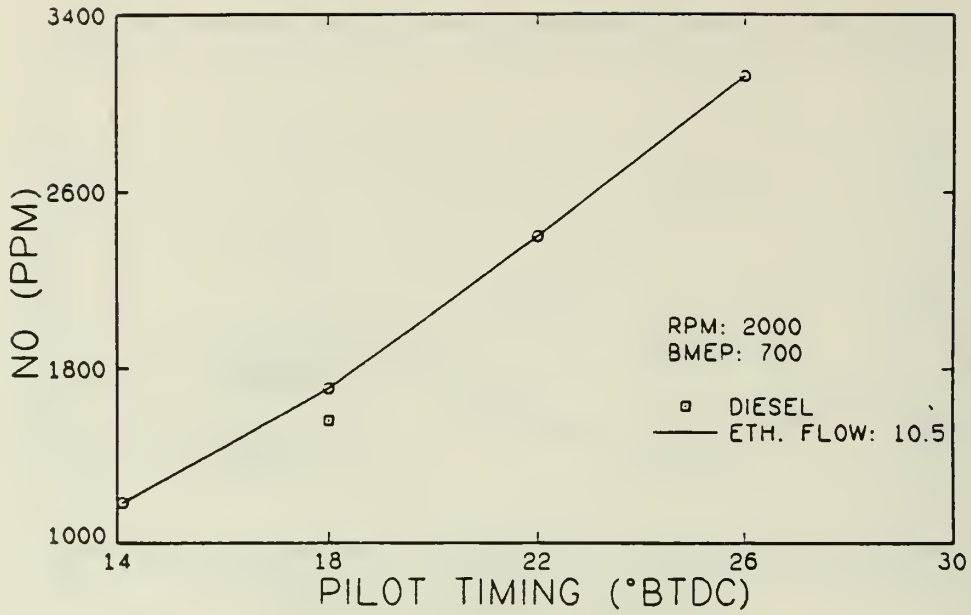

(a) RPM = 2000, BMEP = 700 kpa.
Ethanol flow setting = 10.5

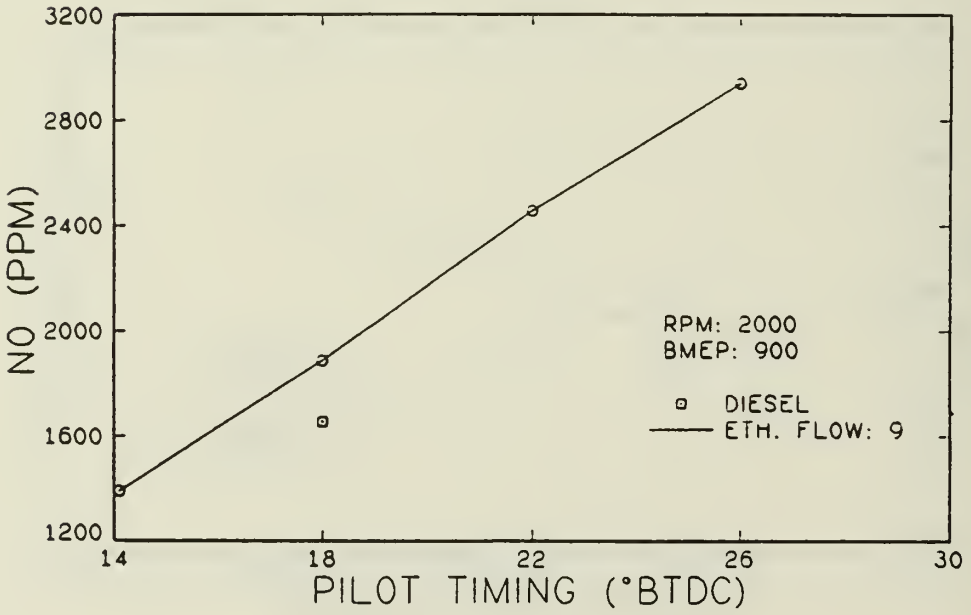

(b) RPM = 2000, BMEP = 900 kpa.
Ethanol flow setting = 9.

Figure 5.35 Effect of pilot fuel timing on nitric oxide concentration.

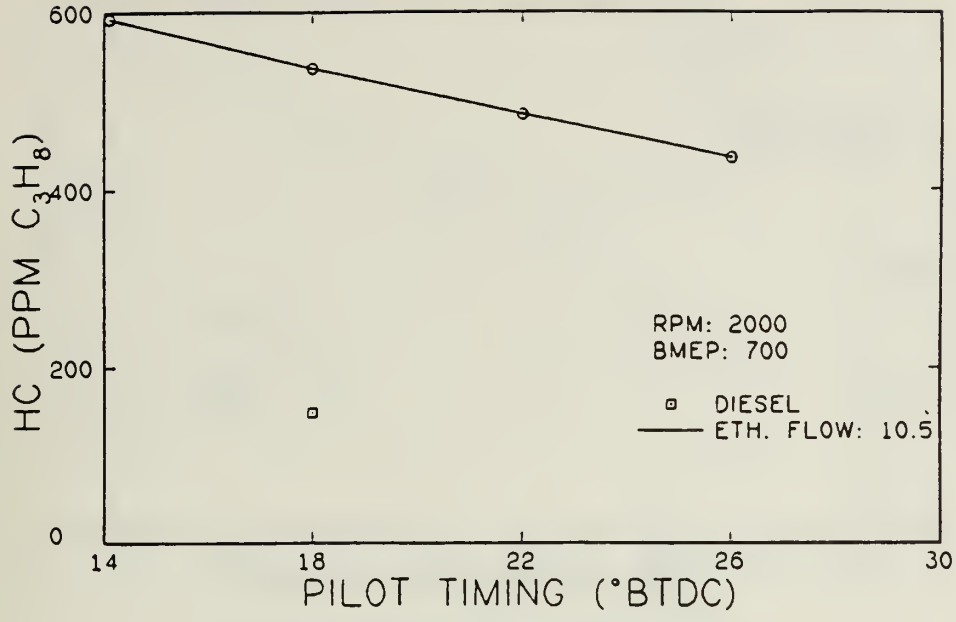

(a) RPM = 2000, BMEP = 700 kpa.
Ethanol flow setting = 10.5

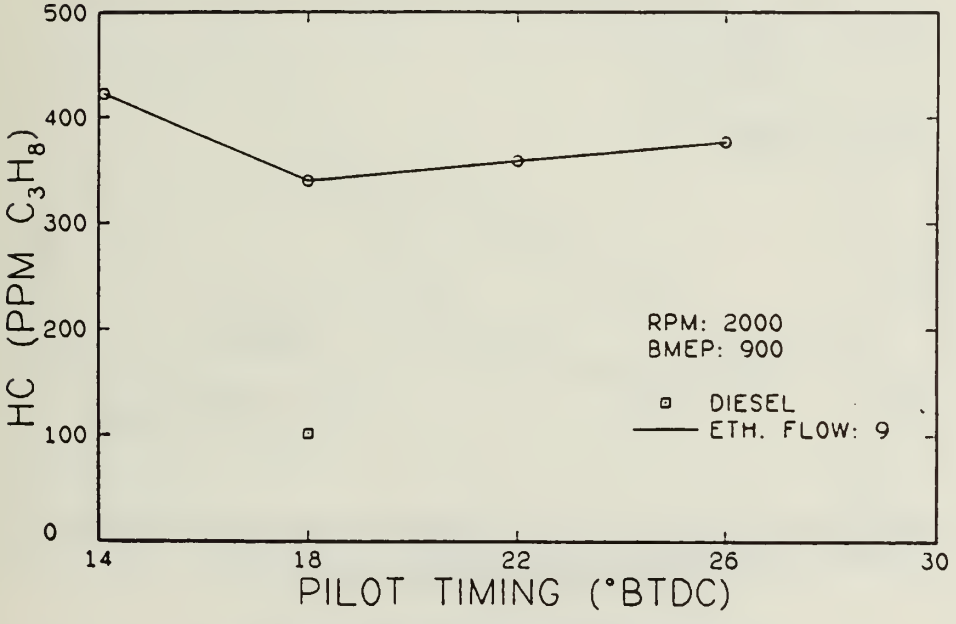

(b) RPM = 2000, BMEP = 900 kpa.
Ethanol flow setting = 9.

Figure 5.36 Effect of pilot fuel timing on hydrocarbon concentration.

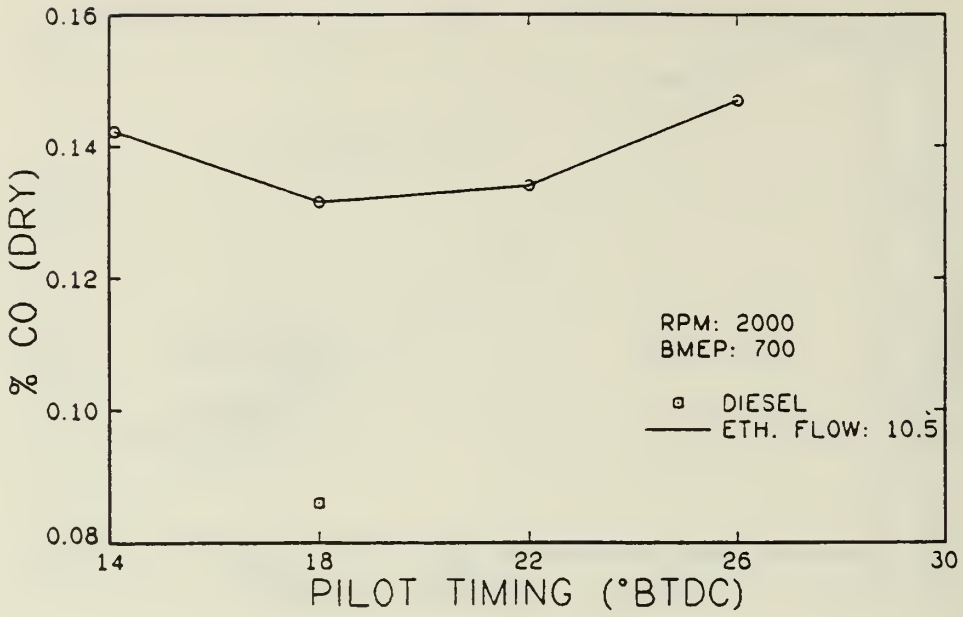

(a) RPM = 2000, BMEP = 700 kpa.
Ethanol flow setting = 10.5

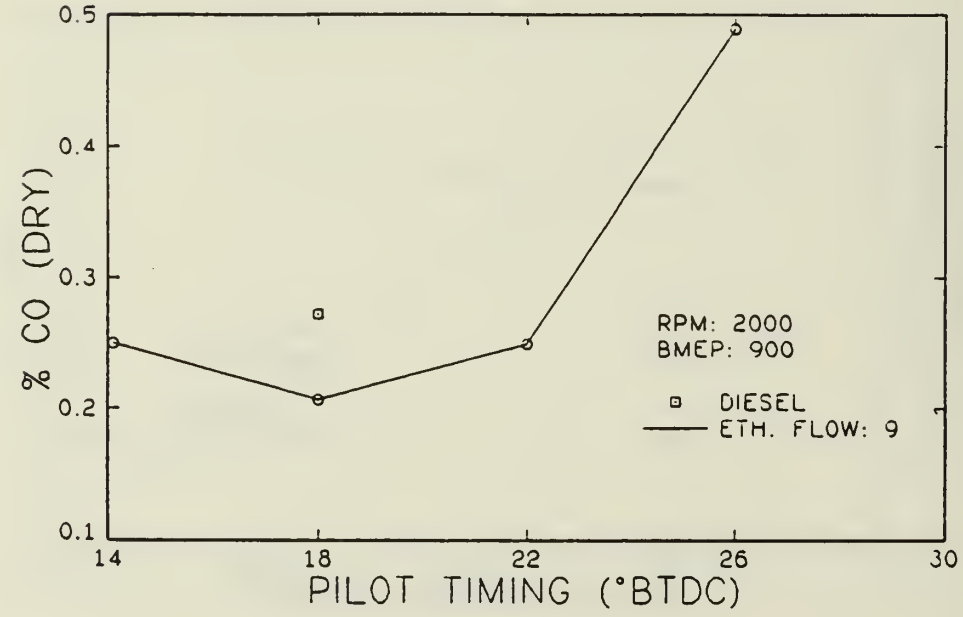

(b) RPM = 2000, BMEP = 900 kpa.
Ethanol flow setting = 9.

Figure 5.37 Effect of pilot fuel timing on carbon monoxide concentration.

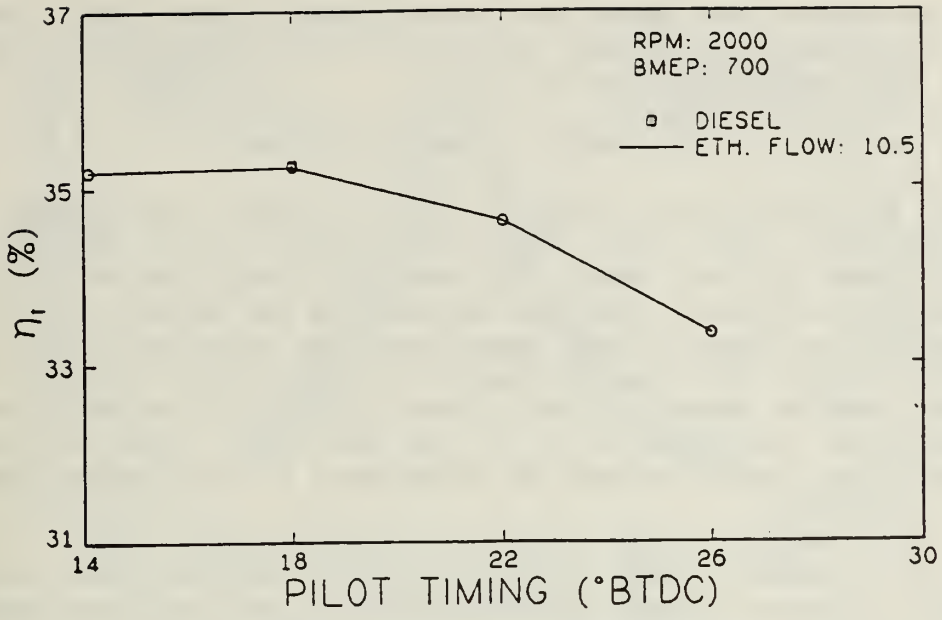

(a) RPM = 2000, BMEP = 700 kpa.
Ethanol flow setting = 10.5

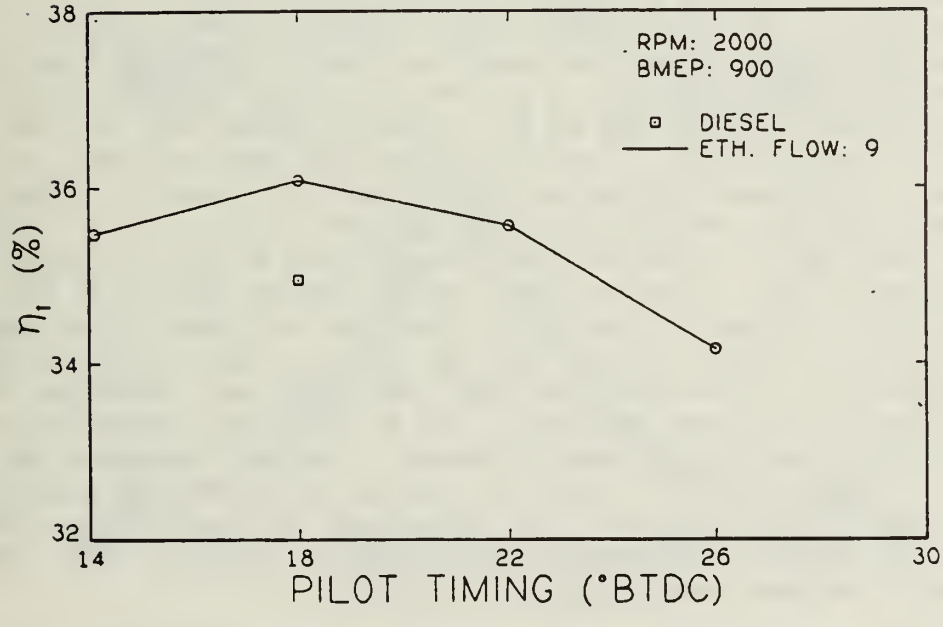

(b) RPM = 2000, BMEP = 900 kpa.
Ethanol flow setting = 9.

Figure 5.38 Effect of pilot fuel timing on thermal efficiency.

percentages of ethanol had to be used due to knock limitations. The results of this test indicate that changes in pilot timing would probably be most effective at a BMEP between 300 and 500 kPa.

5.3 Results for 2000 and 4000 RPM at a BMEP of 400 kPa

The test at 2000 rpm and various loads indicated that changes in pilot fuel injection timing were likely to be most effective at a BMEP between 300 and 500 kPa. Based on this result, further tests were done at 2000 and 2400 rpm with a BMEP of 400 kPa. The test at 2400 rpm was performed to see if the higher turbulence and higher charge temperatures at the time of pilot fuel injection would enhance the effectiveness of advanced pilot timing. Data was taken for both engine speeds at the various pilot fuel timings with ethanol injector controller settings of 8, 9, 10, and 11. Table 5.3 lists the controller settings and corresponding percentages of fuel energy supplied as ethanol for each test.

Figures 5.39 through 5.42 are plots of cylinder pressure versus crank angle for four different ethanol flow rates at the two test conditions. Each plot has three curves: one for diesel and one fur dual fuel at a pilot timing of 18 degrees BTDC, and one for dual fuel at an advanced timing of 29 degrees BTDC. Figures 5.39(a) and (b) show cylinder pressure versus crank angle for 2000 and 2400 rpm with an ethanol flow of 8. In both cases, advancing the pilot timing significantly shifted the dual fuel pressure curves. At 2000 rpm, the dual fuel at advanced timing followed the baseline diesel curve. At 2400 rpm, combustion started earlier for the dual fuel at advanced timing than for baseline diesel. At both speeds, peak pressures were higher for the dual fuel with advanced timing than for baseline diesel. Figures 5.40(a) and (b) show cylinder pressure curves for an ethanol flow of 9. The results were similar to those for an ethanol flow of 8. Figures 5.41(a) and (b) show cylinder pressure curves for an ethanol flow of 10. At 2000 rpm, the peak pressure for the dual fuel at advanced timing was below that for baseline diesel. Thus, timing advance was less effective for an alcohol flow of 10. At 2400 rpm, however, the dual fuel at advanced timing had a peak pressure higher than that for lower alcohol flows. The dual fuel at 18 degrees BTDC also had a higher peak pressure for an ethanol flow of 10 than for the lower flow rates at the same pilot timing. Figures 5.42(a) and (b) show cylinder pressure curves for an ethanol flow of 11. The plot for 2000 rpm shows that advancing the timing had little effect on cylinder pressure. But at 2400 rpm, advancing the timing still had a major effect on cylinder pressure. The peak pressure for the dual fuel was even higher at this flow for the advanced timing than for lower flows. It should be noted that the percentage of fuel energy supplied as ethanol at 2400 rpm was approximately the same as that at 2000 rpm for all ethanol flows rates (see Table 5.3).

Figures 5.43(a) and (b) show maximum cylinder pressure versus pilot timing. At 2000 rpm, an increase in ethanol flow rate resulted in lower peak pressures. Also, peak pressures decreased at maximum pilot timing advance for the higher ethanol flows. At 2400 rpm, however, higher ethanol flow rates resulted in higher peak pressures at advanced pilot timings. Also, peak pressure consistently increased with advance in pilot timing. Thus, changes in pilot timing seem to be much more effective at 2400 rpm that at 2000 rpm.

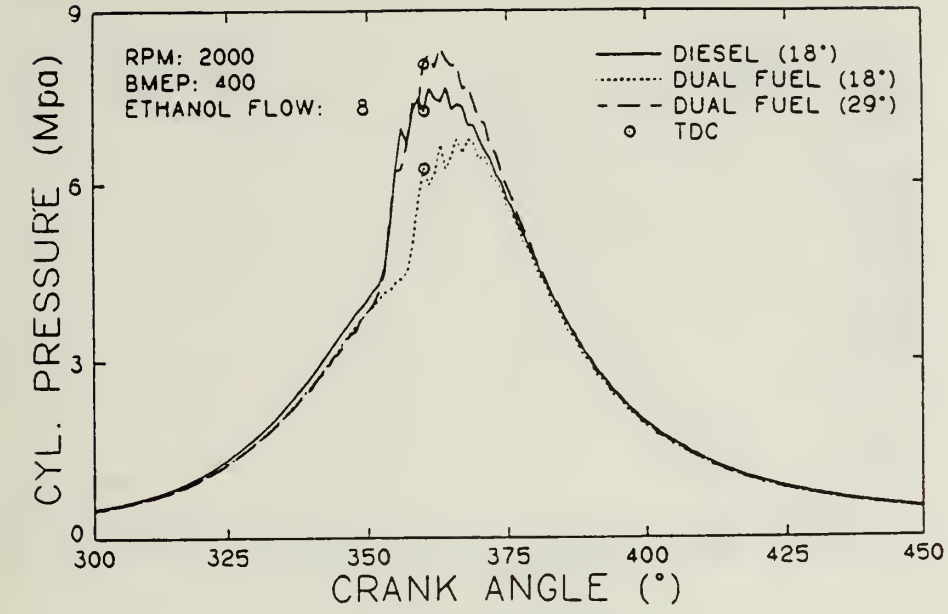

(a) RPM = 2000, BMEP = 400 kpa.
Ethanol flow setting = 8.

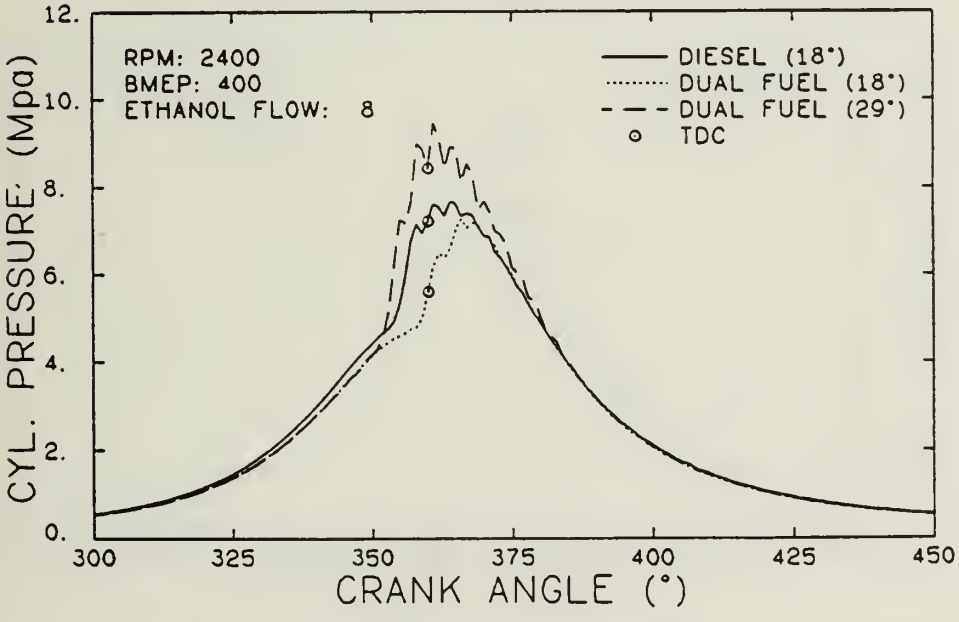

(b) RPM = 2400, BMEP = 400 kpa.
Ethanol flow setting = 8.

Figure 5.39 Effect of maximum pilot timing advance on cylinder pressure.

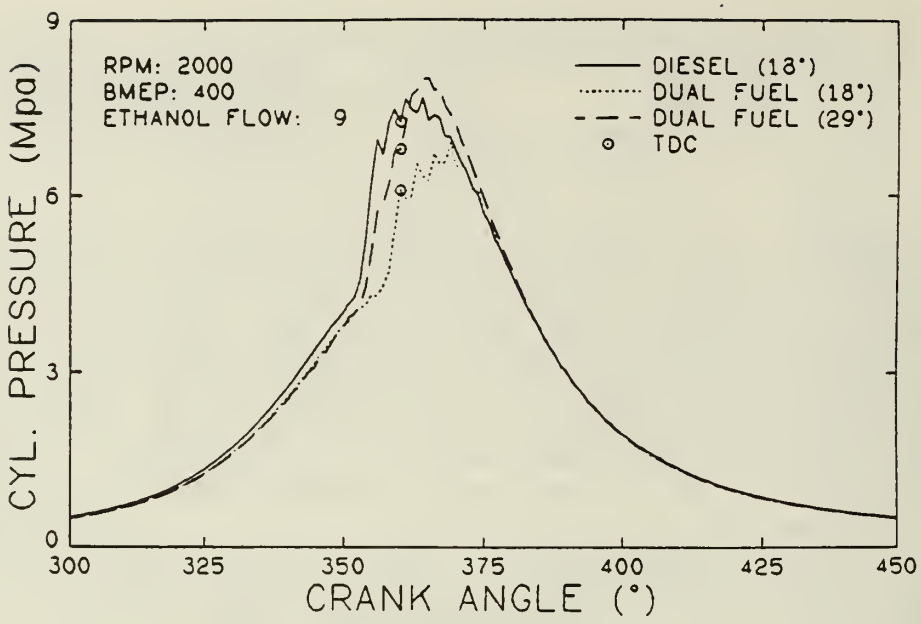

(a) RPM = 2000, BMEP = 400 kpa.
Ethanol flow setting = 9.

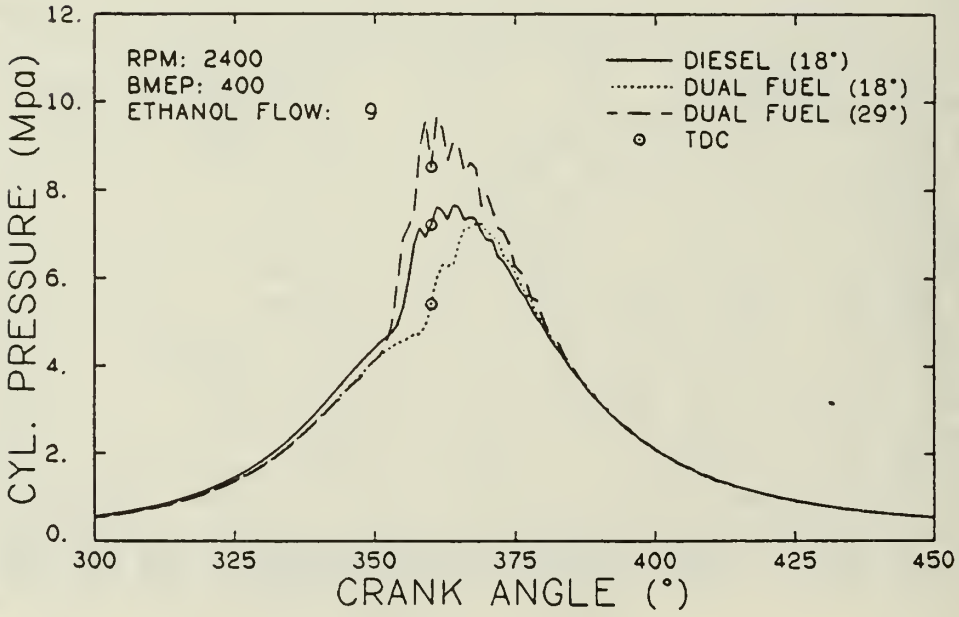

(b) RPM = 2400, BMEP = 400 kpa.
Ethanol flow setting = 9.

Figure 5.40 Effect of maximum pilot timing advance on cylinder pressure.

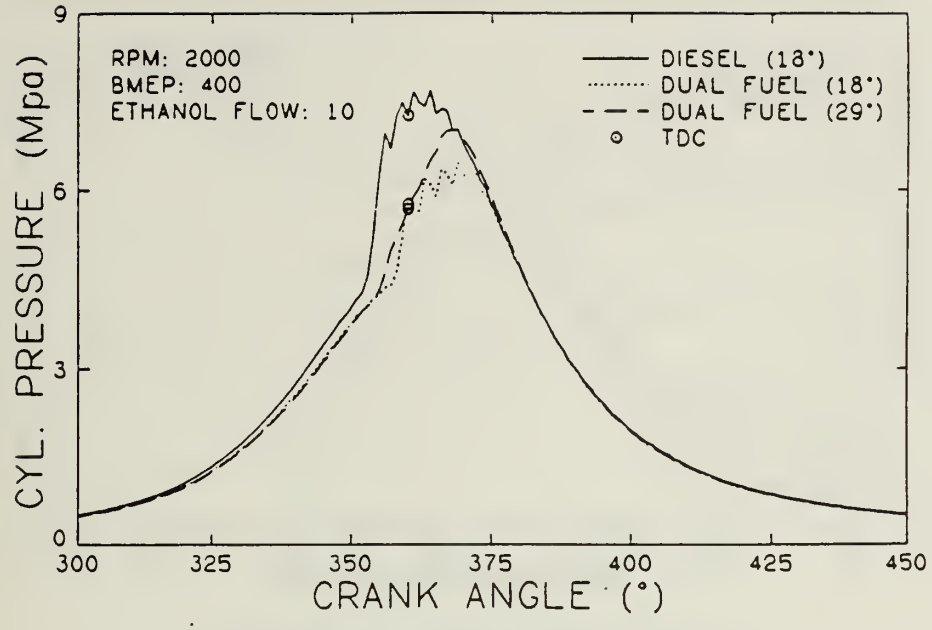

(a) RPM = 2000, BMEP = 400 kpa.
Ethanol flow setting = 10.

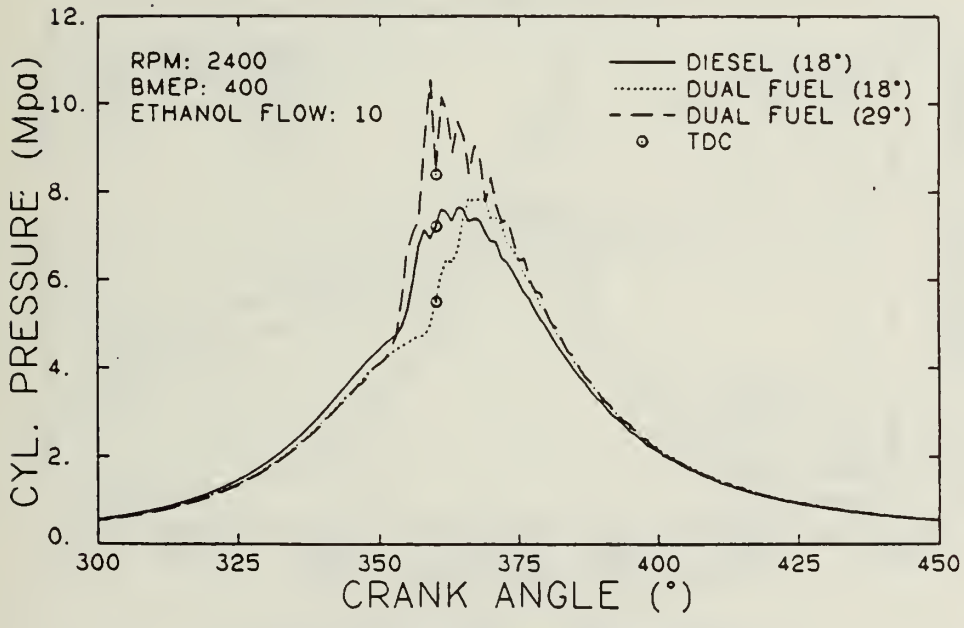

(b) RPM = 2400, BMEP = 400 kpa.
Ethanol flow setting = 10.

Figure 5.41 Effect of maximum pilot timing advance on cylinder pressure.

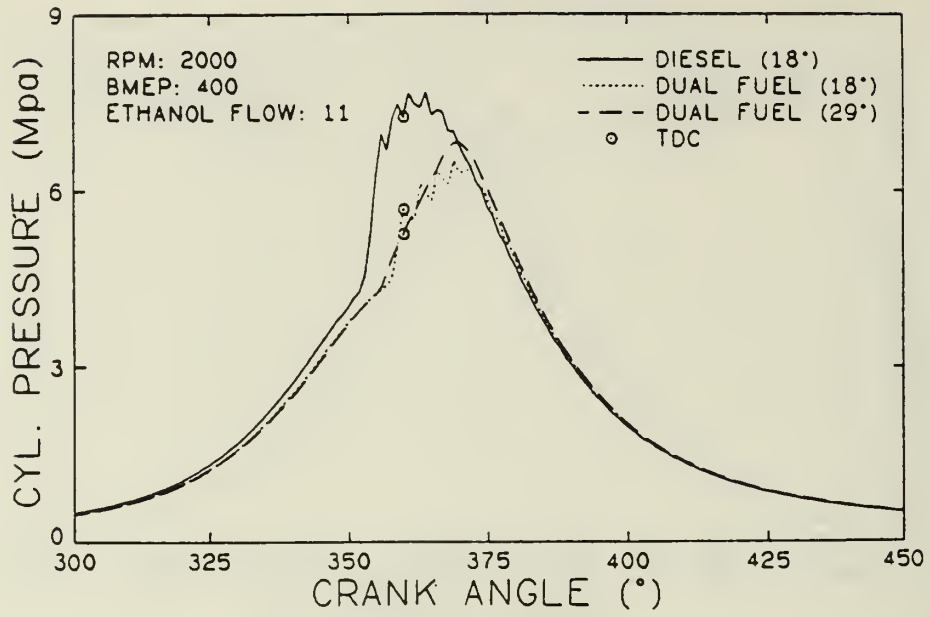

(a) RPM = 2000, BMEP = 400 kpa.
Ethanol flow setting = 11.

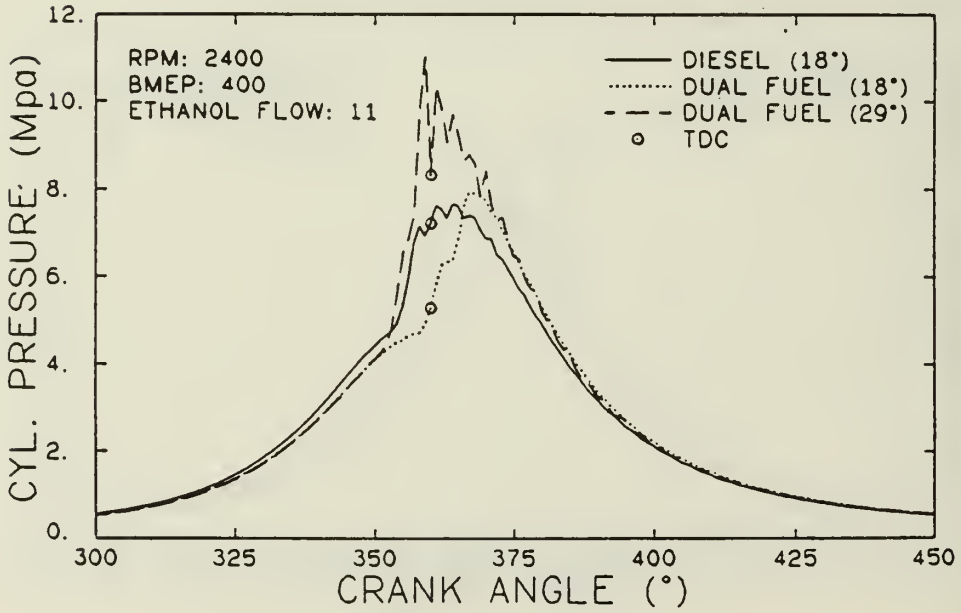

(b) RPM = 2400, BMEP = 400 kpa.
Ethanol flow setting = 11.

Figure 5.42 Effect of maximum pilot timing advance on cylinder pressure.

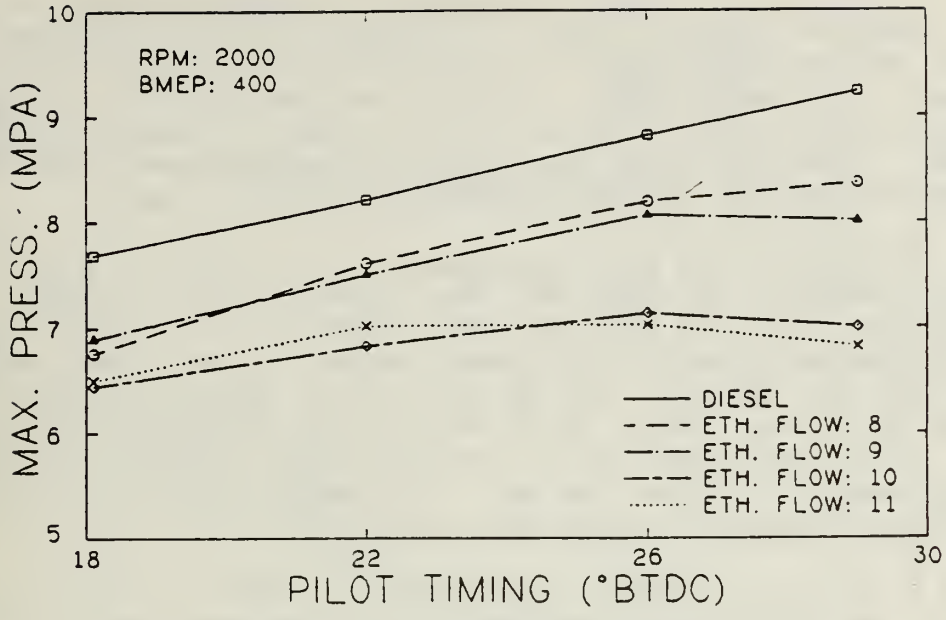

(a) RPM = 2000, BMEP = 400 kpa.

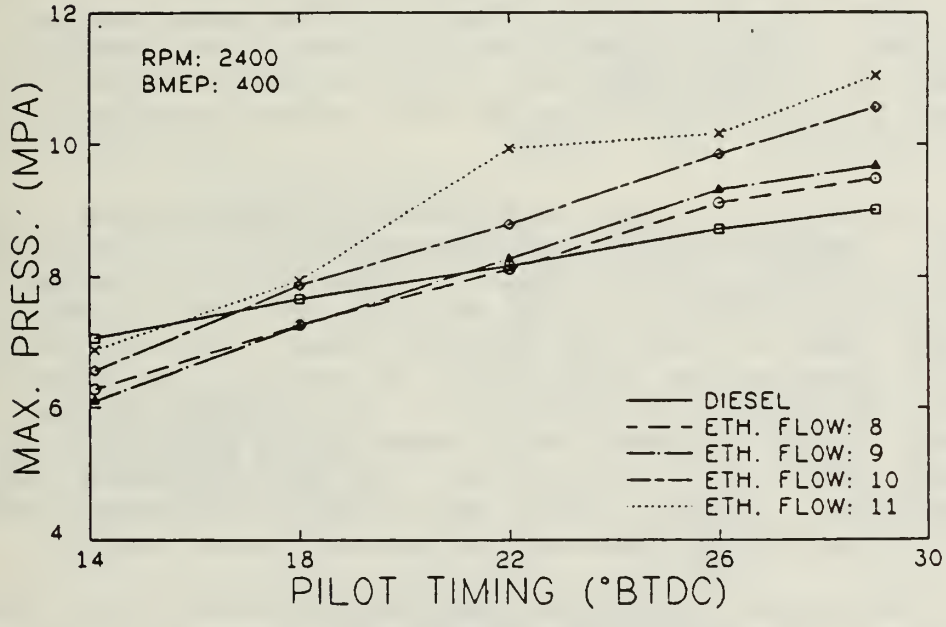

(b) RPM = 2400, BMEP = 400 kpa.

Figure 5.43 Effect of pilot fuel timing on maximum pressure for different ethanol flow rates.

Figures 5.44(a) and (b) show the angle of maximum pressure versus pilot timing. For 2000 rpm, higher ethanol flow rates resulted in peak pressure occurring later in the cycle. Also, peak pressure generally occurred later when timing was set at maximum advance. At 2400 rpm, the angle of maximum pressure for dual fuel at 29 degrees BTDC was close to that of baseline diesel at 18 degrees BTDC. also, as timing was advanced, the angle of maximum pressure generally occurred earlier in the cycle for all alcohol flows.

Figures 5.45(a) and (b) show the maximum rate of pressure rise as a function of pilot timing. For 2000 rpm, the maximum rate of pressure rise decreased as ethanol flow rate was increased. There was also a decrease in maximum rate of pressure rise as timing was advanced at the higher ethanol flow rates. At 2400 rpm, however, the maximum rate of pressure rise was greater for dual fuel at a pilot timing of 29 degrees BTDC than for diesel at 18 degrees BTDC. Also, the maximum rate of pressure rise for dual fuel always increased with advances in pilot timing. This tends to indicate that advanced timing at 2400 rpm resulted in more rapid combustion.

Figures 5.46(a) and (b) show the angle of maximum pressure rise versus pilot timing. At 2000 rpm, the maximum rate of pressure rise occurred later in the cycle as ethanol flow was increased. Also, there was not much change in the point of maximum pressure rise as timing was advanced. At 2400 rpm, the point of maximum pressure rise for an ethanol flow of 11 at a timing of 29 degrees BTDC was about the same as baseline diesel at 18 degrees BTDC.

Figures 5.47(a) and (b) show ignition delay versus pilot timing. Ignition delays for the dual fuel at advanced timing were longer at 2000 rpm than at 2400 rpm. This was probably due to higher charge temperatures at the time of injection and more turbulence in the cylinder at 2400 rpm. At both engine speeds, ignition delay increased with timing advance due to injection of the pilot fuel into a cooler charge.

Figures 5.48(a) and (b) show intake manifold temperature as a function of pilot timing. Manifold temperatures were approximately 15 degrees Celsius higher for 2400 rpm than for 2000 rpm. This may be a contributing factor to the more rapid initial burning at 2400 rpm. For both engine speeds, manifold temperature was lower for dual fuel than for diesel. This was because turbocharger boost decreased by approximately 3 percent (see data tables in appendix) with the addition of ethanol as a result of less energy in the exhaust. Exhaust energy decreased due to more of the combustion occurring at constant volume for the dual fuel mixture. This is indicated by the trend for exhaust temperature. Figures 5.49(a) and (b) show that exhaust temperature decreased with ethanol addition.

Figures 5.50(a) and (b) show NO concentration versus pilot timing. For each engine speed, adding more ethanol resulted in a decrease in NO concentration. At 2000 rpm, NO decreased as timing was advanced for the higher ethanol flowrates. This indicates that lower peak temperatures occurred as timing was advanced. At 2400 rpm, however, NO increased consistently with increasing timing advance. This was because peak temperatures increased as timing was advanced. Note that at 2400 rpm, the No concentrations for the dual fuels at 29 degrees BTDC were not much higher than baseline diesel at 18 degrees BTDC. The decrease in NO due to the addition of ethanol tends to cancel the increase in NO due to pilot timing advance.

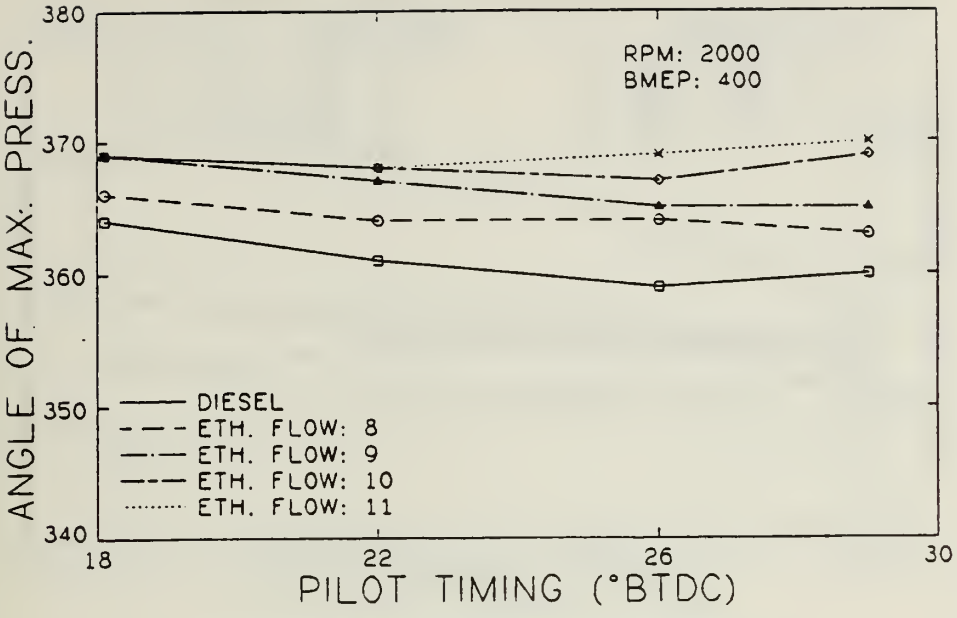

(a) RPM = 2000, BMEP = 400 kpa.

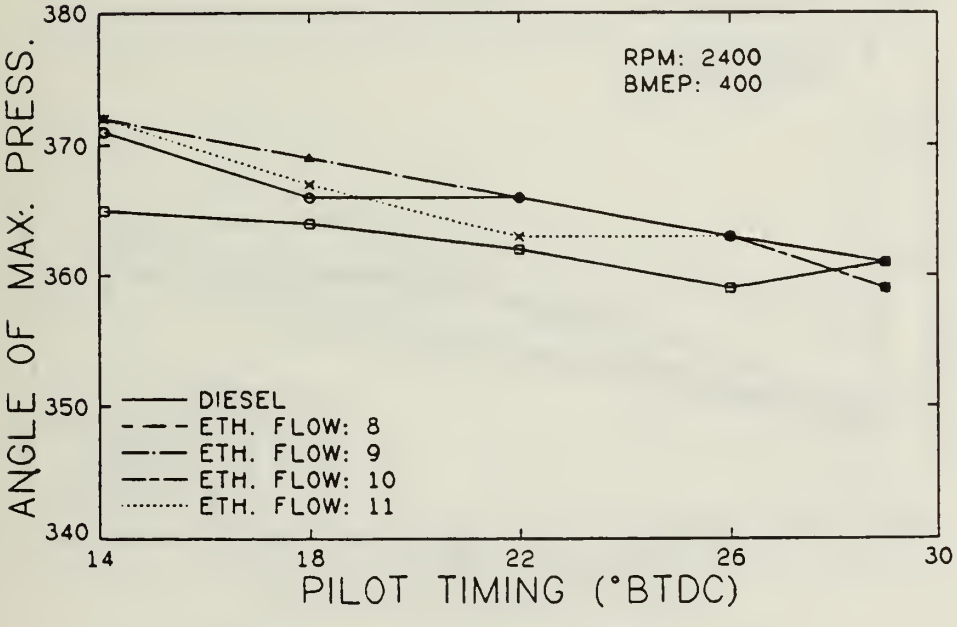

(b) RPM = 2400, BMEP = 400 kpa.

Figure 5.44 Effect of pilot fuel timing on angle of maximum pressure for different flow rates of ethanol.

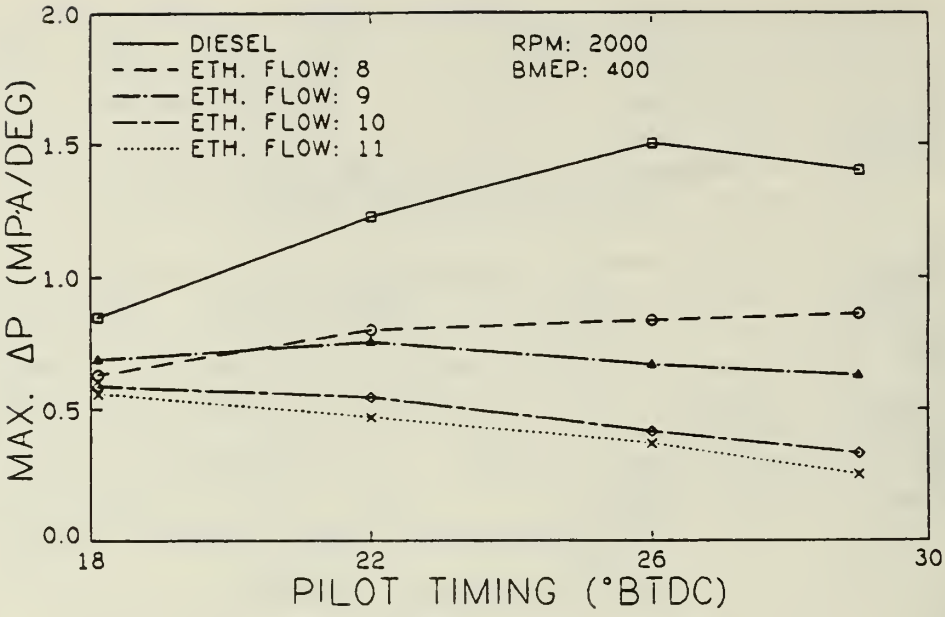

(a) RPM = 2000, BMEP = 400 kpa.

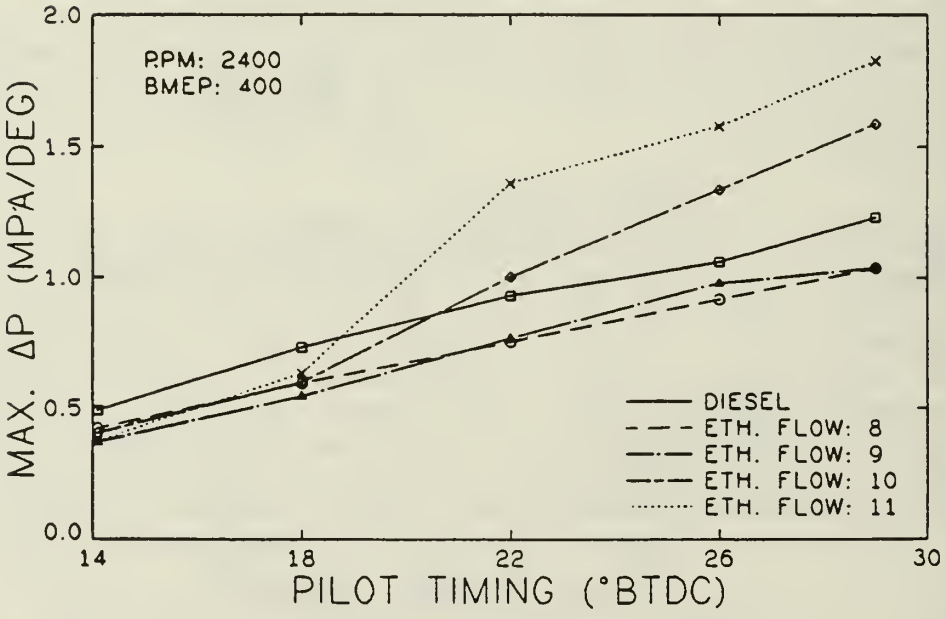

(b) RPM = 2400, BMEP = 400 kpa.

Figure 5.45 Effect of pilot fuel timing on maximum rate of pressure rise for different flow rates of ethanol.

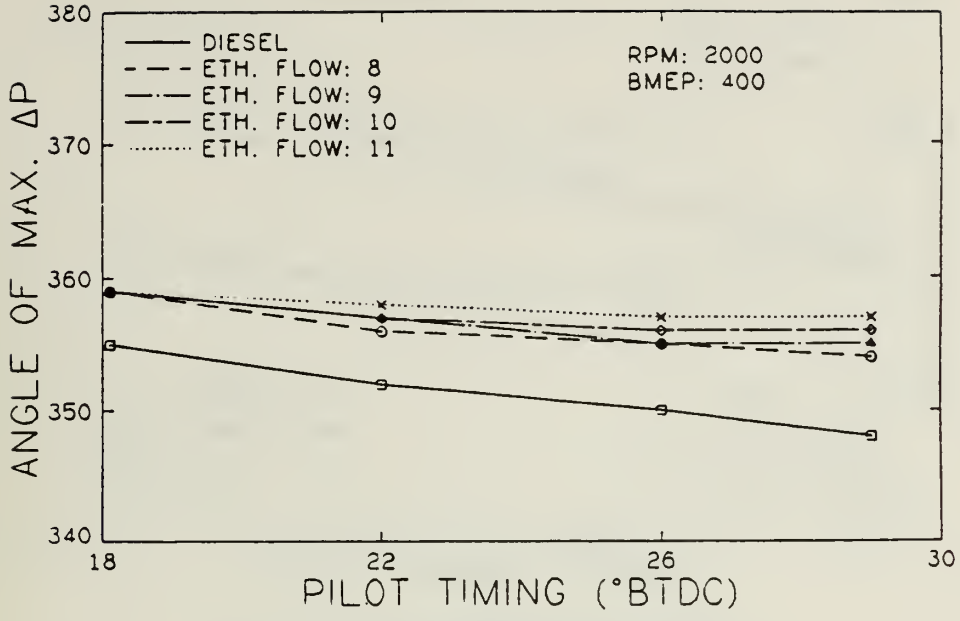

(a) RPM = 2000, BMEP = 400 kpa.

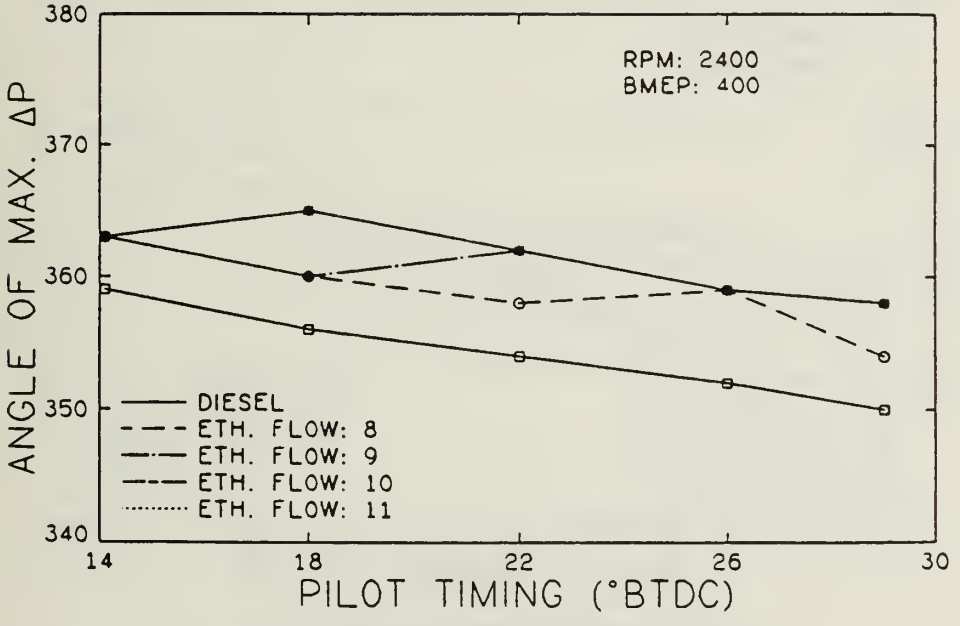

(b) RPM = 2400, BMEP = 400 kpa.

Figure 5.46 Effect of pilot fuel timing on angle of maximum rate of pressure rise for different flow rates of ethanol.

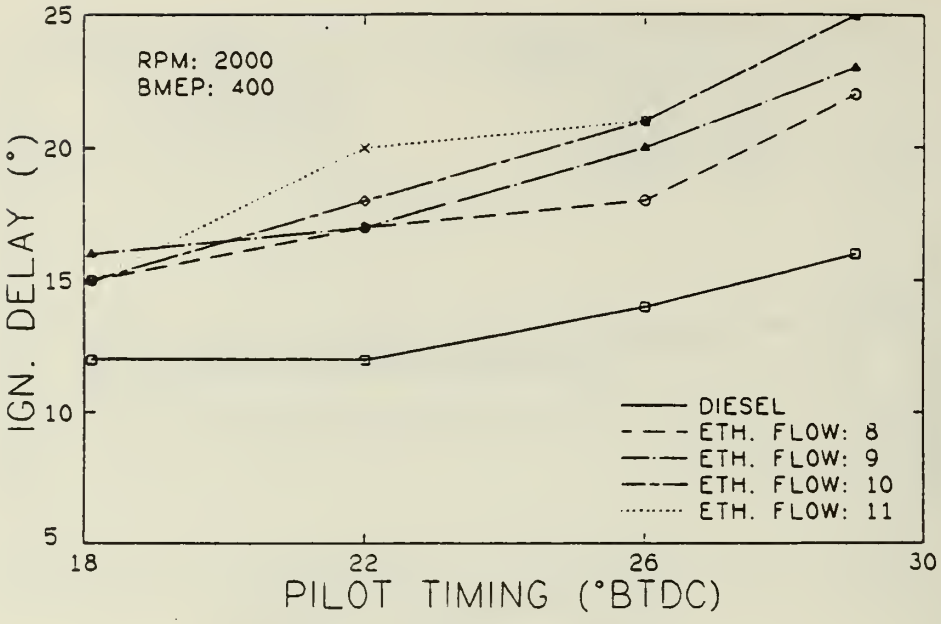

(a) RPM = 2000, BMEP = 400 kpa.

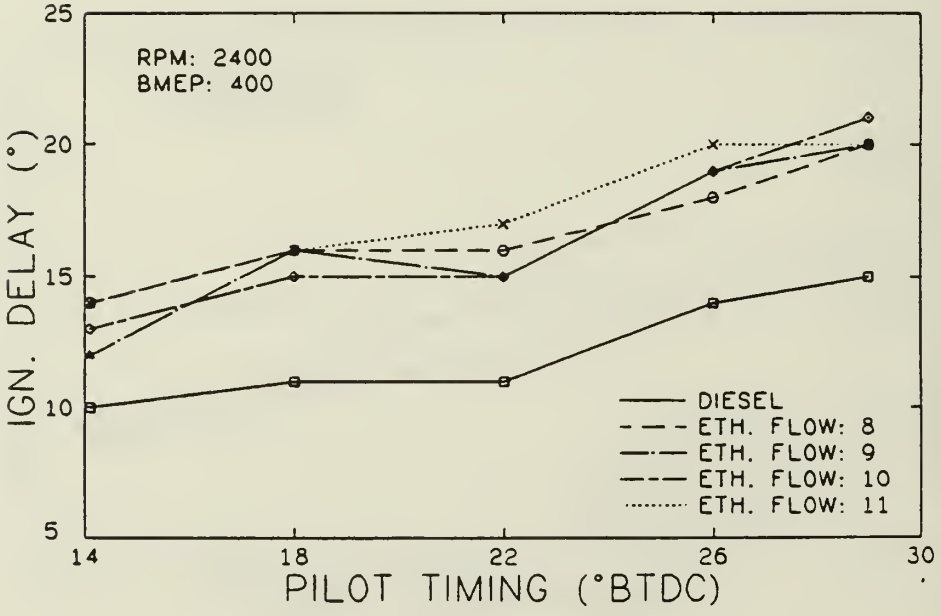

(b) RPM = 2400, BMEP = 400 kpa.

Figure 5.47 Effect of pilot fuel timing on ignition delay for different flow rates of ethanol.

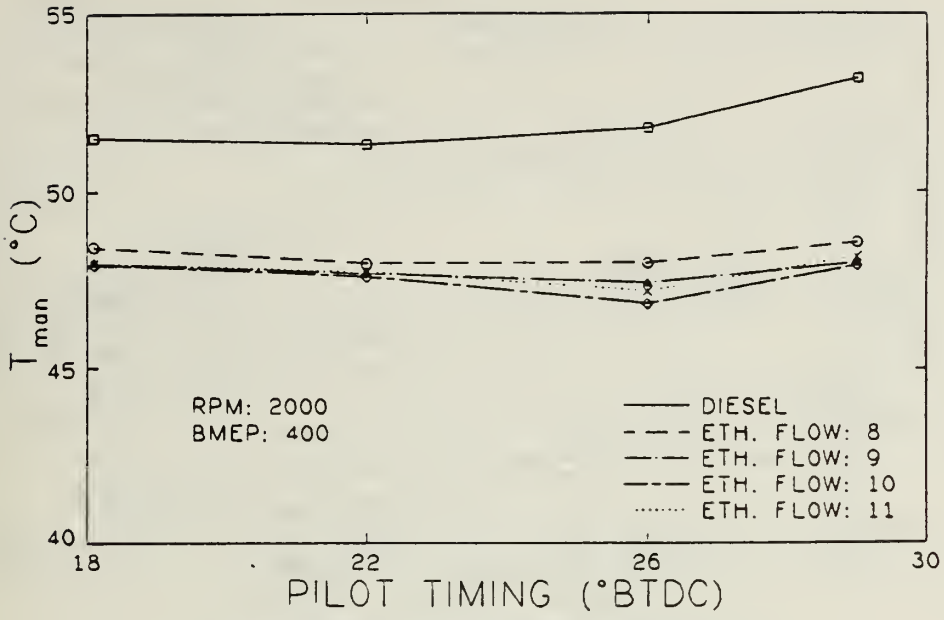

(a) RPM = 2000, BMEP = 400 kpa.

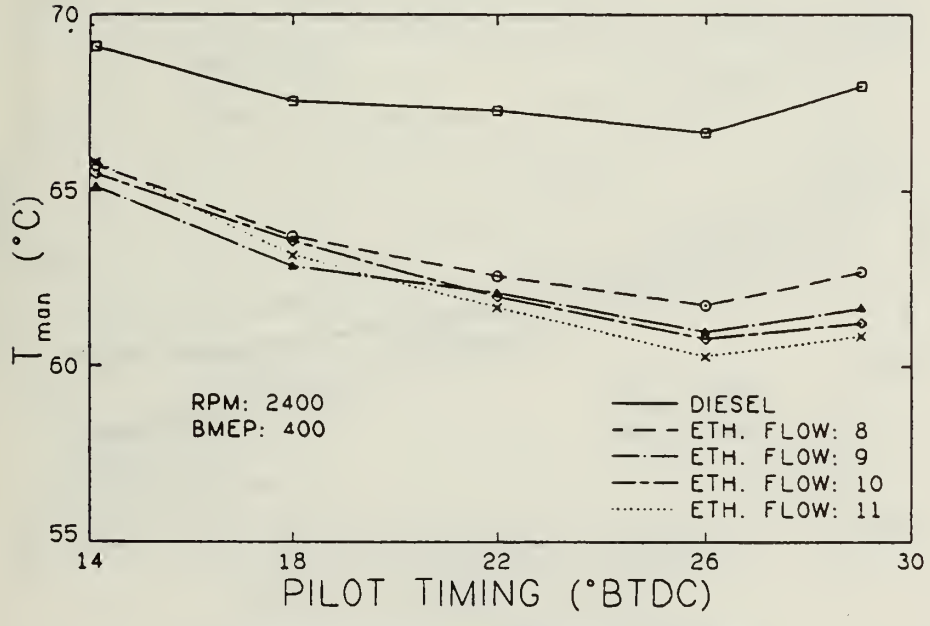

(b) RPM = 2400, BMEP = 400 kpa.

Figure 5.48 Effect of pilot fuel timing on intake manifold temperature for different flow rates of ethanol.

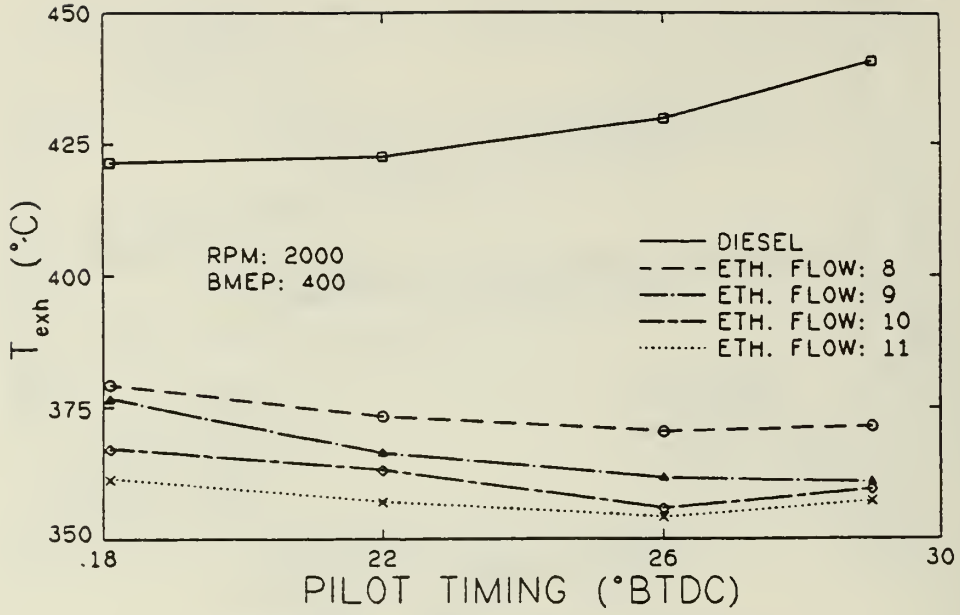

(a) RPM = 2000, BMEP = 400 kpa.

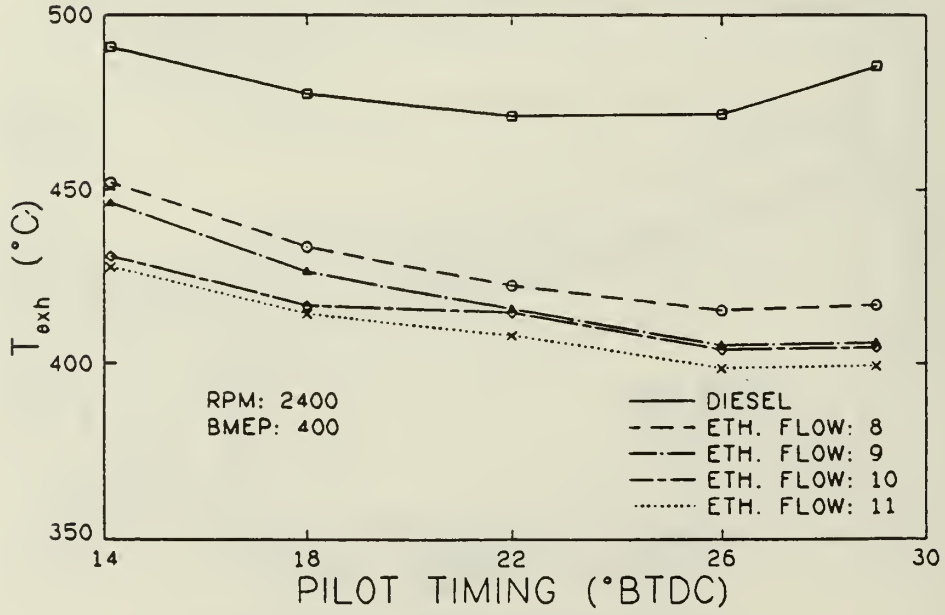

(b) RPM = 2400, BMEP = 400 kpa.

Figure 5.49 Effect of pilot fuel timing on exhaust temperature for different flow rates of ethanol.

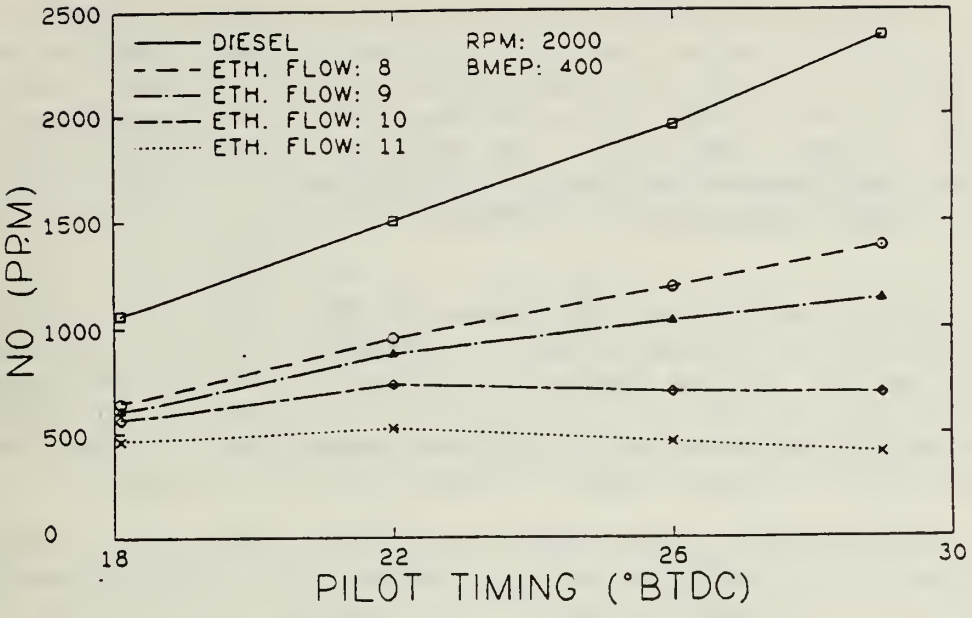

(a) RPM = 2000, BMEP = 400 kpa.

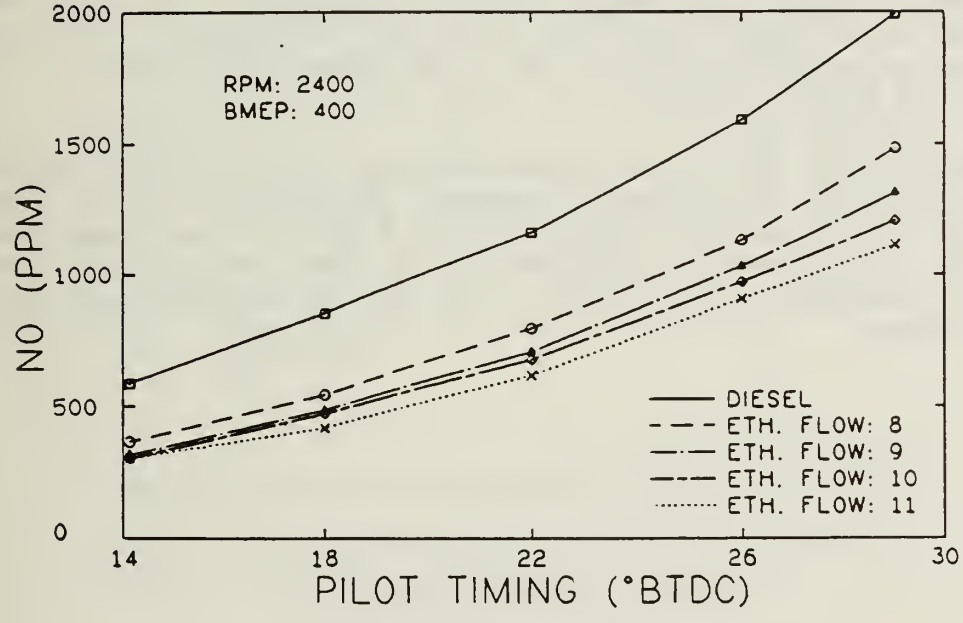

(b) RPM = 2400, BMEP = 400 kpa.

Figure 5.50 Effect of pilot fuel timing on nitric oxide concentration for different flow rates of ethanol.

Figures 5.51(a) and (b) show unburned hydrocarbon concentration versus pilot timing. For both engine speeds, adding more ethanol resulted in higher hydrocarbon levels. This may have been due to the effect of wall quenching on the ethanol-air mixture. Also, the ethanol-air mixture may have been too lean in some regions to burn completely. for 2000 rpm, there was not much change in hydrocarbon concentration as timing was advanced. At 2400 rpm, however, unburned hydrocarbon concentration decreased significantly as timing was advanced.

Figures 5.52(a) and (b) show CO concentration versus pilot timing. For both engine speeds, CO concentration was greater for dual fuel than for diesel. This was due to the combustion characteristics of the homogeneous ethanol-air mixture. At 2400 rpm, CO concentration decreased significantly as timing was advanced indicating more efficient combustion. At 2000 rpm, however, CO concentration did not change as much with pilot timing.

Figures 5.53(a) and (b) show thermal efficiency versus pilot timing. At 2000 rpm, thermal efficiency generally increased with timing advance due to favorable shifts in cylinder pressure. The thermal efficiencies for most ethanol flows at 29 degrees BTDC were higher than baseline diesel at 18 degrees BTDC. For an ethanol flow of 10, advancing the timing from 18 to 29 degrees BTDC resulted in a relative increase in thermal efficiency of 3 percent. At 2400 rpm, the change in thermal efficiency was more pronounced than at 2000 rpm as pilot timing was advanced. The highest thermal efficiency was for an ethanol flow of 11 at a pilot timing of 28 degrees BTDC. Thus, advancing the timing at 2400 rpm allowed a higher percentage of the fuel energy to be supplied as ethanol while maximizing thermal efficiency. For an ethanol flow of 11, advancing the timing fro 18 to 29 degrees BTDC resulted in a relative increase in thermal efficiency of 4 percent.

In summary, advancing the timing was beneficial at both 2000 and 2400 rpm for a BMEP of 400 kPa. At 2400 rpm, however, the advance of pilot timing was more effective. This may be a result of the higher charge temperatures for 2400 rpm at the time of diesel injection. Also, there was probably more swirl in the cylinder at 2400 rpm which may have led to improved ignition of the ethanol-air mixture.

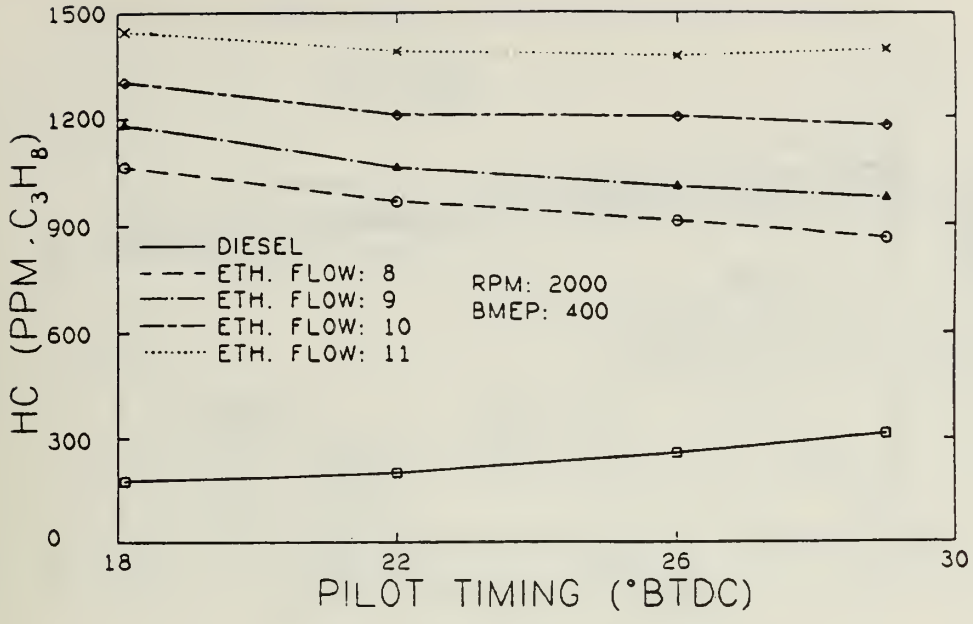

(a) RPM = 2000, BMEP = 400 kpa.

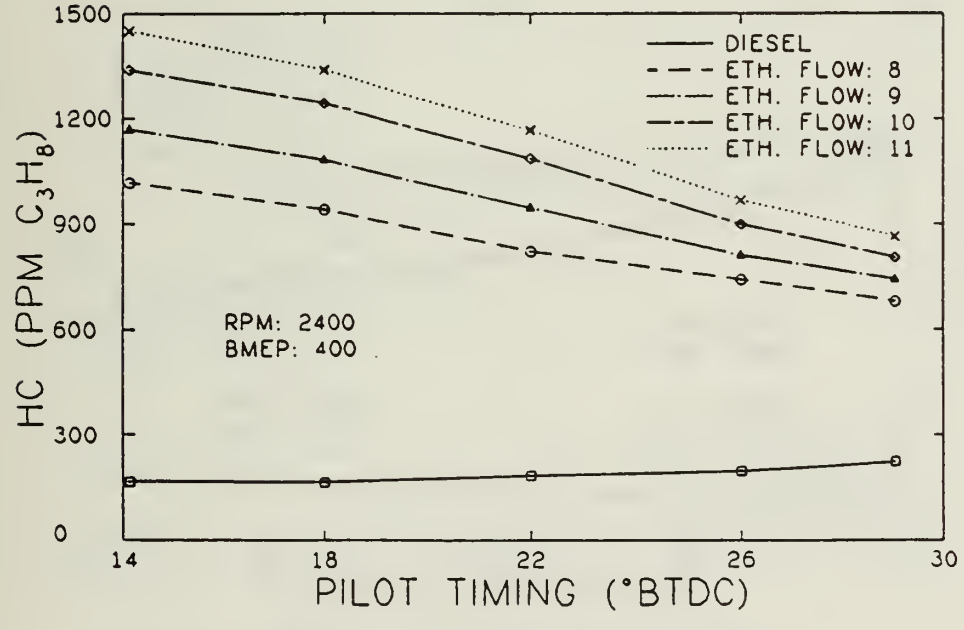

(b) RPM = 2400, BMEP = 400 kpa.

Figure 5.51 Effect of pilot fuel timing on hydrocarbon concentration for different flow rates of ethanol.

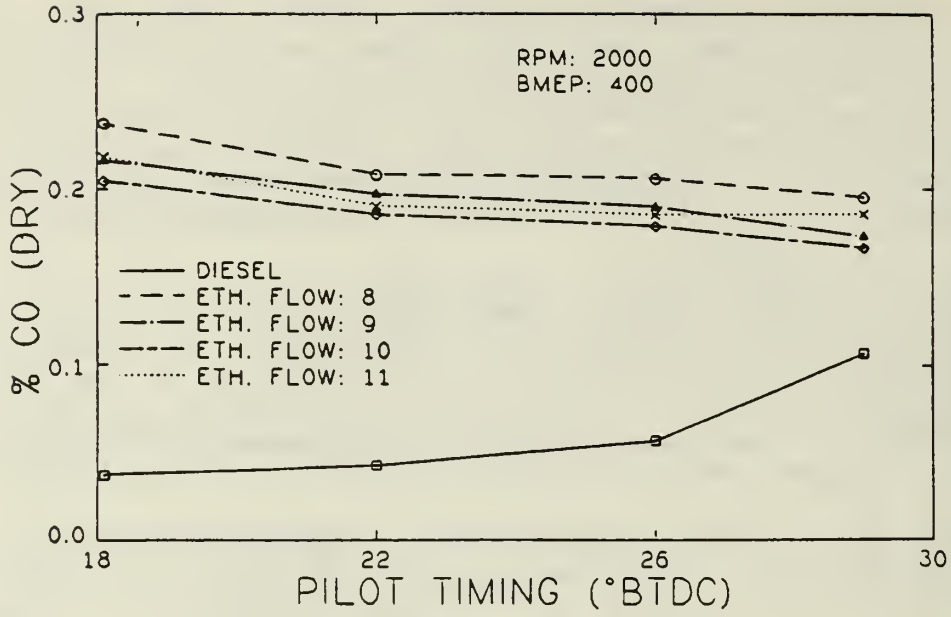

(a) RPM = 2000, BMEP = 400 kpa.

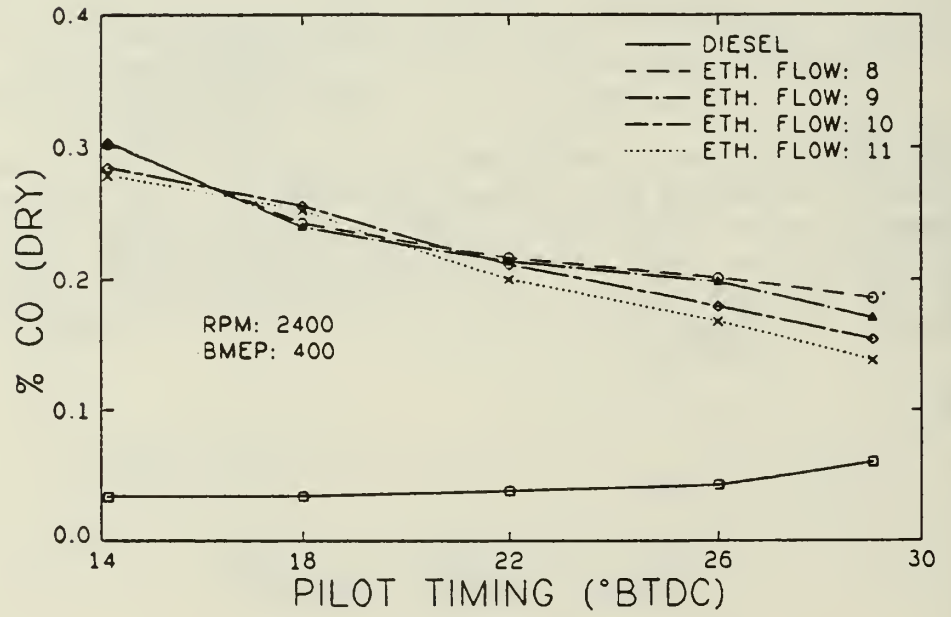

(b) RPM = 2400, BMEP = 400 kpa.

Figure 5.52 Effect of pilot fuel timing on carbon monoxide concentration for different flow rates of ethanol.

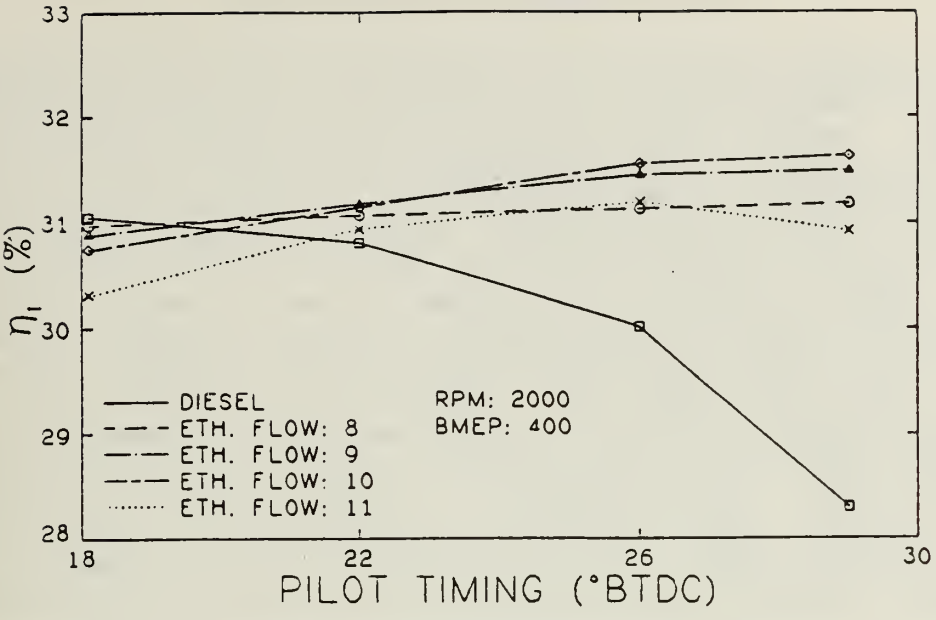

(a) RPM = 2000, BMEP = 400 kpa.

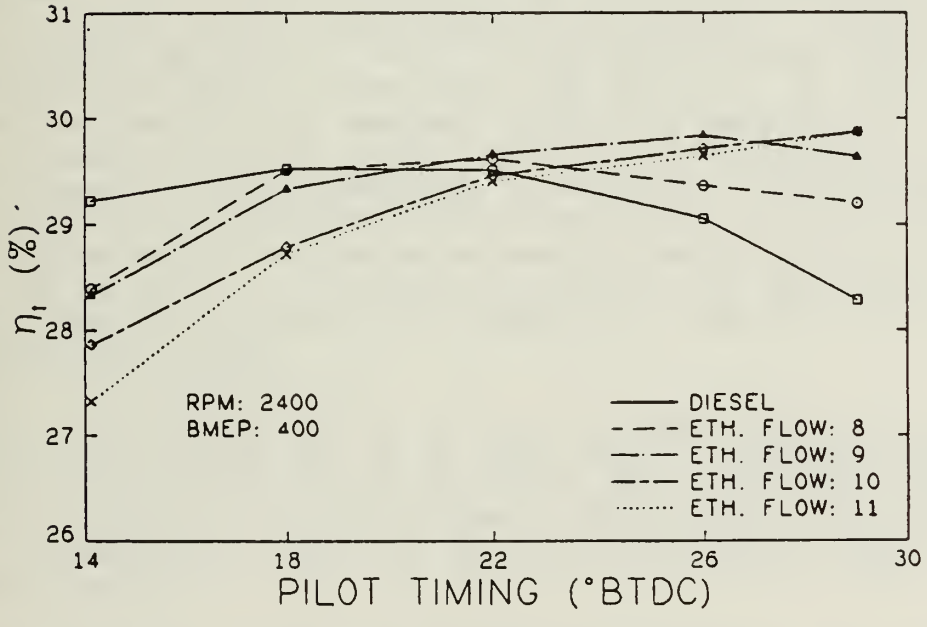

(b) RPM = 2400, BMEP = 400 kpa.

Figure 5.53 Effect of pilot fuel timing on thermal efficiency for different flow rates of ethanol.

6. CONCLUSIONS AND RECOMMENDATIONS

The results of the test at 2000 rpm and various loads indicated that advancing the pilot timing was not effective for BMEP's between 100 and 300 kPa. In fact, advancing the timing increased engine misfire. Thus, lower ethanol flow rates were necessary at advanced timings. One possible explanation for this is that the pilot charge had more time to diffuse when injected earlier. This would result in locally leaner mixtures of pilot fuel at the point of ignition. Also, at low loads the abound of diesel injected was small since a high percentage of the fuel energy was supplied as ethanol. Therefore, the diesel injectors might not distribute the pilot fuel in the cylinder as effectively. At BMEP's of 500 kPa and greater, advancing the timing significantly changed the cylinder pressure. The thermal efficiency, however, decreased with advances in pilot timing due to the shift of peak pressure to a point too early in the cycle. Thus for high loads, the maximum thermal efficiency occurred at a pilot timing of 18 degrees BTDC. These results indicated that changes in pilot timing were likely to be most effective at brake mean effective pressures between 300 and 500 kPa. Here, thermal efficiency should increase due to favorable shifts in the cylinder pressure distribution.

Further testing at 2000 rpm and a BMEP of 400 kPa indicated that a relative increase in thermal efficiency of 3 percent would result if timing was advanced from 18 to 29 degrees BTDC. Tests at 2400 rpm and a BMEP of 400 kPa indicated that changes in pilot fuel timing were much more effective at this spdd than at 2000 rpm. Advancing the timing did not increase engine misfire for high ethanol flow rates but instead led to higher peak pressures and higher initial burning rates. The increased effectiveness of changes in pilot fuel timing at 2400 rpm may be a result of the higher charge temperatures at the time of diesel injection. Also, there was more swirl in the cylinder at 2400 rpm which may have led to improved ignition of the ethanol-air mixture. At 2400 rpm, advancing the pilot timing from 18 to 29 degrees BTDC resulted in a relative increase in thermal efficiency of 4 percent. Advancing the timing also reduced CO and unburned hydrocarbons concentrations significantly. The increase in NO concentration due to advance of the pilot fuel timing was balanced by the decrease in NO concentration due to the addition of ethanol. The net result was a NO concentration comparable to baseline diesel for the dual fuel at advanced timing.

In summary, at 2000 rpm, there was a narrow region where timing advance was beneficial. But at 2400 rpm, it is likely that the effective region would be wider. Further testing needs to be done at 2400 rpm to determine the effective range. Testing should also be done at engine speeds below 2000 rpm to determine if the effective region is too narrow to warrant changes in pilot fuel injection timing.

It has been shown that changes in p pilot fuel injection timing can lead to a relative increase in thermal efficiency of three to four percent for certain engine conditions. Based on these results, it is recommended that pilot fuel injection timing be studied further since it is a promising means of increasing fuel economy.

7. REFERENCES

1. Roberts, B. D., "Performance and Emissions of a Turbocharged Diesel Engine Fumigated with Ethanol," M.S. Thesis, University of Illinois at Urbana-Champaign, Urbana, IL, 1986.

2. Hayes, T. K., "The Effect of Fumigation of Different Ethanol Proofs on a Turbocharged Diesel Engine," M.S. Thesis, University of Illinois at Urbana-Champaign, Urbana, IL, 1986.

3. Donnelly, J., and White, H., "Water and Alcohol Use in Automotive Diesel Engines," U.S. Department of Energy Report DOE/CS/50286-4, 1983.

4. Maynard, A., "A New Electronically Controlled Injection Pumps for Diesels," International Congress and Exposition, Detroit, MI, SAE Paper 850169, Feb. 25-Marcy 1, 1985.

5. Shropshire, G. J., and Goering, C. E., "Ethanol Injection into a Diesel Engine," ASAE Paper 81-1051, June 21-24, 1981.

6. Ecklund, E. E., Bechtold, R. L., Timbario, T. J., and McCallum, P. W., "State-of-the-Art Report on the Use of Alcohols in Diesel Engines," International Congress and Exposition, Detroit, MI, SAE Paper 840118, Feb. 27-March 2, 1984.

7. SAE Recommended Practice, "Measurement of Intake Air or Exhaust Gas Flow of Diesel Engines," SAE J244, SAE Handbook.

8. SAE Recommended Practice, "Measurement of Carbon Dioxide, Carbon Monoxide, and Oxides of Nitrogen in Diesel Exhaust," SAE J117, SAE Handbook.

9. Hayes, T. K., Savage, L. D., and Sorenson, S. C., "Cylinder Pressure Data Acquisition and Heat Release Analysis on a Personal Computer," SAE Paper 860029, 1986.

10. Gao, X., Chen, J., Ye, Z., Foster, D., and Borman, G., "Ignition Delay and Heat Release Analysis of an Ethanol Fumigated Turbocharged Diesel Engine," ASME Paper No. 83-DGP-1, 1983.

8. TABULAR DATA

Test conditions: RPM = 2000
Ethanol flow setting = 0.
Diesel injection timing = 18° BTDC

BMEP (kpa)	100	300	500	700	900
Diesel mass flow (g/s)	1.668	2.910	4.194	5.526	7.159
Eth. mass flow (g/s)	0.	0.	0.	0.	0.
Thermal efficiency	.1673	.2876	.3315	.3526	.3495
% Ethanol by energy	0.	0.	0.	0.	0.
Volumetric efficiency	.8165	.8261	.8427	.8549	.8710
Air mass flow (g/s)	111.5	117.6	128.3	140.4	155.1
Int. man. press. (kpa)	102.3	109.0	120.9	136.0	155.2
Ambient pressure (kpa)	99.27	99.27	99.27	99.27	99.27
Wet bulb temp. (C)	17.22	17.22	17.78	17.78	18.33
Ambient temp. (C)	22.40	22.48	23.28	23.82	25.11
Int. manifold temp. (C)	37.37	44.33	56.11	70.10	88.28
Exh. manifold temp. (C)	237.7	348.7	462.3	554.7	655.8
Stack temp. (C)	224.6	324.4	429.7	512.8	602.4
Coolant temp. (C)	92.66	91.75	93.23	93.57	94.83
Nitric oxide (ppm)	367.0	902.0	1250.	1563.	1655.
HC (ppm propane)	179.4	165.7	155.8	148.6	102.1
Carbon dioxide (% dry)	2.647	4.553	6.238	7.521	8.427
Carbon monoxide (% dry)	.0522	.0351	.0429	.0859	.2722
Bosch smoke no.	.90	1.00	2.10	3.60	5.80
Max. dP/dθ (Mpa/deg)	.5385	.8261	.9013	.7952	.6779
Angle of max. dP/dθ	357	355	354	352	351
Max. pressure (Mpa)	5.631	7.090	8.350	9.789	11.35
Angle of max. pressure	361	362	363	366	365
Ignition delay (deg)	13	12	9	8	7

Table A.1

Test conditions: RPM = 2000
BMEP = 100 kpa
Ethanol flow setting = 5.

Pilot timing (°BTDC)	18	29
Diesel mass flow (g/s)	.9002	.8804
Eth. mass flow (g/s)	1.935	1.926
Thermal efficiency	.1318	.1334
% Ethanol by energy	57.48	57.91
Volumetric efficiency	.8320	.8349
Air mass flow (g/s)	111.7	112.0
Int. man. press. (kpa)	101.3	101.1
Ambient pressure (kpa)	98.77	98.89
Wet bulb temp. (C)	18.61	20.83
Ambient temp. (C)	24.94	25.57
Int. manifold temp. (C)	39.69	39.44
Exh. manifold temp. (C)	238.1	234.5
Stack temp. (C)	219.2	215.3
Coolant temp. (C)	93.93	93.02
Nitric oxide (ppm)	106.0	81.16
HC (ppm propane)	1495.	1437.
Carbon dioxide (% dry)	2.335	2.350
Carbon monoxide (% dry)	.5553	.6470
Bosch smoke no.	.20	.10
Max. dP/dθ (Mpa/deg)	.4457	.2115
Angle of max. dP/dθ	359	356
Max. pressure (Mpa)	5.251	4.896
Angle of max. pressure	363	364
Ignition delay (deg)	16	25

Table A.2

Test conditions: RPM = 2000
BMEP = 100 kpa
Ethanol flow setting = 6.

Pilot timing (°BTDC)	18	26
Diesel mass flow (g/s)	.7745	.7446
Eth. mass flow (g/s)	2.371	2.374
Thermal efficiency	.1232	.1247
% Ethanol by energy	65.81	66.72
Volumetric efficiency	.8294	.8378
Air mass flow (g/s)	111.4	112.4
Int. man. press. (kpa)	101.4	101.3
Ambient pressure (kpa)	98.77	99.01
Wet bulb temp. (C)	18.61	20.83
Ambient temp. (C)	25.03	26.41
Int. manifold temp. (C)	39.94	39.81
Exh. manifold temp. (C)	236.4	233.0
Stack temp. (C)	217.9	214.7
Coolant temp. (C)	92.57	94.67
Nitric oxide (ppm)	76.88	70.41
HC (ppm propane)	1678.	1654.
Carbon dioxide (% dry)	2.278	2.245
Carbon monoxide (% dry)	.6031	.6483
Bosch smoke no.	.20	.20
Max. dP/dθ (Mpa/deg)	.3932	.2698
Angle of max. dP/dθ	359	357
Max. pressure (Mpa)	5.196	5.012
Angle of max. pressure	364	365
Ignition delay (deg)	18	23

Table A.3

Test conditions: RPM = 2000
BMEP = 100 kpa
Ethanol flow setting = 7.

Pilot timing (°BTDC)	18	22	26
Diesel mass flow (g/s)	.6702	.6619	.6619
Eth. mass flow (g/s)	2.787	2.764	2.796
Thermal efficiency	.1152	.1163	.1153
% Ethanol by energy	72.34	72.42	72.65
Volumetric efficiency	.8330	.8362	.8394
Air mass flow (g/s)	112.1	114.2	112.8
Int. man. press. (kpa)	101.6	102.4	101.5
Ambient pressure (kpa)	98.77	99.27	99.01
Wet bulb temp. (C)	18.61	17.78	20.83
Ambient temp. (C)	24.89	22.97	26.74
Int. manifold temp. (C)	39.96	37.65	40.22
Exh. manifold temp. (C)	236.6	231.3	238.1
Stack temp. (C)	218.5	216.9	219.0
Coolant temp. (C)	91.52	92.93	92.63
Nitric oxide (ppm)	57.15	77.42	57.21
HC (ppm propane)	1858.	1812.	1822.
Carbon dioxide (% dry)	2.247	2.354	2.296
Carbon monoxide (% dry)	.6207	.6408	.6439
Bosch smoke no.	.20	.10	.05
Max. $dP/d\theta$ (Mpa/deg)	.3466	.2671	.1474
Angle of max. $dP/d\theta$	360	359	358
Max. pressure (Mpa)	4.985	5.006	4.609
Angle of max. pressure	364	363	363
Ignition delay (deg)	18	20	24

Table A.4

Test conditions: RPM = 2000
BMEP = 100 kpa
Ethanol flow setting = 8.

Pilot timing (°BTDC)	14	18	22
Diesel mass flow (g/s)	.6595	.5921	.5853
Eth. mass flow (g/s)	3.169	3.175	3.169
Thermal efficiency	.1052	.1078	.1082
% Ethanol by energy	75.13	77.13	77.30
Volumetric efficiency	.8295	.8368	.8387
Air mass flow (g/s)	111.4	114.3	114.7
Int. man. press. (kpa)	101.7	102.6	102.7
Ambient pressure (kpa)	98.71	99.27	99.27
Wet bulb temp. (C)	21.39	18.06	17.78
Ambient temp. (C)	27.06	23.63	23.24
Int. manifold temp. (C)	40.75	38.32	38.23
Exh. manifold temp. (C)	252.9	237.4	233.3
Stack temp. (C)	232.9	221.7	221.3
Coolant temp. (C)	95.16	93.80	94.44
Nitric oxide (ppm)	69.57	77.05	73.91
HC (ppm propane)	1974.	1940.	1916.
Carbon dioxide (% dry)	2.359	2.270	2.410
Carbon monoxide (% dry)	.6111	.6152	.6257
Bosch smoke no.	0.	.20	.10
Max. $dP/d\theta$ (Mpa/deg)	.2698	.2240	.1895
Angle of max. $dP/d\theta$	363	361	359
Max. pressure (Mpa)	4.624	4.771	4.785
Angle of max. pressure	364	365	364
Ignition delay (deg)	16	18	21

Table A.5

Test conditions: RPM = 2000
BMEP = 300 kpa
Ethanol flow setting = 6.

Pilot timing (°BTDC)	18	26	29
Diesel mass flow (g/s)	1.564	1.533	1.542
Eth. mass flow (g/s)	2.364	2.364	2.345
Thermal efficiency	.2744	.2772	.2775
% Ethanol by energy	48.73	49.23	48.87
Volumetric efficiency	.8361	.8351	.8358
Air mass flow (g/s)	116.7	115.8	116.0
Int. man. press. (kpa)	107.3	106.4	106.5
Ambient pressure (kpa)	98.77	99.01	98.89
Wet bulb temp. (C)	18.61	20.83	20.83
Ambient temp. (C)	25.03	27.07	26.28
Int. manifold temp. (C)	45.59	45.18	45.05
Exh. manifold temp. (C)	337.8	327.1	327.7
Stack temp. (C)	309.0	301.7	302.2
Coolant temp. (C)	92.86	94.18	93.24
Nitric oxide (ppm)	450.2	810.8	882.5
HC (ppm propane)	1066.	991.2	953.6
Carbon dioxide (% dry)	4.179	4.187	4.308
Carbon monoxide (% dry)	.3187	.2344	.2286
Bosch smoke no.	.20	.30	.35
Max. dP/dθ (Mpa/deg)	.6411	.7900	.7508
Angle of max. dP/dθ	359	355	354
Max. pressure (Mpa)	6.213	6.959	7.195
Angle of max. pressure	363	365	364
Ignition delay (deg)	15	18	22

Table A.6

Test conditions: RPM = 2000
BMEP = 300 kpa
Ethanol flow setting = 8.

Pilot timing (°BTDC)	18	26	29
Diesel mass flow (g/s)	1.107	1.036	1.019
Eth. mass flow (g/s)	3.206	3.181	3.176
Thermal efficiency	.2681	.2757	.2776
% Ethanol by energy	64.55	65.87	66.23
Volumetric efficiency	.8382	.8402	.8363
Air mass flow (g/s)	116.7	116.2	115.7
Int. man. press. (kpa)	106.9	106.1	106.1
Ambient pressure (kpa)	98.77	99.01	98.89
Wet bulb temp. (C)	18.89	20.83	20.83
Ambient temp. (C)	25.41	27.36	26.36
Int. manifold temp. (C)	45.43	45.00	44.83
Exh. manifold temp. (C)	332.4	327.0	326.1
Stack temp. (C)	303.6	297.1	295.9
Coolant temp. (C)	92.93	94.31	93.65
Nitric oxide (ppm)	401.0	562.8	475.2
HC (ppm propane)	1367.	1234.	1250.
Carbon dioxide (% dry)	4.009	4.050	4.078
Carbon monoxide (% dry)	.3248	.2410	.2366
Bosch smoke no.	.20	.20	.20
Max. dP/dθ (Mpa/deg)	.4526	.3880	.2845
Angle of max. dP/dθ	359	357	357
Max. pressure (Mpa)	5.744	5.861	5.673
Angle of max. pressure	364	367	367
Ignition delay (deg)	17	23	25

Table A.7

Test conditions: RPM = 2000
BMEP = 300 kpa
Ethanol flow setting = 10.

Pilot timing (°BTDC)	18	22
Diesel mass flow (g/s)	.7218	.6849
Eth. mass flow (g/s)	4.088	4.068
Thermal efficiency	.2543	.2581
% Ethanol by energy	78.08	78.88
Volumetric efficiency	.8424	.8424
Air mass flow (g/s)	117.4	119.1
Int. man. press. (kpa)	107.2	108.0
Ambient pressure (kpa)	98.77	99.27
Wet bulb temp. (C)	18.89	17.78
Ambient temp. (C)	25.50	24.07
Int. manifold temp. (C)	45.92	43.49
Exh. manifold temp. (C)	330.1	321.4
Stack temp. (C)	306.2	301.2
Coolant temp. (C)	92.75	93.08
Nitric oxide (ppm)	271.1	296.7
HC (ppm propane)	1639.	1574.
Carbon dioxide (% dry)	3.895	4.096
Carbon monoxide (% dry)	.3366	.2818
Bosch smoke no.	.20	.10
Max. $dP/d\theta$ (Mpa/deg)	.4192	.4093
Angle of max. $dP/d\theta$	360	358
Max. pressure (Mpa)	5.484	5.900
Angle of max. pressure	368	368
Ignition delay (deg)	18	20

Table A.8

Test conditions: RPM = 2000
BMEP = 300 kpa
Ethanol flow setting = 11.5

Pilot timing (°BTDC)	14	18	22
Diesel mass flow (g/s)	.6297	.5422	.5602
Eth. mass flow (g/s)	4.687	4.687	4.674
Thermal efficiency	.2340	.2399	.2393
% Ethanol by energy	82.39	84.46	83.99
Volumetric efficiency	.8429	.8443	.8409
Air mass flow (g/s)	118.0	120.2	119.7
Int. man. press. (kpa)	108.3	109.1	108.9
Ambient pressure (kpa)	98.71	99.27	99.27
Wet bulb temp. (C)	21.39	18.06	17.78
Ambient temp. (C)	27.39	24.35	22.84
Int. manifold temp. (C)	47.80	44.67	43.98
Exh. manifold temp. (C)	349.5	325.7	313.5
Stack temp. (C)	325.4	310.4	303.6
Coolant temp. (C)	94.43	92.83	92.69
Nitric oxide (ppm)	182.8	237.6	200.7
HC (ppm propane)	1836.	1807.	1815.
Carbon dioxide (% dry)	3.890	3.822	4.075
Carbon monoxide (% dry)	.3611	.3144	.2689
Bosch smoke no.	.10	.20	.15
Max. dP/dθ (Mpa/deg)	.3037	.2470	.2025
Angle of max. dP/dθ	363	361	360
Max. pressure (Mpa)	5.130	5.179	5.226
Angle of max. pressure	367	368	367
Ignition delay (deg)	15	18	21

Table A.9

Test conditions: RPM = 2000
BMEP = 500 kpa
Ethanol flow setting = 11.5

Pilot timing (°BTDC)	14	18	26	29
Diesel mass flow (g/s)	1.235	1.173	1.369	1.428
Eth. mass flow (g/s)	4.727	4.700	4.687	4.673
Thermal efficiency	.3305	.3368	.3222	.3184
% Ethanol by energy	70.65	71.58	68.29	67.30
Volumetric efficiency	.8405	.8371	.8212	.8255
Air mass flow (g/s)	122.5	121.8	119.9	120.7
Int. man. press. (kpa)	115.1	114.4	114.9	115.4
Ambient pressure (kpa)	98.71	98.77	99.01	98.89
Wet bulb temp. (C)	21.39	19.17	20.83	21.39
Ambient temp. (C)	27.81	25.99	28.28	26.88
Int. manifold temp. (C)	54.40	52.92	53.08	54.17
Exh. manifold temp. (C)	423.2	407.0	412.2	415.4
Stack temp. (C)	390.9	376.7	382.7	387.3
Coolant temp. (C)	94.85	94.06	95.73	94.82
Nitric oxide (ppm)	629.8	970.6	2018.	2443.
HC (ppm propane)	1236.	1067.	701.1	765.5
Carbon dioxide (% dry)	5.633	5.719	6.562	6.698
Carbon monoxide (% dry)	.1776	.1573	.1072	.1049
Bosch smoke no.	.30	.40	.40	.50
Max. dP/dθ (Mpa/deg)	.5097	.6765	1.716	1.641
Angle of max. dP/dθ	362	359	357	356
Max. pressure (Mpa)	6.212	7.640	10.30	11.09
Angle of max. pressure	372	369	363	359
Ignition delay (deg)	15	15	19	20

Table A.10

Test conditions: RPM = 2000
BMEP = 500 kpa
Ethanol flow setting = 12.5

Pilot timing (°BTDC)	18	22
Diesel mass flow (g/s)	.9079	1.047
Eth. mass flow (g/s)	5.104	5.120
Thermal efficiency	.3377	.3259
% Ethanol by energy	77.95	75.47
Volumetric efficiency	.8373	.8229
Air mass flow (g/s)	123.3	121.4
Int. man. press. (kpa)	115.0	115.2
Ambient pressure (kpa)	99.27	99.27
Wet bulb temp. (C)	18.06	18.61
Ambient temp. (C)	25.32	25.35
Int. manifold temp. (C)	50.83	50.63
Exh. manifold temp. (C)	403.6	405.7
Stack temp. (C)	373.6	374.9
Coolant temp. (C)	94.69	95.10
Nitric oxide (ppm)	949.7	1597.
HC (ppm propane)	1106.	861.4
Carbon dioxide (% dry)	5.422	6.568
Carbon monoxide (% dry)	.1441	.1236
Bosch smoke no.	.40	.60
Max. dP/dθ (Mpa/deg)	.5733	1.064
Angle of max. dP/dθ	358	362
Max. pressure (Mpa)	8.092	9.330
Angle of max. pressure	368	363
Ignition delay (deg)	16	17

Table A.11

Test conditions: RPM = 2000
BMEP = 700 kpa
Ethanol flow setting = 10.5

Pilot timing (°BTDC)	14	18	22	26
Diesel mass flow (g/s)	2.820	2.812	2.939	3.132
Eth. mass flow (g/s)	4.322	4.322	4.277	4.311
Thermal efficiency	.3519	.3524	.3462	.3335
% Ethanol by energy	49.08	49.14	47.78	46.39
Volumetric efficiency	.8326	.8400	.8415	.8317
Air mass flow (g/s)	130.8	133.3	133.8	132.0
Int. man. press. (kpa)	128.9	129.3	129.7	130.7
Ambient pressure (kpa)	98.71	99.27	99.27	99.01
Wet bulb temp. (C)	21.67	18.61	18.61	21.39
Ambient temp. (C)	28.98	26.48	26.45	29.49
Int. manifold temp. (C)	67.35	64.50	65.01	68.13
Exh. manifold temp. (C)	527.1	512.7	523.8	545.1
Stack temp. (C)	482.1	472.2	477.5	492.4
Coolant temp. (C)	95.67	95.37	95.66	96.30
Nitric oxide (ppm)	1183.	1711.	2398.	3120.
HC (ppm propane)	592.4	535.6	483.6	434.9
Carbon dioxide (% dry)	7.712	7.226	8.077	8.143
Carbon monoxide (% dry)	.1423	.1315	.1340	.1469
Bosch smoke no.	2.80	1.20	1.00	1.00
Max. dP/dθ (Mpa/deg)	1.787	1.710	1.471	1.823
Angle of max. dP/dθ	361	357	354	351
Max. pressure (Mpa)	10.98	11.76	11.62	12.10
Angle of max. pressure	362	360	360	360
Ignition delay (deg)	10	10	12	16

Table A.12

Test conditions: RPM = 2000
BMEP = 900 kpa
Ethanol flow setting = 9.

Pilot timing (°BTDC)	14	18	22	26
Diesel mass flow (g/s)	4.778	4.650	4.760	5.048
Eth. mass flow (g/s)	3.617	3.633	3.617	3.617
Thermal efficiency	.3547	.3608	.3556	.3416
% Ethanol by energy	32.25	32.94	32.33	31.06
Volumetric efficiency	.8600	.8615	.8641	.8603
Air mass flow (g/s)	148.2	149.2	150.3	149.9
Int. man. press. (kpa)	149.3	148.5	149.6	151.9
Ambient pressure (kpa)	98.71	99.27	99.27	99.01
Wet bulb temp. (C)	21.67	18.33	18.89	20.83
Ambient temp. (C)	26.49	26.57	25.49	26.99
Int. manifold temp. (C)	86.24	82.37	83.40	88.30
Exh. manifold temp. (C)	623.7	615.8	629.3	645.7
Stack temp. (C)	570.9	560.4	567.5	584.4
Coolant temp. (C)	94.61	95.86	95.15	95.17
Nitric oxide (ppm)	1390.	1888.	2457.	2942.
HC (ppm propane)	422.3	339.9	358.8	376.8
Carbon dioxide (% dry)	8.955	8.461	8.931	9.172
Carbon monoxide (% dry)	.2501	.2066	.2496	.4893
Bosch smoke no.	4.35	3.80	3.30	2.80
Max. dP/dθ (Mpa/deg)	1.362	1.201	1.357	1.692
Angle of max. dP/dθ	357	354	351	348
Max. pressure (Mpa)	11.48	12.54	13.15	13.74
Angle of max. pressure	365	363	360	360
Ignition delay (deg)	9	9	11	13

Table A.13

Test conditions: RPM = 2000
BMEP = 400 kpa
Ethanol flow setting = 0.

Pilot timing (°BTDC)	18	22	26	29
Diesel mass flow (g/s)	3.548	3.576	3.671	3.892
Eth. mass flow (g/s)	0	0	0	0
Thermal efficiency	.3105	.3080	.3000	.2830
% Ethanol by energy	0	0	0	0
Volumetric efficiency	.8266	.8225	.8142	.8154
Air mass flow (g/s)	120.1	119.4	118.5	118.9
Int. man. press. (kpa)	113.7	113.6	114.0	114.8
Ambient pressure (kpa)	98.94	98.94	98.94	98.85
Wet bulb temp. (C)	19.44	19.72	19.44	19.44
Ambient temp. (C)	25.51	25.65	25.51	26.03
Int. manifold temp. (C)	51.49	51.29	51.74	53.16
Exh. manifold temp. (C)	421.4	422.6	429.7	440.8
Stack temp. (C)	382.7	384.1	389.4	395.6
Coolant temp. (C)	93.86	93.75	93.88	94.39
Nitric oxide (ppm)	1058.	1503.	1949.	2376.
HC (ppm propane)	177.9	204.1	259.8	312.5
Carbon dioxide (% dry)	5.393	5.565	5.760	5.773
Carbon monoxide (% dry)	.0376	.0433	.0572	.1067
Bosch smoke no.	1.60	1 25	1.40	1.70
Max. dP/dθ (Mpa/deg)	.8490	1.229	1.500	1.401
Angle of max. dP/dθ	355	352	350	348
Max. pressure (Mpa)	7.685	8.212	8.817	9.234
Angle of max. pressure	364	361	359	360
Ignition delay (deg)	12	12	14	16

Table A.14

Test conditions: RPM = 2000
BMEP = 400 kpa
Ethanol flow setting = 8.

Pilot timing (°BTDC)	18	22	26	29
Diesel mass flow (g/s)	1.560	1.538	1.543	1.537
Eth. mass flow (g/s)	3.175	3.194	3.175	3.175
Thermal efficiency	.3097	.3106	.3112	.3118
% Ethanol by energy	56.14	56.63	56.41	56.51
Volumetric efficiency	.8242	.8217	.8145	.8144
Air mass flow (g/s)	118.2	117.3	116.2	115.9
Int. man. press. (kpa)	111.2	110.5	110.5	110.4
Ambient pressure (kpa)	98.94	98.94	98.94	98.85
Wet bulb temp. (C)	19.44	19.44	19.44	19.44
Ambient temp. (C)	25.20	25.35	25.02	25.96
Int. manifold temp. (C)	48.42	47.97	47.98	48.56
Exh. manifold temp. (C)	379.3	373.5	370.5	371.5
Stack temp. (C)	347.2	342.3	340.1	339.8
Coolant temp. (C)	93.47	93.42	93.36	93.87
Nitric oxide (ppm)	647.3	955.0	1190.	1382.
HC (ppm propane)	1064.	965.8	908.5	862.8
Carbon dioxide (% dry)	4.874	5.015	5.084	4.926
Carbon monoxide (% dry)	.2367	.2077	.2055	.1950
Bosch smoke no.	.25	.20	.35	.20
Max. dP/dθ (Mpa/deg)	.6324	.8030	.8367	.8625
Angle of max. dP/dθ	359	356	355	354
Max. pressure (Mpa)	6.760	7.614	8.188	8.367
Angle of max. pressure	366	364	364	363
Ignition delay (deg)	15	17	18	22

Table A.15

Test conditions: RPM = 2000
BMEP = 400 kpa
Ethanol flow setting = 9.

Pilot timing (°BTDC)	18	22	26	29
Diesel mass flow (g/s)	1.298	1.259	1.241	1.224
Eth. mass flow (g/s)	3.609	3.617	3.598	3.617
Thermal efficiency	.3088	.3117	.3144	.3149
% Ethanol by energy	63.62	64.36	64.57	65.01
Volumetric efficiency	.8234	.8193	.8172	.8148
Air mass flow (g/s)	117.8	117.0	116.4	115.7
Int. man. press. (kpa)	110.8	110.4	110.1	110.0
Ambient pressure (kpa)	98.94	98.94	98.94	98.85
Wet bulb temp. (C)	19.44	19.44	19.72	18.89
Ambient temp. (C)	25.19	24.96	24.76	25.75
Int. manifold temp. (C)	47.97	47.69	47.43	47.99
Exh. manifold temp. (C)	376.8	366.5	361.7	360.9
Stack temp. (C)	342.8	336.7	334.3	334.0
Coolant temp. (C)	93.47	93.44	93.76	94.23
Nitric oxide (ppm)	607.2	882.0	1034.	1136.
HC (ppm propane)	1182.	1058.	1002.	973.6
Carbon dioxide (% dry)	4.805	4.943	4.997	4.827
Carbon monoxide (% dry)	.2161	.1968	.1896	.1729
Bosch smoke no.	.20	.15	.20	.10
Max. $dP/d\theta$ (Mpa/deg)	.6900	.7564	.6687	.6285
Angle of max. $dP/d\theta$	359	357	355	355
Max. pressure (Mpa)	6.896	7.508	8.060	8.010
Angle of max. pressure	369	367	365	365
Ignition delay (deg)	16	17	20	23

Table A.16

Test conditions: RPM = 2000
BMEP = 400 kpa
Ethanol flow setting = 10.

Pilot timing (°BTDC)	18	22	26	29
Diesel mass flow (g/s)	1.031	.9732	.9334	.9153
Eth. mass flow (g/s)	4.058	4.078	4.068	4.083
Thermal efficiency	.3074	.3114	.3155	.3163
% Ethanol by energy	71.21	72.49	73.26	73.72
Volumetric efficiency	.8204	.8259	.8148	.8224
Air mass flow (g/s)	117.4	117.4	116.0	116.4
Int. man. press. (kpa)	110.8	110.0	109.9	109.6
Ambient pressure (kpa)	98.94	98.94	98.94	98.85
Wet bulb temp. (C)	19.17	19.44	19.72	18.89
Ambient temp. (C)	24.81	24.71	24.81	25.75
Int. manifold temp. (C)	47.94	47.60	46.84	47.91
Exh. manifold temp. (C)	367.3	363.2	355.9	359.6
Stack temp. (C)	339.0	333.6	329.7	330.3
Coolant temp. (C)	92.78	93.28	93.56	93.99
Nitric oxide (ppm)	566.2	736.4	695.4	688.8
HC (ppm propane)	1302.	1207.	1199.	1175.
Carbon dioxide (% dry)	4.761	4.840	4.799	4.643
Carbon monoxide (% dry)	.2045	.1854	.1787	.1665
Bosch smoke no.	.20	.25	.20	.20
Max. dP/dθ (Mpa/deg)	.5888	.5477	.4169	.3333
Angle of max. dP/dθ	359	357	356	356
Max. pressure (Mpa)	6.450	6.829	7.136	7.002
Angle of max. pressure	369	368	367	369
Ignition delay (deg)	15	18	21	25

Table A.17

Test conditions: RPM = 2000
BMEP = 400 kpa
Ethanol flow setting = 11.

Pilot timing (°BTDC)	18	22	26	29
Diesel mass flow (g/s)	.8145	.7405	.7235	.7356
Eth. mass flow (g/s)	4.485	4.485	4.467	4.497
Thermal efficiency	.3031	.3094	.3119	.3091
% Ethanol by energy	77.59	79.20	79.52	79.36
Volumetric efficiency	.8265	.8235	.8251	.8210
Air mass flow (g/s)	118.5	117.6	117.9	116.8
Int. man. press. (kpa)	111.1	110.5	110.4	110.3
Ambient pressure (kpa)	98.94	98.94	98.94	98.85
Wet bulb temp. (C)	19.17	19.44	19.44	18.89
Ambient temp. (C)	23.77	24.30	23.30	25.78
Int. manifold temp. (C)	47.99	47.74	47.19	48.16
Exh. manifold temp. (C)	361.6	357.1	354.2	357.4
Stack temp. (C)	338.9	333.6	331.6	333.3
Coolant temp. (C)	92.61	92.90	92.96	94.15
Nitric oxide (ppm)	466.1	529.0	461.9	405.6
HC (ppm propane)	1446.	1387.	1371.	1395.
Carbon dioxide (% dry)	4.660	4.708	4.720	4.548
Carbon monoxide (% dry)	.2181	.1902	.1850	.1858
Bosch smoke no.	.20	.25	.20	.20
Max. $dP/d\theta$ (Mpa/deg)	.5617	.4725	.3714	.2532
Angle of max. $dP/d\theta$	359	358	357	357
Max. pressure (Mpa)	6.505	7.020	7.026	6.816
Angle of max. pressure	369	368	369	370
Ignition delay (deg)	15	20	21	25

Table A.18

Test conditions: RPM = 2400
BMEP = 400 kpa
Ethanol flow setting = 0.

Pilot timing (°BTDC)	14	18	22	26	29
Diesel mass flow (g/s)	4.524	4.477	4.479	4.550	4.674
Eth. mass flow (g/s)	0	0	0	0	0
Thermal efficiency	.2922	.2953	.2951	.2905	.2828
% Ethanol by energy	0	0	0	0	0
Volumetric efficiency	.8731	.8660	.8733	.8629	.8616
Air mass flow (g/s)	153.5	151.3	152.3	151.0	150.5
Int. man. press. (kpa)	120.9	119.6	119.3	119.5	119.8
Ambient pressure (kpa)	98.99	99.03	99.03	99.09	98.94
Wet bulb temp. (C)	24.44	24.44	24.72	24.44	25.00
Ambient temp. (C)	32.61	32.48	32.30	32.09	33.44
Int. manifold temp. (C)	69.09	67.54	67.27	66.65	67.97
Exh. manifold temp. (C)	490.8	477.4	471.0	471.6	485.5
Stack temp. (C)	435.6	425.4	422.6	423.4	430.4
Coolant temp. (C)	96.00	95.60	95.89	95.76	95.80
Nitric oxide (ppm)	588.3	852.7	1163.	1592.	1992.
HC (ppm propane)	167.3	166.5	186.0	198.7	225.2
Carbon dioxide (% dry)	5.763	5.735	5.754	5.919	6.003
Carbon monoxide (% dry)	.0341	.0345	.0386	.0432	.0602
Bosch smoke no.	3.00	2.85	2.40	1.80	1.45
Max. $dP/d\theta$ (Mpa/deg)	.4905	.7303	.9285	1.060	1.230
Angle of max. $dP/d\theta$	359	356	354	352	350
Max. pressure (Mpa)	7.063	7.662	8.165	8.721	9.011
Angle of max. pressure	365	364	362	359	361
Ignition delay (deg)	10	11	11	14	15

Table A.19

Test conditions: RPM = 2400
BMEP = 400 kpa
Ethanol flow setting = 8.

Pilot timing (°BTDC)	14	18	22	26	29
Diesel mass flow (g/s)	2.182	2.013	2.001	2.034	2.072
Eth. mass flow (g/s)	3.934	3.921	3.915	3.924	3.906
Thermal efficiency	.2839	.2951	.2962	.2936	.2919
% Ethanol by energy	53.13	55.05	55.16	54.81	54.24
Volumetric efficiency	.8758	.8707	.8729	.8608	.8570
Air mass flow (g/s)	151.3	149.0	148.6	147.1	146.0
Int. man. press. (kpa)	117.7	115.8	114.9	115.0	115.0
Ambient pressure (kpa)	98.99	99.03	99.03	99.09	98.94
Wet bulb temp. (C)	24.44	24.44	24.72	24.44	25.00
Ambient temp. (C)	31.73	31.98	31.65	31.63	32.85
Int. manifold temp. (C)	65.72	63.70	62.58	61.75	62.72
Exh. manifold temp. (C)	452.0	433.6	422.5	415.3	417.0
Stack temp. (C)	405.7	389.4	382.6	378.3	379.9
Coolant temp. (C)	95.11	95.62	95.34	95.63	95.47
Nitric oxide (ppm)	367.7	546.5	795.5	1133.	1485.
HC (ppm propane)	1016.	940.3	821.6	742.1	680.2
Carbon dioxide (% dry)	5.259	5.264	5.312	5.503	5.551
Carbon monoxide (% dry)	.3020	.2424	.2163	.2010	.1855
Bosch smoke no.	1.30	.90	.70	.50	2.00
Max. dP/dθ (Mpa/deg)	.4226	.5931	.7519	.9155	1.037
Angle of max. dP/dθ	363	360	358	359	354
Max. pressure (Mpa)	6.283	7.271	8.115	9.115	9.484
Angle of max. pressure	371	366	366	363	361
Ignition delay (deg)	14	16	16	18	20

Table A.20

Test conditions: RPM = 2400
BMEP = 400 kpa
Ethanol flow setting = 9.

Pilot timing (°BTDC)	14	18	22	26	29
Diesel mass flow (g/s)	1.883	1.723	1.674	1.662	1.693
Eth. mass flow (g/s)	4.425	4.425	4.425	4.402	4.402
Thermal efficiency	.2833	.2934	.2966	.2984	.2963
% Ethanol by energy	59.63	61.75	62.44	62.48	62.05
Volumetric efficiency	.8737	.8670	.8680	.8559	.8532
Air mass flow (g/s)	151.0	148.5	147.8	146.1	145.2
Int. man. press. (kpa)	117.5	115.7	114.7	114.6	114.5
Ambient pressure (kpa)	98.99	99.03	99.03	99.09	98.94
Wet bulb temp. (C)	24.44	24.17	24.44	24.44	24.72
Ambient temp. (C)	31.42	31.28	31.63	31.52	32.64
Int. manifold temp. (C)	65.11	62.85	62.10	60.99	61.67
Exh. manifold temp. (C)	446.2	426.4	415.8	405.2	406.0
Stack temp. (C)	402.0	385.3	376.8	371.3	372.4
Coolant temp. (C)	95.21	95.20	95.58	95.43	95.39
Nitric oxide (ppm)	319.2	489.3	708.3	1033.	1315.
HC (ppm propane)	1168.	1081.	944.7	810.4	742.8
Carbon dioxide (% dry)	5.124	5.167	5.212	5.385	5.439
Carbon monoxide (% dry)	.3035	.2394	.2136	.1978	.1703
Bosch smoke no.	1.05	.65	.45	.45	.50
Max. dP/dθ (Mpa/deg)	.3703	.5445	.7662	.9784	1.038
Angle of max. dP/dθ	363	360	362	359	358
Max. pressure (Mpa)	6.104	7.249	8.277	9.314	9.674
Angle of max. pressure	372	369	366	363	361
Ignition delay (deg)	12	16	15	19	20

Table A.21

Test conditions: RPM = 2400
BMEP = 400 kpa
Ethanol flow setting = 10.

Pilot timing (°BTDC)	14	18	22	26	29
Diesel mass flow (g/s)	1.648	1.496	1.391	1.348	1.347
Eth. mass flow (g/s)	4.923	4.923	4.923	4.930	4.894
Thermal efficiency	.2786	.2879	.2946	.2972	.2988
% Ethanol by energy	65.25	67.42	68.99	69.70	69.55
Volumetric efficiency	.8763	.8650	.8702	.8610	.8503
Air mass flow (g/s)	151.4	148.3	148.1	146.2	144.0
Int. man. press. (kpa)	117.6	116.0	114.6	114.0	113.8
Ambient pressure (kpa)	98.99	99.03	99.03	99.09	98.94
Wet bulb temp. (C)	24.44	24.44	24.72	24.44	24.44
Ambient temp. (C)	31.28	31.33	31.66	31.28	31.95
Int. manifold temp. (C)	65.48	63.57	61.98	60.79	61.26
Exh. manifold temp. (C)	430.9	416.7	414.7	403.9	404.7
Stack temp. (C)	397.6	383.7	374.9	368.7	367.9
Coolant temp. (C)	95.18	95.44	95.07	95.42	95.19
Nitric oxide (ppm)	305.8	475.0	679.1	971.9	1208.
HC (ppm propane)	1339.	1243.	1085.	898.5	805.4
Carbon dioxide (% dry)	5.106	5.129	5.195	5.370	5.459
Carbon monoxide (% dry)	.2844	.2554	.2113	.1791	.1539
Bosch smoke no.	.80	.75	.40	.35	.65
Max. dP/dθ (Mpa/deg)	.4063	.5982	1.003	1.337	1.588
Angle of max. dP/dθ	363	365	362	359	358
Max. pressure (Mpa)	6.567	7.873	8.798	9.856	10.56
Angle of max. pressure	371	366	366	363	359
Ignition delay (deg)	13	15	15	19	21

Table A.22

Test conditions: RPM = 2400
BMEP = 400 kpa
Ethanol flow setting = 11.

Pilot timing (°BTDC)	14	18	22	26	29
Diesel mass flow (g/s)	1.429	1.199	1.087	1.050	1.028
Eth. mass flow (g/s)	5.420	5.411	5.420	5.420	5.402
Thermal efficiency	.2733	.2872	.2941	.2965	.2987
% Ethanol by energy	70.46	73.94	75.82	76.44	76.77
Volumetric efficiency	.8755	.8646	.8658	.8547	.8491
Air mass flow (g/s)	151.9	148.5	147.5	145.7	143.9
Int. man. press. (kpa)	118.2	116.1	114.7	114.2	113.8
Ambient pressure (kpa)	98.99	99.03	99.03	99.09	98.94
Wet bulb temp. (C)	24.44	24.44	24.44	23.89	24.17
Ambient temp. (C)	30.65	30.21	31.24	30.72	30.79
Int. manifold temp. (C)	65.82	63.17	61.68	60.29	60.89
Exh. manifold temp. (C)	427.8	414.4	408.1	398.7	399.5
Stack temp. (C)	397.5	381.8	371.4	364.5	364.4
Coolant temp. (C)	95.16	94.23	95.32	95.23	94.55
Nitric oxide (ppm)	307.3	421.9	619.8	907.5	1116.
HC (ppm propane)	1451.	1339.	1166.	967.0	865.3
Carbon dioxide (% dry)	5.204	5.116	5.175	5.383	5.494
Carbon monoxide (% dry)	.2787	.2522	.1999	.1679	.1381
Bosch smoke no.	.90	.45	.30	.35	.80
Max. dP/dθ (Mpa/deg)	.3753	.6315	1.361	1.580	1.826
Angle of max. dP/dθ	363	365	362	359	358
Max. pressure (Mpa)	6.886	7.942	9.941	10.17	11.04
Angle of max. pressure	372	367	363	363	359
Ignition delay (deg)	14	16	17	20	20

Table A.23

APPENDIX III

THE EFFECT OF FUMIGATION OF DIFFERENT ETHANOL PROOFS ON A TURBOCHARGED DIESEL ENGINE

Timothy Keith Hayes
B.S., University of Illinois, 1983
M.S., University of Illinois, 1986
Department of Mechanical and Industrial Engineering
University of Illinois at Urbana-Champaign
1206 West Green Street
Urbana, IL 61801

Submitted in partial fulfillment of the requirements
for the degree of Master of Science in Mechanical Engineering
in the Graduate College of the
University of Illinois at Urbana-Champaign, 1986

1. INTRODUCTION

Ethanol offers an attractive supplemental fuel source to farmers, especially to those in grain belt states such as Illinois, Indiana, and Iowa. Fluctuating petroleum prices, which are estimated by analysts to increase in the near future, as well as the ability to convert their surplus and damaged waste crops into ethanol fuel make this an attractive proposition. One advantage to ethanol production on an individual farm basis is that the operator may choose his own slack work periods, such as winter, to produce ethanol. One drawback to small plants is the low quality of the ethanol which is produced. 175 to 180 proof ethanol is generally recognized as the upper limit for small distillation plants [1].

The ethanol produced can be used with diesel powered equipment by utilizing several methods:

1. An ethanol and diesel fuel blend could be produced and used in place of pure diesel fuel with the existing injection equipment.

2. A high pressure ethanol injection system could be added to the high pressure diesel system already present on the engine.

3. The engine could be converted to ethanol operation by lowering the compression ratio and adding a spark assist to ignite the ethanol and air mixture.

4. The ethanol could be fumigated or added to the intake air while the diesel injection system is used to supply the pilot fuel.

All of these methods were discussed in detail by Roberts [2].

Fumigation offers several advantages over the other methods. It requires a minimum of modifications to the engine. High pressure injection equipment is not required for the ethanol, which is advantageous since ethanol's poor lubricating properties may lead to reduced pump reliability. Fumigation allows for quick conversion back to diesel operation since the ethanol injection system is separate from the diesel fuel system. Therefore fumigation offers the greatest flexibility and the fewest modifications to the engine of all the methods for supplementing diesel fuel with ethanol. This should make this technique attractive for agricultural usage, especially if the farmer can produce his own ethanol. However, economically it is only feasible for a small distillation plant to produce approximately 175 to 180 proof ethanol as noted earlier. Due to this latter constraint it was decided to study the fumigation of a typical agricultural diesel engine with various ethanol proofs.

2. LITERATURE REVIEW

Studies with various ethanol proofs as fumigants are not new, but tests using an extensive range of proofs in a turbocharged direct injection diesel engine have not been reported. Heinsy and Lestz [3] tested a single cylinder air cooled diesel engine with 200, 180, 160 and 140 proof ethanol. The ethanol was injected with a single continuous air atomizing nozzle mounted in the intake manifold. The intake air was held at constant conditions at all test points, it was dried in a dehumidifier, and the pressure was held constant. The air was heated to 29°C upstream of the ethanol injector. Tests were run at three rack settings, 1/3, 2/3, and full travel, at 2800, 2400, and 1800 rpm. These settings were determined using diesel fuel and the energy flow rate of the diesel fuel at each rack setting was recorded. When ethanol was fumigated the energy flow rates were held constant. Since the thermal efficiency varied with fumigation, holding the energy flow rate constant meant that the power output of the engine varied at each rack setting as the fumigation rate was increased. Ethanol was fumigated in increasing amounts at each rack setting until the misfire limit was reached.

They reported that the thermal efficiency, CO emissions level, and rate of pressure rise were not affected by lower ethanol proofs. They did not report on hydrocarbon levels. The ignition delay was longer with lower proofs especially at higher flow rates. Nitrous oxide emissions levels were lower with lower proof ethanol. The maximum fumigant level was misfire limited at all loads, and the greatest replacement of diesel fuel was obtained at maximum load.

Shropshire and Goering [4] tested a naturally aspirated four cylinder diesel engine with 190, 150, and 100 proof ethanol as fumigants. They used multi-point continuous injectors mounted in a new intake manifold made for their tests. They conducted tests at bmep's of 600, 400, and 200 kPa, at speeds of 2200, 2000, 1800, and 1600 rpm. When ethanol was fumigated they held the load constant. They increased the flow rate of the fumigant at each load until they reached the knock or misfire limit.

They found that the greatest replacement of diesel fuel with ethanol was at full load. There was little effect on the thermal efficiency with lower ethanol proofs and CO and HC emissions were higher at 150 proof than at 190 proof. They did not report on emissions levels at 100 proof. Their maximum levels of fumigation decreased with lower proof ethanols.

Chen, Gussert, and Gao [5] tested a four cylinder turbocharged diesel engine with 160 and 200 proof ethanol as fumigants. The ethanol was injected using a continuous air atomizing nozzle which was mounted after the compressor in the intake passage. Tests were conducted at full, 3/4, 1/2, and 1/4 loads, at speeds of 2100, 1500, and 1100 rpm. When ethanol was fumigated they held the load constant. The ethanol fumigation rate was increased at all loads until at low loads the misfire limit was reached. At high and medium loads the maximum flow rate was limited by the atomizing injector.

They reported no difference between thermal efficiency, ignition delay, and rate of pressure rise with ethanol proof. They reported emissions data only for 160 proof ethanol. Smoke and NO emissions were below diesel levels with 160 proof ethanol. Carbon monoxide and unburned hydrocarbons increased

three and five times, respectively, above the diesel level with the 160 proof ethanol.

Goering and Wood [6] studied 100 and 160 proof ethanol fumigation into a naturally aspirated three cylinder diesel engine. They used a carburator mounted on the intake manifold to meter the ethanol. Both the choke and the throttle plates were removed to reduce air flow restrictions. The flow rate of the ethanol was controlled by a valve in the fuel supply line to the carburator. The ethanol temperature was raised to 68°C to aid in fuel vaporization. A single test started at 2250 rpm at the high idle rack position. The load on the engine was then increased until the speed of the engine dropped to 1800 rpm, while the rack was held in its original position. Test points were recorded at various points between these speeds. This was first done with diesel fuel, and then repeated with each ethanol proof as a fumigant. Several fumigant flow rates were used. Each ethanol proof was inducted at a constant flow rate while the diesel flow rate was maintained at its baseline level. This meant that the engine was overfueled or produced more power than the original design specifications.

They reported that the results for 160 proof ethanol were very similar to 100 proof; therefore they reported only the 160 proof results. Hydrocarbons were raised five times from the diesel level. The CO level was increased two to three times from the diesel level with 160 proof ethanol.

Baranescu [7] used 200 and 160 proof ethanol as fumigants in a turbocharged six cylinder diesel engine. This was the same engine that was used in this study. A single, continuous spray, high pressure ethanol injector was mounted after the compressor in the crossover pipe. They used a heat exchanger mounted after the injector in the crossover pipe to increase the temperature of the ethanol and air mixture. Tests were conducted at bmep's of 841, 551, and 276 kPa, at speeds of 2500, 1800, and 1200 rpm. The power of the engine was held constant as ethanol was fumigated. The flow rate of the fumigant was increased at each load until the knock or misfire limit was reached.

They found that at 2500 rpm a bmep of 551 allowed the most ethanol to be fumigated and that low loads allowed the least. 160 proof ethanol gave lower rates of pressure rise at low and medium loads with little difference at high loads. The thermal efficiency was slightly worse with 160 proof than with pure ethanol. 160 proof ethanol produced higher levels of unburned hydrocarbons and CO emissions when compared with the emissions with pure ethanol. NO emissions levels were equal or lower than diesel levels as ethanol flow rates were increased with 160 proof ethanol. The NO levels with pure ethanol were higher than the levels with 160 proof ethanol.

Valdmanis and Wulfhorst [8] studied pure water induction into the intake air of a diesel engine. It is of interest to determine the effect of water on diesel fuel combustion. A single cylinder naturally aspirated diesel engine was used. The water was inducted with a single continuous air atomizing injector mounted in the intake manifold. The engine was tested at full load at speeds of 1800 and 2600 rpm. The diesel fuel flow rate at each load was held constant. Several tests were performed, each with a larger amount of water inducted into the intake air. The maximum amount of water that was inducted was 60 percent of the total diesel and water mass flow rate. Since

the diesel flow rate was held constant when water was inducted, the injection timing of the diesel fuel had to be adjusted to obtain the same power output that the engine produced when operating without water.

They indicated that NO levels decreased substantially with water. The smoke level was also reduced. The hydrocarbon emissions increased slightly and there was no noticeable trend in CO emissions with water addition. The ignition delay increased as the water was added.

While several studies have been made with lower proof ethanol in diesel engines, there has not been an extensive study of several ethanol proofs in a multicylinder turbocharged direct injection diesel engine. Therefore it was proposed to use 100, 125, 150, 175, and 200 proof ethanol as fumigants across the load range in a six cylinder turbocharged diesel engine.

3. EXPERIMENTAL EQUIPMENT

Engine

An International Harvester DT436b, turbocharged, four stroke, direct injection diesel engine was used for this study. The engine had six cylinders with a bore of 10.92 cm, a stroke of 12.7 cm, a compression ratio of 16:1 and a total displacement of 7.141 liters. A Midwest MV310 electric eddy current dynomometer was used to load the engine.

Digalog Corporation load and throttle controllers were used to regulate the speed and load of the engine. A Model 1022A was used for load control of the dynomometer and a Model TC was used to control the Colman throttle actuator. Figure 1 shows the equipment layout that was used for the load and throttle controllers.

The engine was modified to accept a fumigation fuel system. Port injection was used to optimize fuel distribution and Bendix type E-10 injectors were mounted in the head, spraying at the valve seat in the intake passage as shown in Fig. 2. The injectors were pulsed twice per power cycle, once when the intake valve was open and again 360 degrees later during the power stroke. This allowed a pair of injectors such as cylinders one and four to be fired at the same time. This simplified the control logic of the injectors.

The ethanol fuel pressure was maintained at 40 psig using a Bosch electric fuel pump and filter. A pressure regulator for the ethanol was referenced to the manifold pressure so that a 40 psi differential was maintained across the injector regardless of the turbocharger boost pressure. The injector controller required two T.T.L. signals which were obtained from encoders on the engine crankshaft. The first signal occurred slightly before top dead center (TDC) of the number one cylinder and reset the injector controller, see Fig. 3. The second signal had three pulses per revolution 120 degrees apart, each pulse triggered the firing of a pair of injectors.

Engine Test Equipment

The engine was operated at existing atmospheric conditions. The mass airflow into the engine was measured by two Meriam Model 50MC2-4F laminar flow meters mounted in parallel. Both meters emptied into a plenum chamber placed upstream of the turbocharger intake. The plenum was used to reduce pressure pulsations which would affect the laminar flow meter readings and was sized according to S.A.E. standards [9]. The pressure drop across each laminar flow element was measured with a D. J. Instruments Model MLR differential pressure strain gage transducer. The mass flow of air was found using the pressure differential across the element and the calibration curve supplied by the manufacturer after corrections were made for ambient conditions.

The intake pressure was measured with a Motorola Model MPX absolute pressure strain gage transducer with a pressure tap mounted in the intake manifold. The exhaust pressure was measured with a Meriam mercury well type manometer, the pressure tap was located in the exhaust manifold before the turbocharger. The exhaust and intake temperatures were measured with type K thermocouples. The respective thermocouple probes were mounted in the same locations as the intake and exhaust pressure taps.

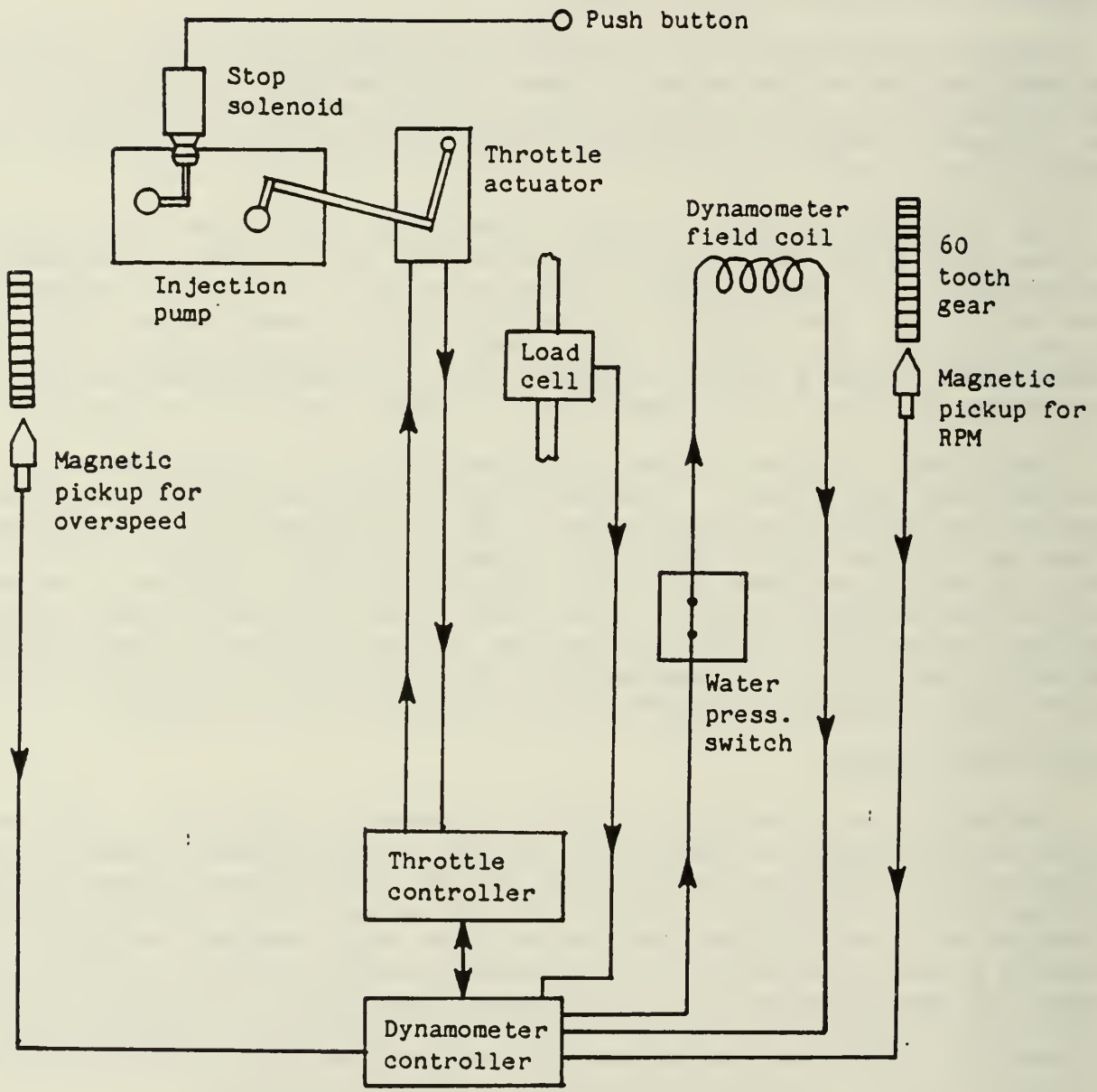

Figure 1 Engine and dynamometer control system.

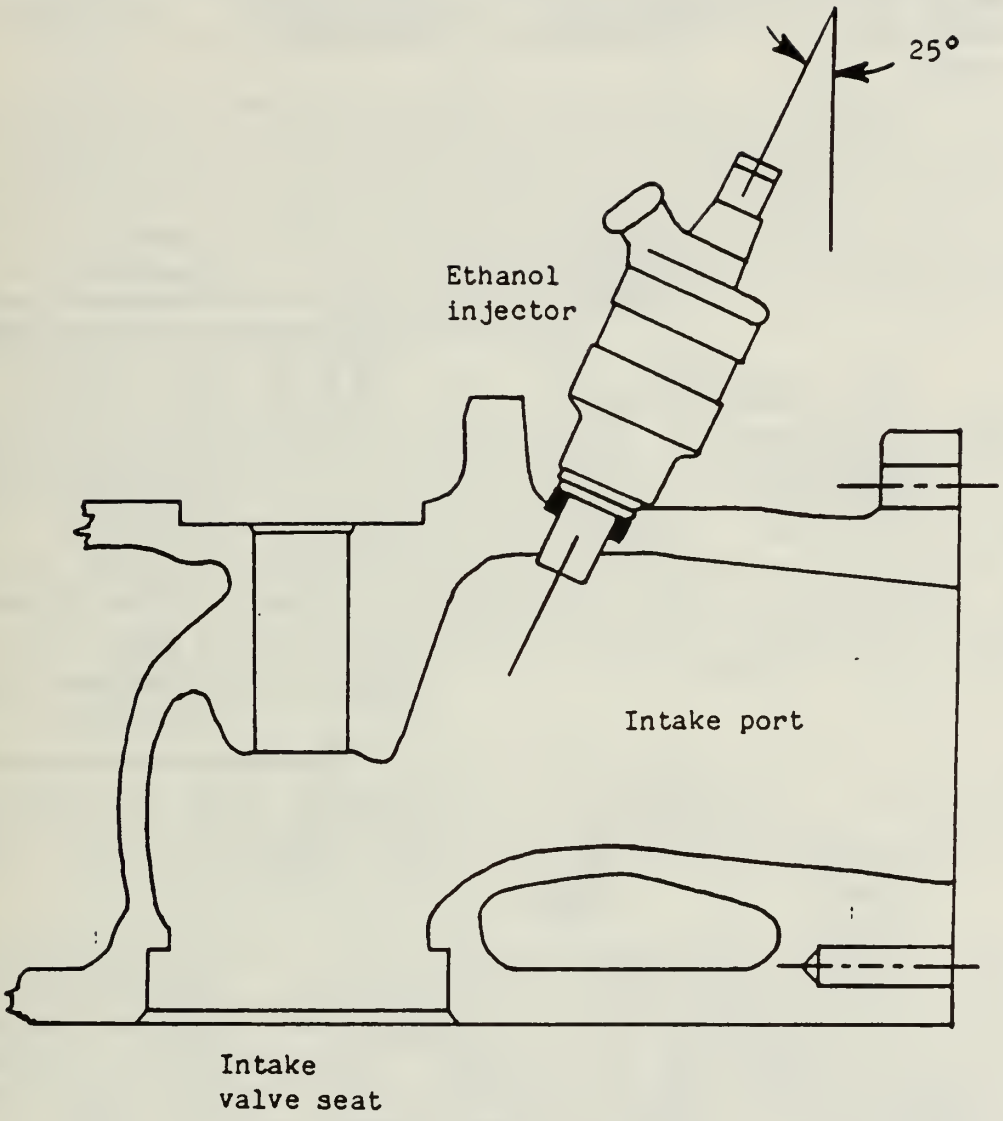

Figure 2 Cross section of cylinder head showing position of ethanol injector with respect to intake valve.

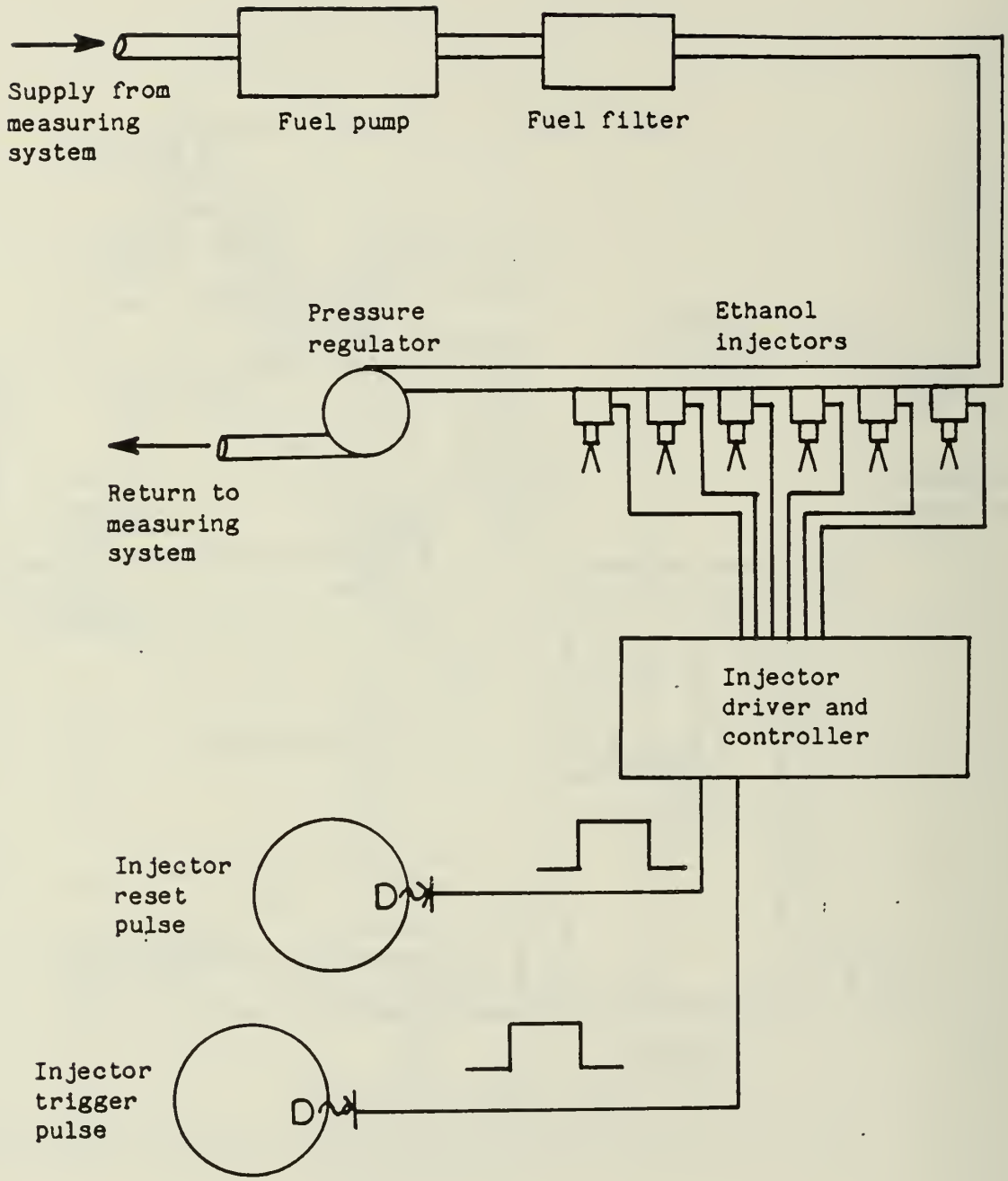

Figure 3 Ethanol fumigation system.

The mass flow rates of ethanol and diesel fuels were found with a series of calibrated burettes, see Fig. 4. The time for the fuel to pass through each volume of the burette was calculated by an Apple computer which used a timer mounted in one of the Apple's backplane floats. The timer was triggered by a float which passed optical sensors mounted on the burettes as the fuel level dropped. The temperature of the fuel in the burettes was measured and the A.P.I. number of the fuel was corrected for variations from the A.P.I. reference temperature. This was necessary due to the heating of the fuel in the return line from the fuel pump on the engine.

An AVL 8QP500ca piezoelectric water cooled pressure transducer was used to measure the pressure in the number one cylinder of the engine. The transducer was slightly recessed from the surface of the combustion chamber. It was mounted vertically in a steel sleeve which passed through the water jacket in the head and through the top of the valve cover. The face of the pressure transducer was coated with silicone rubber to reduce errors caused by thermal strain. The output of the transducer was converted to a voltage with a Kistler Model 504 charge amplifier.

A B.E.I. Model H25D optical shaft encoder was used to correlate the cylinder pressure with the rotation of the engine. The encoder was coupled to a shaft welded on the pulley mounted to the front of the crankshaft. The encoder had two output signals, the first gave a single T.T.L. pulse per revolution and the other gave 360 pulses per revolution. The first of the 360 pulses to rise to a T.T.L. high level after the single pulse from the other channel had risen was orientated with TDC of the number one cylinder. An AVL 41DP 500K strain gage pressure transducer was used to measure the injection line pressure. The mounting block for this transducer was positioned approximately 7.6 cm from the injector.

Emissions measurements made using the system shown in Fig. 5. The sample probe was mounted one meter downstream of the turbocharger. The exhaust gas sample was first drawn through an insulated soot filter and then into a heated sample line. The heated sample line was maintained at a temperature of 350°F.

Beckman instruments were used to measure hydrocarbons, oxygen carbon dioxide and carbon monoxide. A Model 402 F.I.D. hydrocarbon analyzer, Model 315 carbon monoxide and carbon dioxide meters as well as a Model 715 oxygen meter were the specific instruments used. A vacuum type chemiluminescent meter with a heated capillary, the Thermo-Electron Model 10A was used for nitrous oxide measurements. Smoke readings were obtained with a Bosch EFAW 68A meter and a EFAW 65A/6 probe. The emissions equipment and heated line were constructed and operated according to the procedures outlined in the S.A.E. Handbook [9].

The output signals from the emissions, fuel weighing apparatus, and all of the engine temperatures were recorded by an Apple IIe computer. The cylinder and line pressure signals as well as the mass airflow signals were received by an additional Apple II Plus computer. All analog voltage signals were converted to digital signals with an Interactive Structures Corporation AI13 twelve bit A/D converter. The data in its final form was stored on 5 1/4 inch magnetic discs.

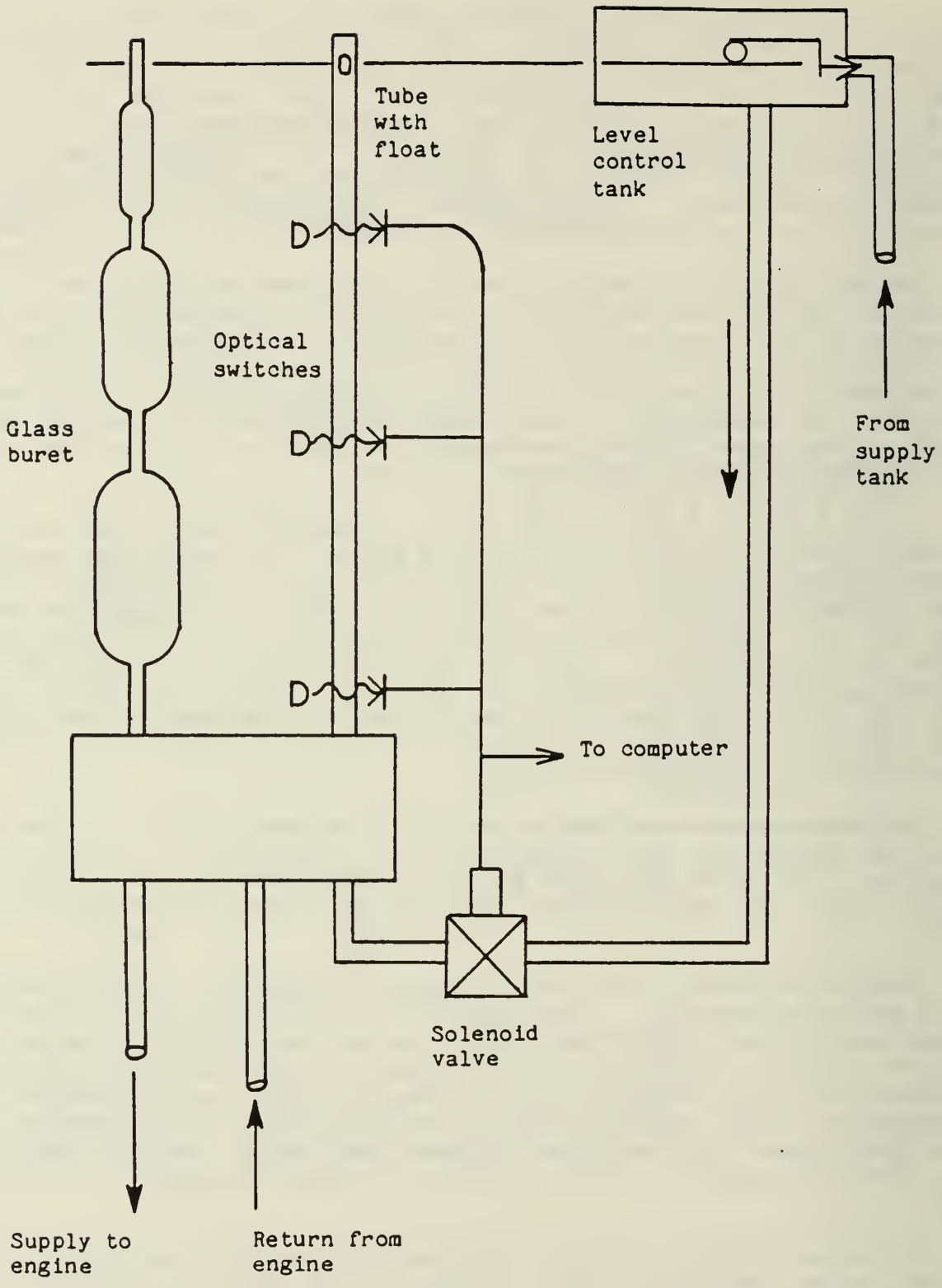

Figure 4 Computer controlled fuel measuring system.

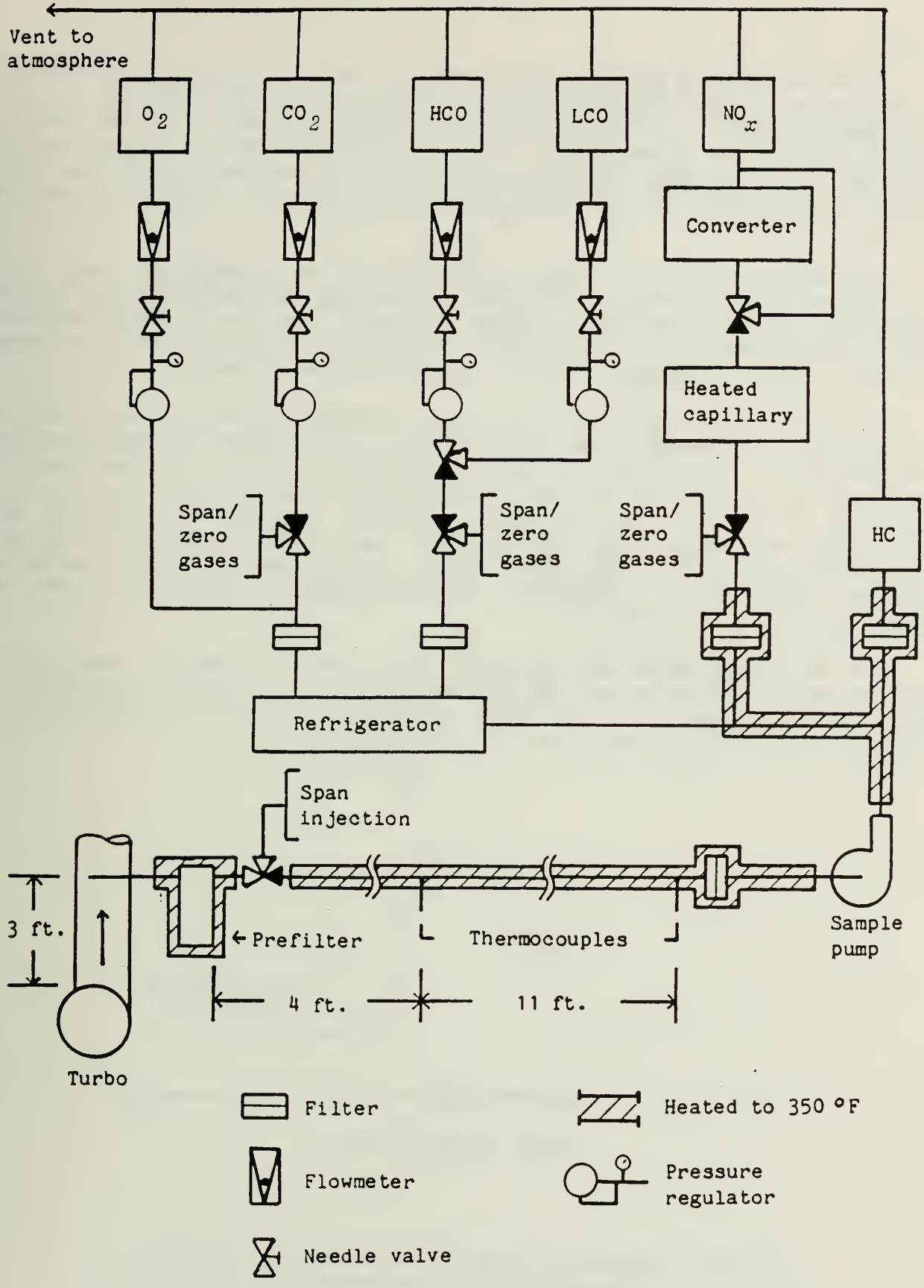

Figure 5 Exhaust gas analysis system.

Data Handling

Cylinder and line pressure data were sampled at every degree of rotation of the engine. The cylinder pressure data was taken first with 128 consecutive power cycles being sampled and then averaged together. This was used to produce one average pressure data array for each test point. Since a piezoelectric transducer measures relative pressure differences the cylinder data had to be referenced to the intake manifold pressure to produce an absolute pressure cycle.

One power cycle of the number one injection line pressure was taken after the cylinder data. Averaging several cycles was not required due to the repeatability of the mechanical injection pump. The line pressure data was used to obtain the start of injection. This occurred at the crankangle where the line pressure reached the opening pressure of the injector.

A numerical derivative of the cylinder pressure allowed the determination of the start of combustion as shown in Fig. 6. The start of combustion was the crankangle at which the derivative deviated at least 10 KPa/deg from the sinusoidal motoring curve. The difference between the start of combustion and the start of injection was the ignition delay. The cylinder pressure data quality was verified by executing a simple heat release subroutine [10], before proceeding to the next test point. The cylinder pressure transducer mounting, calibration, preparation, phasing with crankangle followed the guidelines outlined in Ref. [11].

The emissions, fuel, and air weighing as well all engine temperatures were fed into the computer and then converted to their appropriate engineering units. These values as well as other calculated values, such as thermal and volumetric efficiencies, were then stored on magnetic disc.

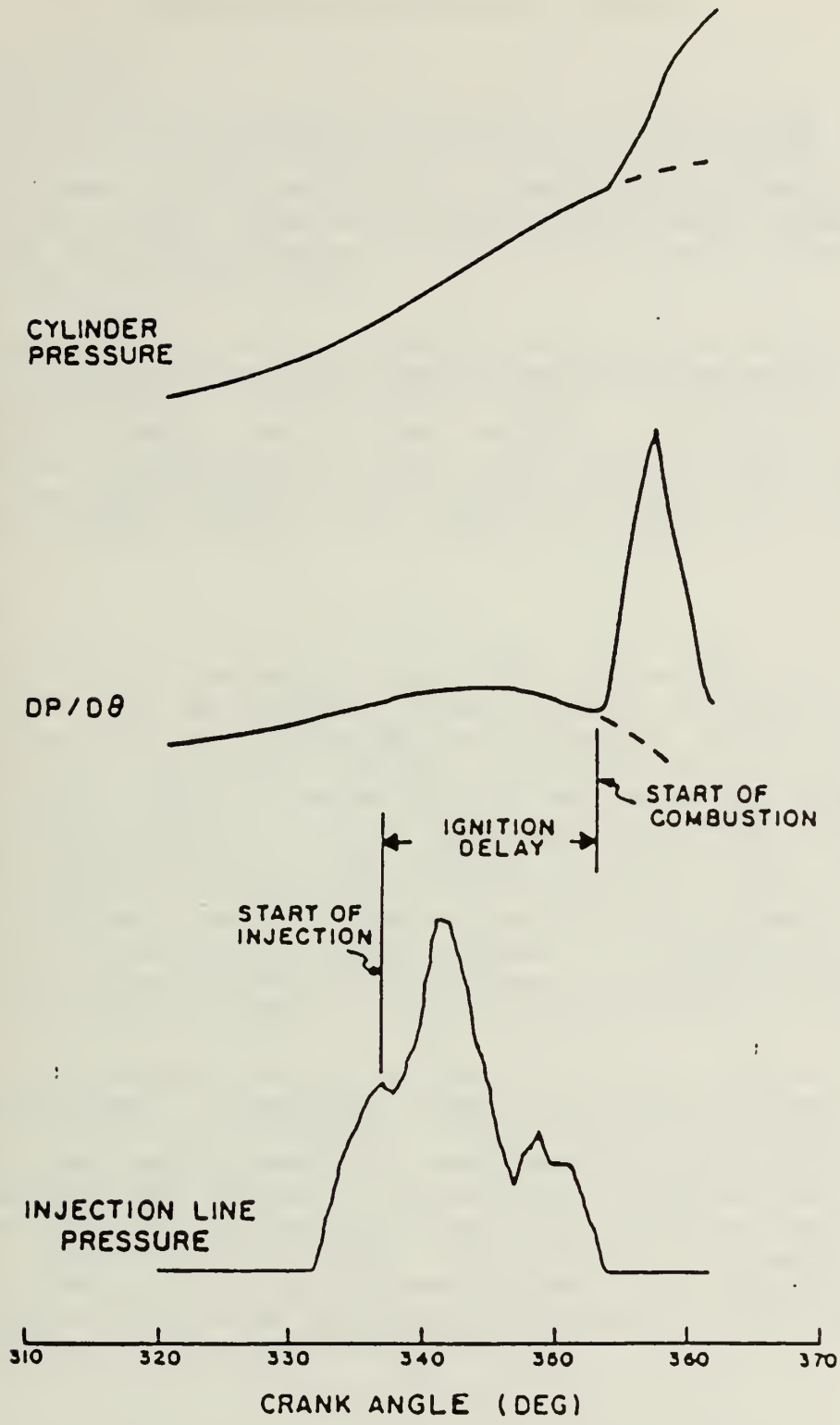

Figure 6 Representative curves of cylinder pressure, derivative of cylinder pressure and injection line pressure versus crank angle.

4. EXPERIMENTAL PROCEDURE AND SCHEDULE

Experimental Procedure

Before testing began, the emissions sample line and the smoke meter were allowed to warm up for several hours prior to starting the engine. The emissions equipment were left on continuously to reduce errors. Next the charge amplifier for the cylinder pressure transducer and all other pressure transducer amplification circuits were zeroed. Then the engine was allowed warm up until the oil was approximately 95°C.

The engine was then loaded to the test point and allowed to come to equilibrium. Equilibrium was determined by monitoring the exhaust, coolant and manifold temperatures. Data acquisition was then initiated beginning with cylinder and line pressure and the fuel weighing. Airflow and emissions followed next and a smoke sample was taken after the emissions readings were complete. After verification of the cylinder pressure data, thermal efficiency, and emissions readings, the engine was loaded to the next test point.

Test Schedule

The engine was first tested at loads of 200, 500 and 800 KPa at 2400 RPM using diesel fuel. The maximum amount of pure ethanol was then determined at these loads. The limit was found by the onset of audible knock at 500 and 800 KPa and by the onset of misfire at 200 KPa. The knock limit was determined by listening and using subjective experience to determine the maximum knock level. The misfire limit was found by observing the pressure time diagram from the number one cylinder on an oscilloscope. The flow rate of the ethanol was increased until the firing spike would occasionally disappear from the pressure time diagram. When this occurred the flow rate of the ethanol was reduced until the firing spike remained constant. This defined the misfire limit. Fractional ethanol energy flow rates were also tested at 1/4, 1/2 and 3/4 that of the maximum pure ethanol energy flow rate found at each load.

At 800 KPa the maximum energy flow rate for 175, 150, 125 and 100 proof ethanol were determined. Comparisons between the various ethanol proofs at constant energy flow rates were desired. Therefore the same energy flow rates were used with lower proof ethanol that corresponded to the 1/4, 1/2, and 3/4 flow rates used with pure ethanol. The energy flow rates were held constant while the mass flow rates varied due to the addition of the inert distilled water used to form the ethanol proofs. This procedure was repeated for 200 and 500 KPa but only with 175 and 150 proof ethanol. The injectors were not able to meet the maximum volume flow rates the engine was capable of burning with 125 and 100 proof ethanol at 200 and 500 KPa.

5. RESULTS AND DISCUSSION

The emissions data and the engine performance parameters are presented in Figs. 8 through 48 as a function of ethanol proof. This was done to clearly show the dependence of the data on ethanol proof. It is common in current literature to plot the engine parameters against the percent of energy by ethanol. This approach was not chosen in this case since the percent of energy by ethanol variable was a function of the thermal efficiency for this engine. It was not possible to hold a constant diesel flow rate to the engine with different ethanol proofs as fumigants because of the internal governor on the diesel fuel pump. Therefore at each test point the load was held constant, and the same energy flow rates of ethanol were fumigated for each proof. This meant that the governor on the fuel pump adjusted the diesel flow rate, according to the thermal efficiency to hold the load constant.

The percent by energy of ethanol is plotted versus ethanol proof in Figs. 7, 8, and 9. At the constant ethanol flow rates, 1, 2, and 3 (a flow rate of zero corresponds to pure diesel operation), the percent of energy by ethanol remains constant indicating that the thermal efficiency did not vary greatly with ethanol proof. At bmep's of 500 and 800 kPa the knock limits, however, show some variation in the percent of energy by ethanol. This can possibly be explained by the subjective nature of determining the knock limit and the fact that the proof tests were run on separate days over a period of several weeks.

In Fig. 10, at a bmep of 800 kPa, the thermal efficiency is seen to rise above the diesel level as the flow rate of ethanol is increased. This is due to the ethanol increasing the ignition delay, see Fig. 31, which allows more of the diesel fuel to vaporize. The ethanol charge, as well the larger volume of vaporized diesel fuel, results in a greater mass of fuel which is able to burn at the onset of combustion. This produces in a more constant volume combustion, rather than the extensive diffusion controlled combustion which occurs with pure diesel operation, with a consequent increase in efficiency.

This is shown in the pressure crankangle diagrams in Figs. 13 through 16 at a bmep of 800 kPa. Each figure is at a different flow rate, and each has a curve of diesel, pure ethanol, and 100 proof ethanol. In Fig. 16, the lowest ethanol flow rate, the ethanol pressure curves are essentially the same as the diesel pressure trace. Figure 14, a flow rate of three, indicates that combustion with ethanol starts later, closer to TDC, and occurs for a narrower region around TDC. This more closely approximates constant volume combustion which results in a higher thermal efficiency.

In Fig. 10 there was a slight increase, 2.4 percent at a flow rate of three, in thermal efficiency as the ethanol proof was lowered. The inert water in the lower proofs produces a more gradual pressure rise during the initial phase of combustion. This is shown in Figs. 14 and 15. The pure ethanol produced a large pressure rise well before TDC while the 100 proof ethanol produced a more gradual pressure rise around TDC. Therefore the 100 proof ethanol would do less work against the compression stroke and this should raise the thermal efficiency slightly over that of pure ethanol.

Figure 11 shows the behavior of the thermal efficiency with varying proofs and ethanol energy flow rates at a bmep of 500 kPa. The thermal ef-

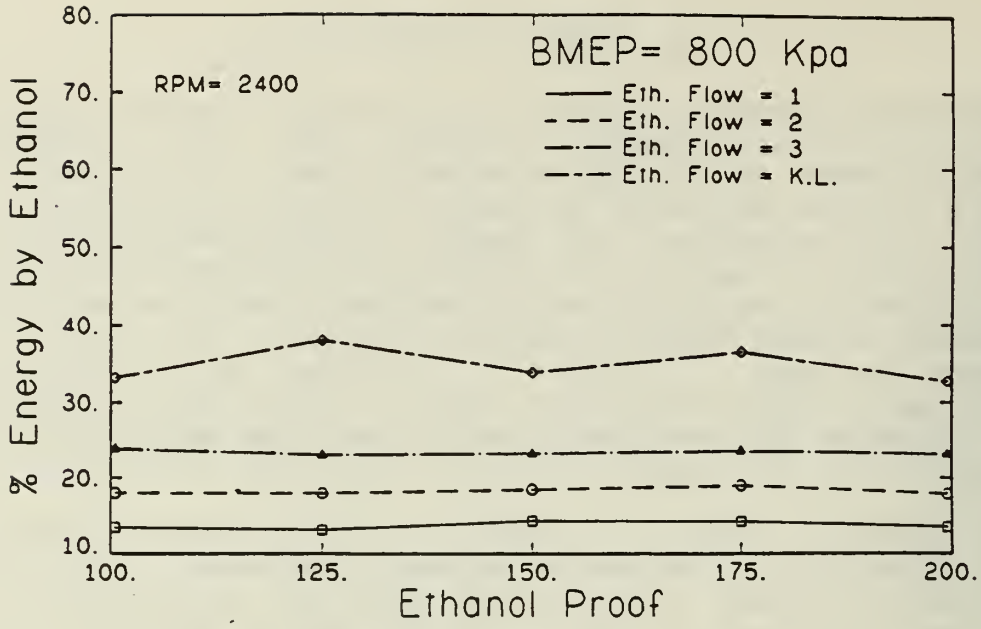

Figure 7 Percent energy of ethanol at a bmep of 800 kPa.

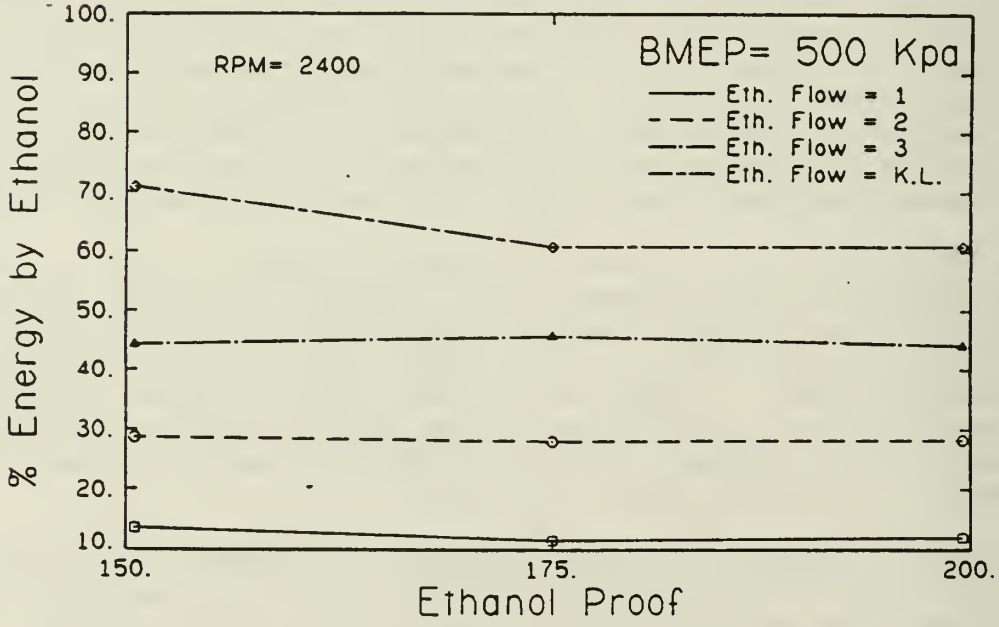

Figure 8 Percent energy of ethanol at a bmep of 500 kPa.

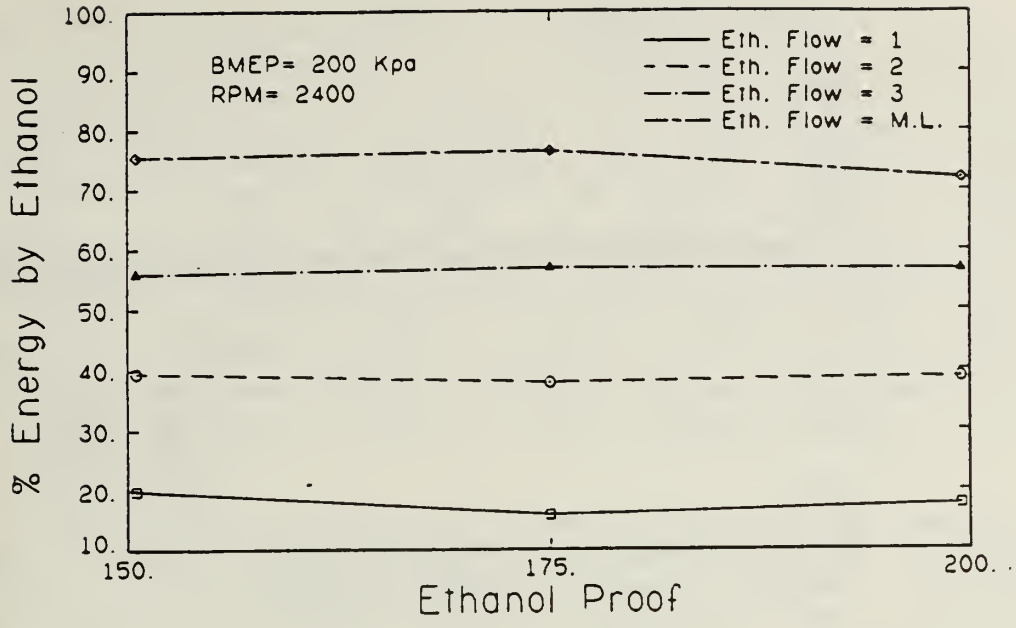

Figure 9 Percent energy of ethanol at a bmep of 200 kPa.

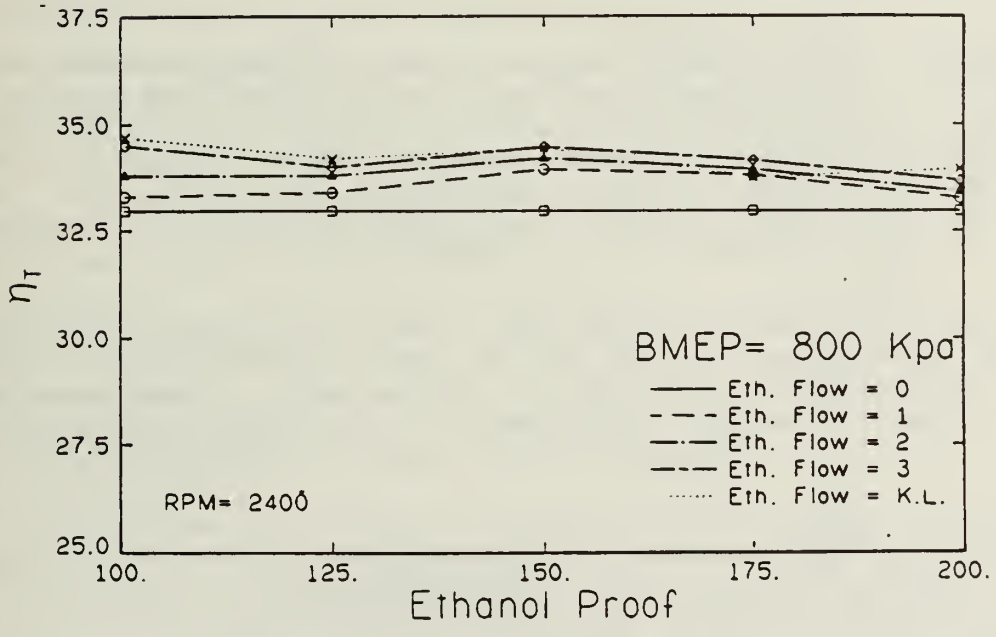

Figure 10 Thermal efficiency at a bmep of 800 kPa.

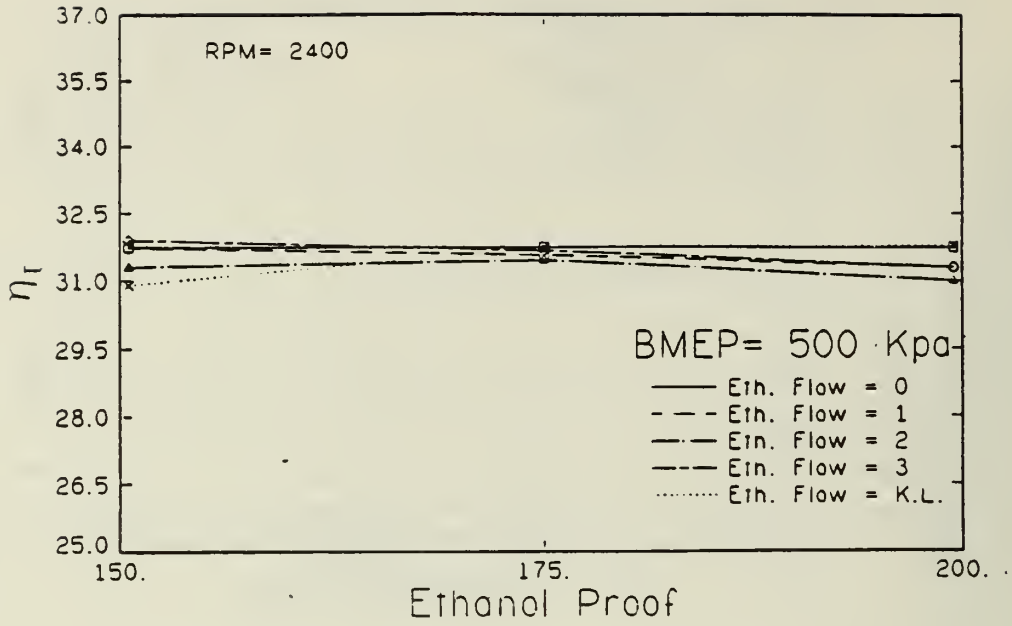

Figure 11 Thermal efficiency at a bmep of 500 kPa.

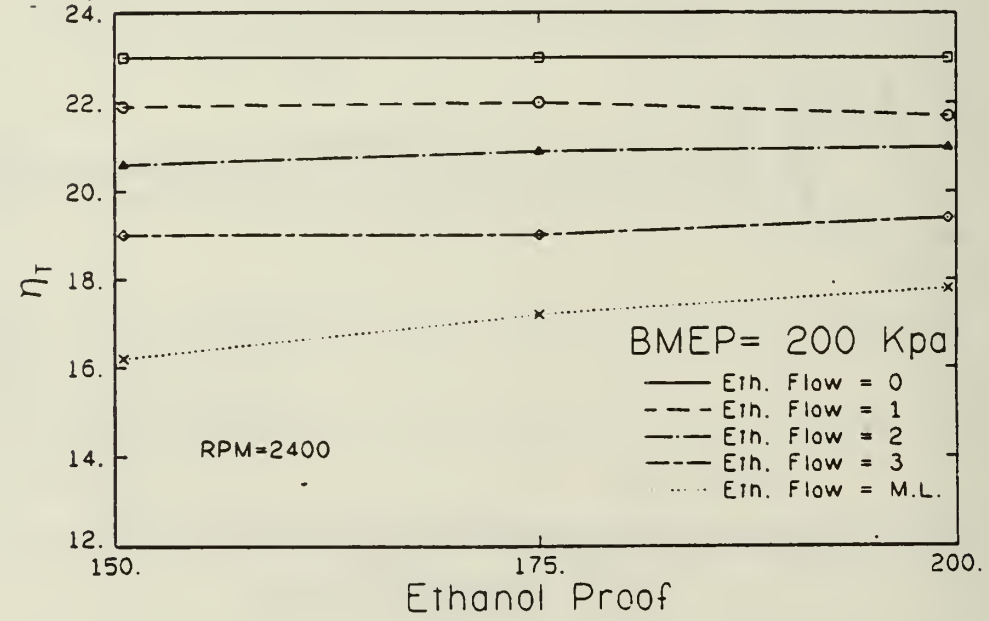

Figure 12 Thermal efficiency at a bmep of 200 kPa.

ficiency remained relatively constant with increasing ethanol flow rate at this load. It initially decreased slightly as the flow rate of ethanol was increased. The smaller ethanol flow rates of 1 and 2 do not significantly increase the ignition delay, see Fig. 32, which would lead to a more constant volume combustion. At these low flow rates, a very lean mixture of ethanol and air is inducted into the cylinder and it is doubtful that this mixture burns efficiently. At higher flow rates, the thermal efficiency increased slightly. At these flow rates, the mixture is richer and the ethanol should burn more efficiently; however, the ignition delay has pushed the start of combustion into the expansion stroke. This is shown in the pressure crankangle plots in Figs. 17 through 20. This offsets some of the gains in thermal efficiency from the richer mixture and more constant volume combustion. There was no indication of any dependency between thermal efficiency and ethanol proof.

Figure 12 shows thermal efficiency at a bmep of 200 kPa. The thermal efficiency dropped slightly, 2 percent at flow rates of 2 and 3, as ethanol proof was lowered. Also as the flow rate of ethanol increased, the thermal efficiency decreased from the diesel level. At the misfire limit, the thermal efficiency decreased 22 to 30 percent from the diesel level. The ignition delay increased with increasing flow rate as shown in the pressure crankangle diagrams in Figs. 21 through 24. The long ignition delay caused combustion to start after TDC at the misfire limit as well as at a flow rate of three. This does not allow the maximum amount of work to be extracted from the cycle and results in a decrease in the thermal efficiency. The slightly lower efficiencies with lower proofs are due to the presence of water which increased the ignition delay.

Figure 25 shows the maximum rate of pressure rise at a bmep of 800 kPa. The rate of pressure rise increased from the diesel level, 1.8 to 3.3 times at the knock limit and 1.6 to 1.9 times at a flow rate of three, as the flow rate of ethanol was increased. This is expected since the ethanol increases the ignition delay. As a result there should be a larger volume of fuel which is available to burn at the start of combustion. This was shown in the pressure crankangle plots and accounts for the larger rates of pressure rise.

At constant flow rates of 2 and 3, the rate of pressure rise decreased from the diesel levels, 11.1 percent and 6.5 percent respectively, as the ethanol proof was lowered. The addition of the inert water acts to lower flame temperature and, therefore, the combustion rate which results in a reduction in the maximum rate of pressure rise.

Figure 26 is the maximum rate of pressure rise at a bmep of 500 kPa. With increasing ethanol flow rate, the rate of pressure rise increased to a maximum at a flow rate of 2 and then decreased with a further increase in flow rate. At ethanol flow rates greater than 2, the start of combustion was at TDC or later as shown in the pressure crankangle plots in Figs. 17 and 18. This accounts for the lower rates of pressure rise at these flow rates since combustion during the expansion stroke will lower the rate of pressure rise. The maximum rate of pressure rise did not vary at this load as the ethanol proof was lowered, except at the knock limit where the rate of pressure rise decreased as the proof was lowered. Figure 8 shows, however, that there was a larger flow rate with the lower proofs at the knock limit. This, instead of the lower proof, probably accounts for the decrease in the rate of pressure rise.

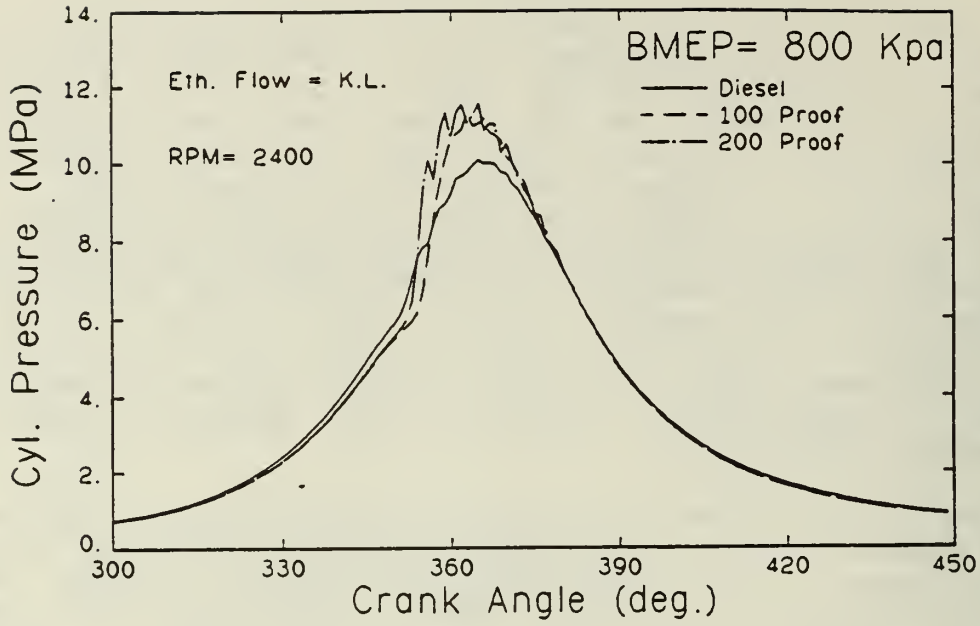

Figure 13 Cylinder pressure versus crankangle at the knock limit for a bmep of 800 kPa.

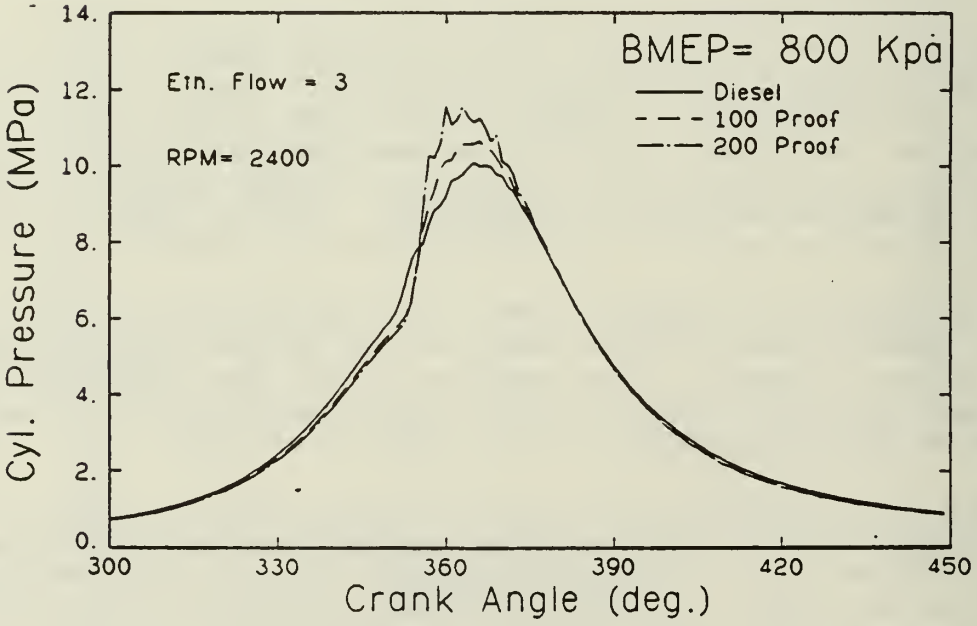

Figure 14 Cylinder pressure versus crankangle at a flow rate of 3 for a bmep of 800 kPa.

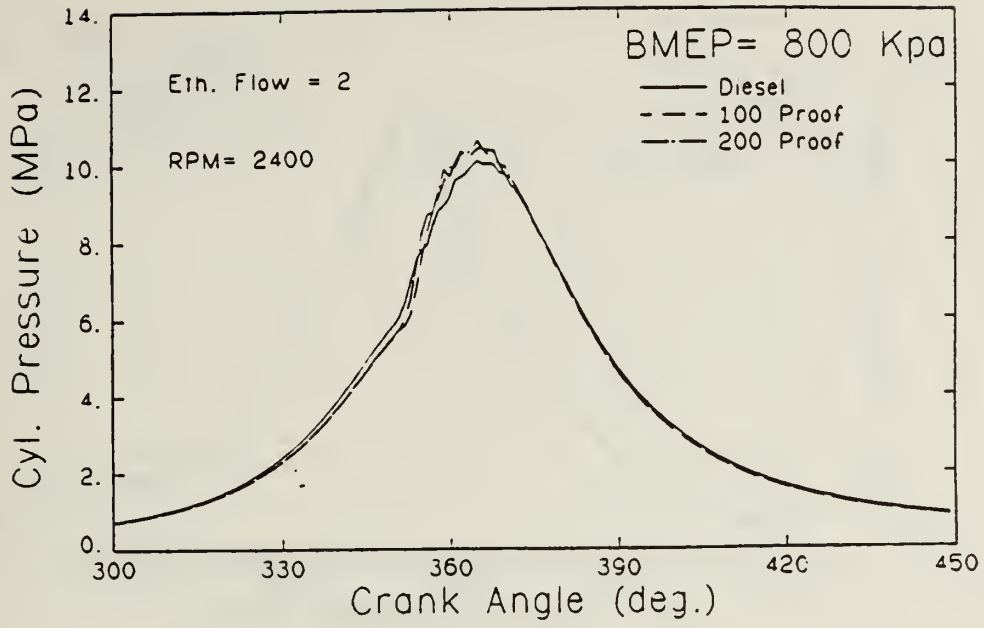

Figure 15 Cylinder pressure versus crankangle at a flow rate of 2 for a bmep of 800 kPa.

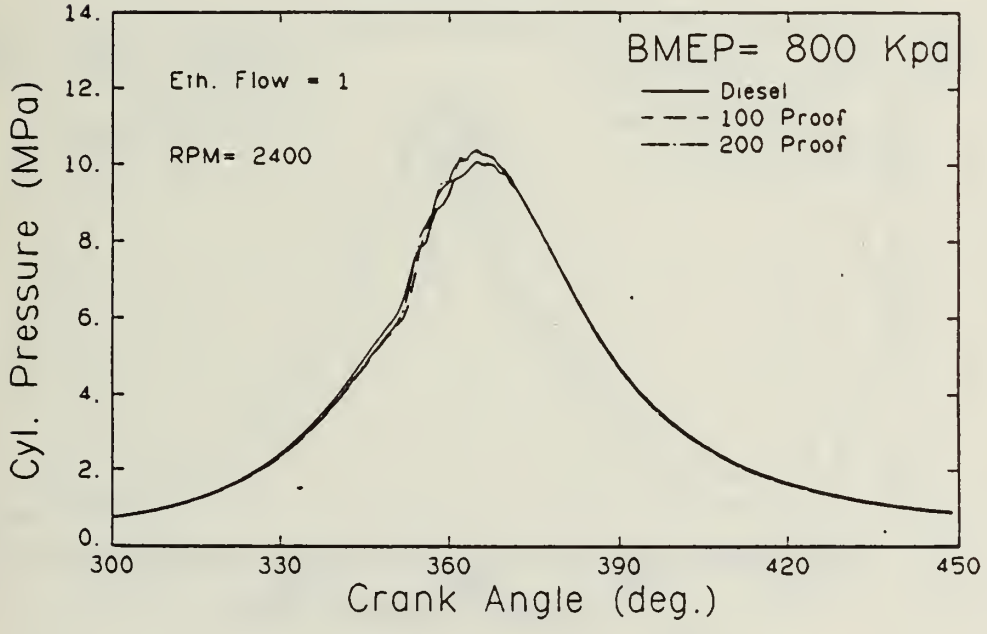

Figure 16 Cylinder pressure versus crankangle at a flow rate of 1 for a bmep of 800 kPa.

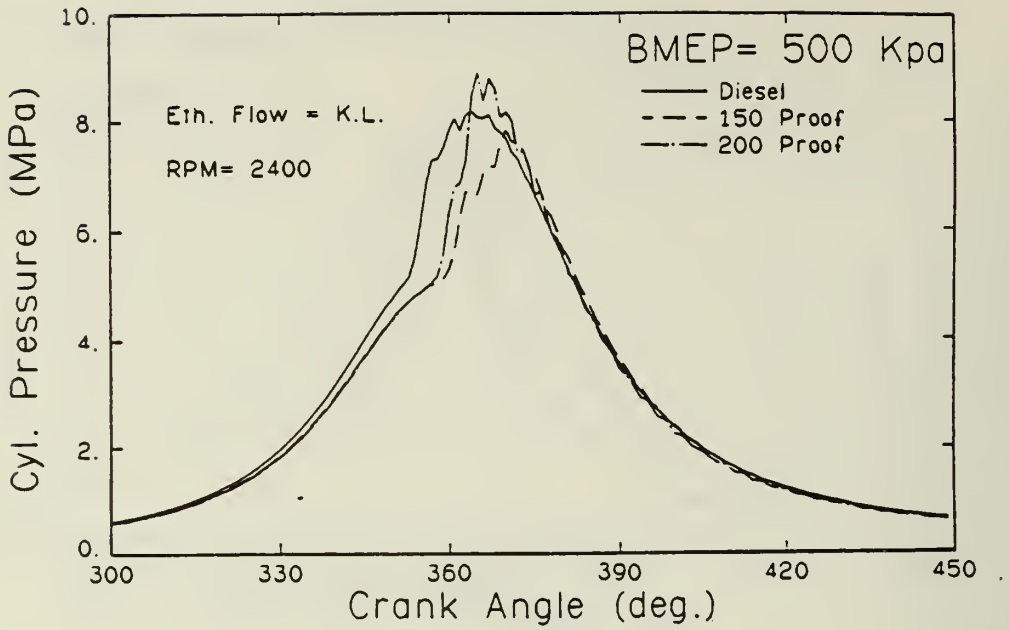

Figure 17 Cylinder pressure versus crankangle at the knock limit for a bmep of 500 kPa.

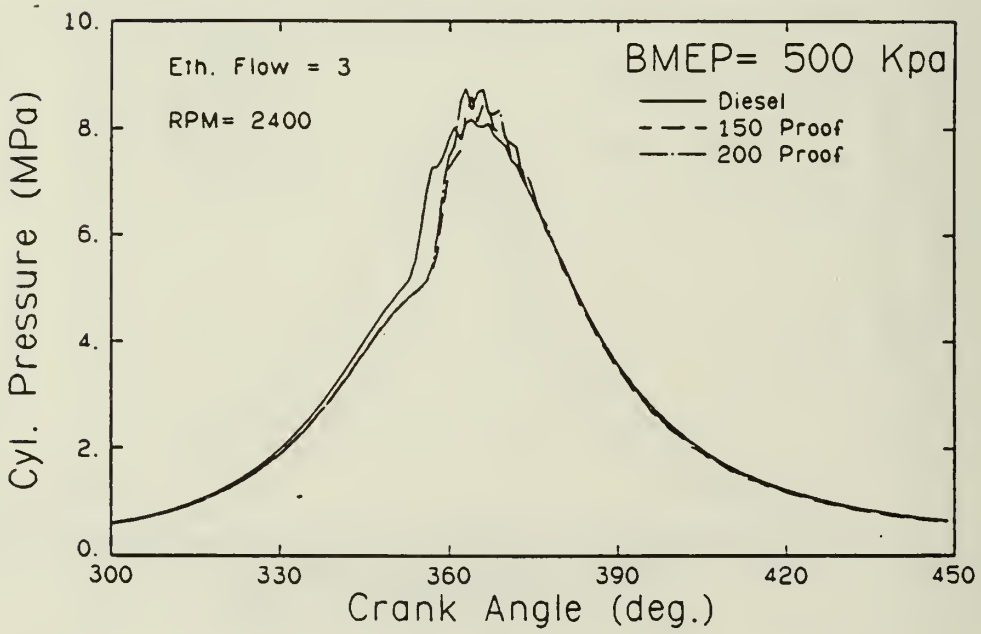

Figure 18 Cylinder pressure versus crankangle at a flow rate of 3 for a bmep of 500 kPa.

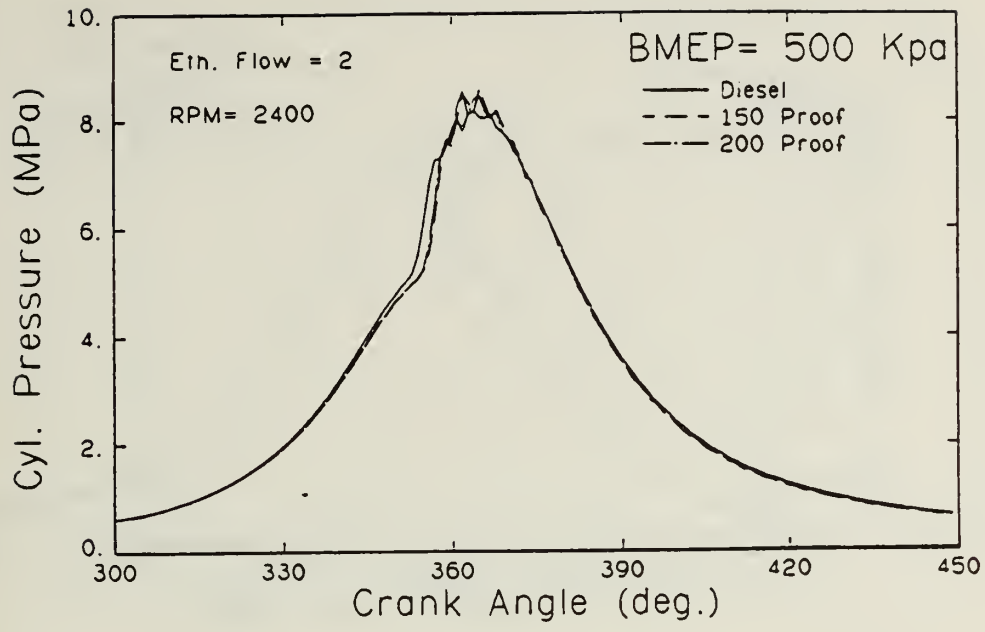

Figure 19 Cylinder pressure versus crankangle at a flow rate of 2 for a bmep of 500 kPa.

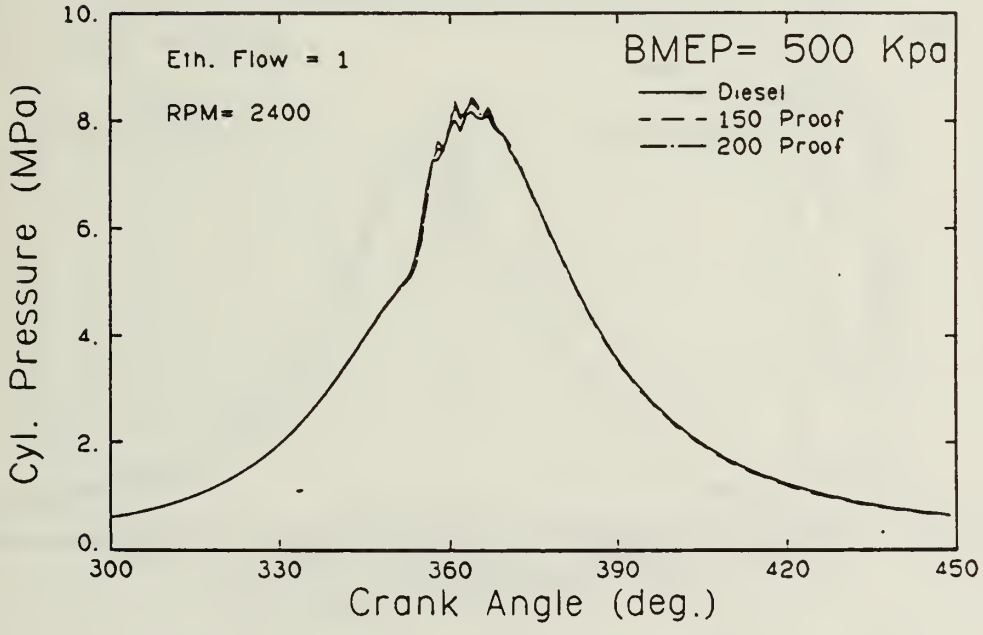

Figure 20 Cylinder pressure versus crankangle at a flow rate of 1 for a bmep of 500 kPa.

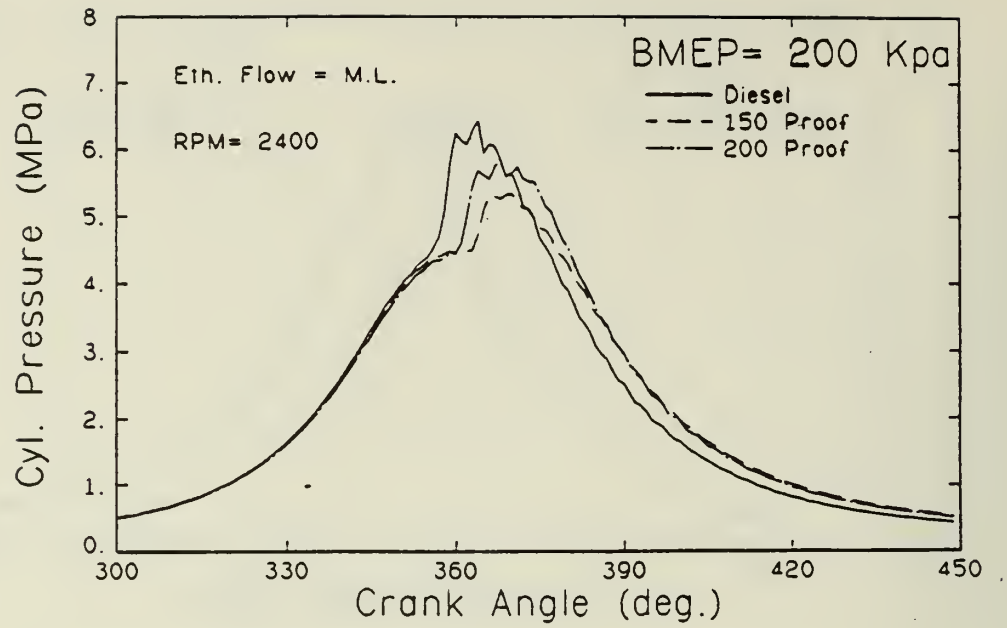

Figure 21 Cylinder pressure versus crankangle at the misfire limit for a bmep of 200 kPa.

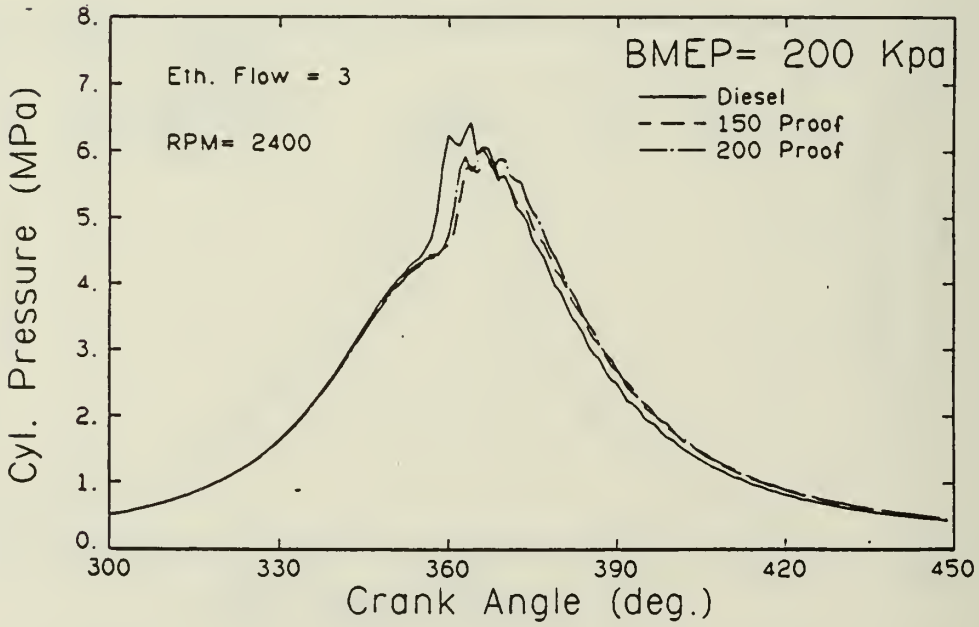

Figure 22 Cylinder pressure versus crankangle at a flow rate of 3 for a bmep of 200 kPa.

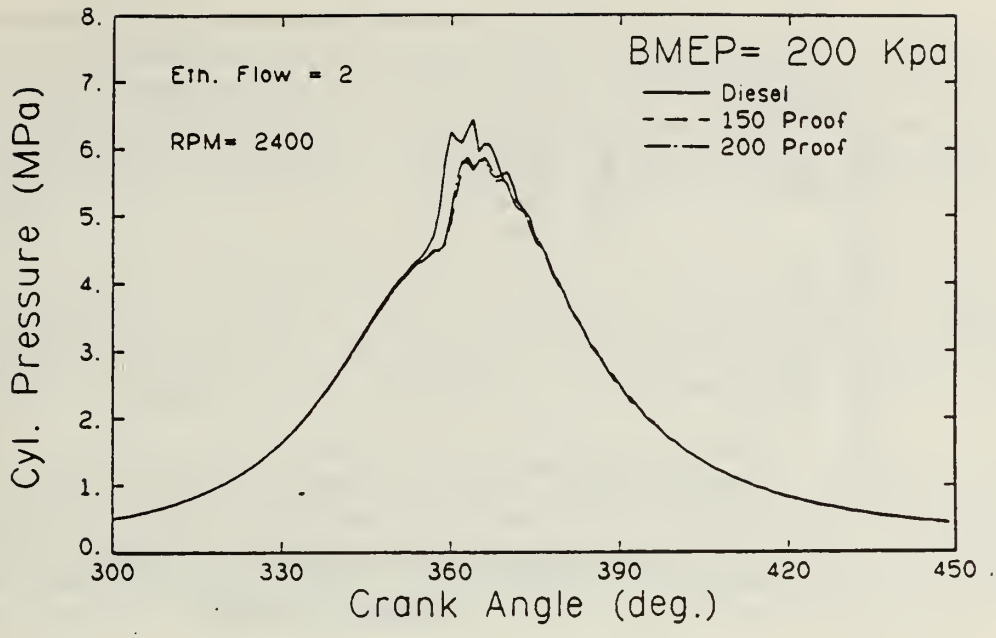

Figure 23 Cylinder pressure versus crankangle at a flow rate of 2 for a bmep of 200 kPa.

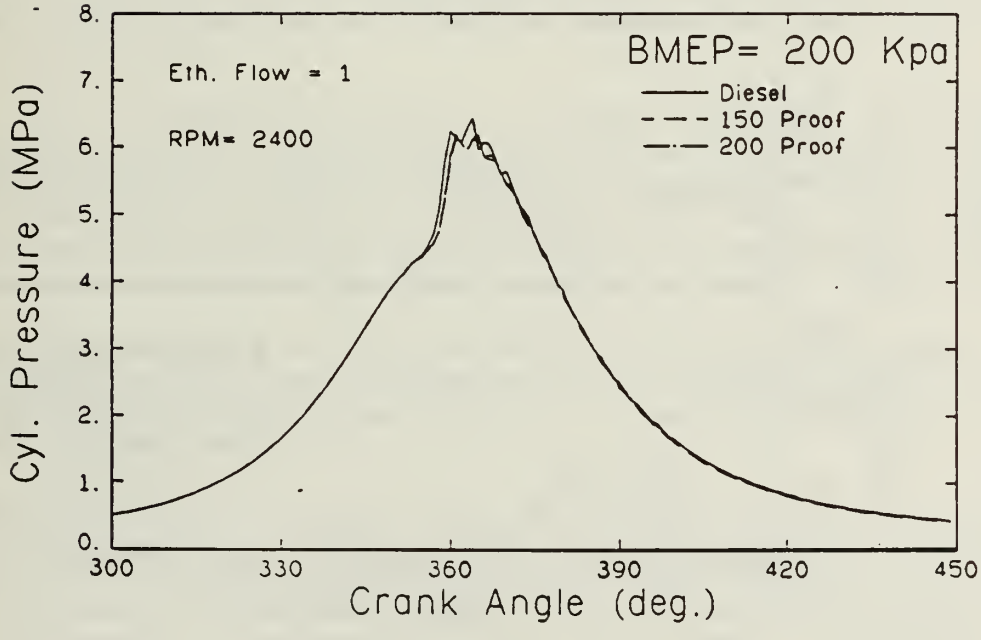

Figure 24 Cylinder pressure versus crankangle at a flow rate of 1 for a bmep of 200 kPa.

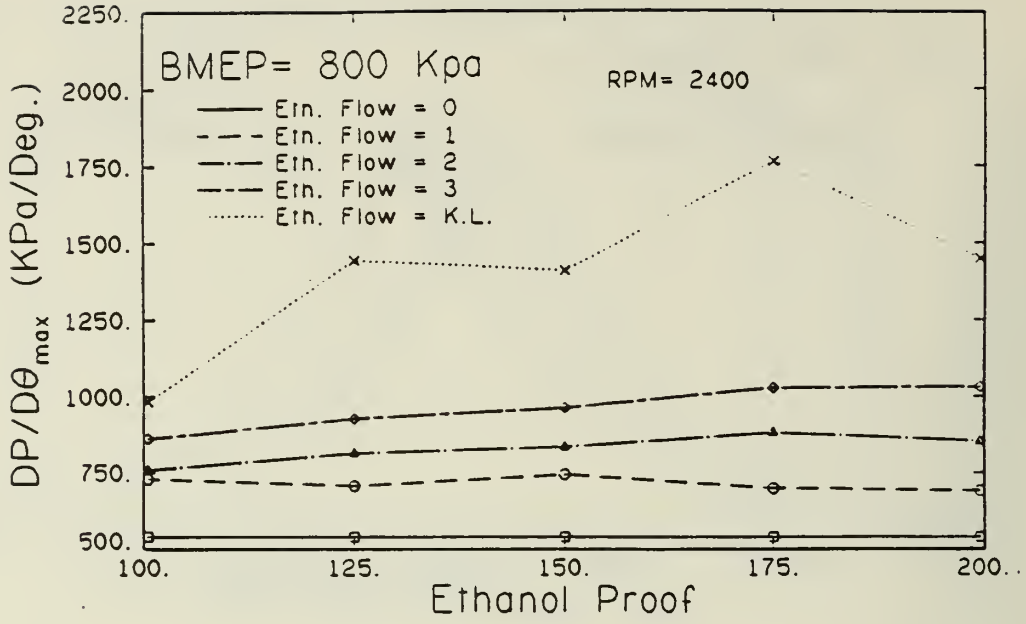

Figure 25 Maximum rate of pressure rise at a bmep of 800 kPa.

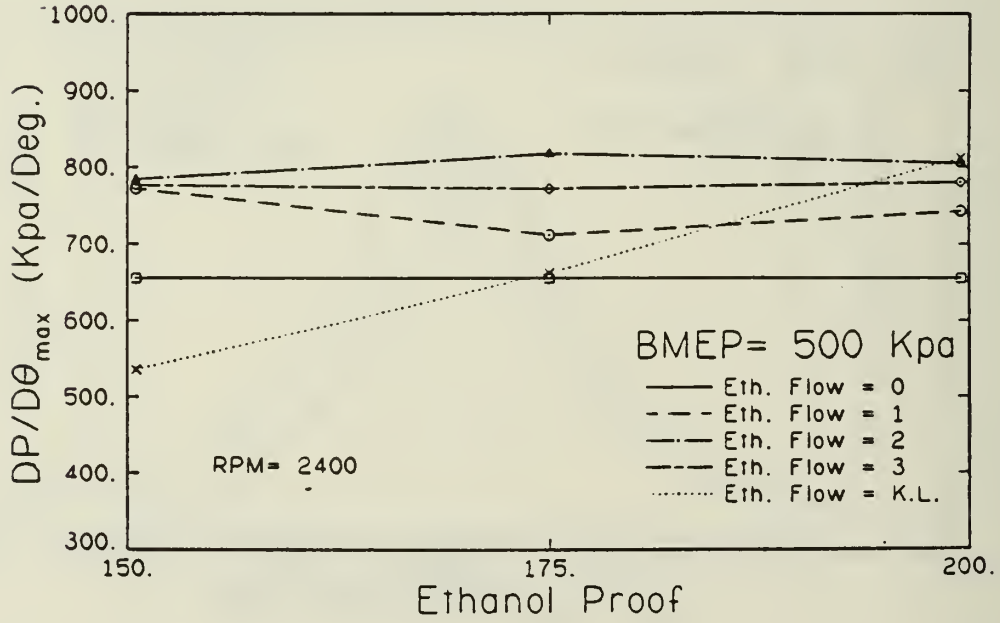

Figure 26 Maximum rate of pressure rise at a bmep of 500 kPa.

Figure 27 is the maximum rate of pressure rise at a bmep of 200 kPa. The maximum rate of pressure rise dropped from the diesel level, 28 to 48 percent at the misfire limit, and 14 to 22 percent at a flow rate of three, as the flow rate of ethanol was increased. The rate of pressure rise decreased, 5.9 percent at a flow rate of three and 2.8 percent at a flow rate of two, as the proof was lowered.

The longer ignition delay, see Fig. 33, with ethanol fumigation pushed the start of combustion past TDC. This is shown in the pressure crankangle diagrams in Figs. 21 through 24. This causes very low rates of pressure rise which were further reduced by the presence of the inert water in the lower proof ethanols.

Figure 28 shows the peak pressure during the cycle at at a bmep of 800 kPa. The maximum pressure increased from the diesel level, 12 to 20 percent at the knock limit and 5.5 to 8.3 percent at a flow rate of three, as the flow rate of ethanol was increased. The longer ignition delay resulted in more constant volume combustion which, in turn, causes a higher peak pressure.

Lower proof ethanol produced slightly lower peak pressures. They dropped, 2.5 percent at a flow rate of three and 2 percent at a flow rate of two, as the proof was lowered. The lower proofs had a longer ignition delay and since the start of combustion was always before TDC as shown in the pressure crankangle diagrams, it might be expected that the peak pressure would increase with lower proofs for the above reasons. The presence of the inert water, however, should lower the flame temperatures and the combustion rates and therefore the peak pressure. This is substantiated by the exhaust temperature plot, Fig. 34.

Figure 29 is the maximum pressure at a bmep of 500 kpa. The maximum pressure increased from the diesel level, 5.4 to 8 percent at a flow rate of three, as the flow rate of ethanol increased. The peak pressure decreased greatly with lower proof ethanol at the knock limit, however, as shown in Fig. 8 the flow rate increased with lower proofs at the knock limit. The peak pressure was not dependent upon the ethanol proof at a constant flow rate.

At lower flow rates the maximum pressure is increased due to more constant volume combustion of a larger volume of fuel. At high and knock limited flow rates, the ignition delay pushes the start of combustion past TDC, reducing the increase in peak pressures.

The maximum pressure at a bmep of 200 kPa is shown in Fig. 30. The maximum pressure decreased from the diesel level, 10 to 18 percent at the misfire limit and 5.8 to 9.3 percent at a flow rate of three, as the flow rate of ethanol was increased to its maximum level. As the proof was lowered, the peak pressure decreased 3.7 percent at a flow rate of three. The addition of the ethanol increased the ignition delay, see Fig. 33, and at ethanol flow rates of 2 or greater combustion started at or after TDC, this reduced the maximum cylinder pressure. The inert water in the lower proof ethanol reduces the combustion temperatures and combustion rates which will lower the peak pressure during the cycle.

Ignition delay at a bmep of 800 kPa is shown in Fig. 31. As the flow rate of ethanol was increased, the ignition delay increased slightly from the

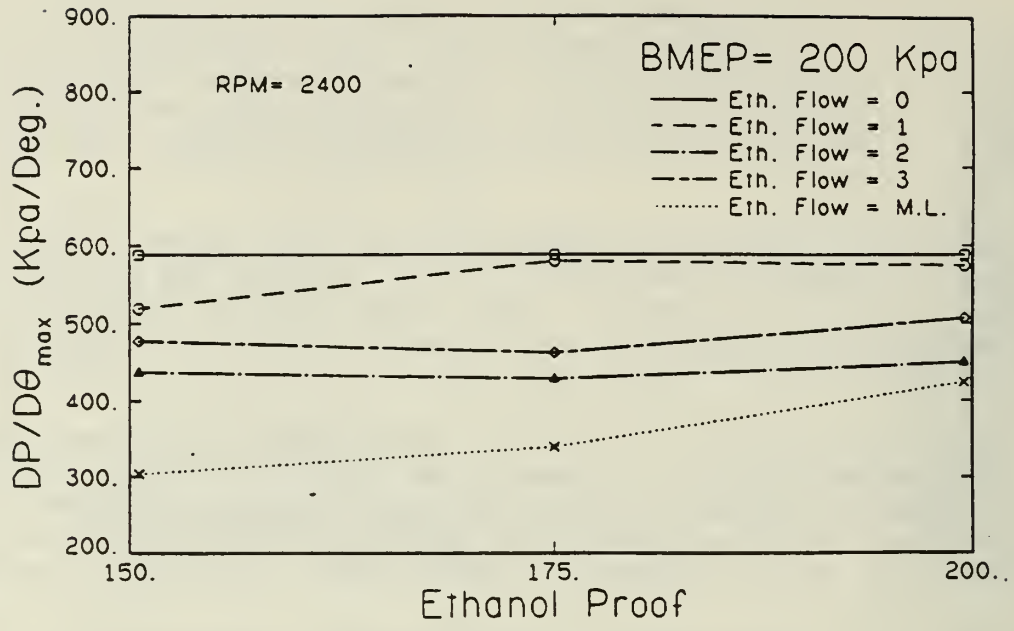

Figure 27 Maximum rate of pressure rise at a bmep of 200 kPa.

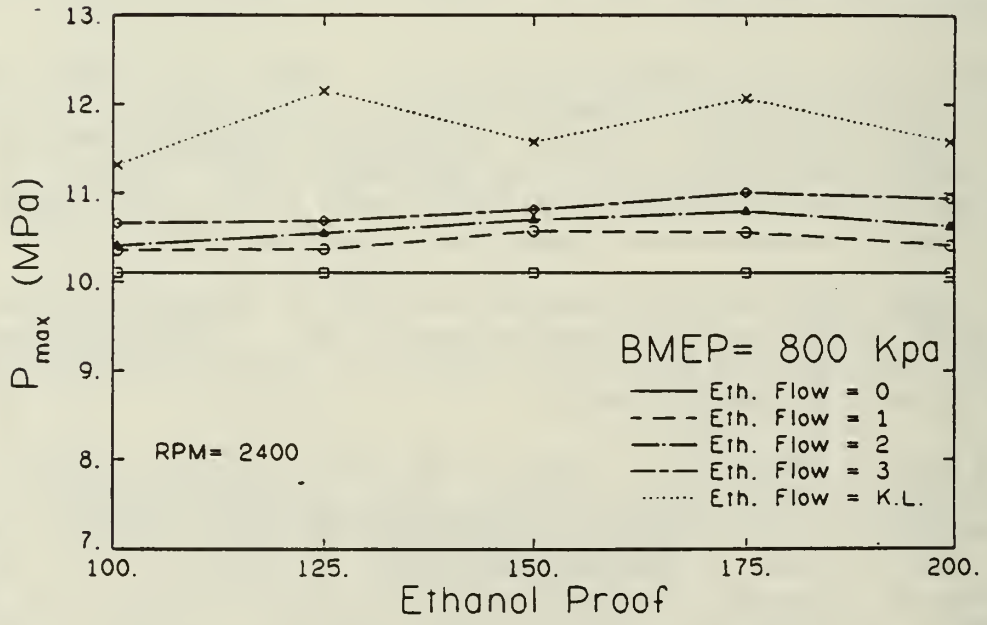

Figure 28 Maximum cylinder pressure at a bmep of 800 kPa.

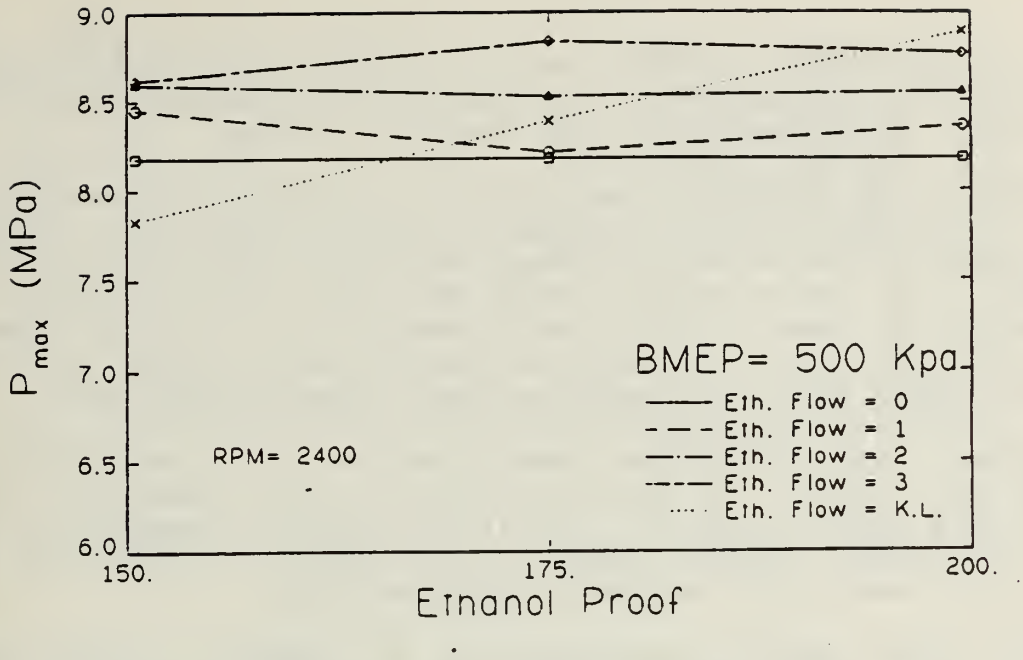

Figure 29 Maximum cylinder pressure at a bmep of 500 kPa.

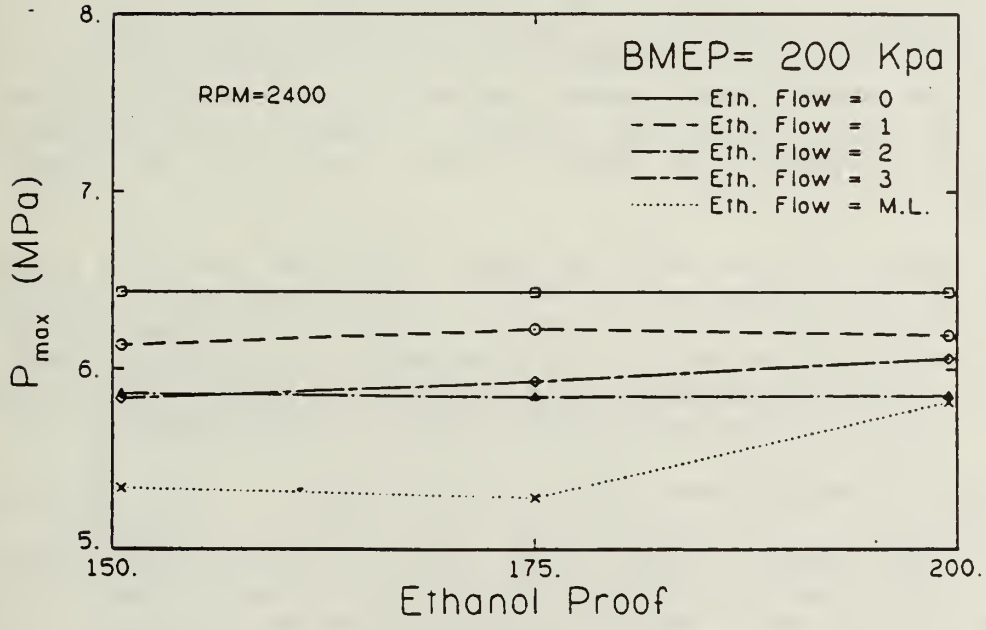

Figure 30 Maximum cylinder pressure at a bmep of 200 kPa.

diesel level, particularly at the lower proofs. The ignition delay is increased due to the addition of the ethanol in the intake air which lowers the temperature and pressure during the compression stroke.

Ethanol has a specific heat ratio of 1.12 while air has a specific heat ratio of 1.4 when both are evaluated at standard conditions. The addition of the ethanol to the intake air lowers the overall specific heat ratio of the mixture. The smaller specific heat ratio for the mixture will lower the temperature and pressure at the end of compression. Steam has a specific heat ratio of 1.327 which is close to the specific heat ratio of air, and the addition of water should not lower the overall specific heat ratio.

Ethanol has a low cetane number compared with diesel fuel. When the diesel fuel diffuses into the ethanol and air, the properties of the mixture become an average of the two fuels (Kanury [12]). Therefore, as ethanol is added, the overall cetane number of the mixture will drop from the diesel level; this should also increase the ignition delay.

The latent heat of vaporization of the ethanol is often claimed as a major cause of the increase in the ignition delay in current literature. It should lower the temperature of the air and ethanol charge but, as shown in Figs. 13 to 24, the cylinder pressure diagrams, the 100 proof ethanol follows the same compression pressure trace as pure ethanol. 100 proof ethanol has equal volumes of water and ethanol, but there is 1.3 times the mass of water. Water has a latent heat of vaporization of 2260 kJ/kg while ethanol has a latent heat of vaporization of 846 kJ/kg. This means that almost 3.5 times the energy is required to vaporize the additional water. If the latent heat of vaporization plays an important role in increasing the ignition delay, the 100 proof ethanol should have a markedly different compression trace than the pure ethanol. Since they do not, it leads to the conclusion that the latent heat of vaporization does not play a large role in increasing the ignition delay.

The longer ignition delay at lower proofs can partially be explained by the fact that the presence of a inert, in this case water, in a fuel mixture acts to narrow the flammability limits. Therefore the major causes of the increase in the ignition delay are the decrease in the specific heat ratio, the lowering of the mixtures cetane number, the inert water, and to a small extent the latent heat of vaporization of the ethanol and the water.

Figures 32 and 33 show ignition delay at bmep's of 500 and 200 kPa. With increasing ethanol flow rate, the ignition delay was increased. This is due to the lower specific heat ratio, and the lower cetane number of the ethanol. There was no discernible effect of lower ethanol proofs on the ignition delay at these loads for constant ethanol flow rates. At the knock and misfire limits, however, the ignition delay increased at the lower proofs. This is probably due to the larger flow rate which was possible with 150 proof ethanol at these limits as shown in Figs. 8 and 9.

The exhaust temperature as a bmep of 800 kPa is shown in Fig. 34. As the ethanol energy flow rate was increased to the knock limit, the exhaust temperature was lowered. At high loads in a diesel engine, a major portion of the fuel is burned after TDC in a diffusion controlled process. This produces high exhaust temperatures as a result of combustion late in the expansion

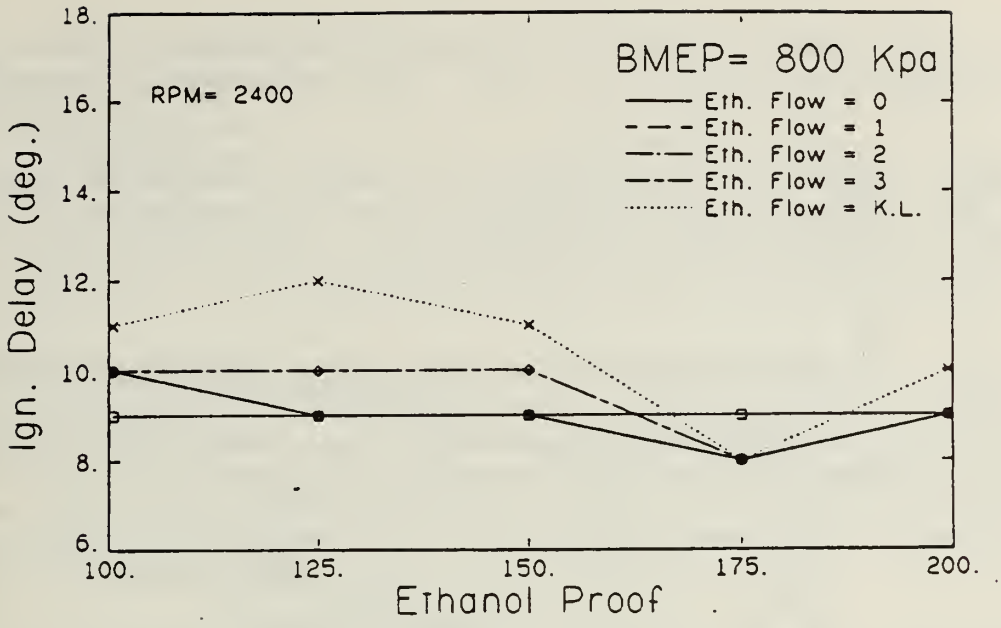

Figure 31 Ignition delay at a bmep of 800 kPa.

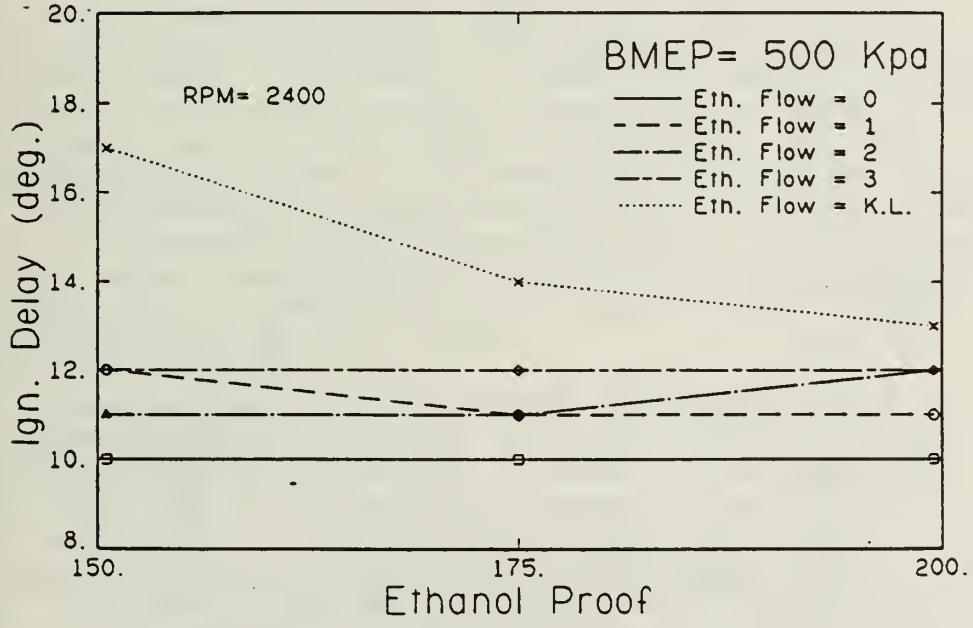

Figure 32 Ignition delay at a bmep of 500 kPa.

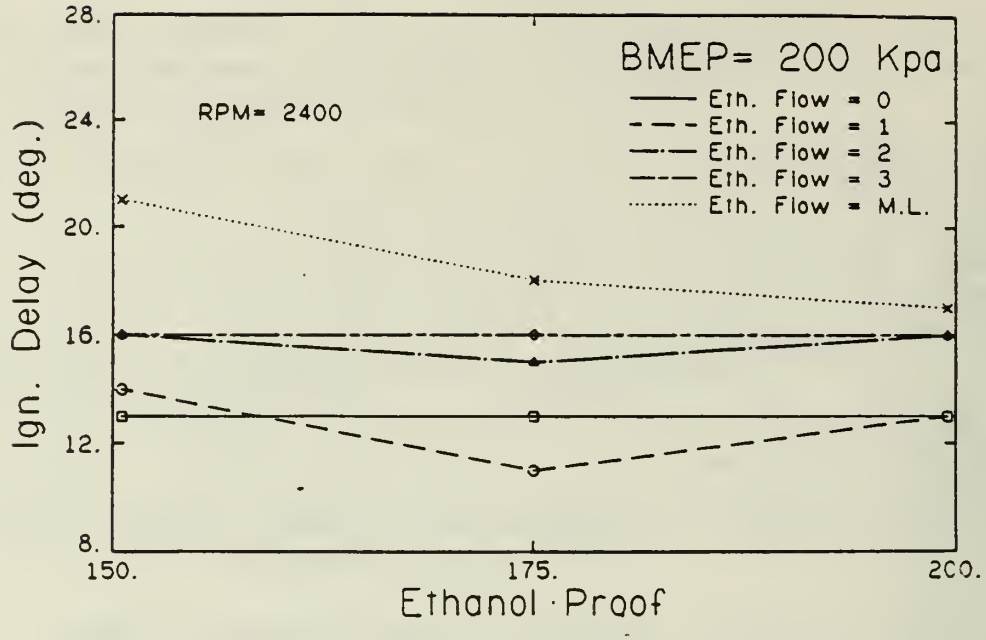

Figure 33 Ignition delay at a bmep of 200 kPa.

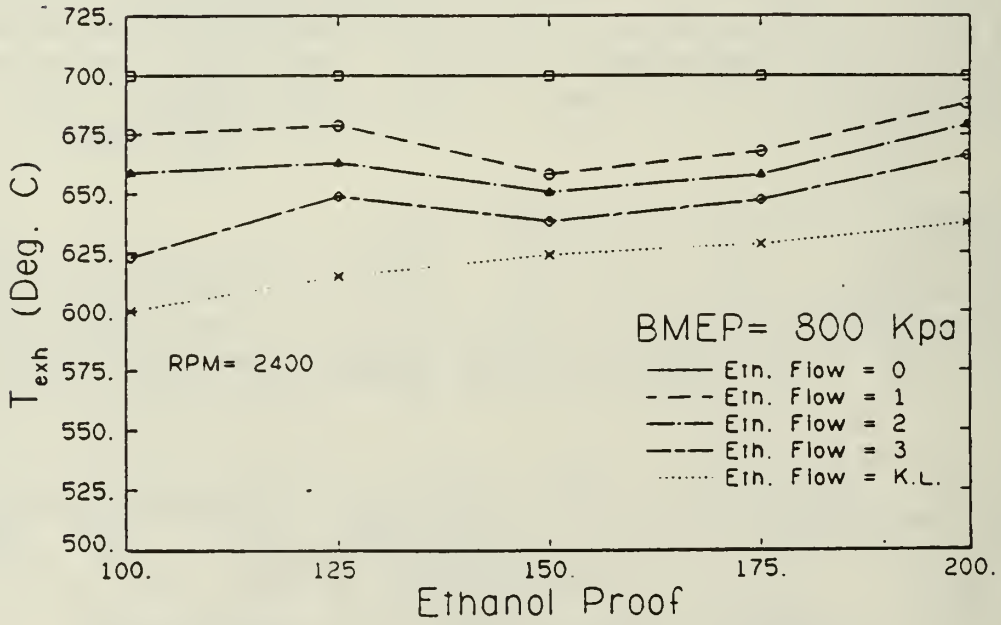

Figure 34 Exhaust temperature at a bmep of 800 kPa.

stroke. As ethanol is added there is more constant volume combustion. This reduces the amount of fuel which burns later in the cycle and therefore drops the exhaust temperature.

The exhaust temperature dropped, 6.5 percent at a flow rate of three and 2 percent at a flow rate of two, as the ethanol proof was lowered. The inert water in the lower proof ethanol lowers the maximum flame temperature and this will lower the temperatures throughout the rest of the cycle including the exhaust temperature.

Exhaust temperature at a bmep of 500 kPa is shown in Fig. 35. The exhaust temperature dropped from the diesel level, 12 to 16 percent at the knock limit and 4.2 to 7.5 percent at a flow rate of three, as the flow rate of ethanol was increased. Lower proof ethanol reduced exhaust temperatures at a constant flow rate. The long ignition delay causes less diffusion burning, lowering the exhaust temperature. The lower temperatures with reduced proofs are a result of the inert water.

Figure 36 shows exhaust temperature at a bmep of 200 kPa. The exhaust temperature dropped from the diesel level, 6.9 to 8.6 percent at the misfire limit and 4.2 to 7.5 percent at a flow rate of three, as the flow rate of ethanol was increased. This load had the smallest change of all the loads tested.

At low loads in a high swirl direct injection diesel, a small amount of diesel fuel is injected each cycle; therefore, the majority of the fuel diffuses and forms a premixed charge. This burns initially near TDC. This reduces the burning late in the cycle and the exhaust temperature drops at low loads in a diesel engine. As ethanol is added, the amount of diesel fuel injected is reduced and there should be essentially a premixed charge of diesel fuel, ethanol, and air at the start of combustion. This should roughly correspond to the same conditions that were present at the start of combustion under pure diesel operation; however, the addition of the ethanol has increased the ignition delay. This pushes the start of combustion past TDC. This will lower the peak temperature during the cycle which, therefore, lowers the exhaust temperature. Lower proof ethanol caused a slight reduction in the exhaust temperature due to the inert water.

Nitrous oxide emissions at a bmep of 800 kPa are shown in Fig. 37. At 150 proof ethanol, there was no change in the NO emissions from the diesel level as the flow rate of ethanol was increased to the knock limit. With proofs greater than 150, the NO emissions increased from the diesel level, 0 to 17 percent at the knock limit and 0 to 8.6 percent at a flow rate of three, as the flow rate of ethanol was increased. The largest increases came with pure ethanol. With proofs lower than 150, the NO emissions decreased from the diesel level, 0 to 30 percent at the knock limit and 0 to 23 percent at a flow rate of three, as the flow rate of ethanol was increased. The largest decreases were with 100 proof ethanol.

With ethanol fumigation the ignition delay leads to more constant volume combustion. This produces higher peak pressures and temperatures. NO levels are strongly dependent on the peak temperature. A larger peak temperature yields greater NO levels. Also the addition of the ethanol will reduce the amount of diffusion burning of the diesel fuel late in the cycle. Therefore

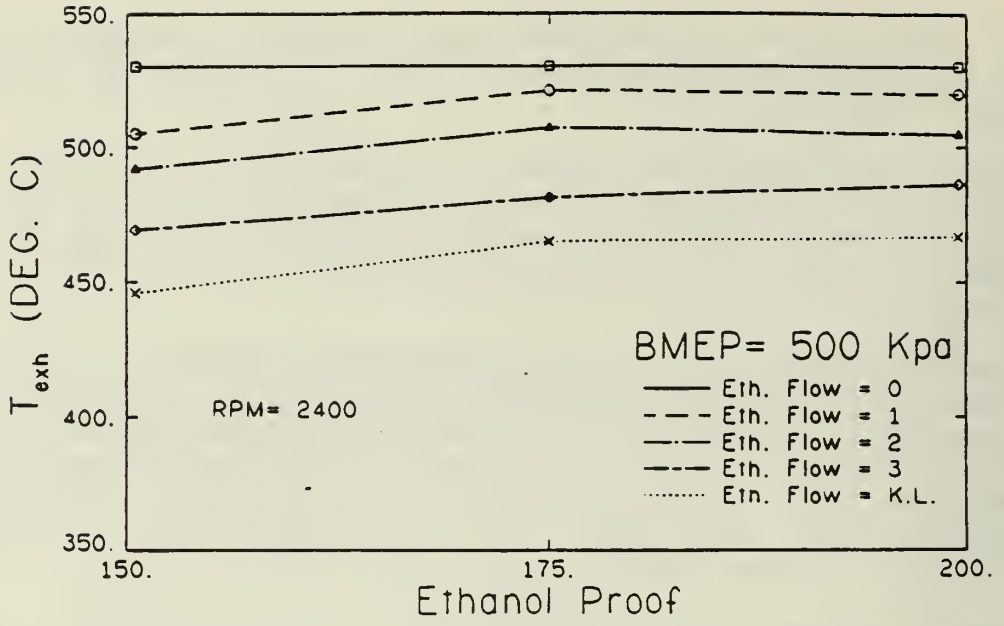

Figure 35 Exhaust temperature at a bmep of 500 kPa.

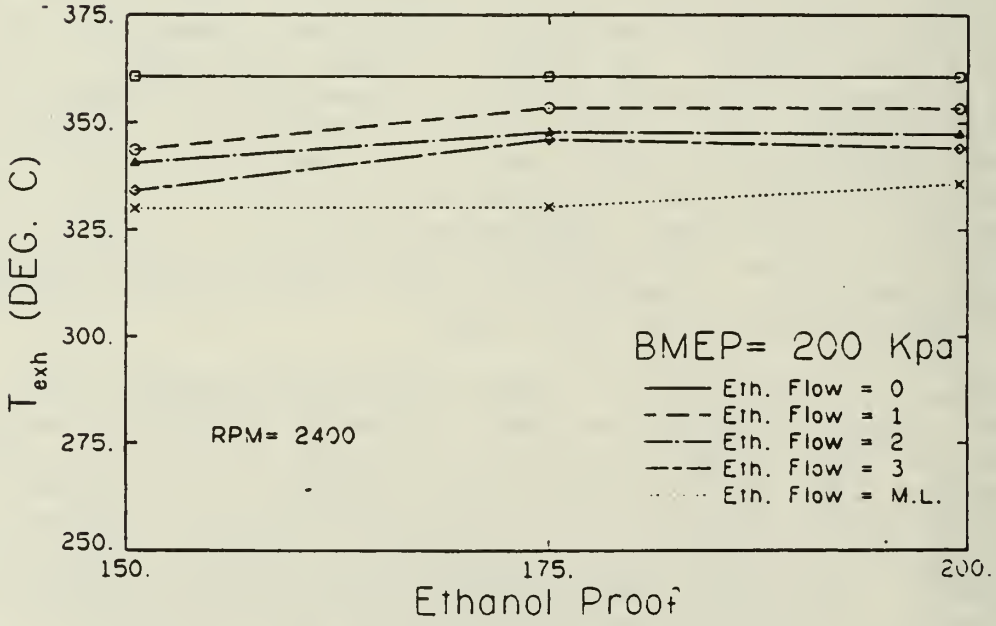

Figure 36 Exhaust temperature at a bmep of 200 kPa.

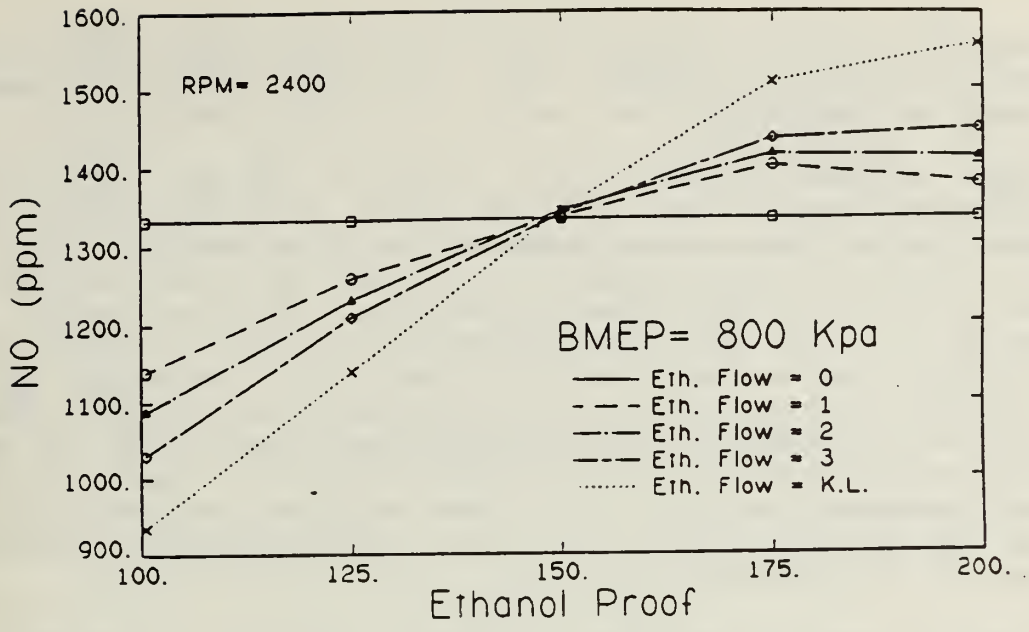

Figure 37 Nitrous oxide emissions at a bmep of 800 kPa.

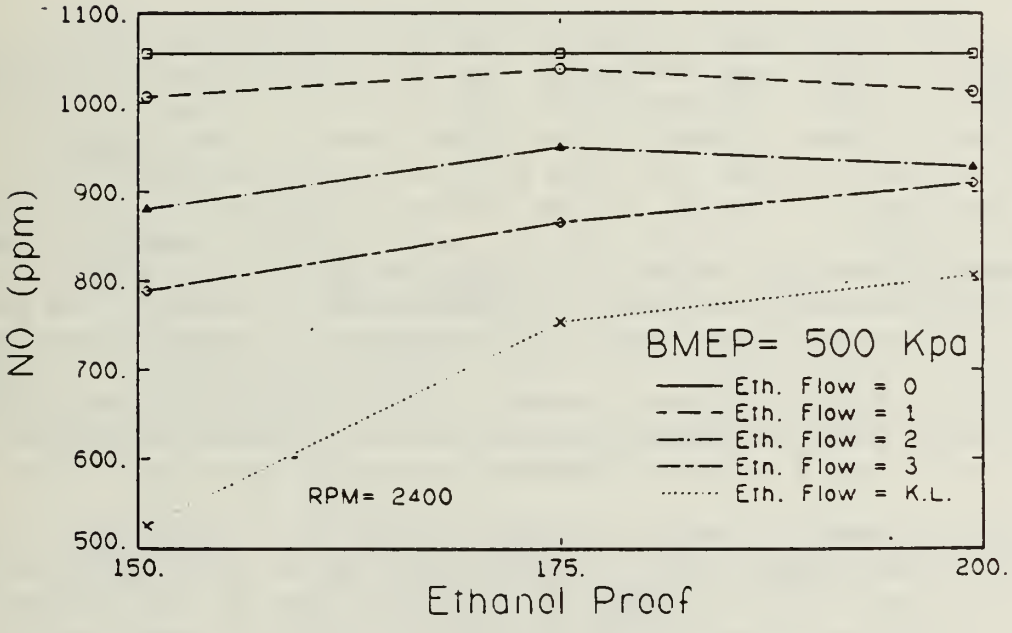

Figure 38 Nitrous oxide emissions at a bmep of 500 kPa.

the combustion products with fumigation will cool faster and freeze the NO equilibrium reactions at a higher level. As water is added with lower proofs, the combustion temperatures are lowered which reduces the NO levels.

Figure 38 shows NO emissions at a bmep of 500 kPa. NO emissions decreased from the diesel level, 24 to 50 percent at the knock limit and 13.7 to 25 percent at a flow rate of three as the flow rate of ethanol was increased. The NO emissions dropped, 13.3 percent at a flow rate of three, and 5.1 percent at a flow rate of two, as the ethanol proof was lowered. The peak pressure curve in Fig. 29, which rose as the flow rate of ethanol increased, indicates that the NO levels should increase with increasing ethanol flow rate, since a higher peak pressure corresponds to a higher peak temperature. The opposite was observed to occur and since a bmep of 500 kPa was in the transition region between misfire and knock limits, it is possible that one of the other parameters controlling the formation of NO, the availability of oxygen and the residence time of the NO at high temperatures, played a larger role than the peak temperature.

Figure 39 shows NO emissions at a bmep of 200 kPa. The NO emissions decreased from the diesel level as the flow rate of ethanol increased. This agrees with the trends of peak pressure in Fig. 30 which dropped with rising flow rates. The lower pressures are due to the ignition delay causing combustion to occur during the expansion stroke. This lowers the peak pressure and temperature during the cycle. The lower peak temperatures should correspond to lower NO levels. There was no noticeable effect of ethanol proof on NO emissions.

Percent CO at a bemp of 800 kPa is shown in Fig. 40. Initially as the flow rate of ethanol was increased, the CO level increased from the diesel level and approached a maximum value. As the flow rate was increased further, the CO level dropped closer to the diesel level. The ethanol air mixture fills the entire cylinder and there will be flame quenching at the walls and in the ring lands. Also at the low ethanol flow rates, 1 and 2, there is a very lean mixture of ethanol and air which causes incomplete combustion. Flame quenching and the incomplete combustion of the lean mixture will cause the increase in the CO levels at the low flow rates. As the flow rate of the ethanol is increased, the ethanol air mixture will become richer and the CO level should drop slightly due to more complete combustion. CO levels were higher with pure and 100 proof ethanol at all flow rates than the CO levels with 150 proof ethanol. No explanation can be given for this trend; however, at this load CO had a very weak dependency on proof and ethanol flow rate.

Figure 41 shows CO levels at a bmep of 500 kPa. The percent CO increased greatly from the diesel level, 4.8 to 6 times at the knock limit and 5.3 to 6 times at a flow rate of three, as the flow rate of the ethanol was increased. There was a very slight increase in the CO levels as the ethanol proof was lowered. At a bmep of 500 kPa, ethanol was fumigated at levels of up to 70 percent by energy. Wall quenching and incomplete combustion lead to the high levels of CO produced at this load. The long ignition delay, see Fig. 32, caused by ethanol reduces the amount of diffusion controlled burning at this load. Therefore the temperatures later in the cycle are lower and this also reduces the amount of CO which reacts with oxygen to form carbon dioxide. This explains why the CO levels are higher at this load than at a bmep of 800 kPa, where there is still a significant amount of diffusion burning.

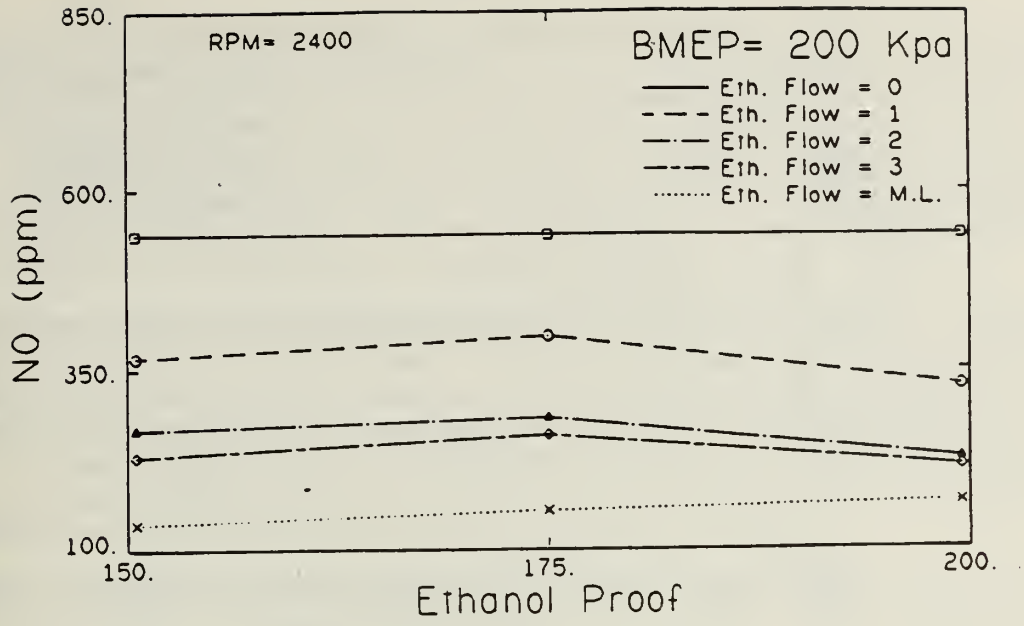

Figure 39 Nitrous oxide emissions at a bmep of 200 kPa.

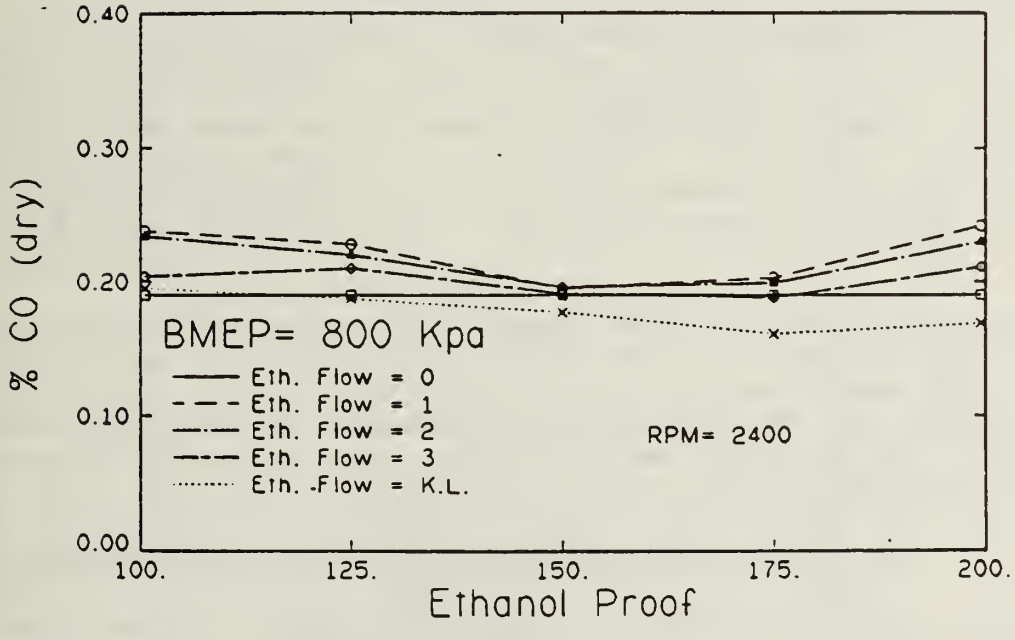

Figure 40 Percent CO at a bmep of 800 kPa.

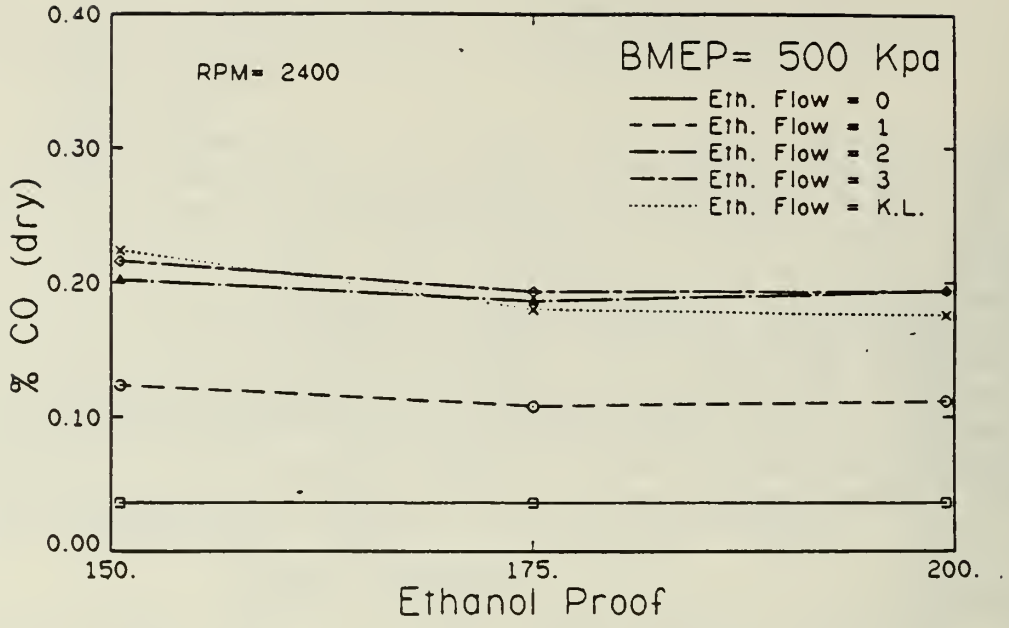

Figure 41 Percent CO at a bmep of 500 kPa.

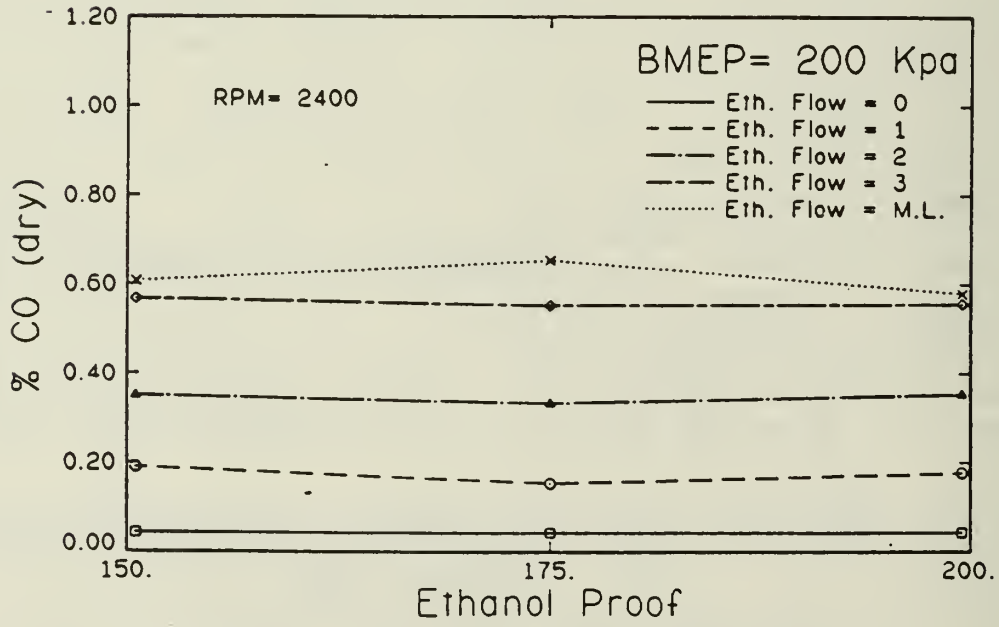

Figure 42 Percent CO at a bmep of 200 kPa.

The percent CO level at a bmep of 200 kPa is shown in Fig. 42. The CO levels increased greatly from the diesel level, 14 to 15.8 times at the misfire limit, and 13.5 times at a flow rate of three, as the flow rate of the ethanol was increased. CO showed no noticeable trend with ethanol proof at this load. Combustion mainly occurs during the expansion stroke at this low load due to the long ignition delay. This causes low combustion temperatures. These low temperatures, flame quenching and incomplete combustion lead to the highest CO levels of all the loads tested.

Hydrocarbon levels at a bmep of 800 kpa are shown in Fig. 43. HC emissions increased from the diesel level, 3.7 to 4.9 times at the knock limit, and 2.8 times at a flow rate of three, as the flow rate of the ethanol was increased. The hydrocarbon levels increased very slightly as the ethanol proof was lowered. Flame quenching at the cylinder walls as well as incomplete combustion in the lean ethanol and air mixture will lead to the high HC levels with fumigation.

This load produced the lowest HC levels of all loads tested, even at the knock limit, with about 40 percent of the energy by ethanol, there was still a significant amount of diffusion burning late in the cycle. This is evident in Fig. 34 for exhaust temperature, which is always greater than 600 degrees centigrade. The high temperatures will cause some of the HC's to burn off during the expansion stroke. This accounts for this load having the lowest hydrocarbon levels of all the loads tested.

Figure 44 shows the hydrocarbons at a bmep of 500 kPa. The hydrocarbon emissions increased greatly from the diesel level, 5.9 to 9 times at the knock limit, and 4.7 times at a flow rate of three, as the flow rate of the ethanol was increased. There was also a very slight increase in HC levels as the ethanol proof was lowered. Flame quenching at the cylinder walls as well as incomplete combustion of the lean ethanol and air mixture account for the increase in the HC levels from the diesel levels. The lower temperatures throughout the cycle, as shown by the low exhaust temperatures in Fig. 35, account for the higher HC levels at this load, when compared with the HC emissions at a bmep of 800 kPa.

Figure 45 shows hydrocarbons at a bmep of 200 kPa. The hydrocarbons increased greatly from the diesel level, 10.5 to 11.7 times at the misfire limit, and 9 times at a flow rate of three, as the flow rate of the ethanol was increased. These were the highest HC levels of all the loads tested. The hydrocarbon levels increased as a result of flame quenching and incomplete combustion. Also the long ignition delay at this load caused combustion to start after TDC during the expansion stroke. As a result the low flame temperatures should also increase the hydrocarbon levels.

Bosch smoke number at a bmep of 800 kPa is shown in Fig. 46. The smoke level decreased from the diesel level as the flow rate of the ethanol was increased to the knock limit. There was no noticeable trend of smoke number with ethanol proof. As ethanol is fumigated the amount of diesel fuel injected decreases, this reduces the amount of the diesel fuel which burns in a diffusion controlled process. Also the longer ignition delay allows a larger fraction of the diesel fuel to diffuse and form a premixed charge before combustion starts. Since the majority of the soot is formed during diffusion combustion the above reasons account for the smaller quantity of smoke pro-

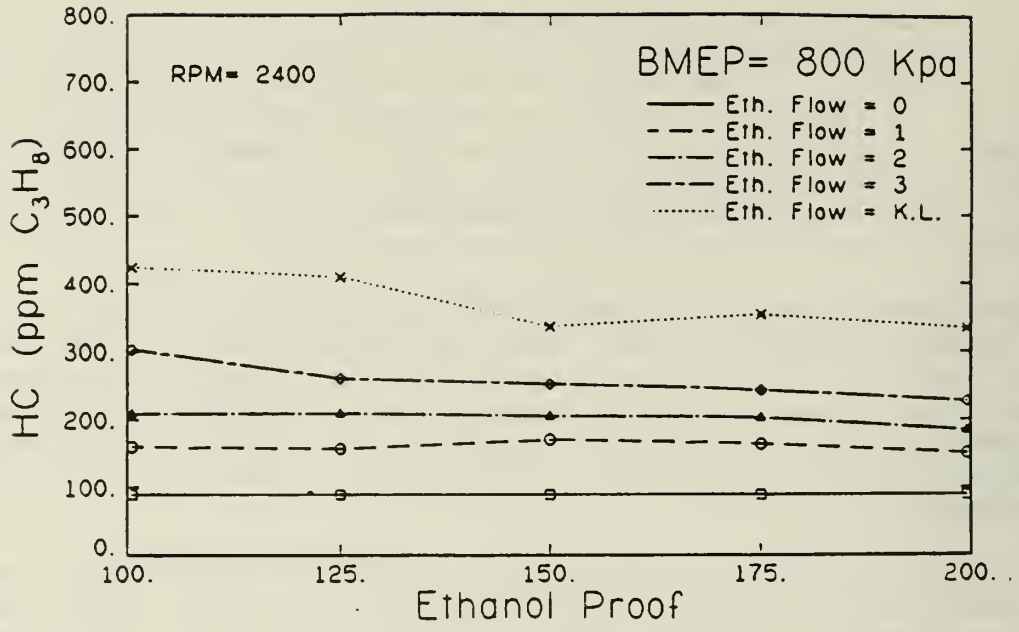

Figure 43 Hydrocarbon levels at a bmep of 800 kPa.

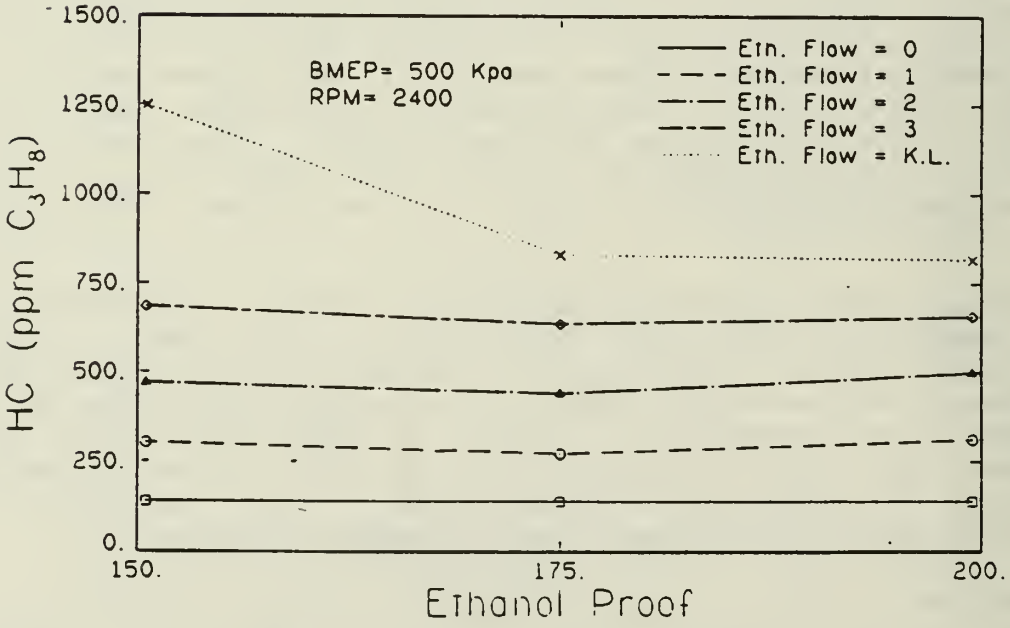

Figure 44 Hydrocarbon levels at a bmep of 500 kPa.

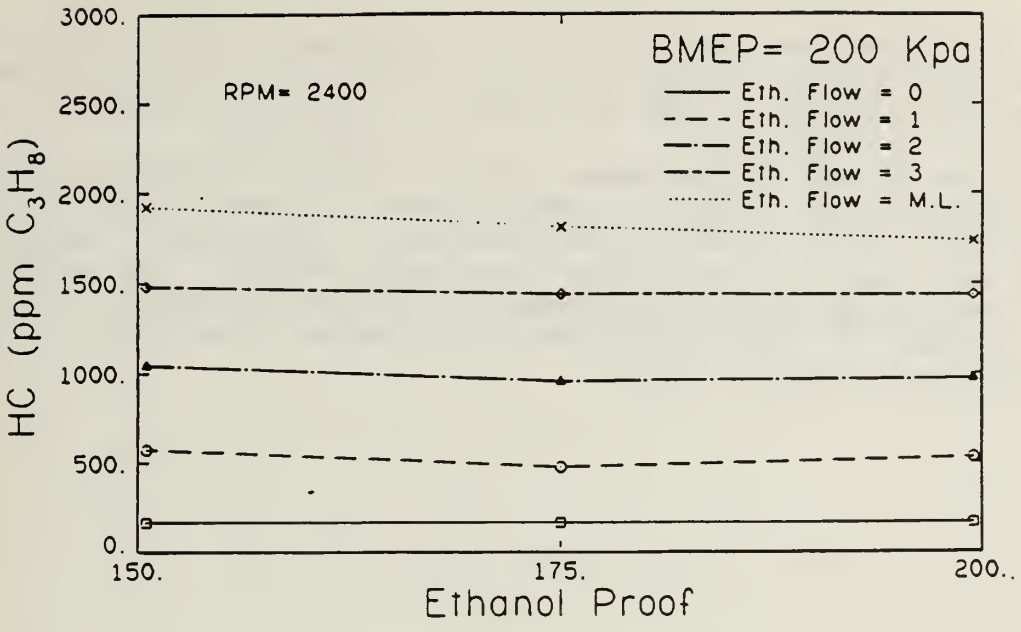

Figure 45 Hydrocarbon levels at a bmep of 200 kPa.

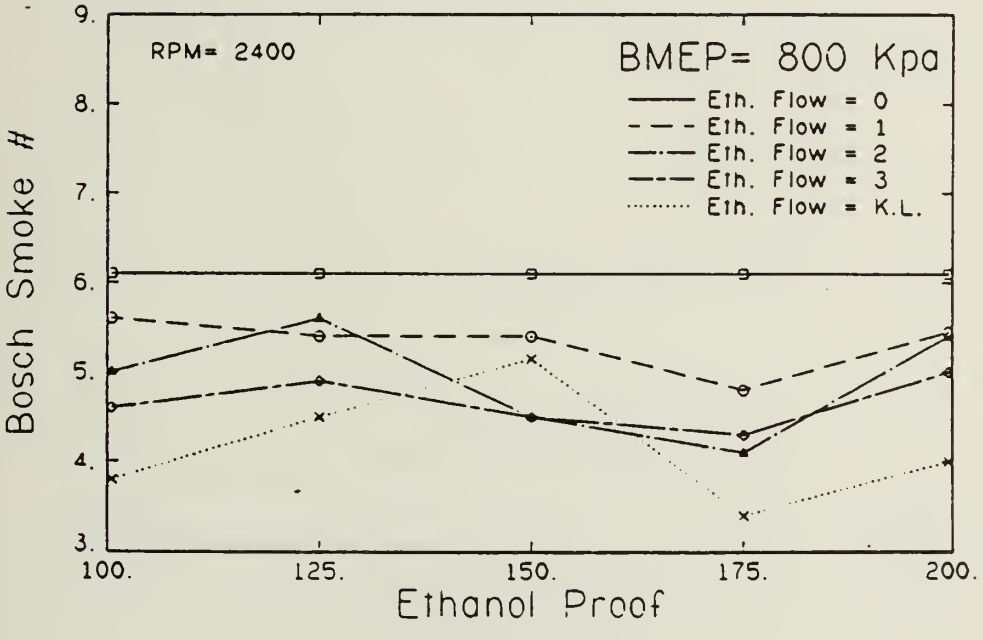

Figure 46 Bosch smoke number at a bmep of 800 kPa.

duced. The ethanol and air mixture should not add any smoke since only a rich premixed fuel charge produces smoke and the ethanol and air mixture at this load is always lower than the stoichiometric level for ethanol and air.

Figures 47 and 48 show smoke levels at bmep's of 500 and 200 kPa. Both plots show the same trends, the smoke number decreased from the diesel level as the flow rate of the ethanol was increased. There was no noticeable trend in the smoke level as the ethanol proof was lowered. The reduction in the smoke level is due to the substitution of part of the diesel fuel with ethanol and as a result of this, a reduction in the amount of the diffusion controlled combustion which produces smoke.

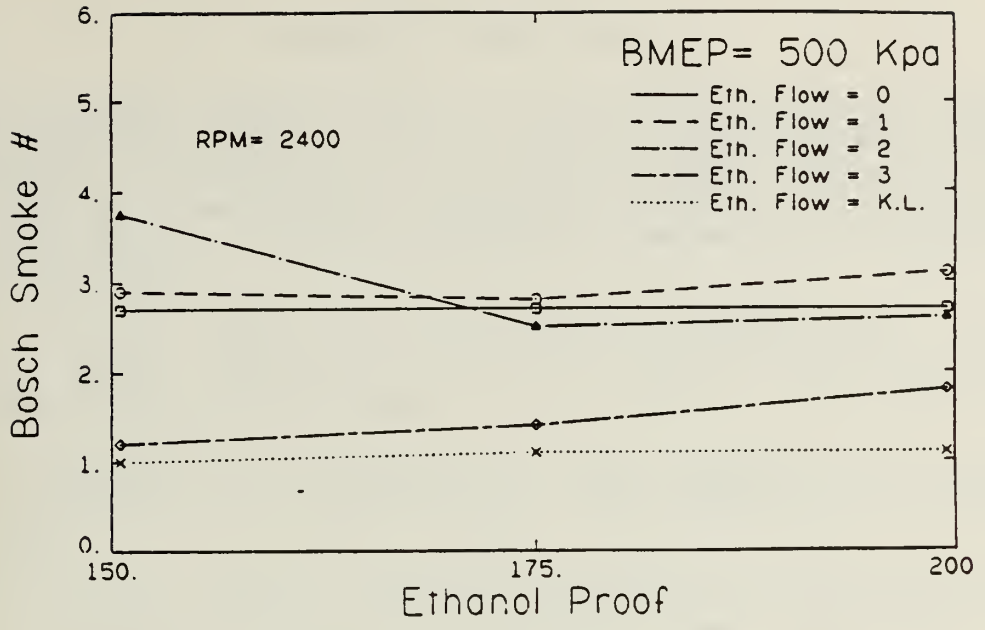

Figure 47 Bosch smoke number at a bmep of 500 kPa.

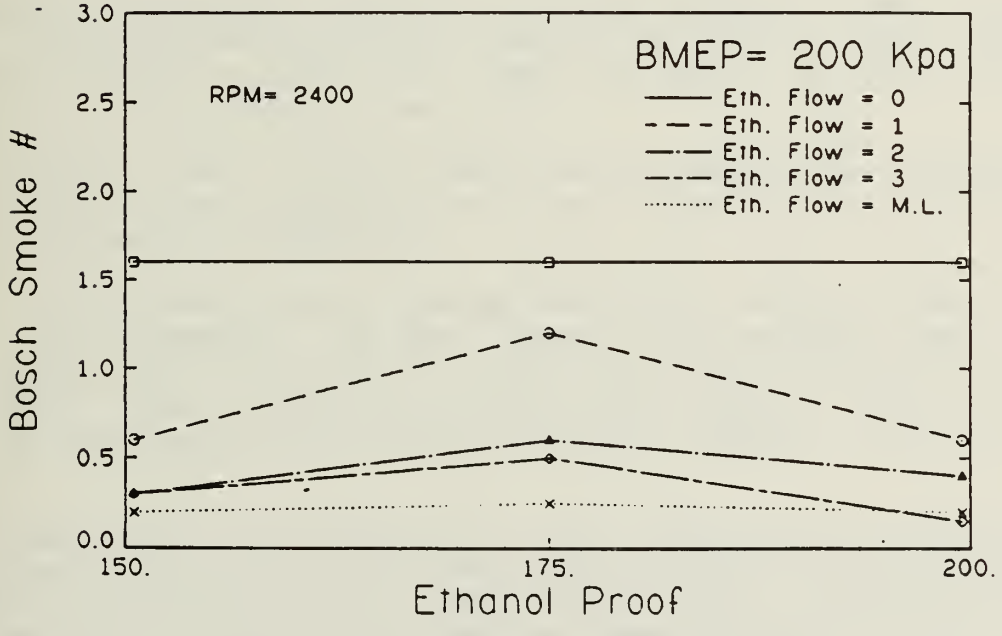

Figure 48 Bosch smoke number at a bmep of 200 kPa.

6. SUMMARY AND CONCLUSIONS

The use of several ethanol proofs as a fumigant in a direct injection diesel engine was investigated. A 7.14 liter International Harvester six cylinder turbocharged diesel engine was used for the tests. Emissions, engine performance parameters, and pressure crankangle histories of the number one cylinder were all measured. From the analysis of the data the following conclusions can be applied:

1. Lower proof ethanol reduced the maximum rate of pressure rise. This was true at all loads. Reductions of up to 20 percent from pure ethanol levels were obtained at high loads.

2. While the maximum rate of pressure rise was reduced with lower proof ethanol at 800 kPa this level was still 59.6 percent higher than the diesel level.

3. Lower proof ethanol slightly reduced the peak pressure from pure ethanol levels. A 2.5 percent decrease was measured at a bmep of 800 kPa.

4. At a bmep of 800 kPa the NO emissions were reduced below the diesel level with the addition of any ethanol proof smaller than 150. If an ethanol proof greater than 150 was added the NO emissions rose above the diesel level. At lower loads the addition of any type of ethanol lowered NO emissions.

5. The unburned hydrocarbon emissions increased greatly. They increased roughly 7.2 times from the diesel level at low load, 6 times at medium load, and 3.8 times at high load. Ethanol proof did not have a significant effect on the hydrocarbon emissions.

6. The CO emissions levels increased greatly as the ethanol flow rate was increased. This was most severe at low loads. Ethanol proof did not have a significant effect on CO emissions.

Judging from the above results, the optimum type of ethanol appears to be 100 proof. It is economical, and easily made on the individual farm with a small distillation plant. It gives the largest reduction in NO emissions from the diesel level. Its use resulted in the largest increase in efficiency at high load, and the lowest peak pressure and rate of pressure rise of all the proofs tested.

The drawbacks with this proof are the large increases in the hydrocarbon and CO emissions. They are several times higher than the diesel emissions, however, these are relatively easily removed catalytically. The peak pressure and the maximum rate of pressure rise have the lowest values of all the proofs tested, but these values are still greater than the diesel levels. And finally for the same energy content the volume of the fuel is doubled.

7. RECOMMENDATIONS

Several other areas should be investigated with lower proof ethanols as fumigants. Since lower proofs increase the ignition delay, above that of pure ethanol, the effect of pilot fuel timing should be investigated. This could be important at medium and high loads where fumigation causes an increase in the maximum rate of pressure rise. This may be harmful to the engine, however, lower proofs reduce the maximum rate of pressure rise. It may be possible to increase efficiency by changing pilot fuel timing, as shown by Schroeder [13] with pure ethanol.

The engine was limited by misfire at low loads and by knock at high loads. There was a transition region in the middle load range where, the same ethanol flow rate would knock at one load yet misfire at a slightly lower load. The effect of intake charge temperature should be studied to determine if it plays a major role in this transition, especially since it is a strong function of load with a turbocharged engine. It may be possible to reduce knock at high loads by cooling the charge, and increase the ethanol flow rate at the misfire limit, as well as efficiency, by heating the intake air charge.

Better instrumentation should be installed for the determination of combustion knock. It was noticed that audibly the engine gave evidence of severe knock yet the pressure trace did not show this from the instrumented cylinder. Possible solutions to this problem would be pressure instrumentation, or knock sensors for all of the cylinders.

8. REFERENCES

1. U. S. National Alcohol Fuels Commission, Fuel Alcohol on the Farm. Washington, DC: U. S. National Alcohol Fuels Commission, 1980.

2. Roberts, B. D., "Performance and emissions of a turbocharged diesel engine fumigated with ethanol," Master of Science Thesis, University of Illinois at Urbana-Champaign, Urbana, Illinois, 1986.

3. Heinsy, J. B., and Lestz, S. S., "Aqueous alcohol fumigation of a Single-Cylinder DI Diesel Engine," SAE Paper No. 811208. SAE, Warrendale, Pennsylvania.

4. Shropshire, G. J., and Goering, C. E., "Ethanol Injection into a Diesel Engine," ASAE Paper No. 81-1051. ASAE, St. Joseph, Michigan.

5. Chen, J., et al., "Ethanol Fumigation of a Turbocharged Diesel Engine," SAE Paper No. 810680. SAE, Warrendale, Pennsylvania.

6. Goering, C. E., and Wood, D. R., "Overfueling a Diesel Engine with Carburated Ethanol," ASAE Paper No. 81-1048. ASAE, St. Joseph, Michigan.

7. Baranescu, R. A., "Fumigation of Alcohols in a Multicylinder Diesel Engine -evaluation of Potential," SAE Paper No. 860308. SAE, Warrendale Pennsylvania.

8. Valdmanis, E., and Wulfhorst, D. E., "The Effects of Emulsified Fuels and Water Induction on Diesel Combustion," SAE Paper No. 700736. SAE, Warrendale, Pennsylvania.

9. Recommended Practice, "Measurement of Intake Air or Exhaust Gas Flow of Diesel Engines," SAE J244, SAE Handbook.

10. Hayes, T. K., Savage, L. D., and Sorenson, S. C., "Cylinder Pressure Data Acquisition and Heat Release Analysis on a Personal Computer," SAE Paper No. 860029. SAE, Warrendale, Pennsylvania.

11. Lancaster, D. R., et al., "Measurement and Analysis of Engine Pressure Data," SAE Paper No. 750026. SAE, Warrendale, Pennsylvania.

12. Kanury, A. M., Combustion Phenomena. New York: Gordon and Breach Science Publishers, 1982.

13. Schroeder, A. R., "The Effect of Diesel Injection Timing on a Turbocharged Diesel Engine Fumigated with Ethanol," Master of Science Thesis, University of Illinois at Urbana-Champaign, Urbana, Illinois, 1986.

9. TABULAR DATA

TABLE 1: DIESEL PARAMETERS A VARIOUS LOADS AND 2400 RPM.

	BMEP (kPa) 800	500	200
Diesel flow (g/s)	8.108	5.256	2.916
Thermal efficiency	32.97	31.75	22.97
Volumetric eff.	89.52	86.79	85.0
Air flow (g/s)	187.2	158.6	138.9
Amb. press. (kPa)	98.91	98.91	98.91
Amb. temp. (C)	31.34	32.43	30.97
Wet bulb (C)	20.83	21.67	21.39
Man. press. (kPa)	157.8	127.2	106.7
Man. temp. (C)	102.2	73.32	51.61
Exh. temp. (C)	700.0	530.2	360.7
NO (ppm)	1333.	1055.	537.6
HC (ppm propane)	89.2	139.3	164.6
Bosch smoke	6.1	2.7	1.6
CO (% dry)	0.190	0.036	0.042
CO2 (% dry)	8.67	6.43	3.92
DP/DCA (kPa/deg)	539.6	655.5	588.6
Ang. max DP/DCA	353	355	359
Max press. (MPa)	10.1	8.18	6.437
Ang. Pmax	365	364	364
Ign. delay (deg)	9	10	13

TABLE 2: ETHANOL FUMIGATION PARAMETERS FOR VARIOUS PROOFS AT THE KNOCK LIMIT FLOWRATE AND A BMEP OF 800 kPa AND 2400 RPM.

	Ethanol proof				
	200	175	150	125	100
Diesel flow (g/s)	5.295	5.029	5.135	4.838	5.151
Ethanol flow (g/s)	4.098	4.593	4.174	4.730	4.062
% Energy by Eth.	32.7	36.48	33.82	38.07	33.2
Thermal efficiency	33.96	33.76	34.45	34.2	34.7
Volumetric eff.	87.98	88.29	86.4	88.9	91.0
Air flow (g/s)	180.6	179.5	177.2	179.2	184.2
Amb. press. (kPa)	98.91	98.87	99.09	98.87	98.87
Amb. temp. (C)	31.98	32.50	26.87	32.87	33.87
Wet bulb (C)	21.67	20.83	16.67	22.36	22.50
Man. press. (kPa)	152.3	151.9	149.8	149.3	151.5
Man. temp. (C)	96.00	98.30	90.20	95.30	99.40
Exh. temp. (C)	637.6	628.9	624.3	615.1	600.2
NO (ppm)	1558.	1508.	1343.	1140.	935.3
HC (ppm propane)	334.4	354.2	336.6	410.3	432.7
Bosch smoke	4.0	3.4	5.2	4.5	3.8
CO (% dry)	0.169	0.161	0.177	0.187	0.195
CO2 (% dry)	8.39	8.63	8.41	8.37	8.04
DP/DCA (kPa/deg)	1449.	1766.	1411.	1445	982.3
Ang. max DP/DCA	354	355	356	357	356
Max press. (MPa)	11.58	12.07	11.58	12.15	11.32
Ang. Pmax	365	359	360	361	363
Ign. delay (deg)	10	8	11	12	11

TABLE 3: ETHANOL FUMIGATION PARAMETERS FOR VARIOUS PROOFS AT A FLOW RATE OF THREE AND A BMEP OF 800 kPa AND 2400 RPM.

	Ethanol proof				
	200	175	150	125	100
Diesel flow (g/s)	6.095	5.976	5.948	6.038	5.894
Ethanol flow (g/s)	2.929	2.941	2.869	2.889	2.945
% Energy by Eth.	23.2	23.63	23.3	23.1	23.9
Thermal efficiency	33.68	34.16	34.48	34.0	34.5
Volumetric eff.	88.10	89.40	87.4	89.4	91.0
Air flow (g/s)	179.1	181.6	179.4	180.5	185.4
Amb. press. (kPa)	98.81	98.87	99.09	98.87	98.87
Amb. temp. (C)	31.18	35.59	29.11	34.83	34.85
Wet bulb (C)	21.67	20.83	17.50	22.36	22.50
Man. press. (kPa)	150.7	152.6	151.4	150.7	153.2
Man. temp. (C)	95.60	100.8	93.60	98.30	101.0
Exh. temp. (C)	666.3	647.7	638.4	649.1	623.0
NO (ppm)	1447.	1435.	1339.	1210.	1031.
HC (ppm propane)	227.4	243.1	252.3	260.7	303.2
Bosch smoke	5.0	4.3	4.5	4.9	4.6
CO (% dry)	0.211	0.188	0.191	0.210	0.204
CO2 (% dry)	8.54	8.50	8.05	8.39	8.11
DP/DCA (kPa/deg)	1032.	1030.	963.5	928.2	862.2
Ang. max DP/DCA	354	354	355	355	355
Max press. (MPa)	10.94	11.00	10.82	10.69	10.66
Ang. Pmax	365	365	365	365	366
Ign. delay (deg)	9	8	10	10	10

TABLE 4: ETHANOL FUMIGATION PARAMETERS FOR VARIOUS PROOFS AT A FLOW RATE OF TWO AND A BMEP OF 800 kPa AND 2400 RPM.

	Ethanol proof				
	200	175	150	125	100
Diesel flow (g/s)	6.565	5.378	6.372	6.473	6.473
Ethanol flow (g/s)	2.281	2.384	2.294	2.266	2.267
% Energy by Eth.	17.9	19.03	18.5	18.0	18.0
Thermal efficiency	33.42	33.94	34.21	33.8	33.8
Volumetric eff.	89.10	89.70	87.9	89.5	90.4
Air flow (g/s)	181.6	183.8	182.5	181.8	182.7
Amb. press. (kPa)	98.81	98.87	99.09	98.87	98.87
Amb. temp. (C)	33.36	36.55	29.87	35.78	35.18
Wet bulb (C)	21.67	20.83	18.06	22.36	24.17
Man. press. (kPa)	151.7	154.5	153.8	152.4	151.4
Man. temp. (C)	97.30	102.1	95.30	100.1	99.70
Exh. temp. (C)	679.2	658.3	650.9	663.2	659.0
NO (ppm)	1410.	1415.	1344.	1232.	1088.
HC (ppm propane)	184.2	202.9	205.4	209.4	208.9
Bosch smoke	5.4	4.1	4.5	5.6	5.0
CO (% dry)	0.230	0.199	0.196	0.220	0.234
CO2 (% dry)	8.52	8.42	7.95	8.38	8.50
DP/DCA (kPa/deg)	854.5	882.5	835.9	815.8	760.0
Ang. max DP/DCA	354	354	354	354	355
Max press. (MPa)	10.63	10.79	10.70	10.55	10.41
Ang. Pmax	365	365	365	365	365
Ign. delay (deg)	9	8	10	9	10

TABLE 5: ETHANOL FUMIGATION PARAMETERS FOR VARIOUS PROOFS AT A FLOW RATE OF ONE AND A BMEP OF 800 kPa AND 2400 RPM.

	Ethanol proof				
	200	175	150	125	100
Diesel flow (g/s)	6.952	6.783	6.745	6.956	6.944
Ethanol flow (g/s)	1.721	1.788	1.793	1.660	1.707
% Energy by Eth.	13.5	14.21	14.3	13.1	13.4
Thermal efficiency	33.27	33.81	33.95	33.4	33.3
Volumetric eff.	88.90	89.70	88.1	89.8	90.4
Air flow (g/s)	182.2	184.2	183.3	183.7	184.0
Amb. press. (kPa)	98.91	98.87	99.09	98.87	98.87
Amb. temp. (C)	34.41	37.08	29.70	36.28	35.97
Wet bulb (C)	21.67	20.83	18.06	22.50	22.50
Man. press. (kPa)	153.4	155.3	154.3	154.2	153.5
Man. temp. (C)	99.30	103.6	95.90	101.9	101.9
Exh. temp. (C)	688.3	668.1	658.5	678.9	675.1
NO (ppm)	1376.	1400.	1336.	1259.	1139.
HC (ppm propane)	150.7	164.2	170.8	157.3	160.5
Bosch smoke	5.45	4.8	5.4	5.4	5.6
CO (% dry)	0.242	0.203	0.196	0.228	0.238
CO2 (% dry)	8.47	8.43	7.86	8.34	8.47
DP/DCA (kPa/deg)	692.1	669.8	745.1	708.1	729.8
Ang. max DP/DCA	354	354	354	354	354
Max press. (MPa)	10.41	10.56	10.57	10.37	10.36
Ang. Pmax	365	365	365	365	365
Ign. delay (deg)	9	8	9	9	10

TABLE 6: ETHANOL FUMIGATION PARAMETERS FOR VARIOUS PROOFS AT THE KNOCK LIMIT FLOW RATE AND A BMEP OF 500 kPa AND 2400 RPM.

	Ethanol proof		
	200	175	150
Diesel flow (g/s)	2.043	2.059	1.573
Ethanol flow (g/s)	5.088	5.082	6.093
% Energy by Eth.	61.0	60.8	70.9
Thermal efficiency	31.80	31.75	30.90
Volumetric eff.	86.10	87.80	86.8
Air flow (g/s)	153.7	154.8	157.2
Amb. press. (kPa)	98.91	98.87	99.09
Amb. temp. (C)	30.25	32.79	28.20
Wet bulb (C)	21.11	20.83	17.22
Man. press. (kPa)	121.9	121.0	123.7
Man. temp. (C)	66.60	68.40	66.70
Exh. temp. (C)	466.8	465.0	445.9
NO (ppm)	806.4	753.9	525.5
HC (ppm propane)	817.7	830.5	1250.
Bosch smoke	1.1	1.1	1.0
CO (% dry)	0.176	0.180	0.224
CO2 (% dry)	5.89	5.99	5.70
DP/DCA (kPa/deg)	813.0	662.3	535.3
Ang. max DP/DCA	364	364	362
Max press. (MPa)	8.892	8.390	7.830
Ang. Pmax	365	368	370
Ign. delay (deg)	13	14	17

TABLE 7: ETHANOL FUMIGATION PARAMETERS FOR VARIOUS PROOFS AT A FLOW OF THREE AND A BMEP OF 500 kPa AND 2400 RPM.

	Ethanol proof		
	200	175	150
Diesel flow (g/s)	2.978	2.859	2.919
Ethanol flow (g/s)	3.752	3.831	3.687
% Energy by Eth.	44.2	45.7	44.3
Thermal efficiency	31.30	31.67	31.90
Volumetric eff.	86.30	87.40	85.6
Air flow (g/s)	155.3	155.8	155.9
Amb. press. (kPa)	98.91	98.87	99.09
Amb. temp. (C)	30.71	32.79	27.47
Wet bulb (C)	21.39	20.83	17.22
Man. press. (kPa)	123.7	123.0	124.3
Man. temp. (C)	68.80	70.20	66.60
Exh. temp. (C)	486.3	481.3	469.1
NO (ppm)	910.3	865.8	789.0
HC (ppm propane)	657.6	636.0	685.2
Bosch smoke	1.8	1.4	1.2
CO (% dry)	0.194	0.193	0.216
CO2 (% dry)	6.02	6.11	5.93
DP/DCA (kPa/deg)	781.0	771.8	776.5
Ang. max DP/DCA	358	359	359
Max press. (MPa)	8.768	8.836	8.617
Ang. Pmax	363	366	364
Ign. delay (deg)	12	12	12

TABLE 8: ETHANOL FUMIGATION PARAMETERS FOR VARIOUS PROOFS AT A FLOW OF TWO AND A BMEP OF 500 kPa AND 2400 RPM.

	Ethanol proof		
	200	175	150
Diesel flow (g/s)	3.861	3.819	3.798
Ethanol flow (g/s)	2.419	2.361	2.433
% Energy by Eth.	28.3	28.0	28.7
Thermal efficiency	31.00	31.46	31.30
Volumetric eff.	86.60	87.90	86.1
Air flow (g/s)	157.9	158.0	158.8
Amb. press. (kPa)	98.91	98.87	99.09
Amb. temp. (C)	30.99	32.84	27.02
Wet bulb (C)	21.39	21.08	17.22
Man. press. (kPa)	126.2	125.1	126.6
Man. temp. (C)	71.00	73.20	68.60
Exh. temp. (C)	504.8	507.2	491.9
NO (ppm)	928.2	950.0	880.7
HC (ppm propane)	499.6	441.9	471.1
Bosch smoke	2.6	2.5	3.8
CO (% dry)	0.194	0.186	0.202
CO2 (% dry)	6.09	6.32	5.98
DP/DCA (kPa/deg)	805.7	818.2	784.5
Ang. max DP/DCA	357	357	357
Max press. (MPa)	8.551	8.526	8.594
Ang. Pmax	362	362	365
Ign. delay (deg)	12	11	11

TABLE 9: ETHANOL FUMIGATION PARAMETERS FOR VARIOUS PROOFS AT A FLOW OF ONE AND A BMEP OF 500 kPa AND 2400 RPM.

	Ethanol proof		
	200	175	150
Diesel flow (g/s)	4.696	4.679	4.540
Ethanol flow (g/s)	1.020	0.963	1.141
% Energy by Eth.	12.0	11.5	13.6
Thermal efficiency	31.30	31.57	31.73
Volumetric eff.	86.60	87.70	85.9
Air flow (g/s)	158.9	158.8	159.4
Amb. press. (kPa)	98.91	98.87	99.09
Amb. temp. (C)	31.17	32.69	26.78
Wet bulb (C)	21.39	22.50	17.50
Man. press. (kPa)	127.5	126.2	127.6
Man. temp. (C)	72.40	73.60	69.00
Exh. temp. (C)	519.9	521.1	505.0
NO (ppm)	1013.	1038.	1007.
HC (ppm propane)	312.6	272.6	303.4
Bosch smoke	3.1	2.8	2.9
CO (% dry)	0.112	0.108	0.124
CO2 (% dry)	6.17	6.36	6.08
DP/DCA (kPa/deg)	743.3	711.8	772.0
Ang. max DP/DCA	356	356	356
Max press. (MPa)	8.363	8.215	8.452
Ang. Pmax	364	364	364
Ign. delay (deg)	11	11	12

TABLE 10: ETHANOL FUMIGATION PARAMETERS FOR VARIOUS PROOFS AT THE MISSFIRE FLOW RATE AND A BMEP OF 200 kPa AND 2400 RPM.

	Ethanol proof		
	200	175	150
Diesel flow (g/s)	1.053	0.915	1.008
Ethanol flow (g/s)	4.299	4.727	4.952
% Energy by Eth.	72.0	76.5	75.5
Thermal efficiency	17.80	17.20	16.20
Volumetric eff.	85.30	86.30	84.8
Air flow (g/s)	140.0	140.8	142.7
Amb. press. (kPa)	98.91	98.87	99.09
Amb. temp. (C)	29.63	31.82	25.88
Wet bulb (C)	21.11	22.50	16.67
Man. press. (kPa)	107.3	107.1	109.6
Man. temp. (C)	51.90	53.60	50.90
Exh. temp. (C)	335.8	330.4	330.0
NO (ppm)	165.6	154.2	135.3
HC (ppm propane)	1739.	1811.	1923.
Bosch smoke	0.2	0.3	0.2
CO (% dry)	0.579	0.654	0.607
CO2 (% dry)	3.32	3.34	3.25
DP/DCA (kPa/deg)	423.9	340.0	304.5
Ang. max DP/DCA	362	364	364
Max press. (MPa)	5.820	5.285	5.339
Ang. Pmax	368	365	370
Ign. delay (deg)	17	18	21

TABLE 11: ETHANOL FUMIGATION PARAMETERS FOR VARIOUS PROOFS AT A FLOW OF THREE AND A BMEP OF 200 kPa AND 2400 RPM.

	Ethanol proof		
	200	175	150
Diesel flow (g/s)	1.488	1.517	1.554
Ethanol flow (g/s)	3.110	3.179	3.135
% Energy by Eth.	56.8	56.9	55.9
Thermal efficiency	19.40	19.00	19.00
Volumetric eff.	85.20	86.00	84.0
Air flow (g/s)	140.0	140.0	140.5
Amb. press. (kPa)	98.91	98.87	99.09
Amb. temp. (C)	29.61	31.44	25.67
Wet bulb (C)	21.11	22.50	16.94
Man. press. (kPa)	107.2	106.7	108.4
Man. temp. (C)	51.70	53.10	49.40
Exh. temp. (C)	344.1	346.1	334.1
NO (ppm)	215.3	259.2	229.7
HC (ppm propane)	1438.	1438.	1481.
Bosch smoke	0.2	0.5	0.3
CO (% dry)	0.556	0.552	0.567
CO2 (% dry)	3.40	3.52	3.33
DP/DCA (kPa/deg)	506.9	462.1	477.4
Ang. max DP/DCA	361	362	362
Max press. (MPa)	6.062	5.937	5.838
Ang. Pmax	366	366	367
Ign. delay (deg)	16	16	16

TABLE 12: ETHANOL FUMIGATION PARAMETERS FOR VARIOUS PROOFS AT A FLOW OF TWO AND A BMEP OF 200 kPa AND 2400 RPM.

	Ethanol proof		
	200	175	150
Diesel flow (g/s)	1.952	1.990	1.968
Ethanol flow (g/s)	1.971	1.923	2.036
% Energy by Eth.	38.8	37.8	39.4
Thermal efficiency	21.00	20.90	20.60
Volumetric eff.	84.60	85.70	83.7
Air flow (g/s)	138.8	139.0	139.2
Amb. press. (kPa)	98.91	98.87	99.09
Amb. temp. (C)	28.70	30.92	25.64
Wet bulb (C)	20.83	22.50	16.67
Man. press. (kPa)	106.9	105.9	107.6
Man. temp. (C)	50.80	52.00	48.80
Exh. temp. (C)	347.4	347.9	340.6
NO (ppm)	226.1	283.1	266.9
HC (ppm propane)	974.0	955.4	1046.
Bosch smoke	0.4	0.6	0.3
CO (% dry)	0.354	0.333	0.351
CO2 (% dry)	3.52	3.61	3.46
DP/DCA (kPa/deg)	449.7	428.3	436.8
Ang. max DP/DCA	360	360	361
Max press. (MPa)	5.854	5.849	5.866
Ang. Pmax	366	366	366
Ign. delay (deg)	16	15	16

TABLE 13: ETHANOL FUMIGATION PARAMETERS FOR VARIOUS PROOFS AT A FLOW OF ONE AND A BMEP OF 200 kPa AND 2400 RPM.

	Ethanol proof 200	175	150
Diesel flow (g/s)	2.544	2.568	2.454
Ethanol flow (g/s)	0.863	0.765	0.968
% Energy by Eth.	17.6	15.8	19.9
Thermal efficiency	21.70	22.00	21.90
Volumetric eff.	84.30	85.50	83.6
Air flow (g/s)	138.6	138.9	139.1
Amb. press. (kPa)	98.91	98.87	99.09
Amb. temp. (C)	28.93	30.81	25.48
Wet bulb (C)	21.11	22.50	16.67
Man. press. (kPa)	107.1	106.2	107.6
Man. temp. (C)	51.10	52.10	48.60
Exh. temp. (C)	353.4	353.5	343.6
NO (ppm)	327.0	396.5	367.2
HC (ppm propane)	531.6	476.1	574.4
Bosch smoke	0.6	1.2	0.6
CO (% dry)	0.177	0.153	0.190
CO2 (% dry)	3.72	3.82	3.63
DP/DCA (kPa/deg)	574.5	580.3	519.2
Ang. max DP/DCA	359	359	359
Max press. (MPa)	6.194	6.230	6.138
Ang. Pmax	361	365	365
Ign. delay (deg)	13	11	14

APPENDIX IV

EXTENDED PERFORMANCE OF ALCOHOL FUMIGATION IN DIESEL ENGINES THROUGH DIFFERENT MULTIPOINT ALCOHOL INJECTION TIMING CYCLES

L. D. Savage, Associate Professor and R. A. White, Professor;
S. Cole and G. Pritchett, Research Assistants
Department of Mechanical and Industrial Engineering
University of Illinois at Urbana-Champaign
1206 West Green Street
Urbana, IL 61801

Published as SAE Paper No. 860308

and

Presented at International Fuels and Lubricants
Meeting and Exposition
Detroit, Michigan

6-9 October 1986

ABSTRACT

This paper reports on the results of using multipoint port injection alcohol fumigation of a four-cycle turbocharged diesel engine in which the fumigation injection cycle was varied. The three cycles, dual with one-half of the alcohol injection on each engine revolution (DIT), single with all of the alcohol injected during the open intake valve revolution (SIO), and single with all of the alcohol injected during the closed intake valve revolution (SIC), lead to significant differences in the engines pressure-volume history and alcohol energy replacement tolerance. The engine was fumigated with both industrial grade ethanol and methanol and complete performance and emissions data (excluding aldehydes) were measured at low, medium, and high values of BMEP and rpm.

The results help to explain recently published data showing limited energy replacement, apparent excessive rate of cylinder pressure change, and emissions for single point injection in the same engine. Additionally the results point to the limiting operational processes that control alcohol fumigation of diesel engines. Changes in the definition of knock for fumigated diesel engine operation are suggested. The dual injection cycle mode allows the widest range of energy replacement and does not produce the excessive rates of pressure rise common to single point injection and which occurs under limited conditions with SIO and SIC.

Multipoint dual cycle fumigation of alcohol appears to be a viable approach to dual fueling of diesel equipment.

1. INTRODUCTION

Alcohol fumigation of diesel engines has attracted considerable attention in recent years as a method of dual fueling which avoids many of the problems associated with low cetane alternate fuels. Most of these studies have used single point injection either upstream of the turbocharger or in the crossover pipe between the turbocharger and intake manifold. The amount of energy replacement possible for single point injection has typically been in the 20 to 70 percent range [1]. None of these investigations have examined multipoint port injection in any detail nor studied the effects of varying the port injection cycle.

The results reported in this paper are based on a multipoint port injection study to examine the limits of energy replacement possible using multipoint port injection and the concurrent effects on emissions. The initial study [2] used an International Harvester (now Navistar International) DT-436B four-cycle, six-cylinder turbocharged engine with an injection cycle in which one-half of the alcohol was injected during the engine revolution with the valve closed and one-half during the engine revolution with the valve open. The results reported on by Roberts [2] showed that up to 90 percent energy replacement was possible at low loads and about 35 percent energy replacement at high loads.

The alcohol fumigation also leads to increased ignition delay [1,2] suggesting that changes in diesel fuel injection time may be desirable. This was studied by Schroeder [3] and resulted in measurable improvements in efficiency. Schroeder [3], however, did not examine changes in the fumigation

timing cycle. Since alcohol production at the farm level typically produces proofs in the 150 range, (75% ethanol, 25% water), Hayes [4] continued the work of Roberts [2] and Schroeder [3] with the multipoint port injection system using ethanol concentrations of 50% to 100% (absolute alcohol). He concluded that the optimum alcohol was 50% ethanol and 50% water based on both emissions and efficiency consideration. He, like Schroeder, did not vary the fumigation injection cycle.

Baranescu [1] reported results from the same engine tested in Refs. [2-4] and this study but with single-point crossover pipe injection indicating that maximum energy replacement with acceptable pressure rise rates in the cylinders, but with heavy knock, was in the 20 to 35 percent range. The significant difference between these replacement values and those of Refs. [2-4] suggest an important characteristic of diesel engine alcohol fumigation can be explained in part by examining the injection method and injection timing cycle and their effect on the intake charge and its combustion. In Ref. [1] it is stated that such large differences are too wide to be a consequence of the fumigation configuration and attributes the difference primarily to the criteria used for the knock limit. The differences referred the discrepancies between the work of Ref. [1] and the results of the current literature. The results of Ref. [2-4] had not been published at the time. Additionally the high rates of the pressure rise were related to knock limit. Similar increases in pressures rise rate and peak cylinder pressure have been measured in this study as well as others [2-4]. However, where these high rates occur relative to top dead center is also important. Thus Hayes [4] reports pressure-volume diagrams under certain test conditions which are similar to the Otto cycle combustion rather than diesel. Consequently knock limit conditions may change for fumigated engines as discussed later in this paper.

The results reported on in this paper are from the same International Harvester (Navistar) Engine of Refs. [1-4] with multipoint port injection using three different fumigation timing cycles. These are:

1. Dual injection with one-half of the alcohol injection on each engine revolution (DIT) (as used by Roberts [2]), Schroeder [3], and Hayes [4].

2. Injection timing with all alcohol supplied during the intake valve open revolution (SIO), and

3. Injection timing with all alcohol injected during the intake valve closed revolution (SIC).

These differences in the timing cycle produce different air-alcohol mixture compositions and stratification levels of the ingested air and alcohol due to residence time in, and heat addition to, the alcohol from the port and valve area of the block and manifold. These changes in turn result in modifications to the burning characteristics of the alcohol including the tendency for predetonation. The maximum amount of alcohol the engine can tolerate is typically limited by excessive knock at high load and misfire at low loads.

A comprehensive investigation of changes in fumigation cycle using the three types listed above is the basis of this paper. Complete performance, emission data (excluding aldehydes), and cylinder pressure history were

measured for industrial grade ethanol and methanol and are compared to diesel fuel values. The effects of varying the fumigation cycles are discussed and changes in the definition of knock for fumigated engines and its relation to cylinder pressure rise rates are suggested.

2. EXPERIMENTAL PROCEDURE

An International Harvester model DT-436B, six-cylinder turbocharged diesel engine was used for these experiments. The nominal specifications of this engine are given in Table 1.

The alcohol fumigation system added to the engine included six ND* model E-10 electronic fuel injectors and associated hardware. The injectors were positioned in the head as shown in Fig. 1. The angle of 25° from vertical was chosen to facilitate placing as much alcohol near the intake valve as possible. Reference pressure for the injector pressure regulator was taken from the intake manifold so that turbocharger boost would not change the 40 psig (282 kPa) pressure differential across the injectors. The alcohol injection timing cycles and their relation to top dead center and crank angle position are defined schematically in Fig. 2. Injection was triggered by three equally spaced signals obtained from an optical encoder placed at the end of the dynamometer shaft opposite the engine.

Data acquisition was carried out by means of an Apple II plus for emission data and an Apple IIe was used to gather air flow, diesel fuel line pressure, and cylinder pressure. Both computers were equipped with an Interactive Structures Corp. model AI-13, 16 channel 12 bit analog-to-digital converter. The frequency response capability of the analog-to-digital converter and associated software limited the acquisition of cylinder pressure data to once every crank angle degree. Cylinder pressure data were taken only from cylinder number one, since an earlier investigation by Roberts [2] showed insignificant cylinder to cylinder variations. To reduce the extraneous effects of cycle to cycle variations, 128 consecutive cycles of pressure data were summed in real time for each crank angle position and recorded as the average test condition.

Emission samples were taken downstream of the turbocharger. These samples were analyzed with standard emission equipment, and gave the total emission level of NO, HC, CO, CO_2, O_2 and smoke in the exhaust from the engine.

The alcohol fumigation tests were conducted using industrial anhydrous methanol and power ethanol (absolute ethanol denatured by 5 percent gasoline). The test matrix consisted of three engine speeds (1200, 1800, and 2400 rpm) and a high, medium, and low load at each speed (nominally BMEP values of 900, 500, and 200 KPA). At 1200 rpm with ethanol fumigation, only the two high loads were run because the dynamometer load/throttle position control system employed is unstable at very low speeds and light loads.

*Formerly reported by Roberts [2] as Bendix Injectors.

Table 1 Test Engine Characteristics

Engine Type	Diesel, 4-Cycle
Configuration	In-Line 6-Cylinder
Displacement	436 CU IN (7.141 L)
Bore x Stroke	4.30 x 5.00 IN 109.2 x 127 MM
Compression Ratio	16.3:1
Aspiration	Turbocharged
Rated Power @ rpm	170 BHP @ 2500 rpm
Peak Torque @ rpm	415 ft-lb @ 1800 rpm
Combustion System	Open Chamber
Direct Injection	
Injection System	Distributor Pump Differential 4-Hole Nozzles Needle Opening Pressure = 3700 psi

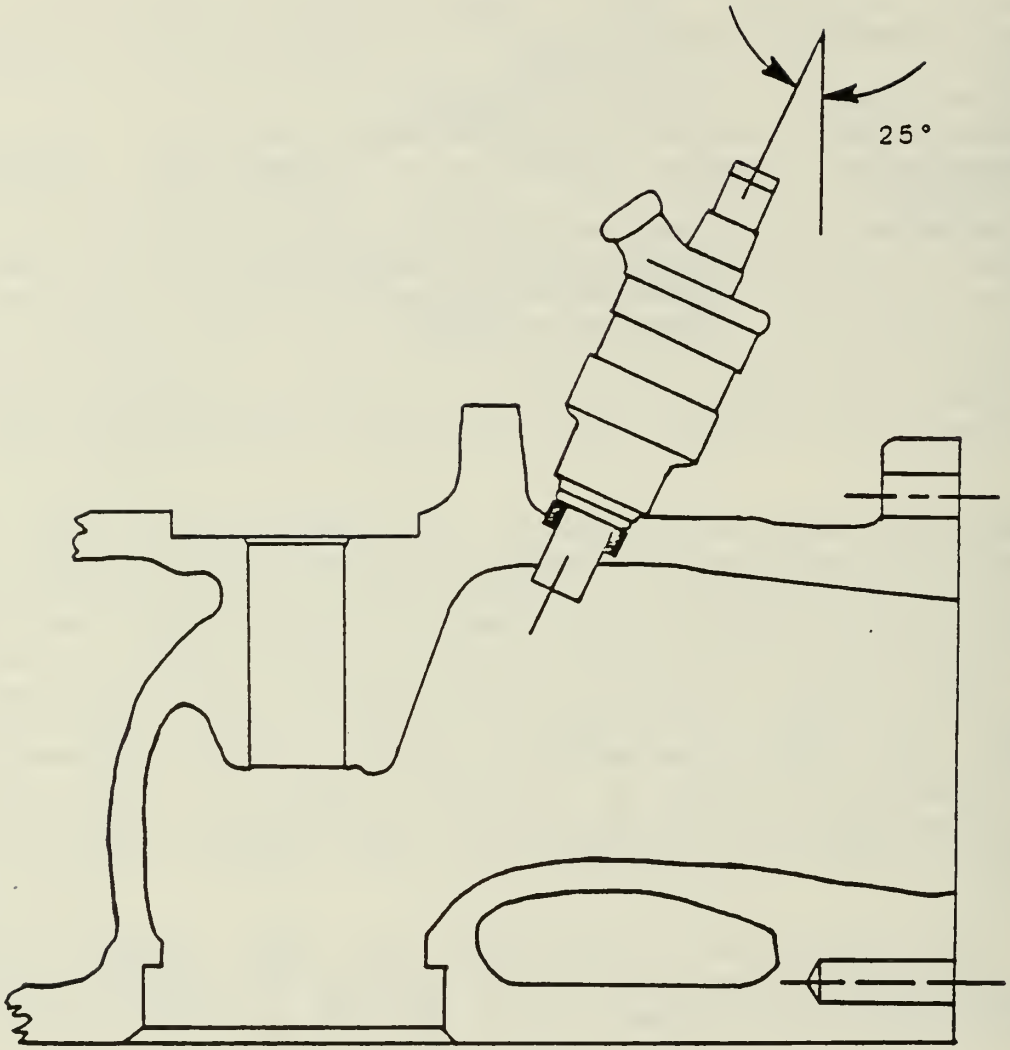

Figure 1 Cross Section of the Engine Head showing the Alcohol Injector Installation

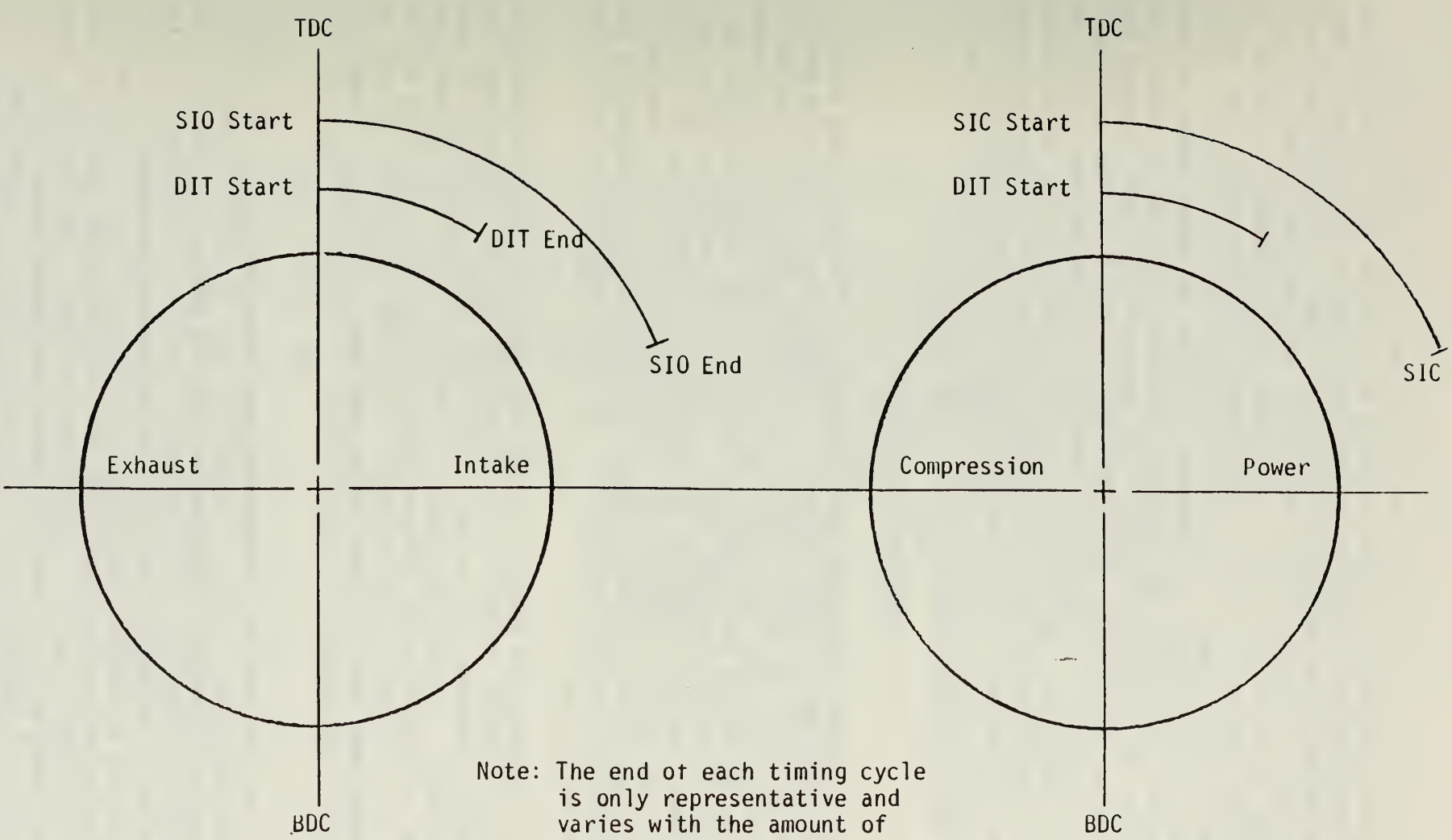

Figure 2 Alcohol Injection Timing and Angular Duration Relations for the Three Cycles Studied

The engine was started and warmed up using only diesel fuel. The desired test point was then selected and the engine stabilized at this point. Next the alcohol fumigation system using the DIT cycle was activated and the amount of alcohol injected was adjusted until an audible level of knock that was considered excessive occurred (or visual inspection of the pressure trace on an oscilloscope showed engine misfire). The alcohol injection amount per cycle was then reduced until the knock level was considered acceptable (or misfire ceased) and then the test data was recorded. After data was taken at this condition the alcohol flow rate was adjusted to lower substitution values and data was then taken at these conditions. The procedure was then repeated for the SIO cycle and the SIC cycle. An example of the data file that was generated for each test point is in Table 2. Throughout the studies Ref. [2-4] and this work, once stabilized, the results were so repeatable that the pressure oscillations which appeared on the oscilloscope readout of the pressure traces also appeared on the average of 128 pressure traces presented digitally. This contrasts dramatically with the cycle to cycle and cylinder to cylinder variations observed with the single-point results from Navistar [1].

3. EXPERIMENTAL RESULTS

The results of these fumigation tests are shown for methanol and ethanol, respectively, at 1200 rpm in Figs. 3a and b, at 1800 rpm in Figs. 4a and b, and at 2400 rpm in Figs. 5a and b. HC and NO emission data are presented as ratios of the fumigation results to the baseline diesel levels. The diesel baseline data for HC and NO are listed in Table 3. The data shows that both methanol and ethanol follow the same general trends. It should be noted that the maximum methanol substitution rate at 1200 rpm and a BMEP value of 352 kPa was dynamometer load control limited, and not a knock limit, i.e., the throttle controller could not reduce the governor setting enough to compensate for the energy contribution of the fumigation. The data labeled with an "N" are the results reported in Ref. [1].

In general the emission results agree both quantitatively and qualitatively with those presented in Ref. [1]. The maximum alcohol replacement considered acceptable, however, is as much as three times as large at some operating conditions. The maximum rates of pressure rise reported here are higher than the average rate of pressure rise for the six cylinders as reported in Ref. [1]. However, the cylinder to cylinder variation of the results of this experiment were not measurable, and those of Ref. [1] showed individual cylinders with rates of pressure rise in excess of those of this study.

Throughout the test program, the engine operated smoothly and was audibly similar to diesel operation. The only exceptions were at 1800 rpm and 911 kPa BMEP as discussed below and at 1200 rpm and 528 kPa BMEP with the SIO cycle with ethanol, where extremely large pressure rises were encountered at the start of combustion. In one of the first cases when this phenomena occurred the cylinder pressure transducer was damaged. The peak pressure for both alcohols and all injection cycles (except for the high load 1800 rpm points with SIO and SIC using ethanol and all cycles with methanol, see Table 4, where these points are marked with an asterisk) are within 10 percent of diesel conditions. For the five starred points, the peak pressure is approximately 50 percent greater than diesel levels. These points are approaching the conditions, SIO and 1800 rpm with ethanol in Table 4, where the cylinder pressure

Table II Typical Data and Processed Results for a Single Test Point

```
FILE:M3183D   DATE:4/26/86   HR:318.2   TIME:1110
      RPM= 1800
      TORQUE= 300  (Nm)
      IP= 79.3747195  (KW)
      BP= 56.5488  (KW)
      IMEP= 741.023381  (kpa)
      BMEP= 527.926061  (kpa)
      MDOT DIES.= 2.85278626E-03  (kg/s)
      MDOT ETH.= 2.20584416E-03  (kg/s)
      IND. THERM. EFF.= .477441445
      BRAKE THERM. EFF.= .340142819
      % ETHANOL BY ENERGY= 29.2484692
      VOL. EFF.= .805674565
      MASS AIR= .0854603177  (kg/s)
      AIR/ETHANOL RATIO = 38.7426816  (kg air/kg eth)
      MAN. PRESS.= 92.58  (kpa)
      AMB. PRESS.= 98.856122  (kpa)
      WET BULB= 24.7222222  (C)
      AMB. TEMP.= 32.0382264  (C)
      HUMID AIR DENSITY = 1.06279505  (kg/m3)
      DRY AIR DENSITY = 1.08972006  (kg/m3)
      RELATIVE HUMIDITY = 78.562666  %
      HUMIDITY RATIO = .0160209529
      COMP. INLET TEMP.= 30.6948551  (C)
      COMP. OUTLET TEMP.= 52.597223  (C)
      TURB. INLET TEMP.= 437.452892  (C)
      TURB. OUTLET TEMP.= 406.750118  (C)
      COOLANT TEMP.= 96.5991495  (C)
      OXYGEN= 12.8849487  %
      NO= 1469.59229  (ppm)
      HC= 465.1326  (ppm)
      CO2= 6.52090071  %
      CO= .161334107  %
      SMOKE # = 1.1

     PMAN= 92.5837606 KPA

     PEXH= 119.192776 KPA

     BAR= 98.86 KPA

     Q-DOT= .0757158083 M^3/SEC

     MAX DP= 2021.05347 KPA/DEG AT 356 DEG.

     MAX PRESS= 11210.4017 KPA AT 361 DEG.

     INJ. STARTS AT 339 DEG

     COMB. STARTS AT 353 DEG.

     IGNITION DELAY= 14 DEG.
```

Table 3 Unburned Hydrocarbons and Nitric Oxide Levels for Diesel Fuel Operation

Baseline Diesel

Speed (rpm)	Load (Nm)	HC (ppm)	NO (ppm)
1200	200	188	926
	300	160	1294
	481	139	1080
1800	100	164	728
	300	131	1579
	518	60	1772
2400	100	124	607
	300	118	1311
	460	46	1432

Table 4 Peak Pressures for Multipoint Fumigation and Diesel Operation

Maximum Ethanol High Load

Pressure (kPa)

Speed (rpm)	DIT	SIO	SIC	Diesel
1,200	12,524	12,622	12,529	11,154
1,800	12,256	16,516*	15,746*	10,826
2,400	10,681	11,108	11,141	10,106

Maximum Methanol High Load

Pressure (kPa)

Speed (rpm)	DIT	SIO	SIC	Diesel
1,200	11,995	12,306	12,387	11,154
1,800	15,346*	14,945*	14,852*	10,826
2,400	10,355	10,274	10,144	10,106

*Near "predetonation."

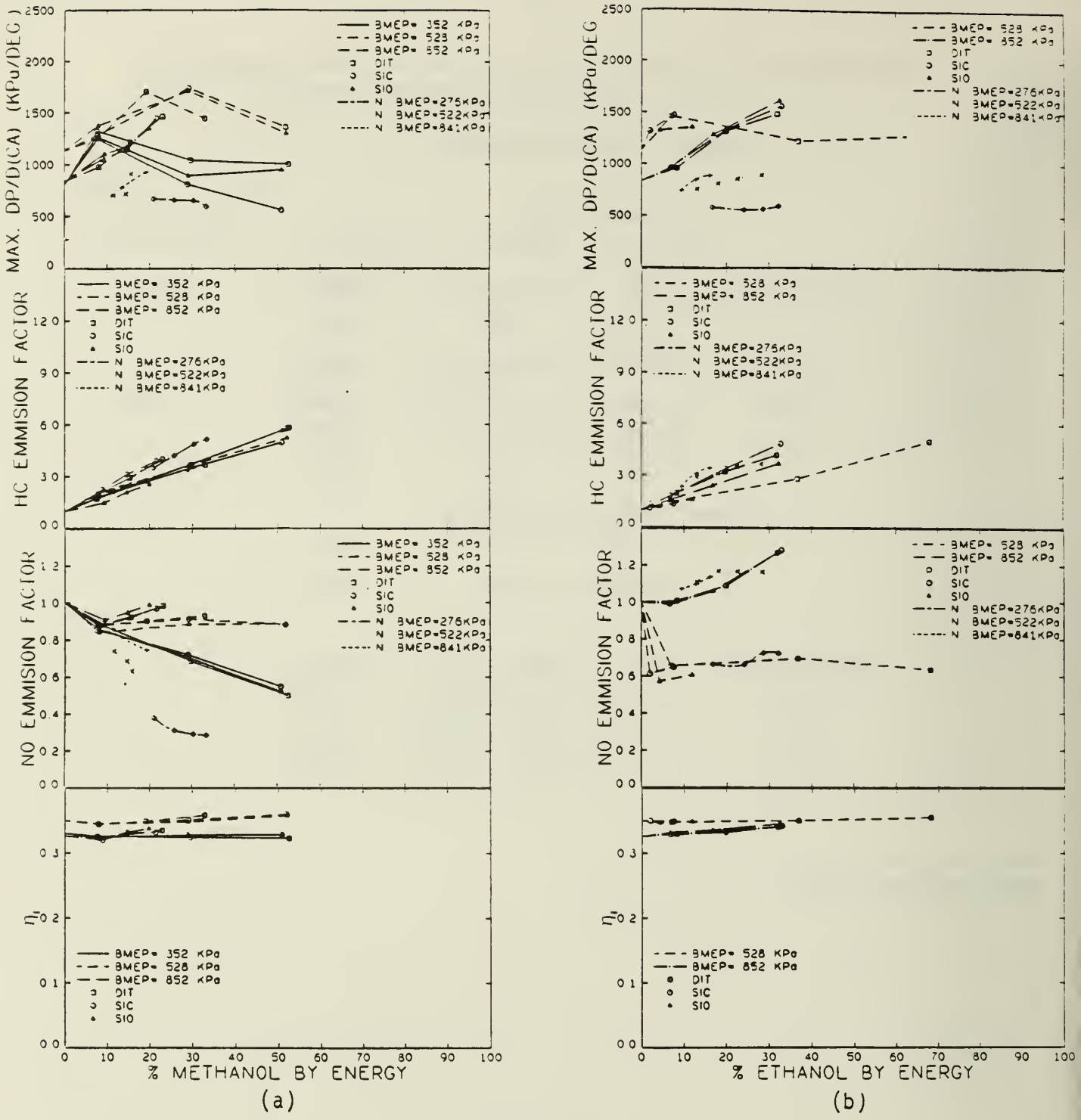

Figure 3 Effect of Fumigation on Angular Pressure Gradient HC Emission Factor, No Emission Factor, and Thermal Efficiency at 1200 RPM
(a) Methanol (b) Ethanol

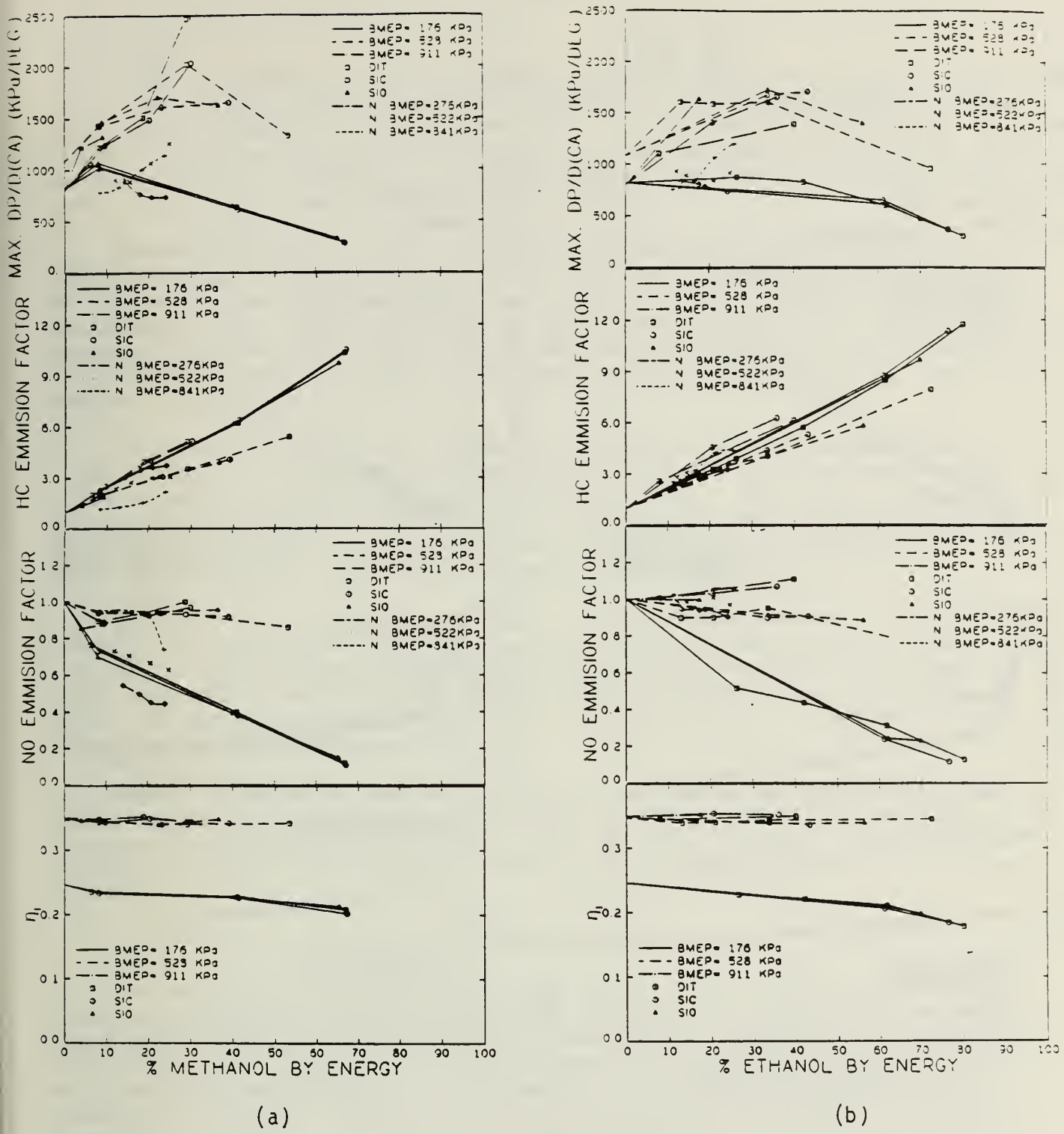

Figure 4 Effect of Fumigation on Angular Pressure Gradient HC Emission Factor, No Emission Factor, and Thermal Efficiency at 1800 RPM
(a) Methanol (b) Ethanol

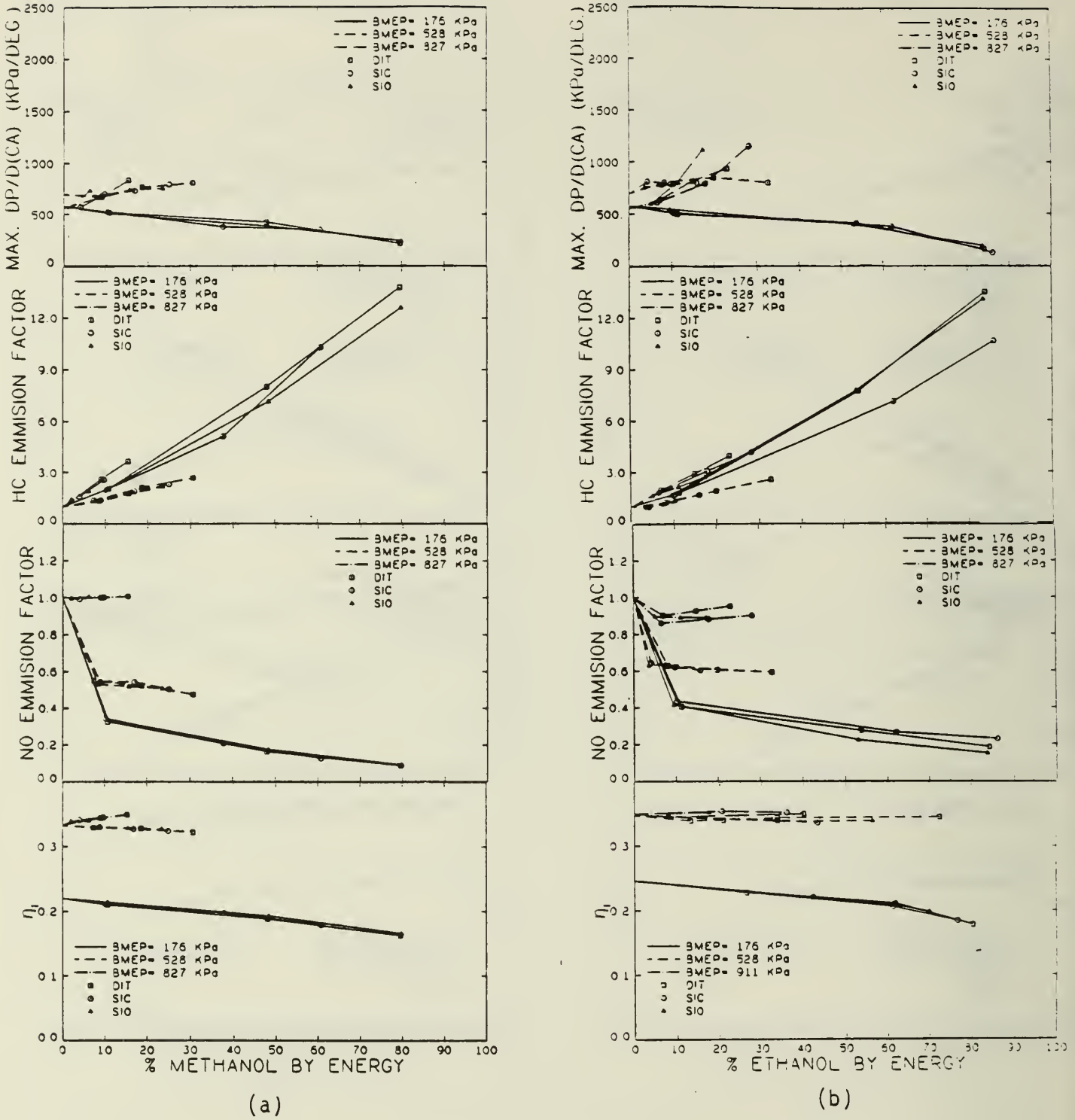

Figure 5 Effect of Fumigation on Angular Pressure Gradient, HC Emission Factor, No Emission Factor, and Thermal Efficiency at 2400 RPM
(a) Methanol (b) Ethanol

transducer was damaged. It was obvious to the test personnel based on knock, that these test conditions were not satisfactory operating states and they consequently reduced the fumigation rate. The implications of this are discussed in the next section. For the DIT cycle fumigated with ethanol, the maximum cylinder pressure was 13 percent higher than that for straight diesel and for most points less than 10 percent greater.

Other than for the conditions mentioned above, the rate of pressure rise does not appear to be directly related to the audible knock limit since most of the medium and high load data shows that the rate of pressure rise has a maximum and then remains constant or decreased as the knock limit is approached. At low loads, the rate of pressure rise data shows a steady decrease with increasing alcohol replacement until the engine misfire limit is reached at maximum percent alcohol.

The occurrence of maximum pressure rise rate was at 2-4 degrees after the start of combustion regardless of the alcohol injection cycle or amount of alcohol injected (including the straight diesel case). This delay is the same as reported in Ref. [1]. Peak pressure showed the same relation except the delay from the start of combustion was 8-12 degrees. By contrast, ignition delay was measurably increased by the addition of alcohol, see Fig. 6.

At low and medium loads even small percentages of alcohol substitution results in a substantial decrease in NO. This reduction is clearly seen in Fig. 3b for 1200 rpm and 528 kPa BMEP with ethanol fumigation. In general at high loads, NO formation is not significantly different with alcohol replacement. By contrast, HC emissions show a steady increase with percent alcohol regardless of the other parameters.

Thermal efficiency remains relatively constant with increased alcohol substitution, showing a slight increase at high loads, and slight reduction at low loads toward the engine misfire limit, see Figs. 4a and b. Away from individual maximums, the different injection cycles produce essentially the same results.

4. DISCUSSION OF RESULTS

The results of the current investigation reported in the previous section show that fumigation using multipoint port injection is strongly influenced by the alcohol injection cycle and alcohol type and that fumigation using ethanol is viable over a wide range of load and speed. Indeed, increases in thermal efficiency can be obtained at high loads with little attendant negative consequences in terms of emissions. At low loads the strong increase in unburned hydrocarbons may be a limiting consideration based on possible pollution standards although that, to some degree, may be mitigated by the decrease in NO emissions.

Considerable concern has been raised in the literature about the rate of pressure rise and peak pressures from fumigation both with respect to possible reduction in engine life and the determination of the knock limit. The rates of pressure rise for fumigated combustion generally are larger than those for pure diesel fuel combustion at the same conditions, see Figs. 3, 4, or 5; however, at low loads at all speeds they are lower than the rates for diesel fuel alone. This is also reflected in the results reported by Baranescu [1] al-

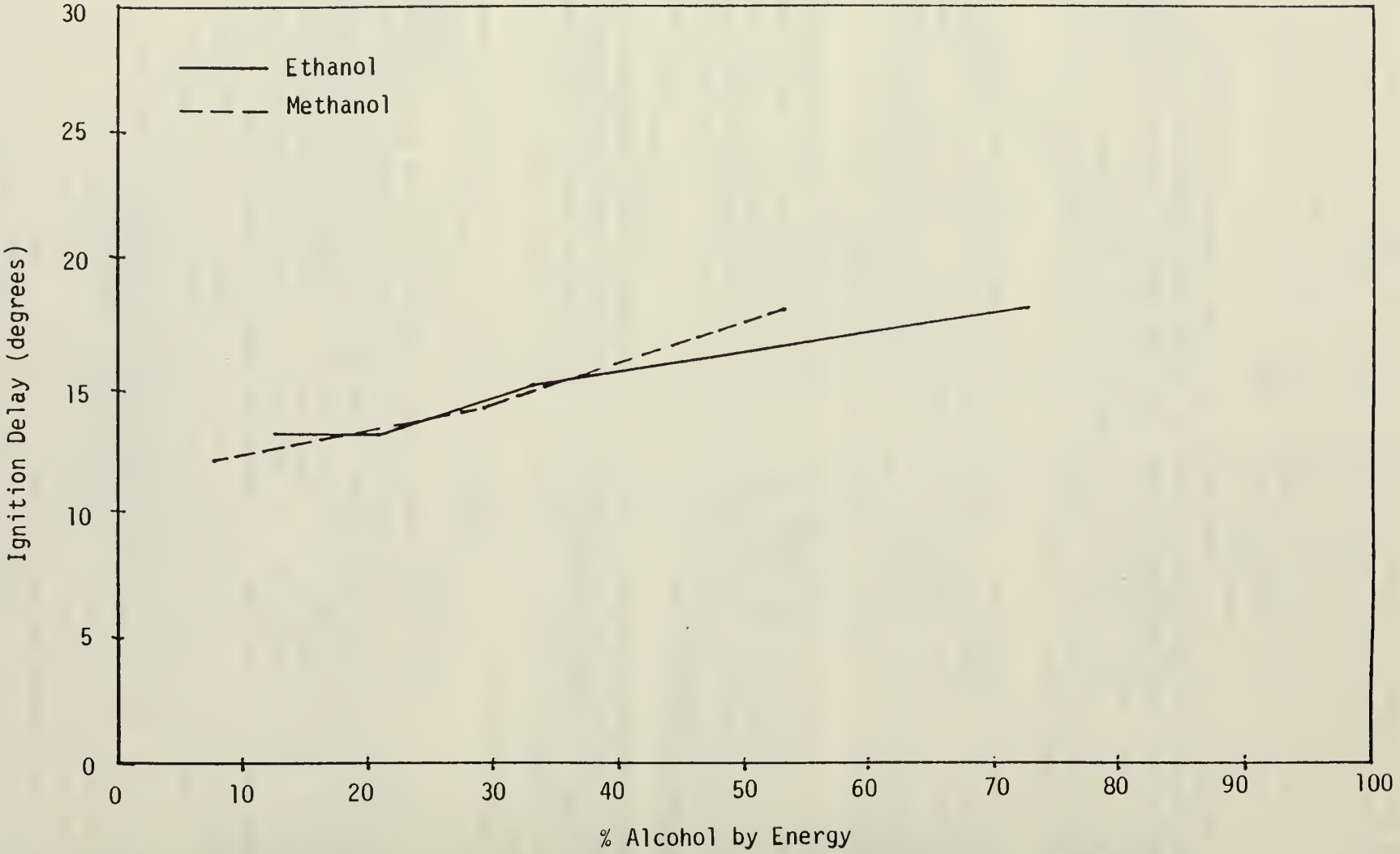

Figure 6 Increases in Ignition Delay due to Alcohol Fumigation for Typical Operating Conditions

though the Navistar results were terminated (apparently by a "knock limit") at a much lower energy replacement level than was feasible with the multipoint port injection system.

Baranescu [1] rejects alcohol fumigation systems based on the fact that the angular rate of pressure rise exceeds that observed for diesel fuel combustion. Since this parameter is often used by designers as a criterion for engine life, a derating of life expectancy with increased rate of pressure rise would be appropriate. She further implies that the attempt to fumigate will lead to disastrous values of the rate of pressure rise which is a reasonable extrapolation of the results of the Navistar experiments. The results of this experiment, however, contradict that extrapolation and indicate that there is in fact for most cases a maximum for the gradient as a function of alcohol substitution, see Fig. 4b. In some cases the knock limit is reached before a maximum is achieved. This maximum is more clearly shown and indicated in the results for ethanol than for methanol.

Careful inspection of figures such as Figs. 4a and b indicate that in general the knock limit (the right hand termination of the gradient as a function of energy substitution) is independent of the rate of pressure rise within the cylinder. For a limited number of cases (as discussed in the last section and noted in Table 4 at maximum load) very early detonation occurred leading to very high pressures and rates of pressure rise, indeed in one case these effects were severe enough to damage the pressure transducer. This has never occurred with the DIT cycle using ethanol. Further this phenomenon was associated with a distinctly different audible knock which for lack of a better description could be called "clanging". Based on the consequence of rate of pressure rise and peak cylinder pressures and their correlation with operator determination of limit knock, it appears that peak pressures greater than some arbitrary value above straight diesel values and not rate of pressure rise should be the criterion for maximum alcohol substitution levels.

Again, this value may exceed the design value selected for durability, thus requiring a derating of life expectancy for dual fueling.

Thus, identification of that characteristic of the DIT cycle (and of the SIC and SIO cycles for most conditions) which allows operation at high pressure rise rates without excessive peak pressures, noise, and roughness is essential to the understanding of the fumigation of diesel engines. As alluded to in the introduction, the knock limit is dependent upon where in the cycle the knock occurs and the amount of mixture that participates in the reaction assuming that knock is the consequence of a homogeneous reaction in some volume of combustible mixture. The knock undergoes a transition from diesel cycle diffusion burning and early cycle low frequency pressure oscillations to an Otto cycle form of pressure-volume history with associated high frequency oscillations after (or at) top dead center with possible end gas "detonation". This is shown in Fig. 7 which is a comparison of cylinder pressure histories. The Otto cycle form of pressure volume history is particularly notable for the DIT injection cycle. The combination of ignition delay and homogeniety or stratification of the A/F ratio in the cylinder normally produces an Otto cycle type pressure history and associated end gas detonation after the initial rapid rise in pressure initiated by the diesel source. Occasionally for the SIO cycle "predetonation" has been detected and excessively high peak cylinder pressures appear to be precursors to the "predetonation."

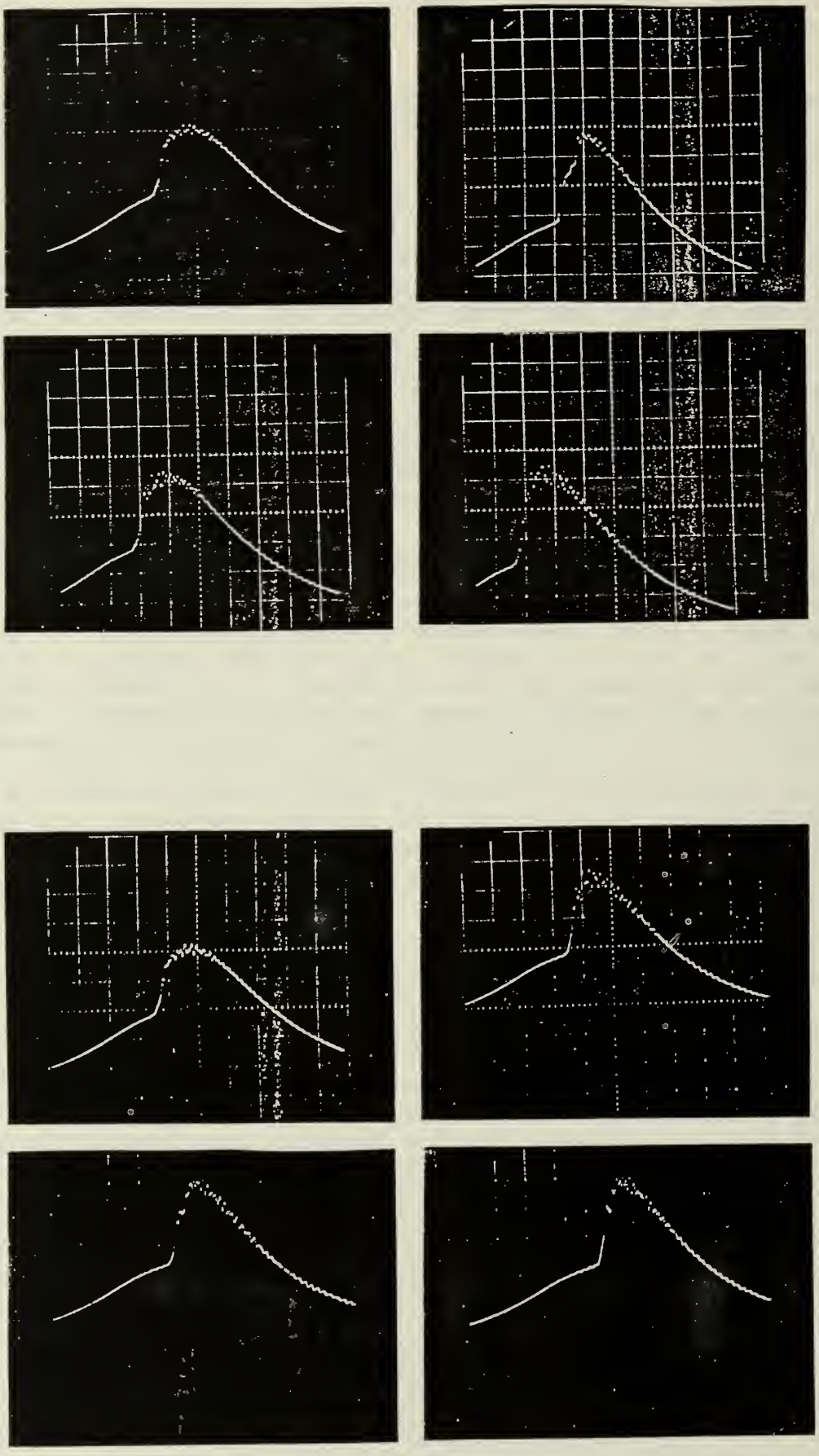

Figure 7 Representative Cylinder Pressure Histories Illustrating the Differences Between Diesel Combustion and that Occurring for the Three Alcohol Injection Cycles

Thus, some of the variation of allowable fumigation levels is attributable to changes in knock conditions. The three types of knock observed with multipoint port fumigation can be categorized as:

1) Heavy diesel knock with low frequencies occurring early in the burning cycle. This occurs primarily while increasing load at low or zero fumigation levels.

2) Predetonation at essentially initial diesel fuel injection characterized by potentially damaging pressure rise rates, pressure levels, and audibly different frequency content of this knock.

3) Transition to an Otto cycle type pressure-volume diagram and higher frequency pressure oscillations near and after peak pressure.

The multipoint port alcohol injection cycles only lead to type 2 knock for limited conditions as discussed previously. It is not clear from the information presented in Ref. [1] whether more than one form of knock was experienced during the conduct of the experiment. Failure to recognize the differences in knock form associated with the fumigation method could account for the widely varying tolerability of engines to fumigation. The DIT cycle which provides a smooth transition to type 3 knock without experiencing type 2, consequently, allows for high energy replacement values without serious consequences. Further, care must be taken in not simply associating high pressure rise rates with knock limit or audible noise. Since the fumigated system promotes involvement of all of the fuel in an energy release process that is similar to the Otto cycle of the spark ignition engine one should expect a wide range of knock sensitivities for diesel designs when fumigated.

5. CONCLUSIONS

Differences in the method of alcohol fumigation such as single-point and multipoint injection as well as the injection cycle lead to substantial differences in alcohol tolerance and onset and type of knock. Thus, diesel engines being designed for use with fumigation should include consideration of end gas detonation. Of the multipoint injection cycles examined in this study, dual injection (DIT) is the simplest cycle to implement and leads to extended performance for alcohol fumigation. Alcohol energy replacement of 90 percent at low loads and 35 percent at high loads with only small changes in thermal efficiency is possible using multipoint dual injection cycles. Thus, multipoint alcohol fumigation appears to have considerable potential for use by the farm and transportation communities. Engines designs for dual fueling should include considerations of higher peak pressures and higher efficiencies that result from fumigation.

While changes in diesel timing show improvements in fumigation performance [3], changes in timing with respect to TDC of the fumigation cycle remain to be studied. The effects of proofs, which have been shown by Hayes [4] to yield an optimum alcohol based on cost and performance of 50 percent ethanol and 50 percent water, may effect the knock phenomena and particularly the tendency for predetonation and consequently should be examined. Although both methanol and ethanol are viable fuels for fumigation, methanol has a lower energy replacement limit and is more prone to predetonation. Peak pressures should be used to establish the limit of replacement with a value of 20 percent over straight diesel values as a suggested limit.

REFERENCES

1. Baranescu, R. A., "Fumigations of Alcohols in a Multicylinder Diesel Engine--Evaluation of Potential," SAE Paper 860308, International Congress and Exposition, Feb. 24-28, 1986, Detroit, MI.

2. Roberts, B., "Performance and Emissions of a Turbocharged Diesel Engine Fumigated with Ethanol," M.S. Thesis, Department of Mechanical and Industrial Engineering, University of Illinois at Urbana-Champaign, Dec. 1985.

3. Schroeder, A. R., "The Effect of Diesel Injection Timing on a Turbocharged Diesel Engine Fumigated with Ethanol," M.S. Thesis, Department of Mechanical and Industrial Engineering, University of Illinois at Urbana-Champaign, May 1986.

4. Hayes, T.K., "The Effect of Fumigation of Different Ethanol Proofs on a Turbocharged Diesel Engine," M.S. Thesis, Department of Mechanical and Industrial Engineering, University of Illinois at Urbana-Champaign, May 1986.

5. Checked, D. M., and Douglas, J., "Computerized Knock Production from Engine Pressure Records," SAE Paper 860028, International Congress and Exposition, Feb. 24-28, 1986, Detroit, MI.

6. Sorenson, S., Hayes, T. K., and Savage, L. D., "Cylinder Pressure Data Acquisition and Heat Research Analysis on a Personal Computer," SAE Paper 860029, International Congress and Exposition, Feb. 24-28, 1986, Detroit, MI.

272 - 101

EPORT DOCUMENTATION PAGE	1. REPORT NO. ILENR/AE-87/02	2.	3. Recipient's Accession No.

Title and Subtitle

A Practical System for the Use of Alcohol in Diesel Engines

5. Report Date: Published November 1987

6.

Author(s)

Dr. L.D. Savage and Dr. R.A. White

8. Performing Organization Rept. No.

Performing Organization Name and Address

University of Illinois at Urbana-Champaign Department of Mechanical and Industrial Engineering
1206 West Green Street
Urbana, IL 61801

10. Project/Task/Work Unit No.

11. Contract(C) or Grant(G) No.
(C)
(G) AE13 and 3-ALT

Sponsoring Organization Name and Address

Illinois Dept. of Energy & Natural Resources
Office of Solid Waste and Renewable Resources
325 West Adams, Room 300
Springfield, IL 62704-1892

13. Type of Report & Period Covered: Final

14.

Supplementary Notes

Abstract (Limit: 200 words)

his study investigated the fumigation of ethanol and methanol into diesel engines with the im of developing a simple and practical microchip controlled alcohol injection system uitable for all engine operating conditions. In contrast to most previous fumigation ystems, the method selected used multiple injectors with one at each inlet valve location. his provided for uniform cylinder-to-cylinder air-alcohol mixtures in order to avoid re- uction in energy replacement potential due to one cylinder setting the limiting condition nd allowed the use of different alcohol injection cycles. The latter is important since t provides a method for controlling the composition of the air-alcohol charge in terms of ne percent vapor or droplets and consequently the tendency to detonate (knock) or burn ith the pilot diesel fuel.

ne results of the investigation have shown that ethanol fumigation of diesel engines is ractical in terms of energy replacement and in terms of proof level of ethanol needed.

two-step injection process allows energy replacement levels of up to 90 percent at low oads and 35 percent at high loads.

Document Analysis a. Descriptors

Multifuel engines, fueling systems, diesel fuels, ethyl alcohol, methyl alcohol, fumigation.

b. Identifiers/Open-Ended Terms

Alcohol fuels

c. COSATI Field/Group

Availability Statement Limited copies available from:
nergy Information Clearinghouse
325 West Adams
Springfield, IL 62704
1-800-252-8955

19. Security Class (This Report)	21. No. of Pages 322
20. Security Class (This Page)	22. Price Free

Printed by the authority of the State of Illinois